FORSCHUNGSZENTRUM
ROSSENDORF e.V.

FZR

INSTITUTE OF BIOINORGANIC AND RADIOPHARMACEUTICAL CHEMISTRY

Annual Report 1994

Editor: B. Johannsen

FZR-73
Februar 1995

Forschungszentrum Rossendorf e.V.
Postfach 51 01 19 · D-01314 Dresden
Bundesrepublik Deutschland

Telefon (0351) 591 3170
Telefax (0351) 591 3232
E-Mail johannsen@fz-rossendorf.de

CONTENTS

I.
INTRODUCTION

This annual report covers the research activities of the **Institute of Bioinorganic and Radiopharmaceutical Chemistry** of the **Research Center Rossendorf Inc. (FZR)** in 1994. Significant progress has been made since the start of the Institute in 1992. The year 1994 is best described as a year of further consolidation.
The subjects of our work in 1994 are presented in this volume in 37 reports dealing with various aspects of radiotracers.

Our main objectives are derived from an awareness of the very important role modern nuclear medicine is playing, as expressed explicitly in the synonym *in vivo* biochemistry. Radiopharmaceuticals are the molecular probes used for the diagnosis and cure of disease. For full exploitation of its potential, this discipline of *in vivo* biochemistry requires great commitment to interdisciplinary research into tracers. The emphasis is on fundamentals on the molecular level, leading to new approaches in tracer design : the tracer chemistry and structure-biodistribution relationships.

The goals imply exploiting technetium coordination chemistry. New classes of complexes of technetium or rhenium, the convenient model nuclide for radioactive technetium, have been synthesized and characterized. Technetium has an intricate coordination chemistry that does not go well with the organic nature of biochemical substrates. One of the main achievements of the year was the successful approach to make complexes of technetium biochemically reactive by functionalization of a coordinate ligand. Functionalization is focused on two areas. The first is specific binding, as in ligand-receptor interactions. The second is enzymatic hydrolysis in the target or a nontarget. The studies also constitute a contribution to applied bio-inorganic chemistry.

A second part of this report describes the progress in our synthetic work on ^{11}C-tracers and precursors. These studies follows the concept of labelling substances in metabolically stable positions. During the year further peparatory work has been done to start PET studies in patients. The preparation of PET radiopharmaceuticals presents unique issues for the legal and regulatory communities. To assure that the

in-house prepared radiopharmaceuticals meet the standards of safety and efficacy according to Good Manufacturing Practice, a comprehensive system of in-house standards as well as documentation covering the entire process of preparation and quality assurance has been established.

The biological and biochemical section of this report informs on the progress attained in 1994 in methodological work on an *in vitro* model of the blood-brain barrier and the *in vivo* microdialysis technique. Transport through the blood-brain barrier and uptake of tracers in normal and tumour cells have been studied. Different *in vitro* binding assays have successfully been used to identify and quantify binding of various new ligands to brain receptors.

The research activities of our Institute have been performed in the following three organisational units:

> The SPECT Tracer Group (Head: H. Spies) deals with the design, synthesis and chemical characterization of metal coordination compounds, primarily technetium complexes.
>
> The PET Tracer Group (Head: J. Steinbach) is engaged in the chemistry and radiopharmacy of ^{11}C and ^{18}F labelled compounds, and in the setup of the Rossendorf PET Center, which is jointly run by the Institute and the Clinic and Polyclinic of Nuclear Medicine of the University Hospital.
>
> The Biochemical Group (Head: P. Brust) is working on SPECT and PET relevant biochemical and biological projects. This includes the characterization and assessment of new compounds developed in the two synthetically oriented groups mentioned above.

The achievements attained so far have only been possible because of the dedication and commitment of the permanent and temporary staff, the Ph.D. students and collaborators inside and outside the Rossendorf Research Center. I would like to express my thanks to all of them.

Bernd Johannsen

II.

RESEARCH REPORTS

1. TECHNETIUM AND RHENIUM COMPLEXES WITH THIOETHER LIGANDS

6. OXORHENIUM(V) COMPLEXES DERIVED FROM THE POTENTIALLY TETRADENTATE LIGAND 1,8-DIHYDROXY-3,6-DITHIAOCTANE

H.-J. Pietzsch, H. Spies, P. Leibnitz[1], G. Reck[1]

[1]Bundesanstalt für Materialforschung Berlin

Recently we found that ligand exchange reaction of the potentially tetradentate ligand 1,8-dihydroxy-3,6-dithiaoctane ("$S_2(OH)_2$") with $[ReOCl_4]^-$ leads to the formation of a violet microcrystalline complex of the general formulation $[ReO("S_2O(OH)")Cl_2]$ **(1)** [1].

Now the proposed structure is confirmed by X-ray diffraction. The molecular structure is shown in Fig. 1. Selected bond distances and angles are contained in Table 1.

By analogy with the appropriate technetium complex [2] the rhenium compound consists of discrete monomolecular units containing the $[O{=}Re{-}O{-}]^{2+}$ core.

While in the binuclear oxorhenium(V) derived from neutral dithiaalkanes [3] the position *trans* to the $[Re{=}O]^{3+}$ core is occupied by a bridging oxygen, the *trans* position in **(1)** is occupied by an oxygen of one of the terminal hydroxy groups. The second hydroxy group remains non-coordinated.

The infrared spectrum shows the characteristic stretching vibration indicating the $Re{=}O^{3+}$ core at 940 cm^{-1}.

Due to the presence of diverse leaving groups in the coordination sphere of **(1)**, namely the only weakly bonded chelate, the two chloro ligands and the non-coordinated hydroxy group, manifold subsequent reactions can be anticipated.

First attempts to functionalize the "free" hydroxy group are described in the following.

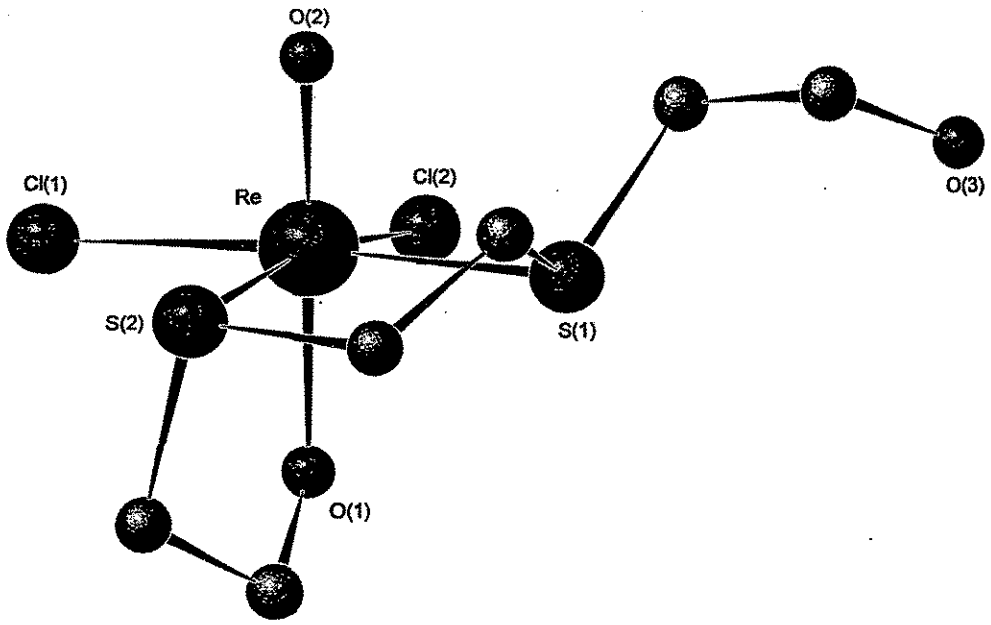

Fig. 1: Structure of [ReO{8-hydroxy-3,6-dithiaoctan-1-olato-(O,S,S)}Cl_2] (1)

Table 1: Selected bond distances (Å) and angles (deg) of [ReO{8-hydroxy-3,6-dithiaoctan-1-olato-(O,S,S)}Cl_2] (1)

Re-Cl(1)	2.437(6)	Re-S(2)	2.439(7)
Re-Cl(2)	2.388(6)	Re-O(1)	1.92(2)
Re-S(1)	2.428(6)	Re-O(2)	1.71(2)
Cl(1)-Re-Cl(2)	90.2(2)	Cl(2)-Re-O(2)	104.5(7)
Cl(1)-Re-S(1)	174.4(2)	S(1)-Re-S(2)	84.9(2)
Cl(1)-Re-S(2)	90.1(2)	S(1)-Re-O(1)	86.1(5)
Cl(1)-Re-O(1)	90.5(5)	S(1)-Re-O(2)	88.0(7)
Cl(1)-Re-O(2)	94.2(7)	S(2)-Re-O(1)	78.6(5)
Cl(2)-Re-S(1)	94.1(2)	S(2)-Re-O(2)	86.9(7)
Cl(2)-Re-S(2)	168.5(3)	O(1)-Re-O(2)	164.8(8)
Cl(2)-Re-O(1)	89.9(5)		

Experiments to the derivatization of the „free" hydroxy group by esterification

When an acetonic solution of **(1)** reacts with acetyl chloride (or acetic anhydride) at ambient temperature the colour of the reaction mixture changes from violet to turquoise. The product crystallizes as dark green crystals by slow evaporation of the reaction mixture (Fig. 2).

X-ray structure analysis shows that esterification with acetyl chloride (or acetic anhydride) surprisingly leads to the cleavage of the Tc-O_{trans} bond and subsequent formation of the μ-oxo bridged compound **(2)** containing four ester groups (reaction way B). The same product is obtained by ligand exchange reaction starting from $[ReOCl_4]^-$ in acetone/acetyl chloride (reaction way A).

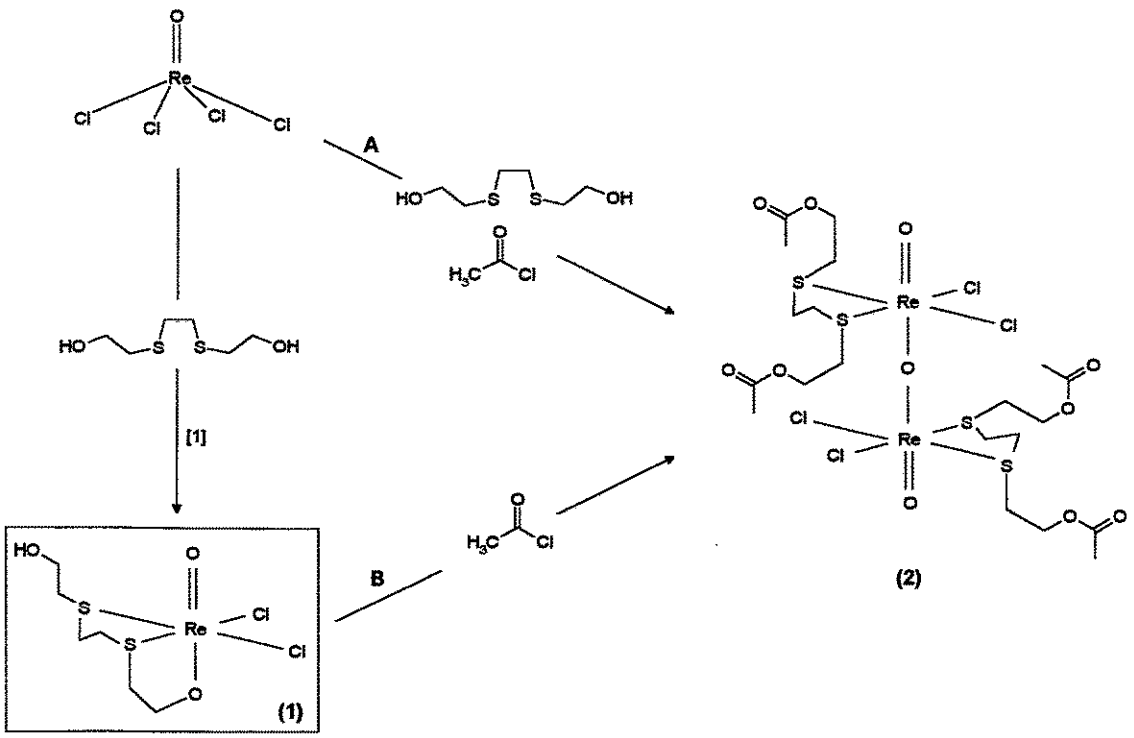

Fig. 2: Formation of the binuclear complex **(2)** while esterification of the mononuclear compound **(1)** with acetyl chloride

Complex **(2)** shows an intense and characteristic stretching vibration band between 650 and 700 cm^{-1} indicating the Re-O-Re moiety, as reported previously for similar $[M_2O_3]^{4+}$ species (M = Tc, Re) [3,4]. Absorptions between 900 and 1000 cm^{-1} which

can be assigned to the $Re{=}O^{3+}$ core are not observed. The bands indicating the ester groups are found at 1744 cm^{-1}.

The molecular structure of the binuclear compound **(2)** is shown in Fig. 3. Selected bond distances and angles are listed in Table 2.

(2) consists of two independent $[ReO\{CH_3C(O)O\text{-}(CH_2)_2\text{-}S\text{-}(CH_2)_2\text{-}S\text{-}(CH_2)_2\text{-}O(O)\text{-}CCH_3\}Cl_2]$ units bridged by an oxygen atom. The characteristic feature is the presence of the O=Re-O-Re=O backbone which shows a considerable deviation from linearity.

In this respect the structure is comparable to those found for the technetium complex $[TcO("S_2")Cl_2]_2O$ ("S_2" = 5,8-dithiadodecane) [2] as well as for the corresponding rhenium complexes $[ReO(Bu\text{-}S\text{-}CH_2CH_2\text{-}S\text{-}Bu)Cl_2]$ [5], $[ReO(pyr)_2Cl_2]_2O$ (pyr = pyridine) [6] and $[ReO(1\text{-}Meim)_2Cl_2]_2O$ (1-Meim = 1-methylimidazole) [7].

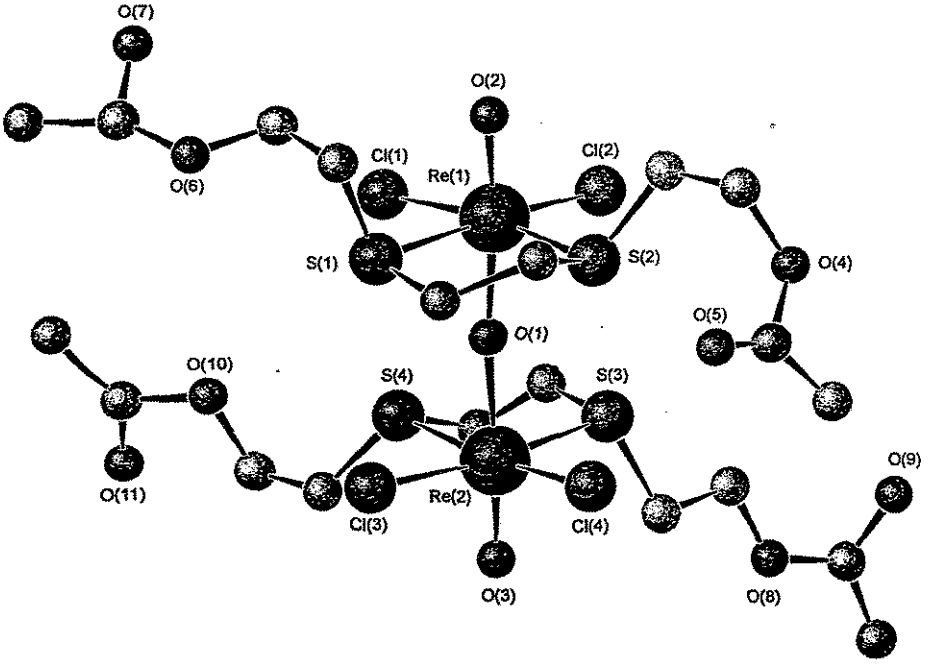

Fig. 3: CELLGRAF [8] drawing of
μ-oxo-bis[(1.8-diacetoxy-3,6-dithiaoctane)dichlorooxorhenium(V)] **(2)**

As illustrated in Fig. 3 the rhenium atoms are centred in an octahedron with the equatorial plane formed by an S_2Cl_2 donor set.

The molecule adopts a staggered conformation in which the ReS_2Cl_2 planes are mutually rotated by approximately 170 ° about the O=Re-O-Re=O axis.

Table 2: Selected bond distances (Å) and angles (deg) of μ-oxo-bis[(1.8-diacetoxy-3,6-dithiaoctane)dichlorooxorhenium(V)] **(2)**

Re(1)-Cl(1)	2.504(9)	Re(2)-Cl(3)	2.47(1)
Re(1)-Cl(2)	2.350(8)	Re(2-Cl(4)	2.36(1)
Re(1)-S(1)	2.51(1)	Re(2)-S(3)	2.40(1)
Re(1)-S(2)	2.351(9)	Re(2)-S(4)	2.46(1)
Re(1)-O(1)	1.88(2)	Re(2)-O(1)	1.97(2)
Re(1)-O(2)	1.72(2)	Re(2)-O(3)	1.67(2)
Cl(1)-Re(1)-Cl(2)	88.8(3)	Cl(3)-Re(2)-Cl(4)	89.6(3)
Cl(1)-Re(1)-S(1)	90.3(3)	Cl(3)-Re(2)-S(3)	172.3(3)
Cl(1)-Re(1)-S(2)	172.3(3)	Cl(3)-Re(2)-S(4)	89.9(4)
Cl(1)-Re(1)-O(1)	90.9(6)	Cl(3)-Re(2)-O(1)	89.5(6)
Cl(1)-Re(1)-O(2)	95.9(7)	Cl(3)-Re(2)-O(3)	96.7(8)
Cl(2)-Re(1)-S(1)	175.9(3)	Cl(4)-Re(2)-S(3)	93.7(4)
Cl(2)-Re(1)-S(2)	94.3(3)	Cl(4)-Re(2)-S(4)	172.3(3)
Cl(2)-Re(1)-O(1)	95.4(7)	Cl(4)-Re(2)-O(1)	92.6(6)
Cl(2)-Re(1)-O(2)	98.2(8)	Cl(4)-Re(2)-O(3)	99.4(8)
S(1)-Re(1)-S(2)	86.1(3)	S(3)-Re(2)-S(4)	86.0(4)
S(1)-Re(1)-O(1)	80.6(7)	S(3)-Re(2)-O(1)	83.3(6)
S(1)-Re(1)-O(2)	85.9(8)	S(3)-Re(2)-O(3)	89.7(8)
S(2)-Re(1)-O(1)	81.6(9)	S(4)-Re(2)-O(1)	79.7(6)
S(2)-Re(1)-O(2)	90.7(7)	S(4)-Re(2)-O(3)	88.2(8)
O(1)-Re(1)-O(2)	165.(1)	O(1)-Re(2)-O(3)	166.(1)

References

[1] Pietzsch, H.-J. et al., Annual report 1993, p. 82, Institute of Bioinorganic and Radiopharmaceutical Chemistry, FZR-32

[2] Pietzsch, H.J. et al., Polyhedron **12** (1993) 187

[3] Tisato, F. et al., Inorg. Chim. Acta **164** (1989) 127
[4] Tisato, F. et al., J. Chem. Soc. Dalton Trans. (1991) 1301
[5] Pietzsch, H.-J. et al., Polyhedron, in press
[6] Lock, C. et al., Can. J. Chem. **56** (1978) 179
[7] Pearson, C. et al., Acta Crystallogr. Sect.C **50** (1994) 42
[8] Reck, G. et al., CELLGRAF- a programme for representation of organic and inorganic crystal structures, Analytical Centre, Berlin (1989/1991)

2. UNUSUAL FORMATION OF A MONOCARBONYL RHENIUM(III) COMPLEX. MOLECULAR STRUCTURE OF [Re{N($CH_2CH_2S)_3$}(CO)]

M. Glaser, H. Spies, F. E. Hahn[1], T. Lügger[1], K. Klostermann[2]
[1]Institut für Anorganische und Analytische Chemie, Freie Universität Berlin
[2]Institut für Analytische Chemie, TU Dresden

Introduction

Up to now only a few technetium complexes containing a tripodal ligand with sulphur donors have been described [1-3] and characterized by X-ray analysis [4,5]. Recently we reported synthesis and structural characterization of some trigonal bipyramidal technetium and rhenium complexes obtained using tris(2-mercaptoethyl)amine [6]. In the context of our efforts to use the terminal ester group in [Re($NCH_2CH_2S)_3$($CNCH_2CO_2R$)] (R = Me, Et) for binding the rhenium chelate to biomolecules we found that mild alkaline hydrolysis leads to the formation of the carboxylic acid [Re($NCH_2CH_2S)_3$($CNCH_2CO_2H$)] **2** but treatment with acidic solution results in the unexpected carbonyl complex [Re($NCH_2CH_2S)_3$(CO)] **3**. We describe here the synthesis and characterization of both compounds.

Experimental

Preparations:

[Re(NS_3)(CNR)] **1**: The required isocyanide complexes **1a-e** were prepared according to procedures described earlier [6,7].

[Re(NS$_3$)(CNCH$_2$CO$_2$H)] **2**: The ester complex **1a** (50 mg, 101 μmol) was dissolved in THF (5 cm^3) and a solution of LiOH x H_2O (7 mg, 167 μmol in 0.5 cm^3 water) was added. After stirring for 1 h at room temperature the THF was evaporated by a nitrogen stream. The remaining aqueous phase diluted with water (1 cm^3) was suspended with cation-exchange resin (10 cm^3, DOWEX 50 WX8, 100 - 200 μm). After 2 h the acid complex **2** was extracted with MeCN (4 x 2 cm^3). Removal of the solvent and recrystallization (MeCN/H_2O = 10/1) produced olive green needles.

Yield: 27.4 mg, (58 %), m.p. 197 - 205 °C (decomp.)

Elemental analysis: (Found C, 23.33; H, 3.38; N, 5.96; S, 20.18, $C_9H_{15}N_2S_3O_2Re$ requires C, 23.22; H, 3.25; N, 6.02; S, 20.66 %)

IR absorptions: ν_{max}/cm^{-1} 1924vs (CN), 1720 (CO) (KBr)

UV/VIS absorptions: λ_{max}/nm (MeCN) (ε/dm^3 mol^{-1} cm^{-1}) 438 (11000), 313 (5000), 354 (1000) and 438 (1400)

NMR data: δ_H (90 MHz; solvent $CDCl_3$; standard $SiMe_4$) 11.81 (1H, br m, CO_2H), 5.37 (2H, s, CH_2NC) and 2.88 (12H, m, 3 SCH_2CH_2).

[Re(NS$_3$)(CO)] **3**: *(a):* To a solution of the complex **1a** (50 mg, 101 μmol) in CH_2Cl_2 (1 cm^3), toluene (10 cm^3) and concentrated hydrochloric acid (1 cm^3, 37 %) were added. The mixture was stirred and refluxed for 1 h under nitrogen. The organic layer was separated, washed with water (3 x 5 cm^3) and dried over Na_2SO_4 and the solvent evaporated in vacuo. Recrystallization of the residue from CH_2Cl_2/EtOH produces rhomboedric red-orange coloured crystals suitable for X-ray structural analysis.

Yield: 26.4 mg (64 %), m.p. 235 - 237 °C (decomp.)

Elemental analysis: (Found C, 20.56; H, 2.70; N, 3.24; S, 24.31; $C_7H_{12}NS_3ORe$ requires C, 20.59; H, 2.94; N, 3.43; S, 23.54 %)

FAB-MS: M^+ 409.

IR absorptions: ν_{max}/cm^{-1} (KBr) 1876 (CO)

UV/VIS absorptions: λ_{max}/nm (CH_2Cl_2) 257 (ε/dm^3 mol^{-1} cm^{-1}) 498 (22900), 321 (1500), 367 (1100), 398 (1300) and 498 (200)

NMR data: δ_H(90 MHz; solvent $CDCl_3$; standard $SiMe_4$) 3.22 (m, SCH_2CH_2).

(b): To a solution of the complex **1b** (10 mg, 19 μmol) in CH_2Cl_2 (1 cm^3), toluene (5 cm^3) and concentrated hydrochloric acid (1 cm^3, 37 %) were added. The reaction

continued as described in *(a)* and the isolation of the complex 3 was carried out in the same manner as above (4.6 mg, 60 %). The identity with the former product was confirmed by its R_f (TLC), m.p. and IR spectrum.

Reaction of 2c-e with hydrochloric acid: Under reaction conditions used for the preparation of 3 described above after 3 hours of refluxing the carbonyl complex was formed only in small traces according to TLC (acetone/$CHCl_3$ = 1/6, R_f = 0.4) and the starting complexes were unchanged.

Results and discussion

Preparation of the isocyanide complexes: Trigonal bipyramidal rhenium(III) complexes $[Re(NS_3)(CNR)]$ 1 are prepared by substitution reaction using the corresponding phosphane complex $[Re(NS_3)PPhMe_2]$ [6,7].

Reactions of the co-ordinated isocyanides: The ester group in 1a is saponified under mild conditions. Treatment with LiOH in THF formes the lithium salt, which is converted to the acid complex 2 without isolation or purification by means of a cation-exchange resin. The olive green compound 2 shows a similar UV/VIS spectrum as the original ester compound, suggesting no significant modification in the coordination sphere.

Saponification carried out in the two-phase system toluene/concentrated hydrochloric acid under a nitrogen atmosphere takes a different course. After refluxing under nitrogen for 1 hour the water phase turns an orange colour during bleaching of the organic phase. On continuation of the reaction, an orange lipophilic compound is formed as indicated by the increasing colouring of the organic layer. Working up results in a crystalline complex which reveals a strong IR absorption at 1876 cm^{-1}, suggesting a coordinated carbonyl group. Both streams we applied are given in Scheme 1.

The composition and structure of complex 3 are confirmed by the FAB mass spectrum and X-ray structural analysis [see also Fig. 1]. Trigonal bipyramidal rhenium complexes owing to an analogous pattern of coordination but without chelating ligand are described [11,12].

The formation of 3 has also been observed with the oxo-free complexes 1b-e. While the N-2-ethyl-morpholinyl isocyanide complex 1b delivers 3 in significant yields, this

reaction also takes place with the oxo-free *t*-butyl, phenyl or cyclohexyl isocyanide derivatives 1c-e but in less amounts.

Scheme 1: Formation of the acid complex 2 and the carbonyl complex 3 starting from {Re[N($CH_2CH_2S)_3$]CNR} 1

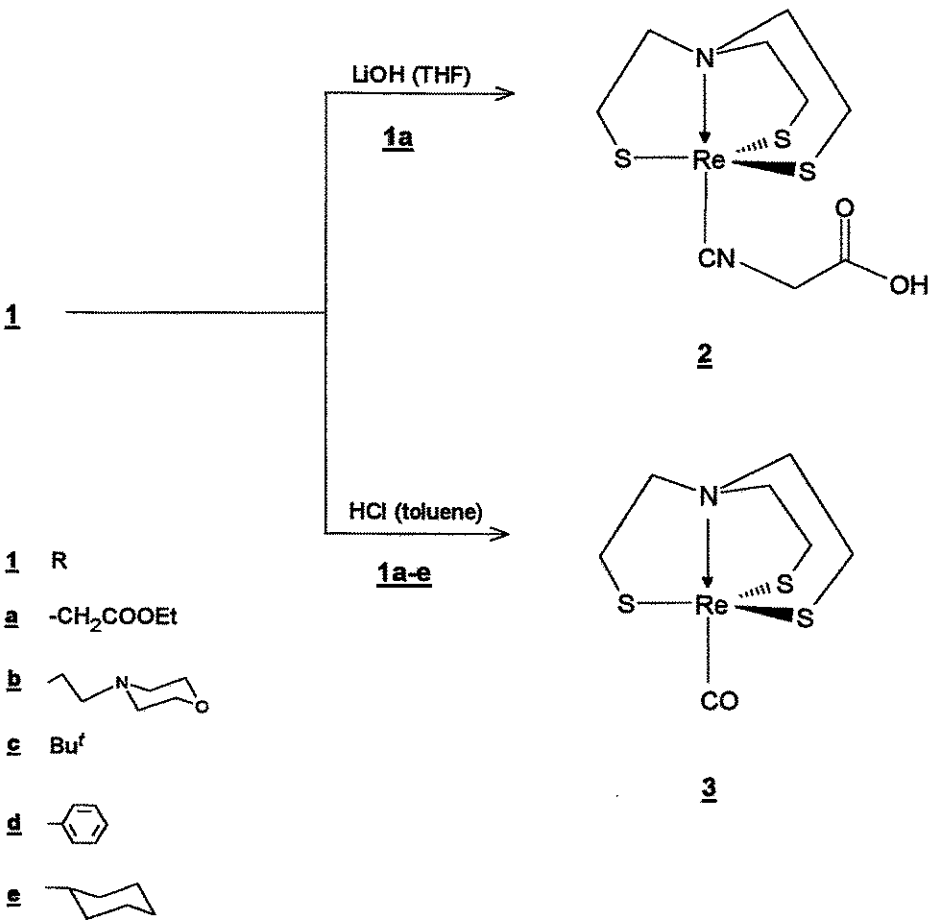

It is difficult to reconcile these results with a mechanism which involves rearrangement at the ester carbonyl group. A possible explanation is a reaction sequence including hydrolysis of the isocyanide group.

Protonation of isocyanide nitrogen (a) leads to the orange coloured species which is observed in the water phase. This phenomenon also corroborates a general change at the rhenium chromophore. The isocyanide carbon atom is attacked by a water molecule (b) leading to a dipolar tautomeric structure and subsequent elimination of the amine produces 3 (c). Comparable pathways shown for a technetium complex [8]

and a platinum co-ordinated isocyanide [9] both leading to carbonyl complexes encourage us to propose a possible explanation of formation (Scheme 2).

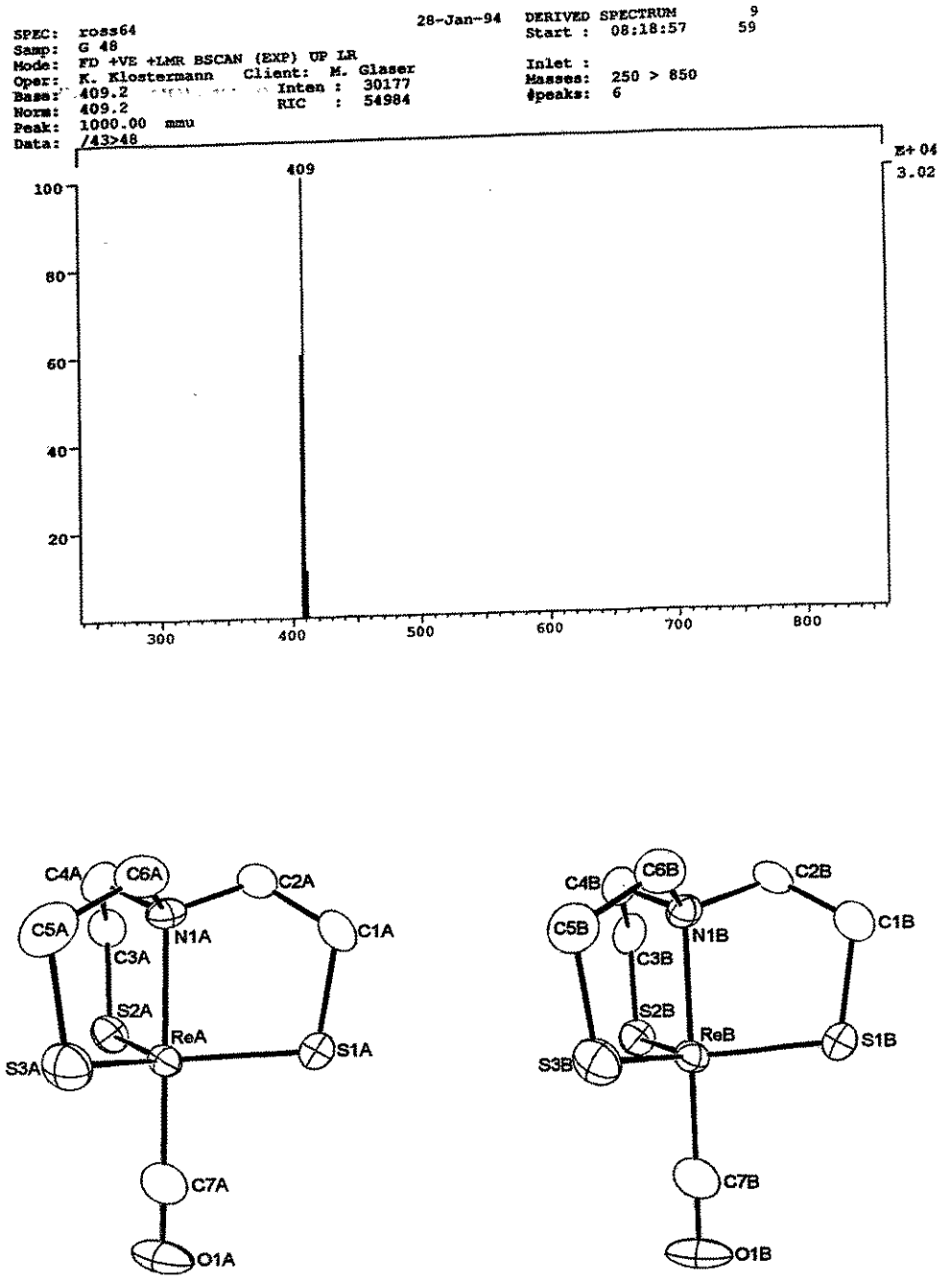

Fig. 1: FAB mass spectrum and ORTEP-drawing of 3

We suppose that low yields of product 3 from 1c-e may be due both to steric constraints at the isocyanides and to the lack of a heteroatom, which causes an inductive electron-withdrawing effect. The intactness of the tripodal chelate unit [Re(NS$_3$)] under applied conditions can be considered evidence of the high stability of this coordination type.

Scheme 2: Proposed mechanism for the formation of the carbonyl complex [Re(NS$_3$)(CO)] 3.

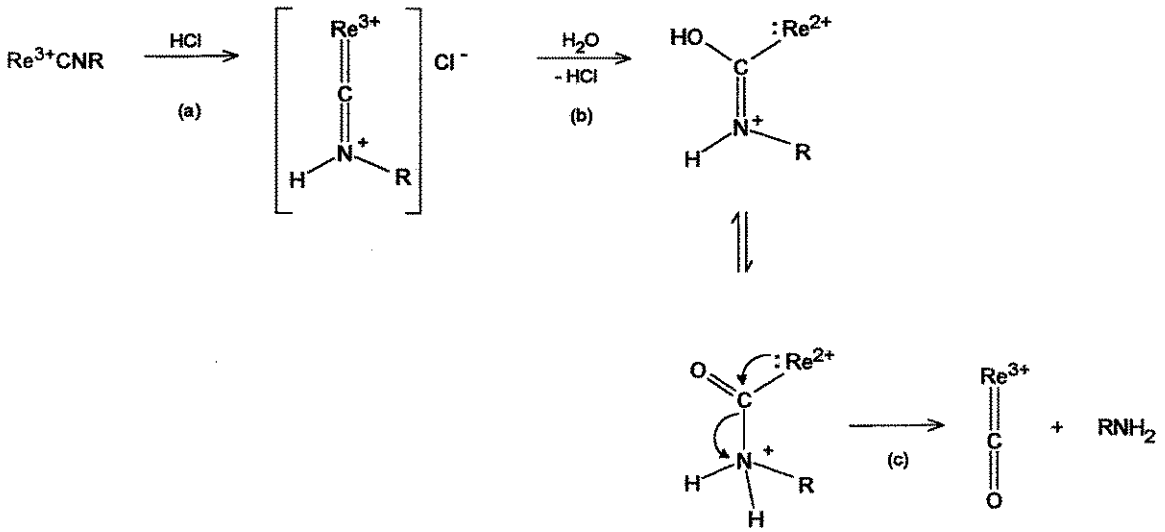

References

[1] Mastrostamatis, S., et al., J. Med. Chem. **37** (1994) 3212

[2] DE 4128183 C1

[3] Nicholson, T. et al., Inorg. Chim. Acta **218** (1994) 97

[4] deVries, N. et al., Inorg. Chem. **30** (1991) 2662

[5] deVries, N. et al., Inorg. Chim. Acta **165** (1989) 9

[6] Spies, H. et al., Angew. Chem. **106** (1994) 1416

[7] Spies, H., unpublished work

[8] Baldas, J. et al., J. Chem. Soc., Dalton Trans. (1982) 651

[9] Crociani, B. et al., Eur. J. Nucl. Med. **7** (1982) 187

[10] Blower, P. J. et al., J. Chem. Soc., Dalton Trans. (1985) 2305

[11] Bandoli, G. et al., J. Chem. Soc., Dalton Trans. (1978) 373

[12] Fletcher, S. R. et al., J. Chem. Soc., Dalton Trans. (1974) 486

3. A NEW OXO RHENIUM COMPLEX WITH BIS(2-THIOLATOETHYL)AMINE AND BENZENETHIOLATE

M. Glaser, H. Spies, F. E. Hahn,[1] T. Lügger,[1] K. Klostermann,[2] D. Scheller [2]
[1]Institut für Anorganische und Analytische Chemie, Freie Universität Berlin
[2]Institut für Analytische Chemie, TU Dresden

Introduction

Our earlier work on complex formation of rhenium with the tripodal chelating sulphur ligand tris(2-mercaptoethyl)amine "$N(SH)_3$" reveals the occurrence of five-coordinated Re(III) complexes. Until now, only a few papers dealing with TcO [1-4] or ReO complexes [5] with such a type of ligand are known. Other representatives of oxo-complexes containing a tripodal ligand are known with hydrotris-pyrazolylborate derivatives [6-13] or the remarkable "Kläui-ligand" [14,15].
Surprisingly, we were able to isolate an oxo-rhenium(V) complex in which the metal is coordinated by the tridentate ligand $HSCH_2CH_2NHCH_2CH_2SH$ and benzenethiol.

Experimental

Preparation of {[bis(2-thiolatoethyl)amine][benzenethiolato]}oxorhenium(V) **2**:
A stirred solution of 70 mg (69 μmol) $[BzNEt_3][ReO(SPh)_4]$ [16] and 29 μl (206 μmol) $N(SH)_3$ in 5 ml acetonitrile is refluxed under nitrogen for 3.5 hours. After removal of the solvent using a vacuum evaporator the crude product is dissolved in $CHCl_3$ and put on a silica gel column (Merck Kieselgel 60, 40 - 61 μm, column 15 x 250 mm). Some coloured by-products and the released benzenethiol are eluated with pure $CHCl_3$ followed by a mixture of $CHCl_3$/acetone = 12:1 to obtain 23.8 mg of an olive green compound. Further purification is carried out by semipreparative HPLC (RP 18, linear gradient from 0 - 100 % of eluent acetonitrile/water = 70/30 about 15 min). Recrystallization by covering up a concentrated solution in CH_2Cl_2 with a layer of cyclohexane at room temperature proved to be an alternative possibility for last purification. Crystals obtained here are used for X-ray analysis.
TLC: ($CHCl_3$/acetone = 6:1) R_f = 0.23
Yield: 5.4 mg (18 %); green microcrystals; m. p. 230 - 235 °C (decomp.)

Elemental analysis: (Found C, 27.01; H, 3.11; N, 3.31; S, 21.44; $C_{10}H_{14}NS_3ORe$ requires C, 26.89; H, 3.16; N, 3.14; S, 21.54 %)

FAB-MS: M^+: 446

IR absorptions: ν_{max}/cm^{-1} (KBr) 3128 (NH), 932 (ReO)

UV/VIS absorptions: λ_{max}/nm (CH_2Cl_2) 235.4 (9600), 258.5 sh (7200), 288.0 sh (4900), 368.6 (3800), 393.9 (3700), 583 (140)

^1H NMR data: δ_H(90 MHz; solvent $CDCl_3$; standard $SiMe_4$) 3.09 - 3.38 (8H, m, SCH_2CH_2N), 7.34 (5H, m, CH-Ar), 9.21 (1H, m, NH)

Results and discussion

A FAB experiment and the X-ray structural analysis (see Fig. 1) provided evidences for the formation of 2 instead of 3.

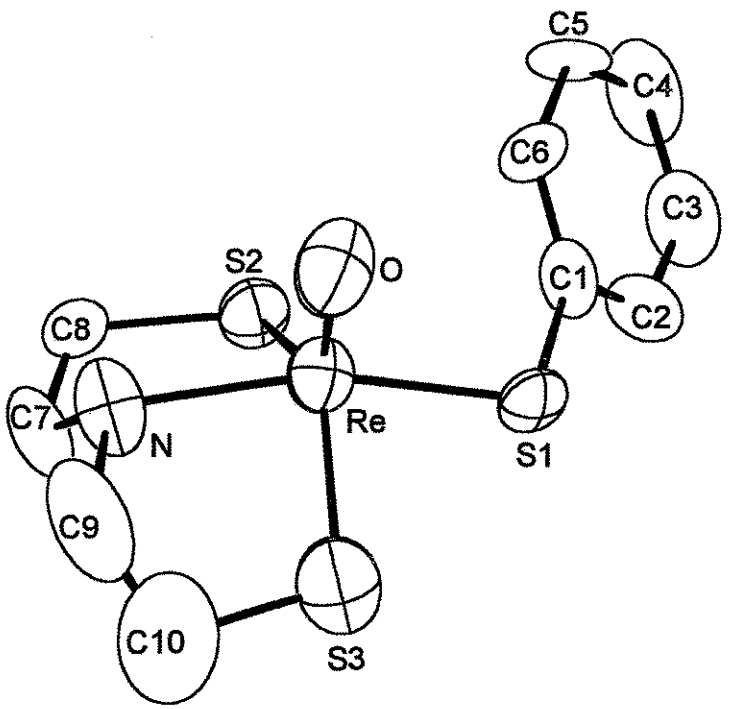

Fig. 1: ORTEP drawing of 2. Selected bond distances (Å) are: Re-S1: 2.304(5), Re-S2: 2.263(6), Re-S3: 2.266(8), Re-O: 1.668(14) and Re-N: 2.166(14).

The existence of a proton bonded to the nitrogen atom of the amine is unambiguously found in the IR and NMR spectra. Thus we synthesized a new representative

of the rare rhenium oxo-complexes containing the "NS_2" podant. This unexpected result may be interpreted in a different manner. First, structural analysis of the trigonal bipyramidal arrangement of a rhenium(V) oxo core has not been described hitherto. So it seems that the system obviously prefers a square-pyramidal coordination. This fact may explain the cleavage of the N-C bond during the reaction. This assumption was supported by a similar CN-cleavage of tertiary amines at a Lewis acid-like transition metal centre [17]. It is more likely, however, that the ligand certified as being $N(SH)_3$ may contain considerable amount of $HN(SH)_2$, from which **2** is formed in a typical "[3+1] reaction" [18]. This is evidenced by the fact that a GC-MS scrutiny of the ligand showed a peak due to an impurity of bis(2-mercaptoethyl)amine of 11 %.

We therefore have to elaborate a procedure for preparing **2** starting from a corresponding pure tris- or bisthiol.

Scheme 1: Formation of $[ReO(NS_2)SPh]$

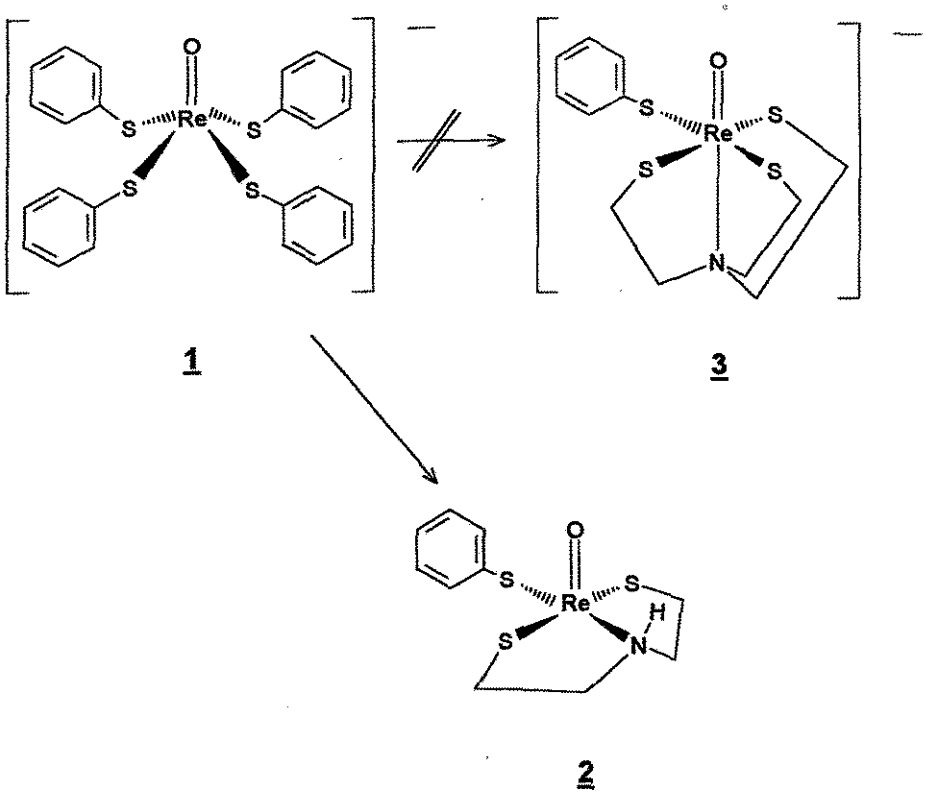

1 **3** **2**

References

[1] Mastrostamatis, S. et al., J. Labelled Compd. Radiopharm. **32** (1993) 1

[2] Schwochau, et al., DE 4128183 C1 (Cl. C07323/25) (1993)

[3] Stepniak-Biniakiewicz, D. et al., J. Med. Chem. **35** (1992) 274

[4] Mastrostamatis, S. G. et al., J. Med. Chem. **37** (1994) 3212

[5] Papadopulus, M. et al. J. Nucl. Med. Biol. **38** (1994) 421

[6] Tisato, F. et al., Inorg. Chem. **32** (1993) 2041

[7] Abrams, M. et al., Inorg. Chim. Acta **82** (1984) 125

[8] Coe, B. J., Polyhedron **11** (1992) 1085

[9] Joachim, J. E. et al., Z. Naturforsch. **48** (1993) 227

[10] Thomas, R. W. et al., Inorg. Chem. **19** (1980) 2840

[11] Thomas, R. W. et al., J. Am. Chem. Soc. **101** (1979) 4581

[12] Thomas, J. A. et al., Inorg. Chim. Acta **190** (1991) 231

[13] Degnan, I. A. et al., Chem. Ber. **123** (1990) 1347

[14] Thomas, J. A. et al., Inorg. Chem. **31** (1992) 1976

[15] Dyckhoff, B. et al., Z. Anorg. Allg. Chem. **614** (1992) 131

[16] McDonell, A. C. et al., Austr. J. Chem. **36** (1983) 253

[17] Murahashi, S. I. et al., J. Chem. Soc., Chem. Commun. (1979) 270

[18] Fietz, T. et al., Inorg. Chim. Acta, in press

4. PREPARATION OF ETHYL-12-ISOCYANLAURATE AND ITS COMPLEXATION WITH RHENIUM

M. Glaser, H. Spies, D. Scheller[1], B. Johannsen
[1]TU Dresden, Institut für Analytische Chemie

Introduction

All attempts to substitute ^{11}C or ^{123}I labelled fatty acids, [1, 2] for myocardium imaging by technetium complexes have failed so far [3]. Having at hand a new chelate group, in which the metal is more strongly shielded than in the polar square-pyramidal oxo complexes [4] we intended to evaluate its suitability as fatty acid tracers. Therefore we prepared a new ω-isocyanide substituted laurinic acid ester for coupling to a lipophilic $Re(NS_3)$ [$N(SH)_3$.= tris(2-mercaptoethyl)amine] moiety. Preparation of the complex {$Re(NS_3)[CN(CH_2)_{11}$ COOH]} **6** is described.

Experimental

12-aminolaurinic acid **1**: It was supplied by Merck.

Preparation of ethyl-12-aminolaurate **2**: A stirred suspension of 10 g (46.4 mmol) 12-aminolaurinic acid in 100 ml ethanol is passed by dry HCl for 30 minutes. After completion of the dissolution the mixture is refluxed for 5 to 6 hours. After removing the solvent and addition of 100 ml of a saturated potassium carbonate solution the product is carefully heated to drive out the carbon dioxide. The crude product is percolated and dried on a tile.

Yield: 6 g (53 %), m. p. 63 - 70 °C,

Elemental analysis: (Found C, 65.32; H, 12.54; N, 5.21 ; $C_{14}H_{29}NO_2 \times C_2H_5OH$ requires C, 66.39; H, 12.19; N, 4.84 %)

IR absorptions: ν_{max} /cm^{-1} (Kbr) 3400 - 3300 (NH_2) and 1725 (CO)

Preparation of ethyl-12-formyllaurate **3**: 567 mg (2.33 mmol) of **2** dissolved in 10 ml ethylformiate are refluxed for 8 hours. After vacuum evaporation of the solvent the product is purified using column chromatography (column 15 x 250 mm, Merck Kieselgel 60, 0.04 - 0.63 mm, $CHCl_3$/acetone = 6:1). The R_f value 0.43 of the thin layer

chromatogram (Kavalier Silufol, $CHCl_3$/acetone = 6:1) corresponds with to that obtained by the method according to [5].

Yield: 254 g (40 %), m. p. 45 - 46 °C

Elemental analysis: (Found C, 66.77; H, 11.65; N, 5.16, $C_{15}H_{25}NO_3$ requires C, 66.38; H, 10.77; N, 5.16 %)

IR absorptions: ν_{max} /cm^{-1} (Kbr) 3300 (NH), 1725 (CO) and 1630 (NH)

Preparation of ethyl-12-isocyanolaurate **4**: To a stirred and cooled solution (0 °C) of 4.4 g (0.0162 mol) **3** and 4 g (0.0402 mol) diisopropylamine in 20 ml $MeCl_2$ 2.5 g (0.0162 mol) $POCl_3$ diluted in 5 ml $MeCl_2$ are added. After stirring at 0 °C for 1 h the mixture is treated with a solution of 4 g Na_2CO_3 (dehydrated) in 16 ml H_2O for 45 min at a maximum temperature of 20 °C. After addition of 50 ml of a saturated sodium chloride solution the organic phase is extracted with $MeCl_2$ (3 x 20 ml) and dried over Na_2SO_4. The solvent is evaporated and the residue purified by column chromatography [column 15 x 250 mm, Merck Kieselgel 60, 0.04 - 0.063 mm, $CHCl_3$/acetone = 12:1 (TLC: R_f = 0.72, Kavalier Silufol, $CHCl_3$/acetone = 6:1).

Yield: 1.4 g (34 %), brown oil, softening point ~ 10 - 20 °C

IR absorptions: ν_{max} /cm^{-1} 2150 (CN) and 1730 (CO)

Preparation of [Re(NS_3)($CN(CH_2)_{11}CO_2Et$)] **5**: To a stirred solution of 50 mg (96.4 µ mol) tris(2-thiolatoethyl)amine-dimethylphenyl-phosphane rhenium(III) in 5 ml $MeCl_2$ 43 µl (173.4 µmol) of **4** in 5 ml $MeCl_2$ are added. The new complex appears in TLC (Kavalier Silufol, toluene) at R_f = 0.07 as opposed to R_f = 0.19 of the starting phosphane complex After stirring for 90 min at room temperature and removing the solvent by a nitrogen stream the product is purified using column chromatography (column 15 x 250 mm, Merck Kieselgel 60, 0.04 - 0.063 mm, $CHCl_3$/acetone = 12:1).

Yield: 40 mg (65 %), green powder, m.p. 108-111 °C

Elemental analysis: (Found C, 40.21; H, 5.93; N, 4.26; S, 14.74. $C_{21}H_{33}N_2S_3O_2Re$ requires C, 40.17; H, 5.30; N, 4.46; S, 15.32 %)

IR absorptions: ν_{max}/cm^{-1} (KBr) 2040 (NC), 1730 (CO)

UV/VIS absorptions: λ_{max}/nm ($MeCl_2$) 248.3 (26900), 278.5 sh (6300), 310.3 (11700), 350.9 (1500), 452.8 (1700) and 595.5 (300)

NMR data: δH (90 MHz; solvent $CDCl_3$; standard $SiMe_4$) 4.76 (2H, q, $CNCH_2$),

4.11 (2H, q, OCH_2CH_3), 2.96 (12H, m, 3 SCH_2CH_2),
2.27 [2H, t, $CH_2C(O)O$], 1.27 [21H, $(CH_2)_9$ + OCH_2CH_3]

Preparation of [Re(NS$_3$)(CN(CH$_2$)$_{11}$CO$_2$H)] **6**: The saponification of **5** is carried out according to the procedure described in our preceding article (this report p....).

TLC (*Silufol Kavalier, $CHCl_3$/acetone* = 12:1) R_f = 0.46.

Yield: 20.3 mg (54 %), green powder, m.p. 100 - 104 °C,

Elemental analysis: (Found C, 38.08; H, 5.46; N, 4.72; S, 15.86, $C_{19}H_{29}N_2S_3O_2Re$
requires C, 38.05; H, 4.87; N, 4.67; S, 16.03 %

IR absorptions: ν_{max}/cm^{-1} (KBr) 2000 br (NC), 1700 d (CO)

UV/VIS absorptions: λ_{max}/nm ($MeCl_2$) 310 (3.91), 348.4 (2.96), 452.2 (3.06),
594 (1.7)

NMR data: δ_H (90 MHz; solvent $CDCl_3$; standard $SiMe_4$) 4.77 (2H, t, $CNCH_2$),
2.97 (12H, m, 3 SCH_2CH_2), 2.34 [2H, t, $CH_2C(O)O$],
1.62, 1.28 [18H, $(CH_2)_9$].

Results and discussion

Fig. 1 illustrates the synthesis of compound **6** which starts from 12-aminolaurinic acid **1** including the dehydration of formamide **3** by affecting $POCl_3$ according to UGI [6] (best-proved way of mild preparation of isocyanides), coupling of **4** to rhenium via the phosphane complex [Re(PPhMe_2)(NS_3)] prepared according [4] and saponification of the terminal ester group using lithium hydroxide in tetrahydrofuran/water

Fig. 2 gives a comparison of an iodine fatty acid [2] and the rhenium complex **6**. The latter formally substitutes the aromatic moiety in iodophenyl fatty acids by the Re(NS_3) unit.

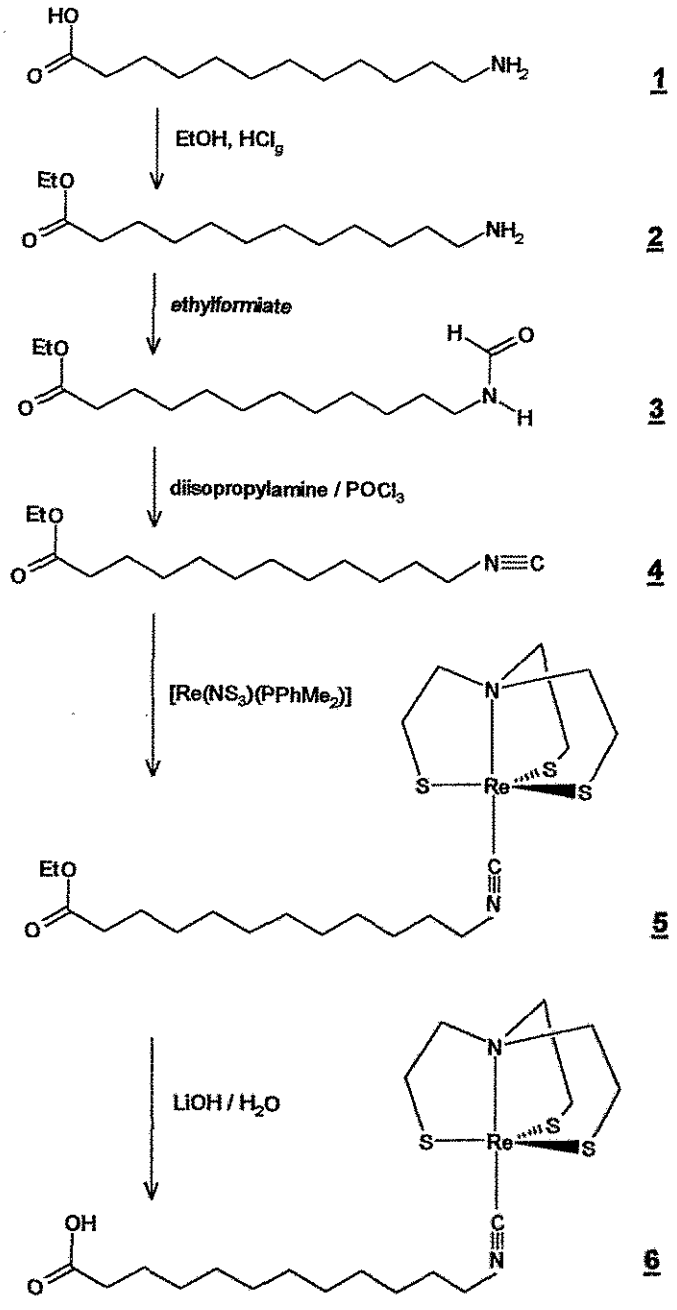

Fig. 1: Preparation of $[Re(NS_3)(CN(CH_2)_{11}CO_2H)]$ 6.

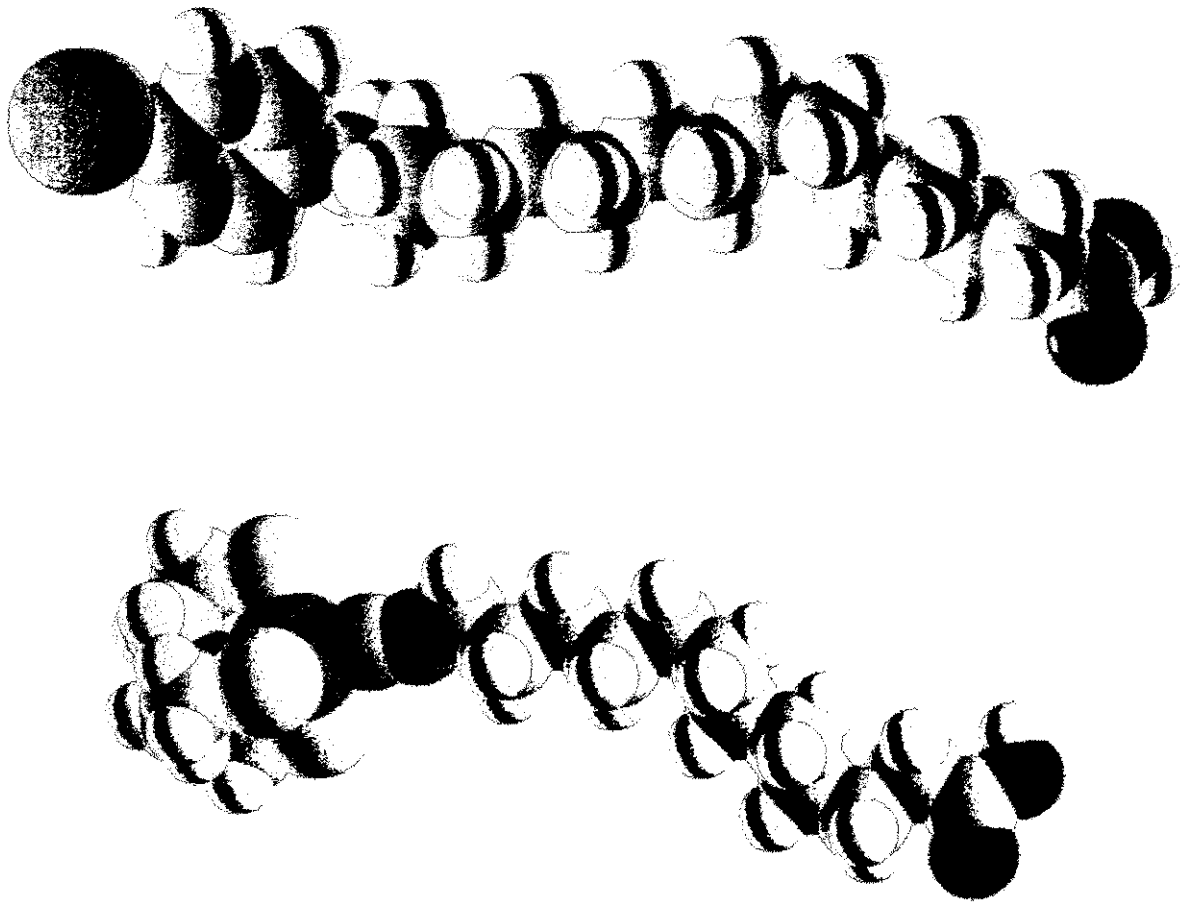

Fig. 2: 15-(4'-[^{123}I]iodophenyl)pentadecanoic acid ([^{123}I]IPPA) versus {$Re(NS_3)[CN(CH_2)_{11}$ COOH]} **6** as space filling models

Experiments were carried out with respect to a radiopharmaceutical preparation of compound **6**. First, phosphane/isocyanide exchange of **5** can be completed in 10^{-4} molar solutions within 5 minutes. Further it is desirable to avoid the preparation of phosphane-substituted precursors and to start from perrhenate directly. Preliminarily, we found that it is possible to reduce ammonium perrhenate in a one-pot-synthesis by a mixture of "$N(SH)_3$", *t*-butyl isocyanide and an excess $NaBH_4$ to give the known compound [$Re(NS_3)$(*t*-butyl isocyanide)].

References

[1] Stöcklin, G. et al., Computed Emission Tomography
(Eds. Ell, P. J.et al., Oxford Univ. Press, Toronto, 1982) p. 299

[2] Eisenhut, M. et al., Nucl. Med. Biol. **20** (1993) 747

[3] Jones, G. S. et al., Nucl. Med. Biol. **21** (1994) 117

[4] Spies, H. et al., Angew. Chem. **106** (1994) 1416

[5] Huffman, C. W., J. Org. Chem. **23** (1968) 727

[6] a) Obrecht, R. et al., Synthesis (1984) 400
b) Tietze, L. F., et al., Organische Synthesechemie,
(Georg Thieme Verlag Stuttgart, New York, 1981) p. 468

5. RHENIUM COMPLEXES WITH BIOLOGICALLY IMPORTANT LIGANDS 1. SYNTHESIS AND MOLECULAR STRUCTURE OF (3-THIAPENTANE-1.5-THIOLATO) (β-D-GLUCOSE-1-THIOLATO) OXORHENIUM(V)

Th. Fietz, H. Spies, P. Leibnitz[1], D. Scheller[2]
[1]Bundesanstalt für Materialforschung, Berlin
[2]TU Dresden, Institut füf Analytische Chemie

Introduction

In order to obtain access to novel technetium and rhenium complexes in radiotracer design, the principle of preparing mixed-ligand complexes in which small-sized chelate units are combined with biologically relevant substituents was applied to 1-thio-β-D-glucose. This paper reports the isolation of two oxorhenium(V) complexes [ReO(SXS)(tgl)] containing 1-thio-β-D-glucose (Htgl) as co-ligand and the molecular structure of [ReO(SSS)(tgl)]. These compounds are meant to illustrate the potential of the '3+1' mixed-ligand approach [1] to obtain small-sized rhenium chelates substituted by carbohydrate moieties.

Experimental

The precursors chloro(3-thiapentane-1.5-dithiolato)oxorhenium(V) 1 [2] and benzyltriethylammonium tetrachlorooxorhenate 4 [3] were synthesized following previously

described methods.

(3-Thiapentane-1.5-dithiolato)(β-D-glucose-1-thiolato) oxorhenium(V) 2:

110.1 mg (504 µmol) 1-thio-β-D-glucose sodium salt are added while stirring to a boiling solution of 170 mg (436 µmol) 1 in 8 ml acetonitrile. Precipitation of a light-brown material from the reaction mixture starts very soon; after 15 minutes reflux the reaction is completed. The solvent is removed *in vacuo* and the residue extracted with hot water, and filtered. The filtrate is allowed to evaporate slowly to give reddish-brown needles which are isolated from the mother liquor, washed with methanol and diethyl ether and dried. Yield: 81 mg (35 %). m.p. (H_2O): 218 - 223 °C (dec.)

Elemental analysis: (Found: C, 21.75, H, 3.50, S, 23.34, $C_{10}H_{19}O_6ReS_4$ requires C, 21.85, H, 3.48, S 23.33 %)

UV/VIS absorptions: λ_{max}/nm (H_2O): 220 (log ε / dm^3 mol^{-1} cm^{-1} = 4.05); 264 (3.90),; 362 (3.56); 504 (2.32).

IR absorptions: ν_{max}/cm^{-1} (KBr) 960s (Re=O).

[3-(Methyl)azapentane-1.5-dithiolato](β-D-glucose-1-thiolato)oxorhenium(V) 3:

129 mg (241 µmol) 4 were dissolved in 2 ml methanol. A mixture of 36.5 mg (241 µmol) 3-(methyl)azapentane-1.5-dithiol and 52.5 mg (241 µmol) 1-thio-β-D-glucose sodium salt in 2 ml chloroform was added at 0 °C while stirring. After one hour, 5 ml chloroform were added and the mixture refluxed for 10 min. Then precipitates were removed by filtration and the solution purified by preparative thin layer chromatography with methanol as the mobile phase. The green zone was removed from the plate, eluted with acetonitrile and the solution evaporated to dryness. The residue was extracted with a small amount of hot water, filtered and the filtrate slowly evaporated to give 13.4 mg (10 %) thin greyish-green plates. The product was washed with methanol and diethyl ether and dried. M.p. (H_2O): 178 - 183 °C (dec.)

UV/VIS absorptions: λ_{max}/nm (H_2O) 264 (log ε / dm^3 mol^{-1} cm^{-1} = 3.85); 366 (3.60), 580 (2.12).

IR absorption: ν_{max}/cm^{-1} (KBr) 948s (Re=O).

Compound 2 was obtained in a 22 % yield by the same reaction. In this case, the isolation was carried out by extracting with water as described for 3 but without chromatography.

Results and discussion

Two new neutral oxorhenium(V) complexes 2 and 3 were obtained by reactions of 1-thio-β-D-glucose sodium salt with appropriate rhenium precursors. 2 and 3 were characterized by UV/VIS, infrared and proton NMR spectroscopy. In addition complex 2 was characterized by X-ray structure analysis. The fourfold sulfur-coordinated 2 can be synthesized from both chloro(3-thia-pentane-1.5-dithiolato) oxorhenium(V) 1 and tetrachlorooxorhenate 4. When starting from 1, the yield is significantly lower than in similar syntheses with other thiols [2]. Since the (alkyl)nitrogen compound analogous to 1 could not yet be isolated, complex 3 is synthesized from 4 and a mixture of thioglucose and 3-(methyl)aza-pentane-1.5-dithiol in a one-pot reaction. This method (Scheme 2) usually gives lower yields when applied to X = S than the two-pot reaction *via* the isolation of 1 and subsequent replacement of the last chlorine ligand by the monothiolic coligand (Scheme 1).

Scheme 1: Synthesis of the thioglucose complex 2.

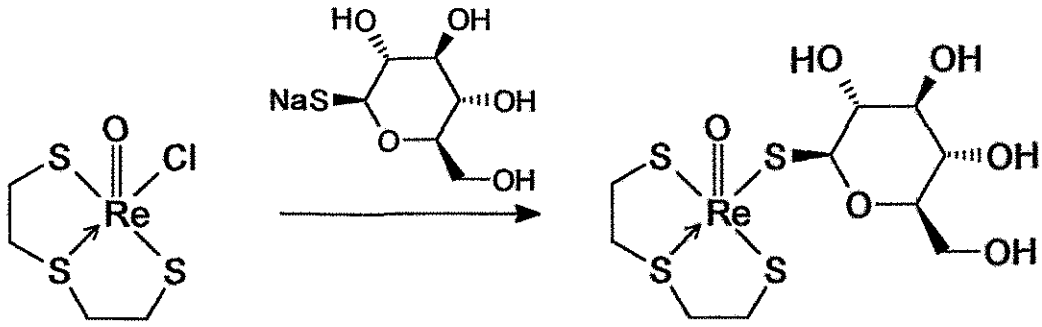

1 2

The 300 MHz proton NMR spectrum of 2 in DMSO-d_6 shows a pattern for the protons of the tridentate ligand (a) as observed before [2,3]. The exact values for these peaks are: 2.30, 3.04, 3.56 and 4.11 ppm (2 H each). The protons of the glucose fragment are depicted as follows: 5.52 ppm (1 H, s, H_e); 4.90, 5.03, 5.11 ppm (1 H each, H_b), 3.23 ppm (4 H, s, H_c), 4.30 (2 H, m, H_d) and 4.11ppm (1 H, H_f; together with 2 H of the tridentate ligand).

Scheme 2: One-pot synthesis of oxorhenium complexes 2 and 3.

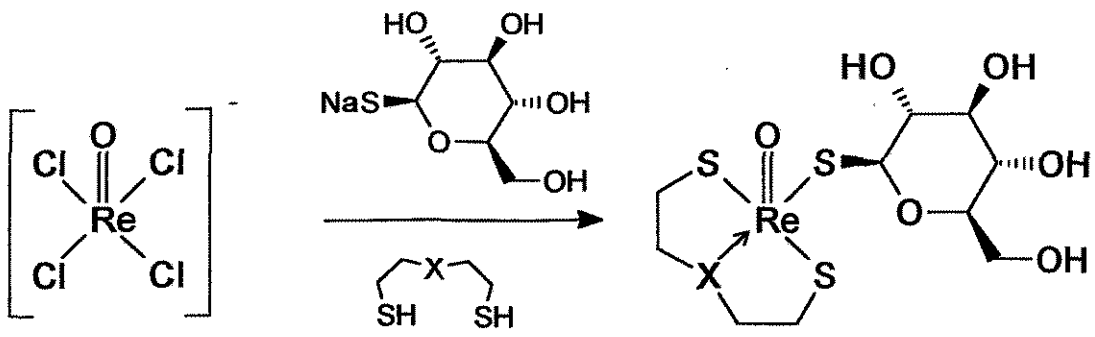

4

2 X = S

3 X = N(CH$_3$)

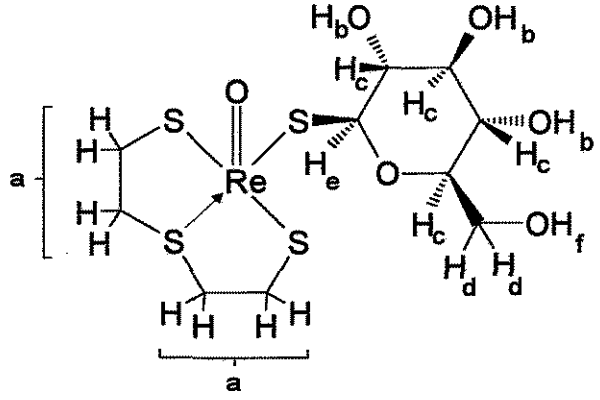

Fig 2: Assignment of the protons in the ^{1}H NMR spectrum

Molecular structure of complex 2

Crystals suitable for X-ray structure analysis were obtained by slow evaporation of an aqueous solution of 2. The compound forms bunches of small reddish-brown needles.

The structure analysis shows distorted square-pyramidal coordination of the sulphur atoms around the central atom which is situated above the basal plane. The shape of the coordination sphere is similar to that in 1 [2] and in (3-thiapentane-1.5-dithiolato)(ethanethiolato) oxorhenium(V) [4]. Furthermore, the crystal structure is characterized by both intensive intermolecular and intramolecular hydrogen bonds *via* the hydroxy groups.

Table 1: Selected bond angles [°] of **2** and their e.s.d.

Atom 1	Atom 2	Atom3	Angle	Atom 1	Atom 2	Atom3	Angle
S1	Re	S2	83.71(8)	S3	Re	O1	113.4(2)
S1	Re	S3	134.10(8)	S4	Re	O1	107.2(2)
S1	Re	S4	81.48(7)	Re	S1	C1	105.8(3)
S1	Re	O1	112.4(2)	Re	S2	C2	108.1(3)
S2	Re	S3	83.07(8)	Re	S2	C3	109.4(3)
S2	Re	S4	149.03(8)	C2	S2	C3	105.0(4)
S2	Re	O1	103.6(2)	Re	S3	C4	107.0(3)
S3	Re	S4	87.96(8)	Re	S4	C5	109.7(3)

Table 2: Selected bond lengths [Å] of **2** and their e.s.d.

Atom 1	Atom 2	Bond distance [Å]
Re	S1	2.309(2)
Re	S2	2.351(2)
Re	S3	2.298(2)
Re	S4	2.328(2)
Re	O1	1.682(6)
S1	C1	1.836(9)
S2	C2	1.812(8)
S2	C3	1.807(9)
S3	C4	1.83(1)
S4	C5	1.821(8)

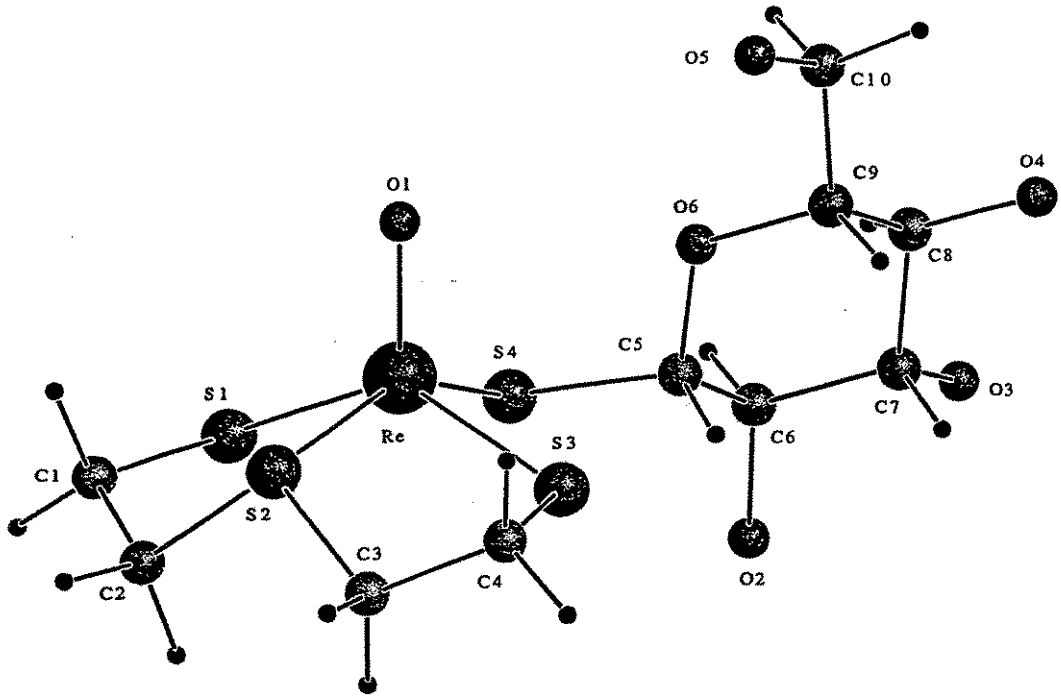

Fig.1: Molecular structure of complex 2

References

[1] Pietzsch, H.-J. et al., Inorg. Chim. Acta **165** (1989) 163

[2] Fietz, Th. et al., Inorg. Chim. Acta, in press

[3] Spies, H. et al., submitted for publication to J. Chem. Soc., Dalton Trans.

[4] Spies, H. et al., unpublished results

6. RHENIUM COMPLEXES WITH BIOLOGICAL IMPORTANT LIGANDS 2. A CHOLESTEROL MOIETY BONDED TO RHENIUM(V)

Th. Fietz, H. Spies

Introduction

Steroids and their metabolism play an essential role in the control of life processes. Therefore it is important to trace the behaviour of steroids and their derivatives *in vitro* and *in vivo*. Radioactive labelled steroids allow a wide range in tracing and modelling experiments as well as in radiodiagnostics and radiotherapy. A number of attempts have been made to label steroids or their derivatives with certain rhenium cores [1-3]. The principle of preparing mixed-ligand complexes in which small-sized chelate units are bound to biologically relevant substituents [4] is applied to thiocholesterol as a substituent. Complexes [ReO(SXS)(SR)] (RSH = cholest-5-ene-3β-thiol; HSXSH = tridentate dithiols HS–CH_2CH_2–X–CH_2CH_2–SH; X = S, O) have been prepared.

Experimental

Chloro(3-thiapentane-1.5-dithiolato)oxorhenium(V) 1 [5] *and benzyltriethylammonium tetrachlorooxorhenate* 4 [6] were prepared according to previously described methods.

(3-Thiapentane-1.5-dithiolato)(cholest-5-ene-thiol-3β-ato)oxorhenium(V) 3:

49 mg (125 µmol) 1 were dissolved in 5 ml boiling acetonitrile. 93.5 mg (232 µmol) cholest-5-ene-3β-thiol were added and the mixture refluxed. After 10 min, a light-brown precipitate was deposited. The whole mixture was evaporated to dryness, the residue dissolved in chloroform and the solution filtered. The product was purified by passing through a silica gel column (20 × 2 cm) with chloroform as eluent. Some ethanol was added to the brown eluate. The eluate was slowly evaporated to give 51.5 mg (54.5 %) brown needles.

Elemental analysis: (Found: C, 49.11; H, 6.85; S, 16.56, $C_{31}H_{53}OReS_4$ requires C, 49.24; H, 7.02; S, 16.96 %)

UV/VIS absorptions: λ_{max}/nm(CH_2Cl_2) 343 (log ε/dm^3 mol^{-1} cm^{-1} 3.42); 392 (3.51), 511 (2.23).

IR absorptions: ν_{max}/cm^{-1} (KBr) 956 s (Re=O), 2936 s (CH_2)

(3-Oxapentane-1.5-dithiolato)(cholest-5-ene-thiol-3β-ato)oxorhenium(V) 4 :

119.2 mg (222 µmol) benzytriethylammonium tetrachlorooxorhenate(V) were dissolved in 3 ml ethanol and cooled to 0 °C. A mixture of 30.7 mg (222 µmol) 3-oxapentane-1.5-dithiol and 89.6 mg (222 µmol) cholest-5-ene-3β-thiol in 2.5 ml chloroform was added while stirring. Cooling and stirring were continued for two hours. The mixture was evaporated to dryness, the residue dissolved in chloroform and the solution filtered. The filtrate was purified by passing through a silica gel column (20 × 2 cm) with chloroform as eluent. Some ethanol was added to the dark-red eluate. The eluate was slowly evaporated to give 70.8 mg (43.1 %) wine-red needles.

Elemental analysis: (Found: C, 50.41; H, 7.33; S, 12.99, $C_{31}H_{53}O_2ReS_3$ requires C, 50.30; H, 7.22; S, 12.99 %)

UV/VIS absorptions: λ_{max}/nm (CH_2Cl_2) 322 (log $\varepsilon/dm^3\ mol^{-1}\ cm^{-1}$ 3.60), 352 (3.65)

IR absorptions: ν_{max}/cm^{-1} (KBr) 968 s (Re=O), 2936 s (CH_2)

Complex 3 can be obtained by the latter method in a 16 % yield. The preferred product (60 % yield) in this reaction is 1.

Results and discussion

Reaction of cholest-5-ene-3β-thiol (Htchol) with both tetrachlorooxorhenate(V) 2 (Scheme 2) and chloro-(3-thiapentane-1.5-dithiolato)oxorhenium(V) 1 (Scheme 1) gave new neutral complexes containing a steroid moiety. The complexes are soluble in chloroform and dichloromethane but insoluble in acetonitrile, alcohols, diethylether and water.

Complex 3 can be obtained with both these methods. However, the yield of pure complex is rather low when starting from tetrachlorooxorhenate(V). This is due to the lower reactivity of the mercapto group in the steroid derivative compared to the reactivity of the thiol groups of the tridentate ligand. A common action of the three thiol groups involved on the Re – Cl bonds is therefore suppressed. That causes the formation of 1 in high yields, which does not react with the monothiol under these conditions. There is, however, a difference in the behaviour of the two tridentate ligands employed in the reaction: the oxygen derivative gave 4 in satisfactory yields.

Scheme 1: Preparation of complex 3.

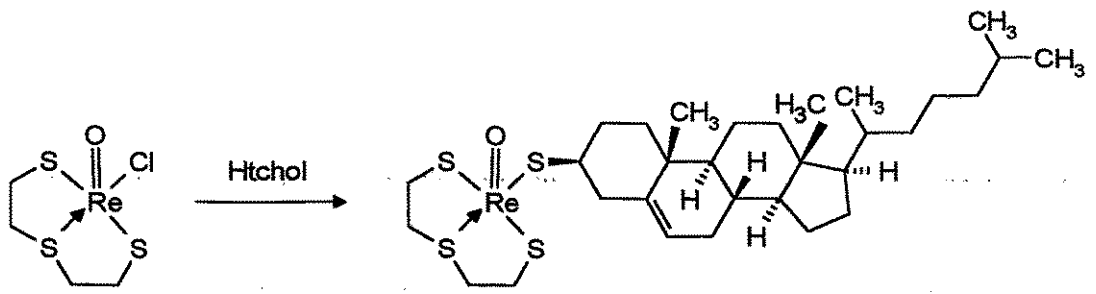

1 3

Scheme 2: Preparation of complex 4

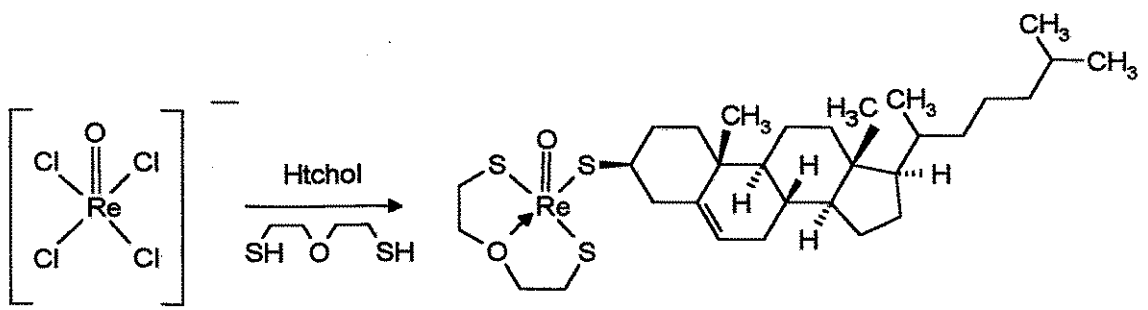

2 4

The preferred formation of 1 during the reaction shows that in this special case the "3+1" method [4] of forming fourfold sulphur coordinated oxorhenium complexes is inferior to the two-pot method [5]. This procedure –where the first step is the formation of 1 from 4 and 3-thiapentane-1.5-dithiol as described in [5]– makes it possible allows to convert even less reactive monodentate thiols into "3+1" complexes.

References

[1] DiZio, J. P. et al., J. Nucl. Med. **33** (1992) 558

[2] DiZio, J. P. et al., Bioconjugate Chem. **2** (1991) 353; CA 115:202038

[3] Top, S. et al., J. Chem. Soc, Chem. Comm. (1994) 453

[4] a) Pietzsch, H.-J. et al., Inorg. Chim. Acta **165** (1989) 163

b) Pietzsch, H.-J. et al., Appl. Radiat. Isot. **41** (1990) 185

[5] a) Fietz, Th. et al., Inorg. Chim. Acta, in press
b) Fietz, Th. et al., Annual Report 1993 p. 66, Institute of Bioinorganic and Radiopharmaceutical Chemistry, FZR-32
[6] Spies, H. et al., submitted for publication to J. C. S., Dalton Trans.

7. NEW MIXED-LIGAND OXORHENIUM(V) COMPLEXES WITH RHENIUM-SELENIUM BONDS. MOLECULAR STRUCTURE OF (3-OXAPENTANE-1,5-DITHIOLATO)(BENZENESELENOLATO)OXORHENIUM(V)

Th. Fietz; H.-J. Pietzsch, H. Spies, P. Leibnitz[1], D. Scheller[2]
[1]Bundesanstalt für Materialforschung, Berlin
[2]TU Dresden, Institut für Analytische Chemie

Introduction

Rhenium complexes with selenium-containing ligands have been scarcely reported [1-6]. According to the HSAB concept [7], S donors are more likely to be bonded to rhenium complex cores than, for example, oxygen atoms. Selenium as the successor of sulphur in the periodic table's 6th main group should do so even more. Despite the high acute toxicity of many selenium compounds and the high sensitivity of –SeH groups towards air and humidity, which prevent a wide application of selenium donor ligands for chemical as well as for pharmaceutical research purposes, we were interested in the basic coordination chemistry of selenium ligands.

Experimental

Benzyltriethylammonium tetrachlorooxorhenate(V) was synthesized according to [11]; *chloro(3-thiapentane-1.5-dithiolato)oxorhenium(V)* 1 was synthesized according to [9]. Crude *sodium benzylselenolate* was synthesized following the method given in [8] and used without previous acidification or isolation.

Benzeneselenol, C_6H_5-SeH, was synthesized from C_6H_5-Se-Se-C_6H_5 by boiling with ethanolic KOH [10]. The solvent was reduced to a small volume by rotary evaporation and deaerated water was added. The mixture was acidified with diluted sul-

phuric acid. The selenol was extracted into chloroform, dried and stored under dinitrogen.

Purification of the complexes: The reaction mixture was evaporated to dryness on a rotary evaporator. The residue was washed with methanol, dissolved in chloroform and filtered to remove some small grey waste (elemental selenium?). The product was purified by column chromatography (silica gel 60; 0.04···0.063 mm; Merck; eluent: chloroform). After addition of ethanol to the eluate, it was allowed to evaporate slowly to a small volume to give crystals. The product was washed with methanol and diethylether and dried.

(3-Thiapentane-1.5-dithiolato)(benzeneselenolato)oxorhenium(V) **2**:

117 mg (300 µmol) **1** were dissolved in 5 ml of boiling acetonitrile and an approximately fivefold excess of the crude benzeneselenol solution was added. The colour of the mixture turned from ink-blue to brown very soon. The mixture was refluxed for 15 minutes and processed as described above. Yield: 104.1 mg (68.6 %) of small brown needles.

UV/VIS absorptions: λ_{max}/nm (CH_3CN) 301 (log ε / $dm^3\ mol^{-1}\ cm^{-1}$ = 3.66); 417 (3.56).

IR absorption: ν/cm^{-1} (KBr) 968s (Re=O)

(3-Thiapentane-1.5-dithiolato)(benzylselenolato) oxorhenium(V) **3**:

87 mg (225 µmol) **1** were dissolved in 8 ml acetonitrile and an excess of crude sodium (phenyl)methaneselenolate solution was added. The mixture turned from blue to brown immediately and was stirred for 5 minutes. It was processed as described above. Yield: 41 mg (34.7 %) of dark brown needles.

UV/VIS absorptions: λ_{max}/nm (CH_3CN) 291 (log ε / $dm^3\ mol^{-1}\ cm^{-1}$ = 3.77), 338 (3.44); 417 (3.57)

IR absorption: ν/cm^{-1} (KBr) 960 (Re=O)

(3-Oxapentane-1.5-dithiolato)(benzeneselenolato) oxorhenium(V) **4** was synthesized by adding a mixture of 38.9 mg (314 µmol) bis(mercaptoethyl)ether and an excess of the selenophenol solution to a cooled (0 °C) and stirred solution of 168.3 mg (314 µmol) $[BzNEt_3][ReOCl_4]$ in 3 ml methanol. A clear reddish brown solution was obtained after another hour of stirring. Yield: 74.2 mg (47.8 %) of large brown needles.

UV/VIS absorptions: λ_{max}/nm (CH_3CN) 287 (log ε / $dm^3\ mol^{-1}\ cm^{-1}$ = 3.69), 392 (3.68).

IR absorption: ν/cm^{-1} (KBr) 976s (Re=O).

Results and discussion

We synthesized three new oxorhenium(V) mixed-ligand complexes with rhenium-selenium bonds according to the "3+1" principle. This principle embodies common [11] or subsequent [9] action of a tridentate dithiol and a monodentate thiol ligand on an appropriate oxorhenium(V) precursor.

Scheme 1: Synthesis of selenium complexes in a two-step procedure [9]

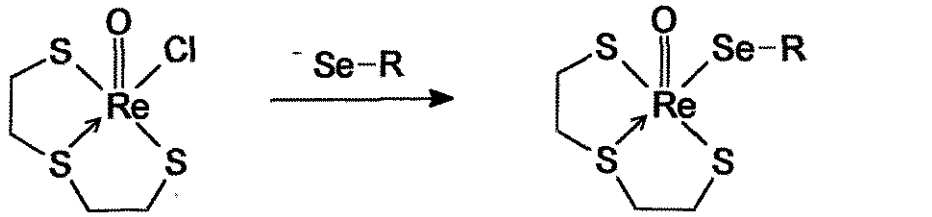

1

2 R = C_6H_5

3 R = CH_2-C_6H_5

Scheme 2: One-pot synthesis of complex 4.

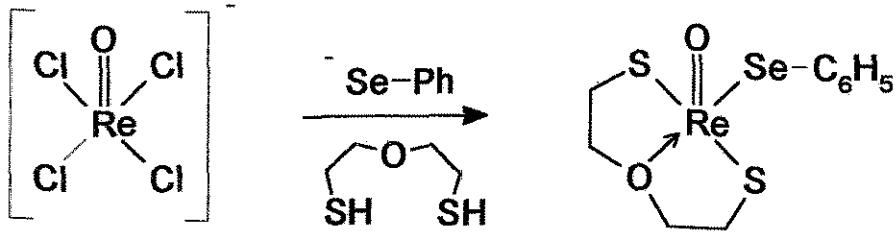

4

The appropriate seleno-organic compounds were synthesized using two different methods: crude benzeneselenol was obtained by alkaline cleavage of diphenyl diselenide in ethanol followed by acidification; sodium benzylselenolate was synthesized by reducing selenium powder with sodium borohydride and subsequent reaction with benzyl chloride in ethanol [8]. The selenols were not isolated due to their high sensitivity towards air. Excessive crude solutions of them were used for complexation experiments. Since the solutions contained varying but remarkable

amounts of the diselenides, it was impossible to determine the exact stoichiometry of the selenol components involved.

Compound	M.p. [°C]†	Elemental analysis		
		% C found (calc.)	% H found (calc.)	% S found (calc.)
2	220 - 222	23.58 (23.53)	2.39 (2.57)	18.61 (18.84)
3	176 - 179	24.62 (25.19)	2.66 (2.88)	18.62 (18.33)
4	177 - 179	24.17 (24.17)	2.50 (2.65)	12.96 (12.97)

†) with decomposition

The 90 MHz proton NMR spectra of complexes 2 and 3 show the typical patterns expected for compounds with 3-thiapentane-1.5-dithiolato ligands [11]. The signals of the protons of the tridentate ligand of 2 are depicted at 1.91 ppm (septet), 3.06 ppm (td), 3.84 ppm (ddd) and 4.19 (dd, 2H each). The aromatic protons are shifted to 7.32 (3H) and 7.81 (2H). In complex 3, the shape of the signals of the tridentate ligand is very similar with only slightly different shifts: 1.91, 3.06, 3.84 and 4.30 ppm. The methylene group is depicted at 5.08 ppm and the aromatic protons in a multiplet at 7.39 (5H).

The spectrum of complex 4, however, exhibits a different pattern of the chemical shift of the protons of the tridentate ligand. They are shown as three multiplets at 3.35 (4H), 3.66 (2H) and 4.62 ppm (2H). The aromatic protons are depicted at 7.34 (3H) and 7.74 ppm (2H). This is very similar to the proton NMR spectrum of ReO(SOS)(SPh) [11].

Molecular structure of complex 4

Large single crystals suitable for X-ray structure analysis were obtained by slow evaporation of a solution of 4 in chloroform and ethanol. This structure analysis is one of the first with an ether oxygen and a basic selenium atom coordinated to oxo-rhenium.

The ligands form a distorted tetragonal pyramidal coordination around the central atom. Most of the features are similar to those in ReO(SOS)(S-Ph-OCH_3(*p*)) [11]. Selected data are given in Tables 1 and 2.

Table 1: Selected bond lengths of 4 and their estimated standard deviations

Atom 1	Atom 2	Bond distance [Å]
Re	Se	2.406(2)
Re	S1	2.288(5)
Re	S2	2.275(5)
Re	O1	1.64(1)
Re	O2	2.10(1)
Se	C5	1.92(2)

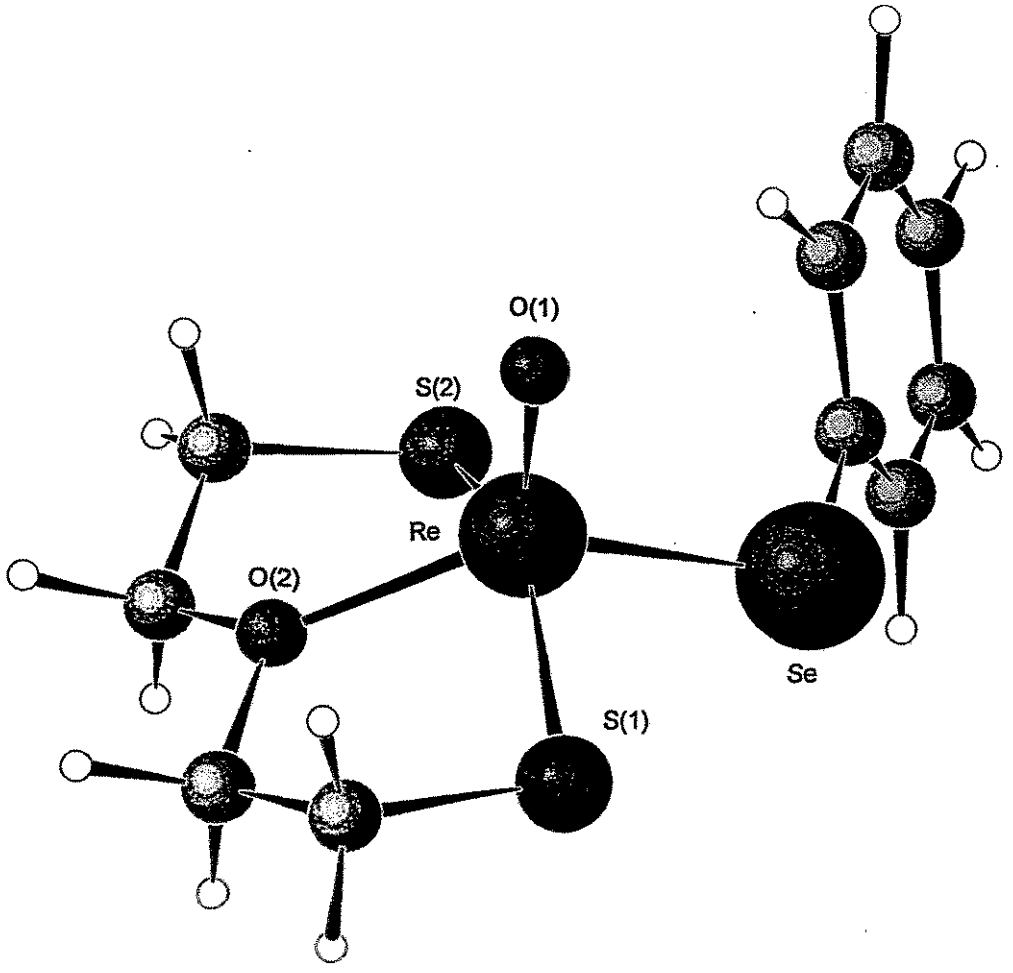

Fig. 1: Molecular structure of (3-oxapentane-1.5-dithiolato)(benzeneselenolato) oxorhenium(V) 4

Table 2: Selected bond angles of **4** and their estimated standard deviations

Atom 1	Atom 2	Atom 3	Angle [°]	Atom 1	Atom 2	Atom 3	Angle [°]
Se	Re	S1	84.9(1)	S2	Re	O2	80.9(4)
Se	Re	S2	90.6(1)	O1	Re	O2	109.8(6)
Se	Re	O1	104.9(5)	Re	Se	C5	108.6(5)
Se	Re	O2	145.1(3)	Re	S1	C1	98.3(6)
S1	Re	S2	139.8(2)	Re	S2	C4	100.5(8)
S1	Re	O1	108.8(4)	Re	O2	C2	123(1)
S1	Re	O2	80.4(3)	Re	O2	C3	121(1)
S2	Re	O1	111.0(4)	C2	O2	C3	110(1)

References

[1] McDonell, A. C. et al., Aust. J. Chem. **36** (1983) 253

[2] Laing, M. et al., J. C. S., Chem. Comm. (1977) 221

[3] Abel, E. W. et al., J. Organomet. Chem. **250** (1983) 373

[4] Bacchi, A. et al., Angew. Chem. **106** (1994) 206

[5] Abram, U. et al., Z. Naturforsch. **46b** (1991) 1183

[6] Herberhold, M. et al., J. Organomet. Chem. **459** (1993) 257

[7] Pearson, R. G. and J. Songstadt, J. Am. Chem. Soc. **89** (1967) 1827

[8] Klayman, D. L. and T. S. Griffin, J. Am. Chem. Soc. **95** (1973) 197

[9] Fietz, Th. et al., Inorg. Chim. Acta, in press

[10] Behaghel, O. and K. Hofmann, Chem.Ber. **72** (1939) 699

[11] Spies, H. et al., submitted for publication to J. Chem. Soc., Dalton Trans.

8. PREPARATION, CHARACTERIZATION AND ENZYMATIC HYDROLYSIS OF MIXED LIGAND Re/Tc COMPLEXES WITH DMSA AND DMS ETHYL ESTERS

S. Seifert, R. Syhre, H. Spies, B. Johannsen

Ester groups can play an important part in technetium tracer design, as is known for Tc-99m-ECD and other complexes [1,2,3]. Studies of their enzymatic hydrolysis have revealed stereoselective and animal species dependent factors governing the hydrolysis rate and kind of products [4]. To gain a greater insight into such factors as well as the interplay of coordinated ester functions, we prepared and studied $[MO(DMSA/ester)_2]^-$ complexes with up to four coordinated ester groups per molecule. Such oxocomplexes of rhenium(V) and technetium(V) with *meso* dimercaptosuccinic acid (DMSA) and/or its esters occur as mixtures of three stereoisomers (syn-endo, syn-exo, anti).

Eperimental

The number and position of ester groups in the complex molecule are symbolized as follows, without distinguishing isomers:

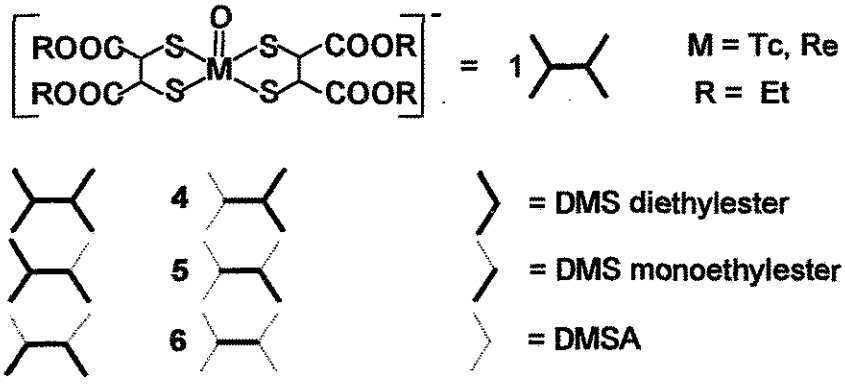

Re complexes **1 - 6** were prepared by ligand exchange reaction of equimolar amounts of $Bu_4N[ReOCl_4]$ and pairs of ligands in an acetonic solution and identified and separated by HPLC. The HPLC analyses were carried out with a PRP-1 column (Hamilton, 250 x 4.1 mm, 10 µm, flow rate 2 ml/min) or a ChiraDex column (Merck, LiChroCART 250 x 4 mm, 5 µm, flow rate 1 ml/min) using a linear gradient system

(t,%B): (5,0), (10,50), (10,50) of 0.1 % trifluoroacetic acid in water (A) and 0.1 % trifluoroacetic acid in acetonitrile (B). The effluent from the column was monitored by UV absorbance at 340 nm.

The corresponding ^{99m}Tc complexes were obtained by stannous chloride reduction of pertechnetate in aqueous acetonic ligand solutions. According to the general procedure 0.2 - 0.8 mg of the ligands, 0.1 mg ascorbic acid, and 7.0 mg $NaHCO_3$ are dissolved in saline and/or acetone and mixed with 1.0 - 2.0 ml pertechnetate eluate. 1 mg $SnCl_2 \times 2H_2O$ dissolved in 10 µl ethanol is added and after 5 min the reaction solution is filtered through a millipore filter. The following ligand quantities needed for preparation (Table 1) were optimized empirically. The relatively high quantities of DMS ethylester are caused by impurities of DMS diethylester in this ligand preparation which could not be obtained in crystalline form. The resulting HPLC chromatograms of the Re/Tc complexes therefore show additional peaks of mixed ligand complexes with the DMS diethylester ligand.

Table 1: Optimized quantities of ligands for preparing the ^{99m}Tc complexes

Complex	DMSA	DMS ethylester	DMS diethylester [µg]
1			250
2		650	60
3		650	
4	280		210
5	230	650	
6	500		

For separation of 400 µl samples of ^{99m}Tc complexes a preparative PRP-1 column (305 x 7 mm, 10 µm, flow rate 4 ml/min) was used.

Fig. 1 shows as an example the HPLC separation of a preparation containing the ^{99m}Tc complexes **1**, **4** and **6**. After separation of the complex **4** fraction the acetonitrile is evaporated by nitrogen bubbling and heating in a boiling water bath. The acidic aqueous solution is neutralized with $NaHCO_3$ and aliquots are used for incubation studies.

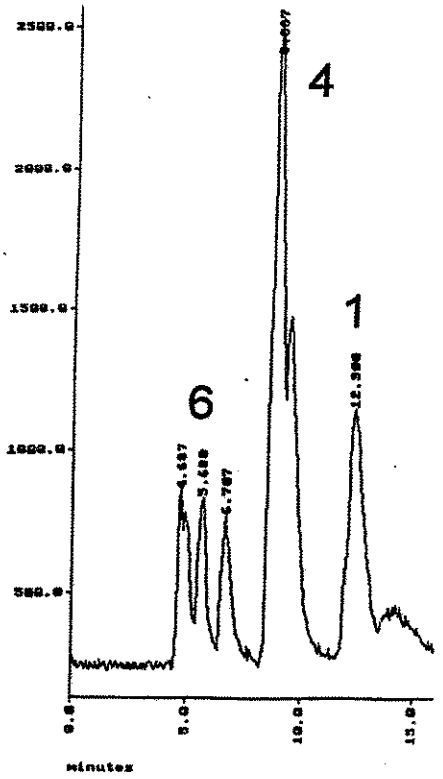

For *in vitro* studies 6 x 10^{-7} mol Re complex or 5 - 10 MBq ^{99m}Tc complex are incubated in a sample volume of 1 ml at 37 °C with 100 U pig liver esterase (PLE, E.C. 3.1.1.1., Fluka) in phosphate buffer of pH 7.4 or blood plasma of rats (RP) or humans (HP) diluted 1:1 with phosphate buffer of pH 7.4.
For *in vivo* studies 0.5 ml complex solution (5 - 10 MBq ^{99m}Tc) are injected into Wistar rats (male, 5 - 6 weeks old).

Fig. 1: HPLC separation (PRP-1) of a complex mixture obtained by stannous reduction of $^{99m}TcO_4^-$ in aqueous acetonic DMSA / DMS diethylester solution

Results and discussion

All the above mentioned types of mixed ligand rhenium complexes 2 - 5 are also obtained if a $[ReO(DMSA)_2]^-$ complex preparation is allowed to stand in ethanolic solution. The gradual esterification is helpful for assignment because the same R_t-values in HPLC are observed as found for direct preparations.

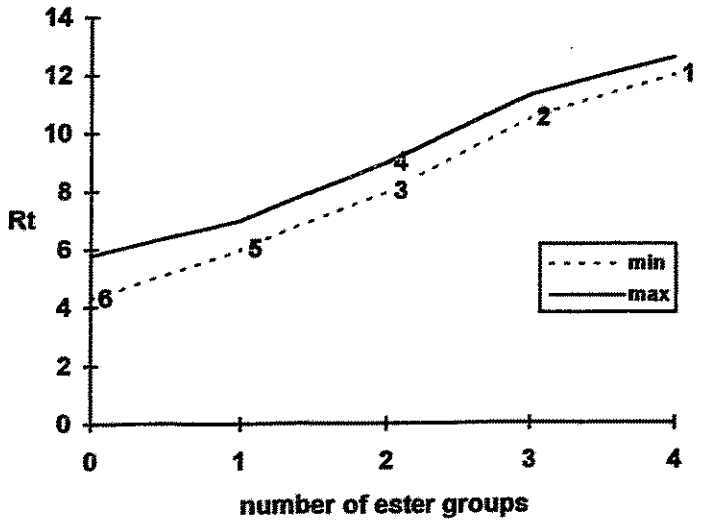

Fig. 2: Dependence of R_t values (PRP-1) of the complexes 1 - 6 on the number of ester groups

As expected the Re/Tc complexes are eluted from the PRP-1 column according to their lipophilicity, which increases with the number of ester groups in the complex molecule (Fig. 2). In Table 2 a summary of the measured data for ^{99m}Tc complexes is given. In contrast to the PRP-1 column, on the ChiraDex column the more lipophilic diethyl ester complex **1** is eluted first, followed by complexes **2**, **4** and **3**. Complexes containing more than two free carboxylate groups are not eluted. A complete separation into the three possible stereoisomers is only possible for complex **6** on the PRP-1 column and for the complexes **1** and **2** on the ChiraDex column. All other complexes are separated incompletely into two peaks.

Table 2: Chemical and biological characterization of ^{99m}Tc complexes **1** - **6**

Comp. No.	log P (oct./wat.)	R_t [min] PRP-1	R_t [min] ChiraDex	enzymatic cleavage in vitro PLE	in vitro RP	in vitro HP	in vivo rat
1	0.7	12.5 - 13.5	12, 15, 16*	+	+	-	+
2	-1.5	10.0 - 11.0	13, 17, 21*	+	+	-	+
3	< -2.0	8.0 - 9.0	24, 30	-	-	-	-
4	< -2.0	8.5 - 9.5	19, 26	-	-	-	-
5	< -2.0	6.0 - 7.0	-	-	-	-	-
6	< -2.0	4.5, 5.2, 5.8*	-				

* Separation of the three possible stereoisomers

Only the complexes **1** and **2** are enzymatically hydrolysed (Fig. 3). While complex **1** reacts with PLE to **2** only, the cleavage in RP solution results also in small portions of the diacid complex **3**.

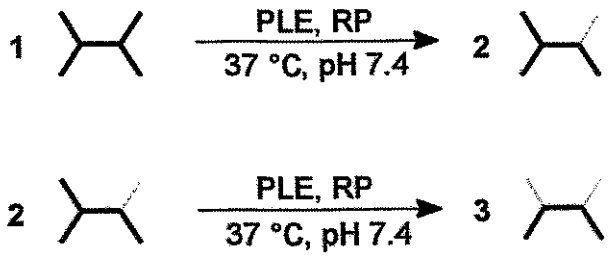

Fig. 3: Enzymatic cleavage of **1** and **2** with PLE and RP

It was found by HPLC with the ChiraDex column that in fact the symmetric complex **3** and not complex **4** is formed. That means that the enzymatic hydrolysis is stopped, when one of the two ester groups of a DMS diester ligand molecule is already hydrolysed. *No hydrolysis is observed in HP solutions.*

References

[1] Walovitch, R.C.et al., J.Cereb.Blood Flow Metab. **14** (1994) S4

[2] Verbruggen, A. et al., in: Technetium and Rhenium in Chemistry and Nuclear Medicine 3 (M. Nicolini, G. Bandoli, U. Mazzi Eds.) Cortina International, Verona, pp.445-452 (1990)

[3] Pasqualini, R. et al., Eur. J. Nucl. Med. **20** (1993) 1001 (abstr.)

[4] Vanbilloen, H. et al., Eur. J. Nucl. Med. **20** (1993) 1001(abstr.)

9. DIFFERENT RATES OF ENZYMATIC CLEAVAGE OF THE THREE STEREOISOMERS OF $[ReO(DMS\ DIESTER)_2]^-$ COMPLEXES

S. Seifert, R. Syhre

The enzymatic cleavage of $[ReO/TcO(DMS\ diester)_2]^-$ complexes with pig liver esterase (PLE) is obviously stopped when one of the two ester groups of a DMS diester ligand molecule is already hydrolysed as described in the preceding article. The individual hydrolysis rates of the syn-endo, syn-exo and anti stereoisomers of the ester complexes were determined by a combination of ^1H NMR and HPLC, which allows to analyse the isomeric pattern and identity of the three stereoisomers.

Experimental

The rhenium complexes $[ReO(DMSR_2)_2]^-$ (R = Me, Et, i-Bu) were prepared by ligand exchange reaction of $Bu_4N[ReOCl_4]$ with stoichiometric amounts of DMS dimethylester, DMS diethylester and DMS diisobutylester. After crystallization of complexes by reducing the volume of the solution, filtration, washing and drying the solids are redissolved in acetone or acetone-d_6 and analysed.

The ^{1}H NMR analyses were carried out in acetone-d_6 solutions using a Varian UNITY 400 system at a ^{1}H frequency of 400 MHz.

For HPLC analyses a ChiraDex column (E.Merck, 250 x 4 mm, 5 µm) filled with β-cyclodextrin chemically bonded to silica gel as chiral stationary phase for the separation of enantiomers was used in conjunction with a linear gradient system of 0.1 % trifluoroacetic acid in water (A) / 0.1 % trifluoroacetic acid in acetonitrile (B); flow rate 1.0 ml/min, (t[min]/% B): (10/20), (10/80) with a gradient +1, (20/80), UV absorbance at 340 nm.

For hydrolysis studies 6 x 10^{-7} mol Re complex are incubated at 37 °C in a sample volume of 1 ml containing 100 U pig liver esterase (PLE, E.C. 3.1.1.1., Fluka) in phosphate buffer of pH 7.4.

Results and discussion

The HPLC system used for the analyses allows a quantitative determination of the isomer ratios of the dimethyl- and diethylester complexes (Fig. 1), the diisobutyl complex, however, was not separated into the three isomers by this method.

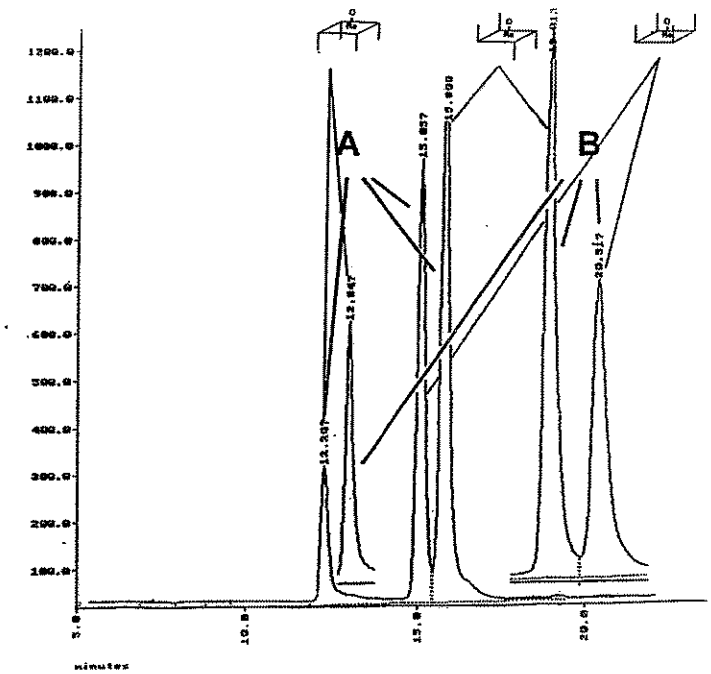

Fig. 1: HPLC analyses of [ReO(DMS diethylester)$_2$]$^-$ (A) and [ReO(DMS dimethylester)$_2$]$^-$ (B) dissolved in acetone

The identity of the isomers was determined by comparing the percentage yields of the isomers measured by HPLC and ^{1}H NMR (Table 1), taking into consideration that the anti form shows two singlets of 1:1 integral ratio in the ^{1}H NMR spectrum (Fig. 2) and that only less than 20 % of the syn-exo form is contained in an acetonic solution [1,2].

Table 1: Average isomer distribution of $[ReO(DMSR_2)_2]^+$ complexes (R = Me, Et, i-Bu) determined by ^{1}H NMR and HPLC

$[ReO(DMSR_2)_2]^+$	^{1}H NMR			HPLC [%]		
R	exo	anti	endo	exo	anti	endo
Me	15	52	33	14	50	36
Et	12	48	30	15	49	36
i-Bu	13	51	36		-	

The elution order of the isomers in HPLC is different: while the DMS diethylester complex is eluted in the sequence syn-exo - syn-endo - anti, the DMS dimethylester complex is eluted in the order syn-exo - anti - syn-endo.

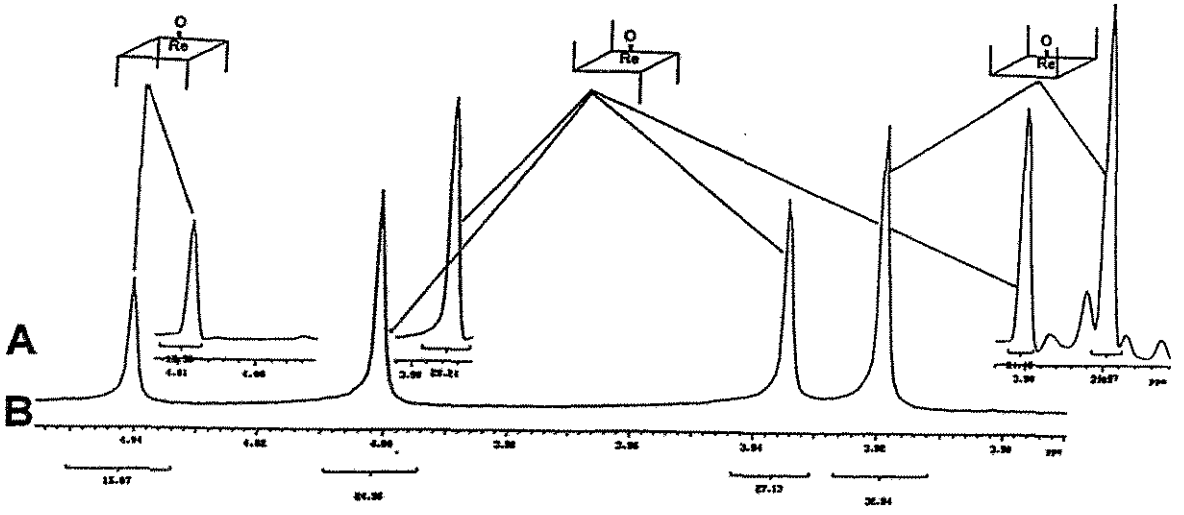

Fig. 2: ^{1}H NMR analyses of C-H proton region (3.8 - 4.1 ppm) of [ReO(DMS diethylester)$_2$]$^+$ (A) and [ReO(DMS dimethylester)$_2$]$^+$ (B) in acetone-d_6

With knowledge of the isomer ratios and identity, the hydrolysis rates of the three $[ReO(DMS\ diester)_2]^-$ isomers during incubation with PLE were determined.
It was found that cleavage of isomers of the DMS dimethylester and DMS diethylester complexes is influenced by stereo-specific factors. After incubation with PLE in both cases, the syn-endo form is hydrolysed significantly faster than the other two isomers (Fig. 3).

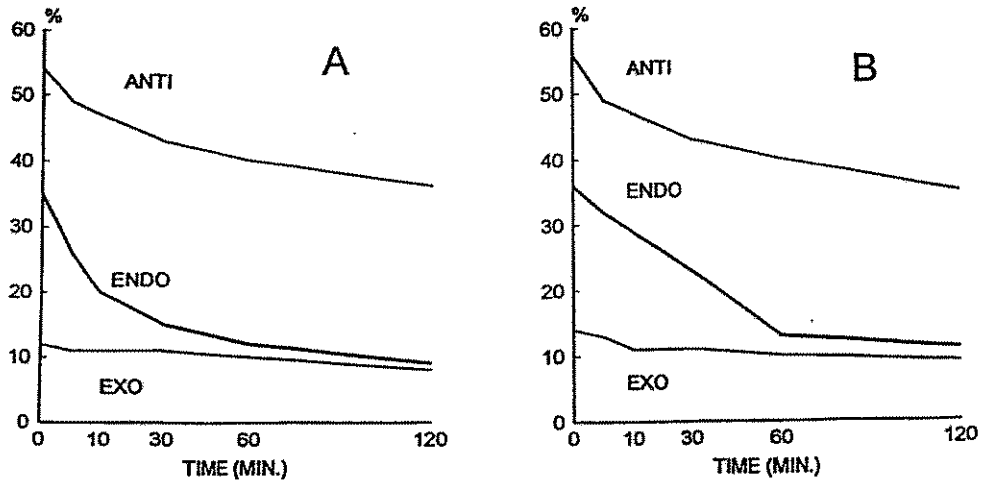

Fig. 3: PLE-hydrolysis rates of stereoisomers of $[ReO(DMS\ dimethylester)_2]^-$ (A) and $[ReO(DMS\ diethylester)_2]^-$ (B) complexes

Acknowledgement

The authors wish to thank Dr. M. Findeisen (Universität Leipzig) for performing ^1H NMR analyses.

References

[1] Blower, P. J. et al., J. Nucl. Med. 32 (1991) 845

[2] Seifert, S. et al., Annual Report 1992 p. 55, Institute of Bioinorganic and Radio pharmaceutical Chemistry, FZR 93-12

10. SYNTHESIS OF TWO FURTHER 4-FLUOROBUTYROPHENONE-CONTAINING RHENIUM COMPLEXES

B. Noll, St. Noll, H. Spies

Synthesis and properties of a rhenium complex [ReO(SXS)(SR)], where R is the p-fluoro-butyrophenone moiety of the D_2 receptor binding compound spiperone and HSXSH is $HSCH_2CH_2XCH_2CH_2SH$ (X = S), was described in [1]. The procedure, which consists in simultaneous action of both the tridentate dithiol ligand and 4-mercapto-(p-fluoro)-butyrophenone (RSH) on rhenium(V) gluconate, was applied to 3-oxapentane-1.5-dithiol and 3-methylazapentane-1.5-dithiol as tridentate ligands. The complexes [ReO(SXS)(SR)] (X = O (**1a**), X = NMe (**1b**)) were obtained in a yield of about 15 % after purification by HPLC. The compounds are another two representatives of "spiperoids", which differ with respect to the nature of X in the chelate.

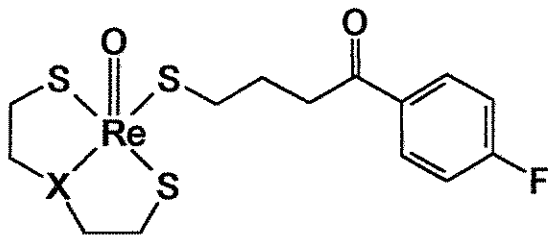

1 X = S
1a X = O
1b X = NMe

Fig.1: [ReO(SXS)(SR)] (1) , **1a** X = O, **1b** X = NMe

Table 1: Experimental and spectroscopic data

	M.p. [°C]	Formula	Analysis [% calc./found] C	H	S
1a	146-47	$C_{14}H_{18}O_3S_3FRe$	31.3	3.4	17.9
			31.3	3.3	18.8
1b	175-177	$C_{15}H_{21}NO_2S_3FRe$	32.8	3.9	17.5
			32.3	3.3	17.2

	UV/VIS [λ_{max} (log ε)]	IR [cm^{-1}]	^1H NMR [ppm] butyrophenone protons	chelate ring protons
1a	242(4.24)	968	a) 3.10 (2H)	f,g) 3.20 - 3.80 m (6H),
	318(3.42)		b) 2.36 m (2H)	4.65 br (2H)
	347(3.47)		c) 3.92 t (2H)	
			d) 7.99 m (2H)	
			e) 7.08 m (2H)	
1b	239(3.92)	968	a) 3.18 t (2H)	f,g) 2.10 - 3.60 m (8H)
	363(3.02)		b) 2.33 m (2H)	h) 3.35 s (3H)
	395(2.92)		c) 3.85 t (2H)	
			d) 7.99 m (2H)	
			e) 7.08 m (2H)	

References

[1] Spies, H. et al., Annual Report 1993, p. 37, Institute of Bioinorganic and Radiopharmaceutical Chemistry, FZR-32

11. Tc AND Re COMPLEXES DERIVED FROM SPIPERONE
4. COMPLEX FORMATION OF TECHNETIUM WITH MAG_2 DERIVATIVES OF ω-AMINO-4-FLUORO-BUTYROPHENONE

H. Spies, St. Noll, B. Noll

The fluorobutyrophenone moiety is a structural part of several organic receptor-binding substances, e. g. of the dopamine D_2-binding ligand spiperone. Introduction of this group as a substituent into Tc and Re complexes may therefore help to lend Tc and Re coordination compounds receptor-binding properties.
With the aim of making more of such compounds [1] available, a new ligand, 4-(p-fluorophenyl)-4-oxobutylamide of mercaptoacetyldiglycine ($FB\text{-}MAG_2$) was prepared. This compound is expected to fulfil the requirement of having good complexing properties and bearing the fluorobutyrophenone substituent. Synthesis of the ligand and experiments concerning complexation with technetium-99 are dealt with.

Synthesis of $FB\text{-}MAG_2$
Synthesis follows the route as shown in Fig. 1.

ω-amino-4-fluoro-butyrophenone (2):
10 g (0.05 mol) ω-chloro-4-fluoro-butyrophenone was dissolved in 140 ml of ethanol. After addition of 50 ml of 25 % ammonia the mixture was refluxed for 4 h. The solvent was removed by rotary evaporation and 50 ml of water and 50 ml of diethyl ether were added to the residue. The layer of diethyl ether was separated and dried with sodium sulphate. The solution was filtered and the diethyl ether evaporated. The yellow oil was treated with methanolic hydrochloric acid and lyophilized. The hydrochloride obtained was dissolved in water and lyophilized again.
Yield: (6.5 g, 60 %)
M.p. 39 °C
TLC: (RP 18//methanol/water 9:1) R_f 0.65 (UV, ninhydrine)
Elemental analysis: (Found: C, 55.85; H, 5.77; N, 6.75; Cl, 16.11, $C_{10}H_{13}ONClF$ requires C, 55.18; H, 6.02; N, 6.43; Cl, 16.29 %)

Preparing the free amine, the hydrochloride was dissolved in water and treated with a sodium bicarbonate solution. The brown oil obtained was extracted with diethyl ether and dried in vacuum.

Yield: (75 %)

M.p. 163°C

TLC: (RP 18//methanol/water 9:1) R_f 0.3 (UV, ninhydrine)

Elemental analysis: (Found: C, 66.89; H, 6.32; N, 8.13, $C_{10}H_{12}ONF$ requires C, 66.28; H, 6.67; N, 7.73 %)

^{1}H NMR data: δ_H(250 MHz; solvent DMSO; standard TMS) 1.88-1.96 (2H, -CH_2), 2.86-2.91 (2H, -CO-CH_2), 3.89-3.93 (2H, -CH_2-N), 7.22-7.27 (2H, arom.), 7.84-7.87 (2H, arom.)

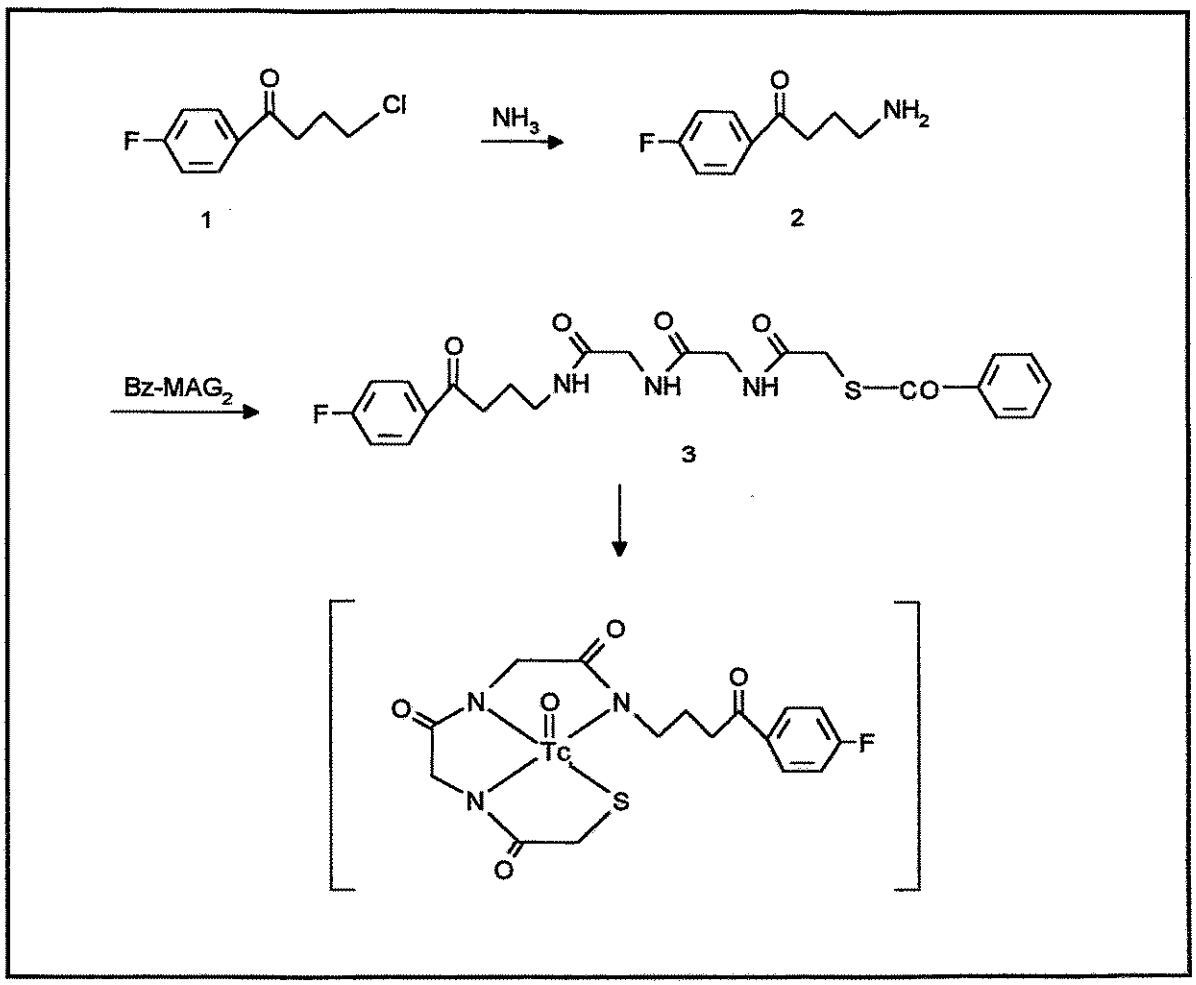

Fig. 1: Reaction scheme of the synthesis of FB-MAG_2 and proposed structure of [Tc-FB-MAG_2]$^-$

Bu-MAG$_2$

310 mg (1 mmol) benzoyl-MAG$_2$ and 330 mg (1 mmol) O-(1H-benzotriazol-1yl)-N,N,N',N'-tetramethyluronium tetrafluoroborate (TBTU) were dissolved in 2 ml of 1-methyl-2-pyrrolidone. After addition of 340 µl (2 mmol) ethyldiisopropylamine and stirring for 3 min, the mixture was added to a solution of 145 mg (0.8 mmol) ω-amino-4-fluoro-butyrophenone in 2 ml of 1-methyl-2-pyrrolidone. The reaction solution was stirred for 4 h at room temperature and then the solvent was removed in vacuum. The residue was dissolved in ethanol/water 1:1 and lyophilized. The brown crystals were extracted with hot water and recrystallized from ethanol.

The separation occurred by MPLC on a Eurosil Bioselect C 18 (300 x 25 mm) column:

Eluent A: methanol

Eluent B: water

Elution: 5 min isocratic 10 % A, 40 min gradient -->50 % A, 20 min isocratic 50 % A

Pump speed: 7 ml/min (1.8 MPa)

detection: 265 nm

The separation product was vacuum-dried.

Yield:(163 mg, 43 %)

M.p. 185 °C

TLC: (RP 18//methanol/water 9:1) R_f 0.58 (UV)

Elemental analysis: (Found: C, 58.03; H, 5.37; N, 8.68; S, 6.81, $C_{23}H_{24}N_3O_5SF$ requires C, 58.34; H, 5.11; N, 8.87; S, 6.77 %)

^{1}H NMR data: δ_H (250 MHz; solvent DMSO; standard TMS) 1.72-1.76 (2H, -CH_2), 2.99-3.03 (2H, -CH_2), 3.11-3.14 (2H, -CH_2), 3.67-3.88 (6H, -CH_2), 7.31-7.36 (2H, arom.), 7.54-7.70 (3H, arom.), 7.72-7.76 (1H, -NH), 7.91-7.93 (2H, arom.), 8.00-8.04 (2H, arom.), 8.14-8.17 (1H, -NH), 8.51-8.53 (1H, -NH).

Complexation reaction

UV/VIS spectra depending on the molar ratio Tc gluconate/MAG derivative were recorded by means of the spectrophotometer Specord M40. The chromatographic behaviour was determined by thin layer chromatography on silica gel with acetone or 95 % methanol as the solvent and by HPLC on the RP 18 column (Eurosphere),

10 min. gradient +1 from 100 % A to 10 % A (eluent A: phosphate buffer pH 5.8, eluent B: acetonitrile).

The S-benzoyl-protected ligand was saponified with sodium methylate and used without further purification. Ligand exchange reactions carried out, starting from the 1.3×10^{-4} M Tc(V) gluconate precursor, varying the molar ratio ligand / Tc in the range from 0.5 : 1 to 2 : 1 in neutral and alkaline solution. Tc gluconate was prepared as previously described.

Results

Gradual addition of an aqueous solution of MAG_2-butyrophenone (4) both to a neutral and alkaline Tc gluconate solution under UV control gives a peak at 330 nm. The maximum extinction is found at a molar ratio of about 1:1 (ligand/Tc). Because the exchange is relatively low, a small excess of the ligand is necessary to consume Tc gluconate quantitatively in appropriate time.

The results of quantitative determination of the ligand exchange reaction depending on the molar ratio MAG_2 butyrophenone/Tc gluconate by HPLC and TLC (listed in Table 1) are in good agreement and pH independent.

Table. 1: Composition of the ligand exchange reaction mixture in dependence on the molar ratio MAG_2 butyrophenone/Tc gluconate, reaction time 30 min

	HPLC		TLC	
molar ratio (MAG_2-but./Tc gluc.)	Tc gluc. R_t = 2.21'	Tc-MAG_2 -bu. R_t = 9.01'	Tc gluc. R_f = 0	Tc-MAG_2-but. R_f = 0.8
neutral	[%]		[%]	
0.5:1	65	35	64	35
1:1	40	60	36	64
2:1*	-	>95	-	>95
alkaline	[%]		[%]	
0.5:1	62	37	57	43
1:1	32	67	26	74
2:1*	-	>95	-	>95

*slight excess of ligand and after 60 min

The charge of the Tc complex obtained could not be determined because of its adsorption on the starting point of the silica gel electrophoretic sheets.
However, the observation that the technetium complex is extractable into methylene chloride only in the presence of an organic counter-cation, such as tetrabutylammonium chloride, is consistent with the assumed anionic character of the Tc-(FB-MAG_2) complex. These preliminary results confirm the formulation of Tc-(FB-MAG_2) as a 1:1-complex, in which one of the four donor atoms is the amide nitrogen derived from the aminobutyrophenone moiety.

Reference

[1] Spies, H. et al., Annual Report 1993, p. 37, Institute of Bioinorganic and Radio pharmaceutical Chemistry, FZR-32

12. OCTANOL/WATER PARTITION COEFFICIENTS OF SOME RHENIUM COMPLEXES

R. Berger, T. Fietz, M. Glaser, B. Noll, H. Spies

The lipophilicity of a molecule is an important characteristic in drug and radiotracer design, which influences the pharmacokinetic and the pharmacodynamic behaviour of a substance (i.e. drug) in the body.
A quantitative measure of the lipophilicity of a solute is its distribution ratio between a water immiscible solvent (e.g. octanol) and an aqueous phase, expressed by the partition coefficient ($P_{O/W}$) as shown in the following relation:

$$P_{o/w} = \frac{c_o}{c_w}.$$

[concentrations: c_O (in octanol), c_W (in the water phase)]

Different methods for the determination and calculation of $P_{O/W}$ have been described [1-6]. This article deals with experimental data of $P_{O/W}$ determination of two series of recently synthesized rhenium complexes **1** and **2** by means of the shaking flask procedure. The structure of these complexes is given in Fig. 1.

In comparison with compound 1, complex 2 does not contain a $Re=O^{3+}$ core.

These compounds are studied in order to see whether and how a "tuning" of lipophilicity may be achieved by small substituent changes in a widely variable monodentate coligand present in both types of complexes (R^1 = substituted alkyl, aryl and others and R^2 = substituted triphenylphosphane and isocyano ligands) [7,8].

The experiments for determining the $P_{O/W}$ values of the selected rhenium complexes were performed by the shaking flask procedure after their dissolution either in the octanol or aqueous (water or buffer with an appointed pH value) phase.

Because of the poor solubility of some complexes the dissolution was accomplished by using auxiliary solvents such as acetonitrile or dimethylsulphoxide (DMSO). In these cases corrections of the volumes of the immiscible phases were indicated.

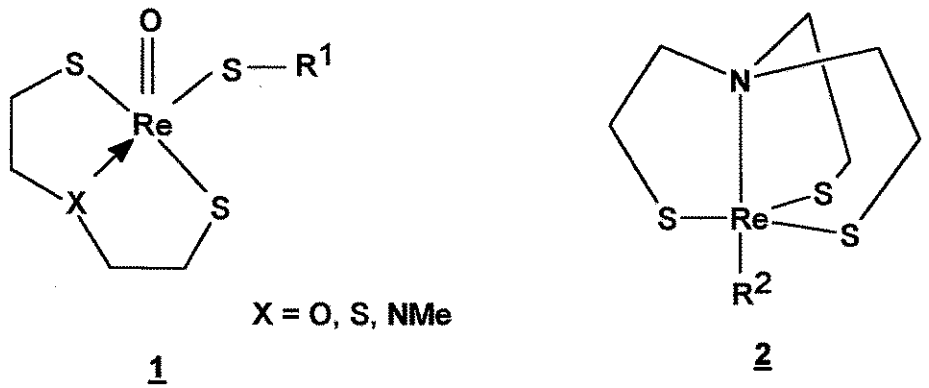

Fig. 1: General structure of rhenium complexes 1 and 2

After separating the two phases, the UV/VIS absorption spectrum of the appropriate rhenium complex within the respective phase was measured. For this purpose the phases added into cuvettes had to be sometimes warmed up for removing a possible clouding before recording the absorption spectrum. The concentrations of the phases could be calculated by means of extinction coefficients had to be determined from typical absorption maxima of corresponding solvents, and equations suitable for necessary volume corrections.

In Tables 1 - 3 the preliminary values of $P_{O/W}$ of the rhenium complexes studied are summarized. These results are supposed to serve as orientation (values obtained by only one or two measurements have to be verified). The aqueous phase consisted of

redistilled water for most determinations and of disodium hydrogen/potassium dihydrogen phosphate buffers containing a free carboxyl or amino group (Tab. 3).

The octanol/water partition coefficients of compounds of particularly high lipophilicity have relatively great errors. This is a result of the poor solubility of some complexes in the aqueous phase.

No substantial influence of the auxiliary solvents can be deduced from the octanol/-water partition coefficients determined. The pH dependence of b reflects deprotonation of the amino group in alkaline media, while a and c are deprotonated in the pH region considered.

Compounds within homologous series show a graduation of the appropriate partition coefficients as expected. This is especially true of the series of aliphatic compounds.

Table 1: Octanol/water partition coefficients of various rhenium complexes 1

R^1 (X = S)	Molecular weight	$P_{o/w}$ solution in octanol	$P_{o/w}$ solution in acetonitrile
$-CH_3$	401.6		28 ± 4 [n=3]
$-C_2H_5$	415.6	39 [n=1]	52 ± 7 [n=2]
$-nC_3H_7$	429.7		247 ± 90 [n=4]
$-nC_4H_9$	443.7		312 ± 200 [n=4]
$-nC_{12}H_{25}$	555.9		≥515 [n=2]
$-C_6H_5$	463.7	63 ± 15 [n=4]	52 [n=1]
$-CH_2C_6H_5$	477.7	≥66 [n=3]	
$-(CH_2)_2C_6H_5$	491.8	≥78 [n=5]	
$-CH_2COOH$	445.6		20 ± 5 [n=3]
$-CH_2COOCH_3$	459.7		21 ± 5 [n=2]
$-CH_2COOC_2H_5$	473.7	18 ± 2 [n=3]	25 ± 8 [n=8]
$-(CH_2)_2N(CH_3)_2$	486.7	6 ± 3 [n=3]	4 ± 2 [n=10]
-thioglucose	549.7	$(3.5 \pm 0.3) \cdot 10^{-2}$ [n=4]	

Table 2: Octanol/water partition coefficients of rhenium complexes 2

R^2	Molecular weight	$P_{O/W}$ solution in octanol	$P_{O/W}$ solution in DMSO
-CN-C_2H_4-N-morpholinyl	520.8	16 ± 3 [n=2]	10 ±3 [n=2]
-CN-C_6H_5	483.7	≥60 [n=2]	
-CN-COOH	465.6	1.0 ± 0,5 [n=2]	
-P-$(CH_3)_2$-C_6H_5	518.7	≥93 [n=2]	≥88 [n=2]

Table 3: Octanol/water partition coefficients of rhenium complexes 1 [R^1 = -CH_2COOH (a), -$(CH_2)_2N(CH_3)$ (b)] and 2 [R^2 = -CN-COOH (c)] depending on pH values

pH value	Rhenium complex		
	a	b	c
5.0	19.1	0.4	0.72
6.0	29.7	0.4	0.40
6.5	27.1	0.5	0.16
7.0	31.1	0.7	0.20
7.5	29.0	1.2	0.15
8.0	26.5	-	-
8.5	21.6	2.2	0.13

References

[1] Leo, A. J. et al., Chem. Rev. **71** (1971) 525

[2] Braumann, T. et al., J. Chromatogr. **261** 1983) 329

[3] Biagi, G. L. et al., J. Chromatogr. A **669** (1994) 246

[4] Minick, D. J. et al., J. Med. Chem. **31** (1988) 1923

[5] Kugel, C. et al., J. Chromatogr. A **667** (1994) 29

[6] Yamagami, C. et al., J. Chromatogr. **662** (1994) 49

[7] Fietz, T. et al., Annual Report 1993 p. 66, Institute of Bioinorganic and Radio pharmaceutical Chemistry, FZR-32

[8] Glaser, M. et al., Annual Report 1993 p. 70, Institute of Bioinorganic and Radio pharmaceutical Chemistry, FZR-32

13. STABILIZING AQUEOUS SOLUTIONS OF LIPOPHILIC SUBSTANCES BY CYCLODEXTRINS

R. Berger, H. Spies

Binding studies on receptor sites may be complicated by poor solubility of the compounds in aqueous solution. That is so in the case of "spiperone-like" rhenium complexes (Fig. 1) [1].

Studies were therefore carried out regarding the miscibility of their dimethylsulphoxide (DMSO) solutions with water and to enhance the solubility by cyclodextrins.

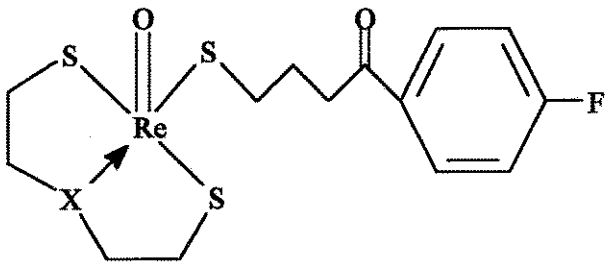

Fig. 1: Structure of a 4-fluorobutyrophenone-containing neutral rhenium complex {X = S (I), O (II) and NCH_3 (III)}

In Fig. 2 the influence of adding water to the DMSO solution of the rhenium complex II is shown.

An addition of water to the DMSO solution in a volume ratio of 1 to 1 does not cause any change of solubility (curve 1), as observed by the corresponding UV/VIS absorption spectrum. If the water is added to the volume of the DMSO solution in a 15-fold excess the mixture becomes turbid with the consequence that the rhenium complex precipitates (curve 2).

For overcoming this disadvantage cyclodextrin was investigated for its applicability as a solubilizer.

Cyclodextrins containing six, seven, or eight glucose units in a circle (α-, β-, or γ-cyclodextrins) are often used to improve the water solubility of poorly-soluble ingredients. For the solubilization of drugs, for instance, concentrations of solubilizer from 5 - 50 % are recommended [2]. The solubility of a lipophilic substance in-

creases usually linearly proportionally to the cyclodextrin concentration in aqueous buffer, due to the formation of a complex. Hydrophobic interactions drive the lipophilic compound into the cyclodextrin cavity, displacing water molecules and forming the guest-host complex [3, 4, 5].

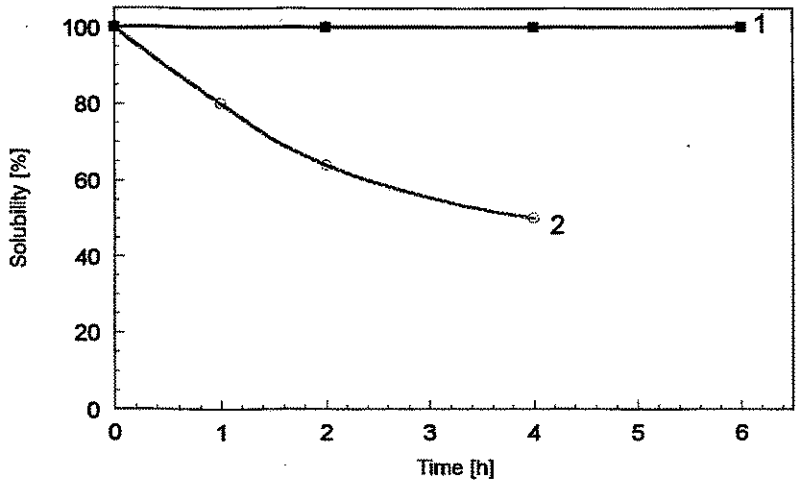

Fig. 2: Time-dependent solubility of rhenium complex II in DMSO after adding an equal (1) and a 15-fold (2) volume of water

The solubility of various substances both in water and in 45 % v/v aqueous 2-hydroxypropyl-β-cyclodextrin (HBC) has been investigated [6].

The usefulness of hydroxypropyl-β-cyclodextrin to enhance the water solubility of the same rhenium complexes as presented in Fig. 1 has been tested.

Although it has been recommended that compounds to be dissolved should be pulverized and added to the clear solution of solubilizer [2], these experiments were generally carried out by dissolving the rhenium complex in a minor volume of DMSO, adding a definite amount of HBC to this solution and finally filling up with small portions of water in a measuring vessel. For further studies of receptor/ligand binding, the aqueous ligand solutions should be stable and contain the DMSO as well as the HBC in concentrations as small as possible.

Pure ligand solutions in DMSO and also acetonitrile are stable over weeks, but for the assessment of binding to biological material (e.g. tissue homogenates) such organic solutions are unsuitable.

In Fig. 3 the results of these experiments are summarized. It can be seen that only in a solution containing 6 % DMSO and 3 % HBC the rhenium complex II remains

stable without forming a precipitation for 8 hours at least. The rhenium complexes I and III show an analogous behaviour.

Because of the small concentration of aqueous HBC solutions used, the appropriate rhenium complex has to be dissolved first in a volume of DMSO designed to produce

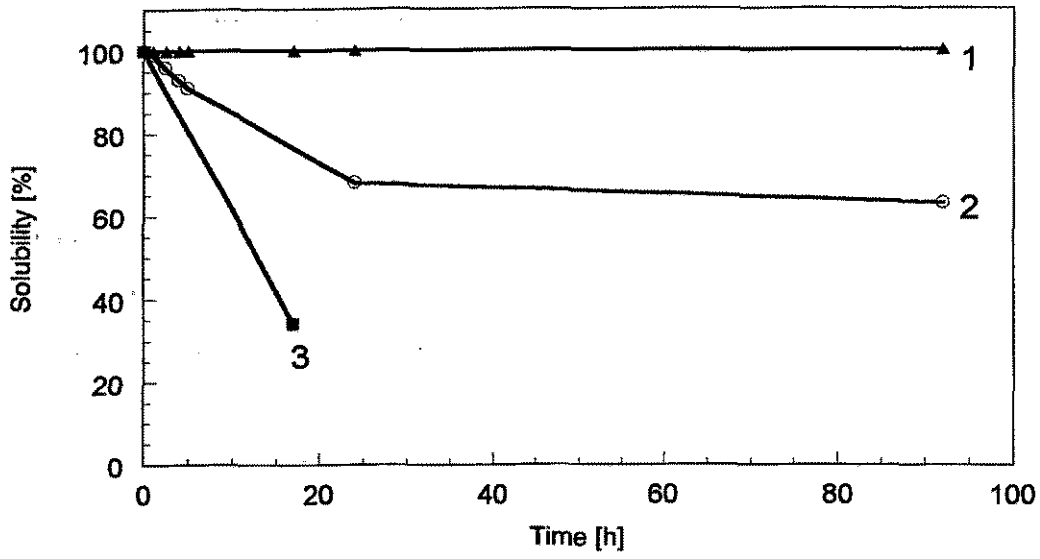

Fig. 3: Time-dependent stability of aqueous $5 \cdot 10^{-4}$ molar solutions of rhenium complex II with different percentages of DMSO and HBC (curves 1, 2, 3 contain 6 % and 3 %, 4 % and 2 %, 1 % and 1 % DMSO and HBC)

a concentration of 6 % (v/v) of DMSO. A relatively diluted HBC solution of only 3 % (v/v) is obviously suited for stabilizing aqueous solutions of these rhenium complexes.

References

[1] Spies, H. et al., Annual Report 1993, p. 37 and 40, Institute of Bioinorganic and Radiopharmaceutical Chemistry, FZR-32

[2] Pitha, J., Neurotransmissions 5/1 (1989) 1

[3] Duchene, D. et al., J. Coord. Chem. **27** (1992) 223

[4] Pitha, J. et al., Life Sciences **43** (1988) 493

[5] Wenz, G., Angew. Chem. **108** (1994) 851

[6] RBI, Research Biochemicals Incorporated, Product Data Sheet, Rev. 7/91

14. DOES CYCLODEXTRIN AFFECT LIGAND/RECEPTOR BINDING STUDIES ?

R. Berger, J. Wober, P. Brust, H. Spies

With respect to our investigations of their potential receptor binding properties, technetium and rhenium complexes have been tested concerning their binding to the dopamine D_2 receptor.

Substances intended to be used as potential brain agents should have properties allowing their penetration through the blood brain barrier. Usually such agents are quite lipophilic and, consequently, only poorly soluble in water. For practical applications there are manifold efforts to increase the water solubility of these and other substances of partial therapeutical interest. In some cases the water solubility of lipophilic compounds can be improved by using 2-hydroxypropyl-β-cyclodextrin (HBC) as a solubilizer [1, 2].

We studied the receptor binding of this agents dissolved in an aqueous medium with and without cyclodextrin as solubilizer.

As antagonist of the receptor dopamine D_2 (+)-butaclamol was selected. The assessment of its binding was carried out by competitive displacement of [^{3}H]spiperone bound to tissue homogenized from rat brain striatum.

When the radiolabelled ligand is incubated with tissue containing specific binding sites for this ligand, a distinct amount of radioactivity is bound. The amount of bound tracer is separated from free radioactivity by filtration over glass-fiber filters. Background binding to non-receptor sites and lipid phases is measured in the presence of an about 1000-fold excess of an unlabelled receptor binding compound, e.g. (+)-butaclamol.

The preliminary results of this binding study are shown in Fig. 1. In this diagram two solutions of (+)-butaclamol of the same concentration but with different solubilizers in aqueous solution are represented by corresponding curves. For solution 1 (+)-butaclamol is dissolved in a small volume of ethanol, and then diluted with water up to a concentration of 2 % (v/v) of ethanolic aqueous solution (curve 1). The aqueous solution 2 of (+)-butaclamol contains HBC and dimethylsulphoxide (DMSO) as solubilizers with concentrations of 3 % (v/v) and 6 % (v/v) (curve 2). For the pre-

paration of solution 2 (+)-butaclamol is dissolved in a small volume of DMSO. To this solution a definite amount of HBC is added and filled up with water in small portions [2]. For curve 2 the value relating to a specific binding of [^{3}H]spiperone of 100 percent had to be corrected. Because the underlying measuring sample did not contain (+)-butaclamol and thus neither HBC nor DMSO, the influence of the last two compounds had to be considered. In the system containing 3 % HBC and 6 % DMSO, the binding of [^{3}H]spiperone is diminished by about 50 percent. This decrease was applied for the correction.

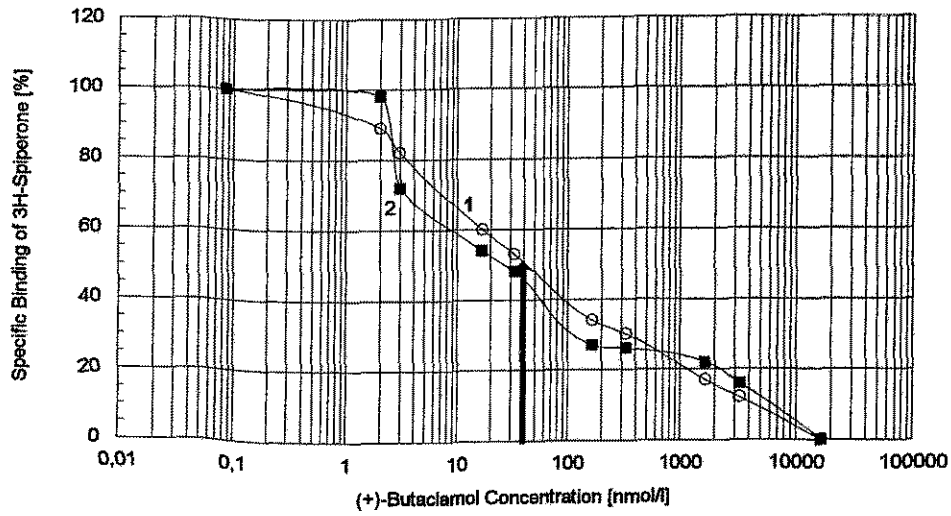

Fig. 1: Displacement of specifically bound [^{3}H]spiperone from rat brain striatum by increasing concentrations of (+)-butaclamol for the determination of IC_{50}-values; (+)-butaclamol solutions without (1) and with (2) HBC

From the curves 1 and 2 the same IC_{50}-value (the concentration of half-maximal inhibition) of about $4 \cdot x\ 10^{-8}$ mol/l can be derived.

Apart from the remark on the Product Data Sheet of the company RBI that the HBC are not recommended in receptor binding assays [3], neither additional arguments nor other related information were found in the relevant literature.

The preliminary results show that the use of HBC even as a solubilizer for relatively poorly soluble substances doesn´t drastically alter the result of the receptor/ligand

binding studies. In particular, solutions of about 3 percent and with a DMSO content of up to 6 percent might be quite suitable.

References

[1] Pitha, J., Neurotransmissions 5/1 (1989) 1

[2] Berger et al., this report, p. 56

[3] RBI, Research Biochemicals Incorporated, Product Data Sheet, Rev. 7/91

15. TECHNETIUM AND RHENIUM COMPLEXES OF DERIVATIZED NUCLEIC ACID COMPONENTS

1. TECHNETIUM COMPLEXES OF URACIL-MAGn LIGANDS

St. Noll, B. Noll, H. Spies, B. Johannsen, L. Dinkelborg[1], W. Semmler[1]

[1]Institut für Diagnostikforschung Berlin

Pyrimidine derivatives seem worth beeing included in our studies on "reactive" Tc tracers. Pyrimidine moieties are of interest because both of the eminent role pyrimidines play as nucleic acid constituents in the organism and their potential as delivery systems for selective transport of technetium into tissues. For instance, the ability of 2-thiouracil to be selectively taken up into melanomas [1] gave rise to the proposal that derivatives of thiouracil should be used as boron-delivering systems for transport of boron into melanomas [2].

On the other hand, they are also of interest from the point of view of coordination chemistry.

The pyrimidine bases may act as "anchor groups" in bifunctional agents, or agents can be designed in which the pyrimidines are integrated parts of the chelate unit, by coupling them with appropriate O, N or S-containing moieties. Considering the ability of, for example, uracil to exist in different tautomeric forms, manifold coordination modes are anticipated to occur in the complexation reactions of Tc or Re with such chelating agents.

Preliminary studies involve two different types of bases, a) uracil as the parent compound, and b) orotic acid as a representative containing a carboxylic group, both

substituted with mercaptoacetyl glycine moieties. The following two papers provide information on preliminary studies concerning ligand synthesis, labelling experiments and bio-behaviour of the resulting complexes.

Synthesis of ligands

Synthesis of ligands follows the routes shown in Fig. 1.

5-mercaptoacetylamino-uracil (MAU)

5-aminouracil reacts with chloroacetyl chloride in 0.2 N sodium hydroxide to 5-chloro-acetylamino-uracil. Subsequent reaction with thiobenzoic acid in sodium methylate/methanol yields 5-benzoylmercaptoacetylamino-uracil. 5-mercaptoacetyl-

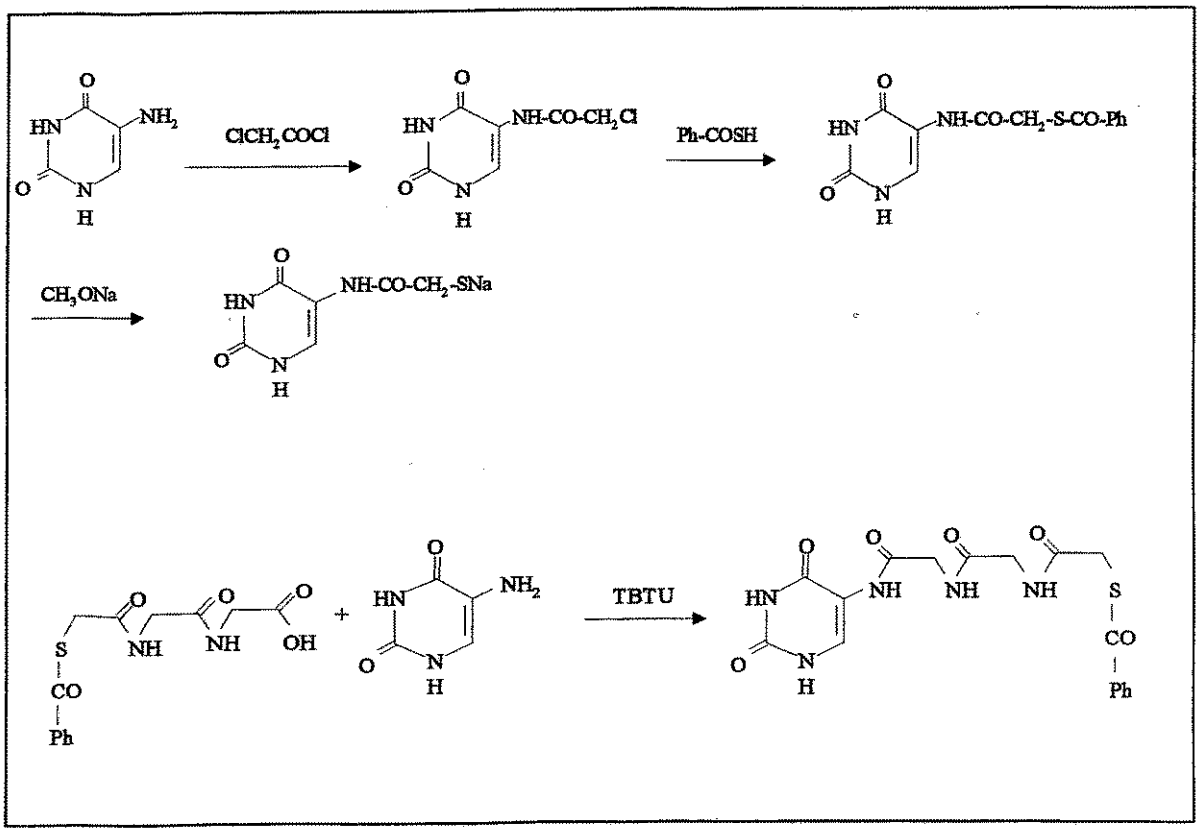

Fig. 1: Reaction scheme

aminouracil was obtained by a special procedure described in [3] in an overall yield of 16 %, based on 5-aminouracil.

Melting point: 240 °C (subl.)

TLC (Silufol//n-butanol/acetic acid/water 2:1:1) R_f 0.75 (UV, 245 nm)

Elemental analysis: (Found: C, 35.64; H, 3.63; N, 20.57; S, 15.87, $C_6H_7O_3N_3S$ requires C, 35.82; H, 3.51; N, 20.88; S, 15.93 %)

^{1}H NMR data: δ_H(250 MHz; solvent DMSO; standard TMS) 2.91 (1H, -SH), 3.50 (2H, $-CH_2$), 8.10 (1H, -CH), 9.35 (1H, NH-CO), 10.66 (1H, NH_{core}), 11.50 (1H, NH_{core})

5-benzoylmercaptoacetyl diglycylamino uracil (Bz-MAG_2-AU)

Benzoylmercaptoacetyl-diglycine was coupled to 5-aminouracil by means of ethyl-diisopropylamine and benzotriazo-1yl-tetramethyluronium-tetrafluorborate.

Yield: 57 %.

Melting point: 293 °C

TLC (Silufol//n-butanol/acetic acid/water 2:1:1) R_f 0.70 (UV, 245 nm)

Elemental analysis: (Found: C, 48.42; H, 4.10; N, 16.43; S, 7.38, $C_{17}H_{17}O_6N_5S$ requires C, 48.68; H, 4.09; N, 16.70; S, 7.64 %)

^{1}H NMR data: δ_H(250 MHz; solvent DMSO; standard TMS) 3.75 (6H, $-CH_2$), 7.54-7.92 (5H, $CH_{arom.}$), 8.18-8.49 (3H, NH-CO), 9.09 (1H, CH_{core}), 10.66 (1H, NH_{core}), 11.45 (1H, NH_{core})

Complex formation

Ligand exchange reactions on Tc(V) gluconate were carried out both at the "c.a." level and at the "n.c.a." level. Tc gluconate was prepared as previously described [4].

MAU and Tc(V)-gluconate at " c.a. " level

MAU was added to Tc(V) gluconate (1.3×10^{-4} M) both in neutral and in alkaline solution. The amount of MAU varies from equimolar ratio ligand/Tc to an eightfold excess.

MAU and Tc(V) gluconate at "n.c.a." level

0.5 mg MAU dissolved in 400 µl 0.1 N sodium hydroxide is added to 2 ml ^{99m}Tc gluconate prepared according to [4]. After a reaction time of 30 min the reaction mixture is neutralized by adding 40 µl 1 N hydrochloric acid.

MAG_2-AU and Tc(V)-gluconate at "n.c.a." level

50 µl 1 M sodium methylate was added to 3,4 mg of S-benzoyl protected amino-uracil-coupled MAG_2 dissolved in 200 µl DMSO. After 20 min the saponified ligand

was added to 2 ml ^{99m}Tc gluconate. The incubation time should not be less than 30 minutes.

Animal studies

The biodistribution and elimination of Tc-99m-MAU and Tc-99m-MAG_2-AU were investigated in mice. 74 kBq of the complexes were intravenously injected into mice. The animals were sacrificed after 0.5, 1, 3 and 5 h. The percentage of the injected dose (% ID) as well as the percentage of the injected dose per gram of tissue (% ID/g) were determined.

Results and discussion

Tc-MAU

At "c.a." level the formation of a 2:1 complex in alkaline solution can be deduced from the extinction at 380 nm in the UV/VIS spectra depending on the molar ratio MAU/Tc. Ligand exchange in neutral solution is incomplete but yields the same compound as shown by the UV/VIS spectra. In electrophoresis, both at pH 7 and pH 2, one anionic component was found with a mobility of $u_{rel} \sim 0.1$. Because there is no difference in the mobilities of the Tc-MAU complexes in the pH scale from pH 2 - 7, the charge of the complex anion is independent of changes in pH.

Investigations at the "n.c.a." level resulted in one component (95 %), detected by TLC (silicagel//ethanol/water 95:5), R_f = 0.70 and by HPLC (Hypersil ODS; 60 % MeOH/40 % phosphate buffer pH7// 10 % MeOH/90 % phosphate buffer pH 7), R_t 2.3 min.

In electrophoresis in phosphate buffer at pH 7 three components were separated: one neutral component (ca. 15 %) and two anions with $u_{rel} \sim 0.1$ (35 %) and $u_{rel} \sim 0.2$ (50 %).

A separation into three compounds was also found in glycine buffer at pH 2: $u_{rel} = 0$ (ca. 5 - 10 %); $u_{rel} \sim 0.2$ (ca. 15 %) and $u_{rel} \sim 0.5$ (ca. 75 %).

Whereas at "c.a." level protonation of any functional group of the ligand molecule can be excluded because of the electrophoretic behaviour , the pH-dependent behaviour of the main component at "n.c.a." level indicates a protonation of a functional group in the ligand molecule.

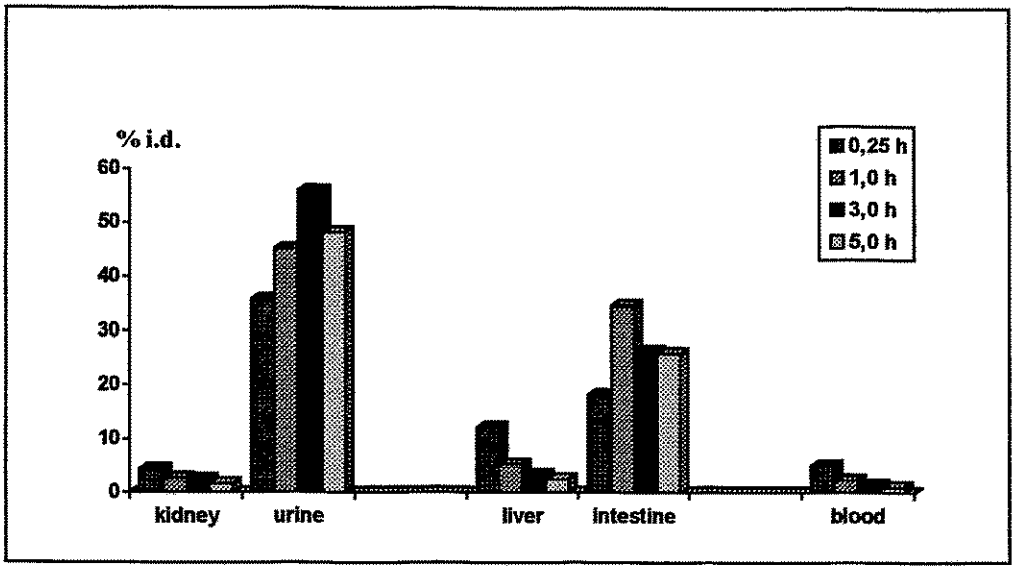

Fig. 2: Biodistribution of ^{99m}Tc-MAU in mice as a function of time

The biodistribution study of ^{99m}Tc-MAU in mice was carried out without further purification of the reaction mixture and is depicted in Fig. 2.

Tc-MAG_2-AU

In comparison with MAU the labelling of MAG_2-AU resulted in a relatively homogeneous product detected by electrophoresis. The by-products (<20 %) are probably Tc complexes of a higher ligand/Tc molar ratio analogeous to the by-products occurring in the preparation of the renal function agent ^{99m}Tc-MAG_3 [5]. The lower ion mobility (u_{rel} ~ 0.25) compared with ^{99m}Tc-MAG_3 (u_{rel} ~ 0.6) at pH 7 can be explained by the fact that there is no carboxylic group in the MAG_2-AU molecule and by the increased molecule size. In TLC (silicagel//methanol/water 95:5) the main component was found at R_f = 0.7 (ca. 80 %), the by-products at R_f = 0.15 and R_f = 0.6. Purification of the ^{99m}Tc-MAU_3 was carried out by HPLC on Kromasil RP 18 column and phosphate buffer pH 5.8/methanol 85/15 as eluent (R_t = 6.0 min).

These preliminary results are in accordance with the proposed speculative structures shown in Fig. 3. MAG_2-AU is expected to form a 1:1 complex analogous to the well known Tc-MAG_3 renal function agent, whereas MAU can form 4:1 or 2:1 complexes because there are only two donor atoms available in the ligand molecule. Investigations with MAG_2-AU at "c.a." level are in progress.

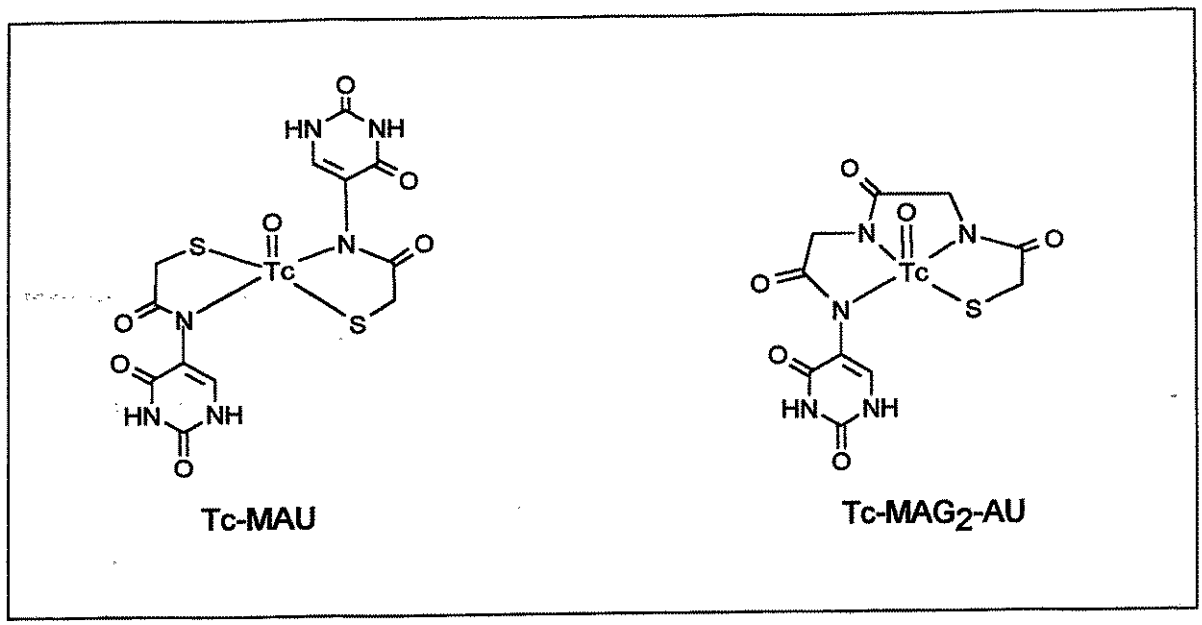

Fig. 3: Proposed structure of Tc-MAU and Tc-MAG_2-AU

The biodistribution study of ^{99m}Tc-MAG_2-AU in mice is depicted in Fig. 4.

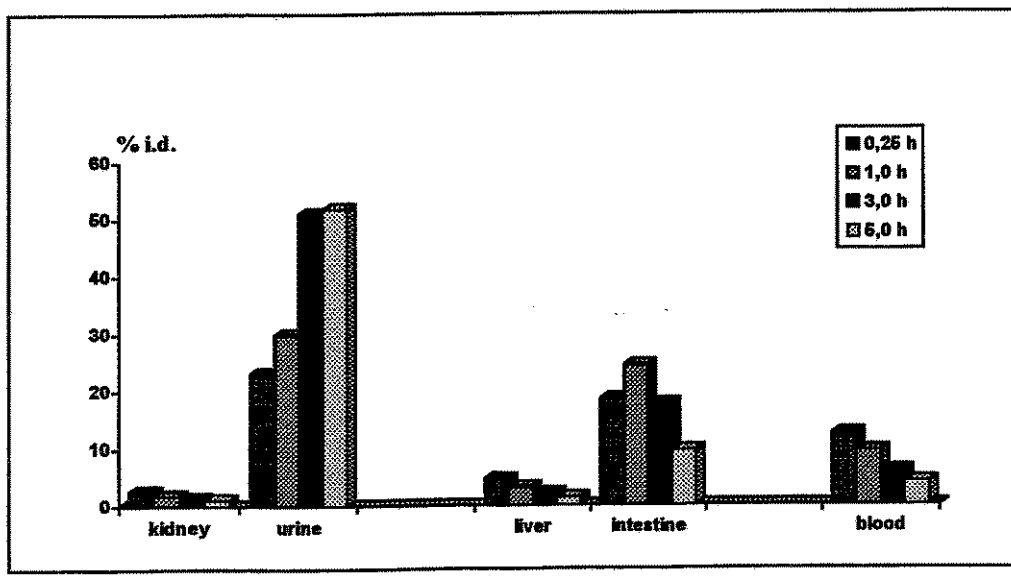

Fig. 4: Biodistribution of ^{99m}Tc-MAG_2-AU in mice as a function of time

References

[1] Dencker, L. et al., Pharmacol. Toxicol. **49** (1981) 141

[2] Hawthorne, M.F., Angew. Chem. **105** (1993) 997

[3] Noll, St. et al., Annual Report 1993, p. 63, Institute of Bioinorganic and Radiopharmaceutical Chemistry, FZR-32
[4] Noll, B. et al., Annual Report 1990, p. 36, ZfK-739
[5] Noll, B. et al., Int. J. Appl. Radiat. Isot. 43 (1992) 899

16. TECHNETIUM AND RHENIUM COMPLEXES OF DERIVATIZED NUCLEIC ACID COMPONENTS
2. TECHNETIUM COMPLEXES OF 5-MERCAPTOACETYLAMINO OROTIC ACID (MAOA)

St. Noll, B. Noll, H. Spies, L. Dinkelborg[1], W. Semmler[1]
[1]Institut für Diagnostikforschung Berlin

Orotic acid (6-carboxyuracil) is included in our studies as an interesting functional derivative of uracil. Whether or not the carboxylic group present in 6-position will participate in the coordination sphere and the influence on bio-behaviour are questions of special interest. From a physiological point of view, orotic acid is capable of crossing the intact blood barrier and of participating in the protein metabolism in the brain.

Synthesis of 5-mercaptoacetylamino orotic acid (MAOA)

Synthesis of the ligand follows the route shown in Fig. 1.

5-mercaptoacetylamino-orotic acid (MAOA)

5-chloroacetylamino-orotic acid was obtained by chloroacetylation of 5-amino-orotic acid in 1 N sodium hydroxide. Subsequent reaction with thiobenzoic acid gives 5-benzoyl-mercaptoacetylamino-orotic acid. 5-mercaptoacetylamino-orotic acid was obtained following the procedure described in [1]. The overall yield is 8 %.

Melting point: 320 °C (decomp.).

TLC (Silufol// n-butanol/acetic acid/water 2:1:1) R_f 0.25 (UV, ninhydrine)

Elemental analysis: (Found: C, 34.07; H, 2.59; N, 17.39; S, 13.22, $C_7H_7O_5N_3S$ requires C, 34.29; H, 2.88; N, 17.14; S, 13.07 %)

^{1}H NMR data: δ_H(250 MHz; solvent DMSO; standard TMS) 2.74 (1H, SH), 3.67

(2H, -CH_2), 9.30 (1H, NH-CO), 10.27 (1H, NH_{core}), 11.28 (1H, Nh_{core})

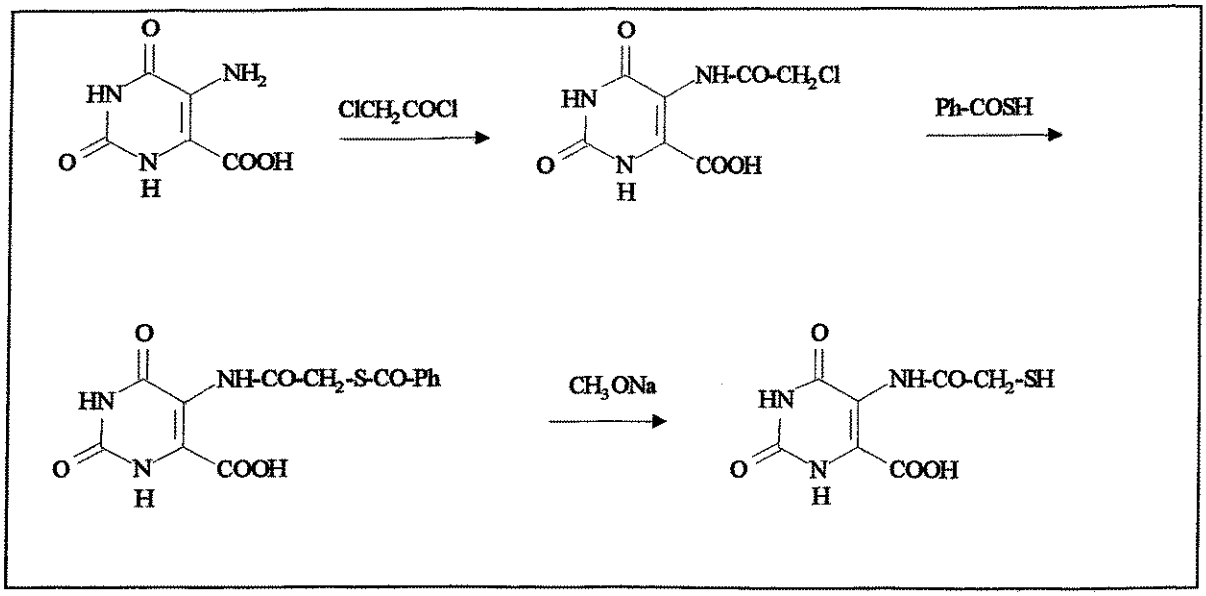

Fig. 1: Reaction scheme

Complex formation

Experiments were carried out with the MAOA ligand in order to obtain some first results concerning the affinity to form complexes with technetium. Reactions at "carrier added" level were performed with the S-protected ligand 5-benzoyl-mercaptoacetylamino-orotic acid because of its higher stability in comparison with the S-unprotected ligand.

MAOA is expected to form a MAOA/Tc 2:1 complex analogous to the Tc-MAU complex previously reported [2].

Preparation of the Tc complex at "c.a." level:

Complexes were prepared by ligand exchange reaction, starting from the Tc-gluconate complex: To $2.1*10^{-5}$ mol Bz-MAOA solved in 400 µl DMSO, 40 µl sodium methylate is added. The solution clouds due to the insolubility of the saponified ligand. By adding 100 µl water, the ligand is solved, and the molar equivalents according to the ligand/Tc molar ratio are added to the Tc-gluconate solution (prepared by addition of $1*10^{-6}$ mol stannous chloride to $1*10^{-6}$ mol potassium pertechnetate in 2 ml 0.05 M sodium gluconate solution).

Preparation of the Tc complex at "n.c.a."level

0.5 mg MAOA solved in 400 µl 0.1 N sodium hydroxide is added to 2 ml ^{99m}Tc gluconate prepared according to [3]. After 30 min the reaction mixture is neutralized by adding 40 µl 1 N hydrochloric acid.

Results and discussion

Addition of MAOA to Tc gluconate under spectrophotometric control leads to an increasing absorption maximum at 360 nm in the UV/VIS spectrum. (This value is compatible with Tc-carboxylic group coordination in the Tc-MAG_2 [4]). The molar ratio of the resulting Tc/MAOA species could not be determined because of incomplete complex formation, which can be explained either by an incomplete saponification of the benzoylic protected ligand or by the pH value of the reaction solution beeing too low. Up to a molar ratio of 8:1 a steady increase of extinction was observed. An analogous behaviour is known from the ligand exchange of MAU/Tc gluconate in neutral solution [2].

All analytical data determined are in good agreement both at "c.a." and "n.c.a." level. In electrophoresis (phosphate buffer pH 7) the incomplete reaction was confirmed. Up to a molar ratio of 4:1, both the Tc-MAOA complex and Tc gluconate are present in the reaction mixture.

It is noteworthy that the Tc-MAOA complex has a higher anionic mobility than the Tc-MAU complex (u_{rel} = 0.7 and 0.1). This high mobility can be explained by an additional negative charge of the Tc-MAOA anion due to the presence of a carboxylic group. The mobility of Tc-MAOA was diminished to u_{rel} = 0.4 in glycine buffer at pH 2 because of protonation of a "free" carboxylic group.

TLC (Silicagel60//ethanol/water 95:5) shows a peak at R_f = 0.2. In HPLC (RP 18 column//phosphate buffer/methanol 90:10) the reaction mixture was separated into three components with R_t = 1.8 min, R_t = 2.4 min and R_t = 2.8 min.

These peaks indicate the formation of several, probably isomeric complexes, which was expected in view of our previous experience with the MAG_n system.

References

[1] Noll, St. et al., Annual Report 1993, p.63, Institute of Bioinorganic and Radiopharmaceutical Chemistry, FZR-32

[2] Noll, St. et al., this report, p. 61

[3] Noll, B. et al., Annual Report 1990, p. 36, ZfK-739

[4] Johannsen, B. et al., Inorg. Chim. Acta **210** (1993) 209

17. TECHNETIUM AND RHENIUM COMPLEXES OF DERIVATIZED NUCLEIC ACID COMPONENTS
3. COMPLEX FORMATION OF TECHNETIUM WITH MAG_2 DERIVATIVES OF CYTIDINE

St. Noll, B. Noll, H. Spies, B. Johannsen

A further extension of our efforts to design Tc and Re complexes of nucleic acid components involves nucleosides. As a first representative, cytidine was allowed to react with S-benzoylmercaptoacetyldiglycine (Bz-MAG_2) to give the corresponding amide S-Bz-MAG_2-Cyt. This compound is expected to react as tetradentate SN_3 ligand after removing the benzoylic group and to form a stable anionic oxotechnetium complex to which the nucleoside as the pendant moiety is bound via the cytidine-amine group. The article describes the synthesis of the ligand S-Bz-MAG_2-Cyt and complexation experiments.

Synthesis of the ligand

Synthesis follows the way described in Fig. 1.

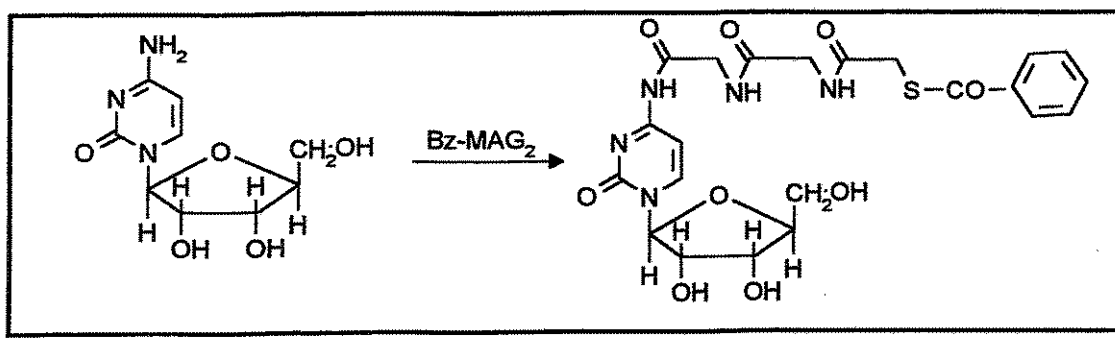

Fig.1: Reaction scheme

To a mixture of 160 mg (0.5 mmol) benzoyl-MAG_2 and 165 mg (0.5 mmol) O-(1H-benzotriazol-1yl)-N,N,N',N'-tetramethyluronium tetrafluoroborate (TBTU) in 1 ml of 1-methyl-2-pyrrolidone 170 µl (1 mmol) ethyldiisopropylamine was added while stirring vigorously. After 3 min the solution was dropped to 97.3 mg (0.4 mmol) cytidine dissolved in 1 ml of 1-methyl-2-pyrrolidone and stirring was continued for 4 h at room temperature. After that the solvent was removed in vacuum, the residue was dissolved in ethanol/water 1:1 and dried again. The brown crystals were extracted with hot water and on cooling the reaction product began to crystallize.

Yield: (144 mg, 67 %)

M.p. 136 °C

TLC: (Silufol// n-butanol/acetic acid/water 2:1:1) R_f 0.75 (UV)

(RP 18//methanol/water 9:1) R_f 0.7 (UV)

Elemental analysis: (Found: C, 49.60; H, 4.81; N, 12.79; S, 5.96, $C_{22}H_{25}N_5O_9S$ requires C, 49.34; H, 4.71; N, 13.08; S, 5.99%)

^{1}H NMR data: δ_H(250 MHz; solvent DMSO; standard TMS) 3.59 (2H, CH_2OH), 3.79 (2H, -CH_2-N), 3.80 (2H, CH_2), 3.98 (2H, -CH_2N), 5.03-5.78 (4H, ribose), 7.12 (1H, heterocycl.), 7.57 - 7.94 (5H, arom.), 8.21 (1H, NH), 8.43 (1H, heterocycl.), 8.53 (1H, NH), 10.91 (1H, NH).

Complexation reaction

UV/VIS spectra depending on the molar ratio Tc gluconate/MAG derivative were recorded by means of the spectrophotometer Specord S10. The chromatographic behaviour was determined by thin layer chromatography on silica gel and 95 % ethanol as the solvent and by HPLC on an RP 18 column (Hypersil ODS), 3 min isocratic, 15 min gradient +1 from 100 % A to 10 % A (solvent A: 0.01 M phosphate buffer pH 5.9, eluent B: methanol).

The S-benzoyl-protected ligand was saponified with sodium methylate and used without further purification. The ligand exchange reactions at "c.a." level were carried out with 5 x 10^{-4} M Tc(V) gluconate precursor by varying the molar ratio ligand/Tc in the range from 0.5 : 1 to 2 : 1 in neutral and alkaline solution.

Tc gluconate was prepared as previously described.

Results

Addition of an aqueous solution of MAG_2-Cyt to a neutral Tc gluconate solution gives a UV absorption at 360 nm, the extinction is increased with the increase of the molar ratio ligand/Tc (Fig. 1). The maximum extinction is only obtained with an excess of the ligand and is not altered by alkalization of this neutral solution.

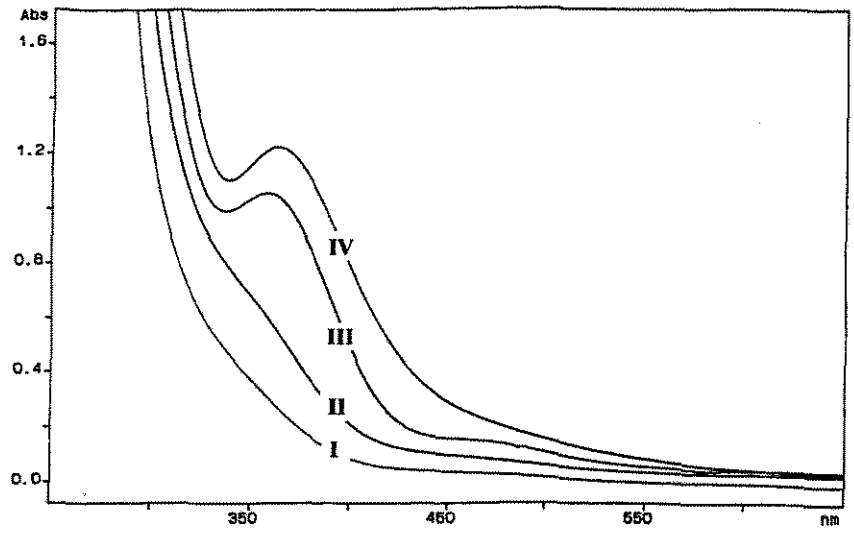

Fig. 1: UV spectra of the ligand exchange reaction Tc gluconate/MAG_2-Cyt at various molar ratios MAG_2-Cyt/ Tc-gluc., I - 0.5 : 1, II - 1 : 1; III - 2 : 1, IV - 4 : 1

If the ligand exchange is carried out in alkaline solution, no characteristic UV absorption is observed. It is therefore assumed that the absorption at 360 nm is caused by the component II obtained by HPLC analysis (Fig. 2). The anionic mobility of this complex was 0.6 related to that of pertechnetate both at pH 7.0 and pH 2.0.

The composition of the reaction mixtures depending on the molar ratio is listed in Table 1.

As indicated by HPLC, ligand exchange reaction with varying ligand/technetium ratio results mainly in two complexes of Tc-MAG_2-Cyt. At a 1:1 molar ratio in neutral solution two com-plexes I and II are obtained as shown in Fig. 2 with I being the predominant species.

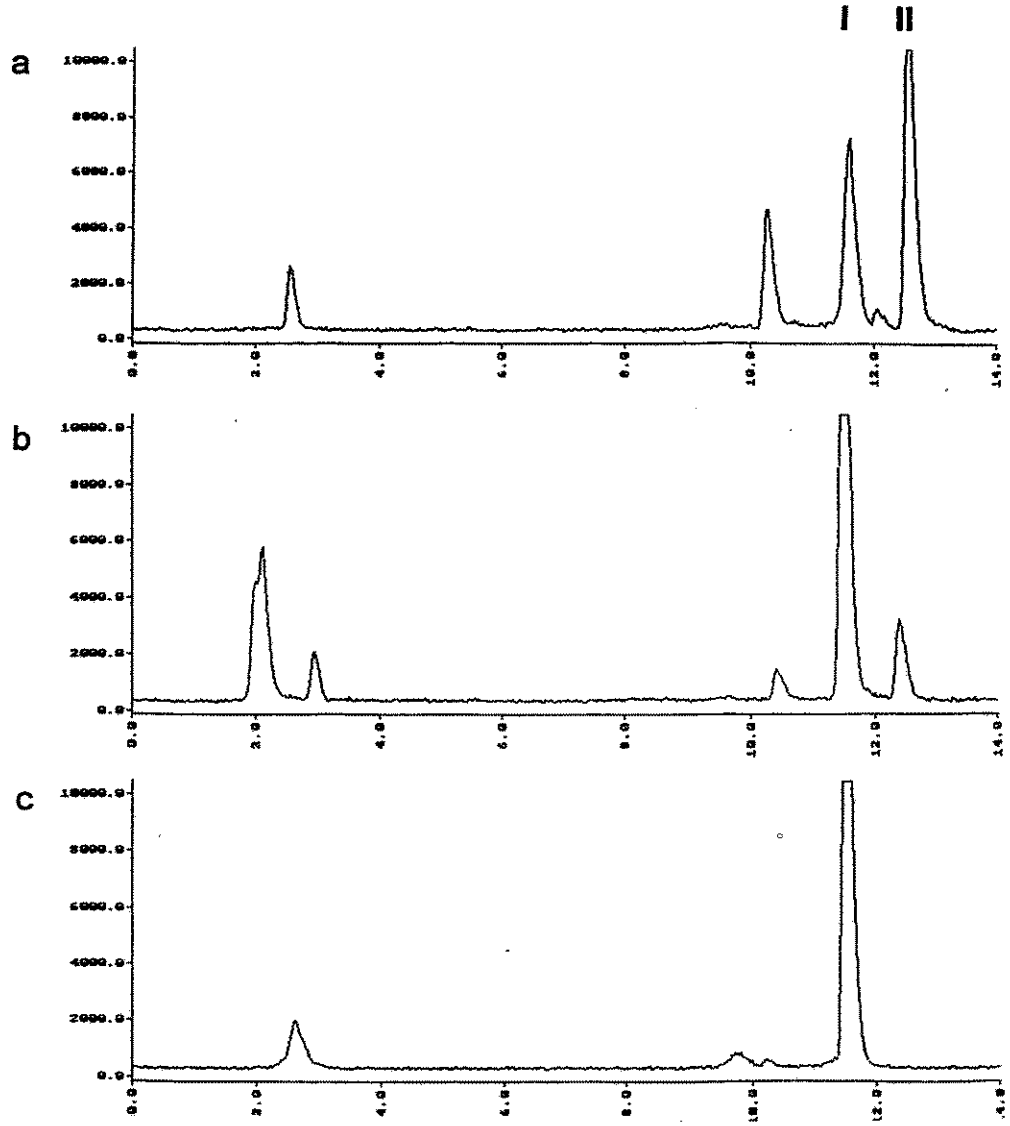

Fig. 2: HPLC separation of the reaction mixtures Tc/MAG_2-Cyt in dependence on the pH-value and the molar ratio (I : predominant complex at molar ratios ≤ 1, II : predominant complex in ligand excess)

a) molar ratio MAG_2-Cyt:Tc-gluc. 2:1; neutral solution

b) molar ratio MAG_2-Cyt:Tc-gluc. 1:1; neutral solution

c) molar ratio MAG_2-Cyt:Tc-gluc. 1:1; alkaline solution

An increase of the molar ratio leads to a reverse of the amounts of I and II. In alkaline solution only the complex I is formed. A similar behaviour was observed in the exchange reaction with MAG_3 as the ligand [1].

Table 1: Composition of the reaction mixture in dependence on the molar ratio MAG_2-Cyt/Tc gluconate and pH, reaction time 30 min

Molar ratio (MAG_2-Cyt : Tc gluc.)	HPLC		TLC	
	Tc gluc.	*Tc-MAG_2-Cyt*	*Tc gluc.*	*Tc-MAG_2-Cyt*
	R_t = 2.21'	R_t = 11.0'	R_f = 0	R_f = 0.8
		R_t = 11.8'		
		R_t = 13.0'		
neutral	[%]		[%]	
0.5:1	60.0	7.0	46	54
		28.0		
		5.0		
1:1	26.0	12.0	22	78
		48.0		
		14.0		
2:1	8.0	17.0	-	>95
		28.5		
		41.5		
alkaline				
	R_t = 2.21'	R_t = 11.8'		
0.5:1	60.0	40.0		
1:1	24.5	75.5		
2:1	8.0	92.0		

A possible explaination is that at low Tc/ligand ratios and at pH>11 the formation of the 1:1 complex is preferred while at any excess of ligand complexes with more than one ligand molecule bound to the Tc are formed. Compound II seems to be the 2:1 complex.

References

[1] Johannsen, B. et al., Radiochimica Acta 63 (1993) 133

18. SYNTHESIS OF N(2-MERCAPTOETHYL)NICOTINAMIDES

Zhi Fen Su, St. Noll, H. Spies

The design of new technetium and rhenium radiotracers may also make use of the ability of certain organic compounds to undergo redox processes *in vivo*.
To explore the principle of Bodor et al. [1], who demonstrated that drugs can be selectively delivered to the brain, using a dihydropyridine/pyridinium salt redox system for the design of redox-sensitive radiotracers, the synthesis of technetium and rhenium complexes equipped with the dihydropyridine/pyridinium redox system is necessary. This requires appropriate ligands with a pyridinium or dihydropyridine moiety. Because in our concept the ligands are intended to react as monodentates to form neutral mixed-ligand "3+1" complexes [2], the synthesis is aimed at the SH-functionalization of nicotinamide derivatives.
In continuing our first efforts concerning redox tracers [3], we now report on the synthesis of derivatives of N-(2-mercaptoethyl)-nicotinamide and derived pyridinium compounds.
Functionalization of the nicotinamide molecule with an -SH group is accomplished by introducing a 2-mercaptoethyl group at the amide N-atom.
Schemes 1 and 2 illustrate two different routes

Route 1, which is based on a procedure reported by Kuhn [4], involves an intramolecular rearrangement of the thiol ester formed in the reaction of thiol acids with aziridine to the corresponding N(2-mercaptoethyl) amides 1. However, the reaction was only successful with thioacetic acid and thiobenzoic acid but has so far failed with thionicotinic acid. Obviously the latter forms dimer products instead of 5 under the conditions used for purification of the reaction mixture.

An alternative route 2 starts with nicotinic acid, from which N-nicotinoylethylene imines 2 were prepared by reaction with ethylene imines in the presence of dicyclohexylcarbodiimide in DMF [5]. The attached ethylene imine rings are activated and can be opened with thiobenzoic acid to give the S-protected compounds 3. Subsequent alkylation results in the S-benzoylated N-alkylpyridinium salts 4. The

compounds are obtained in good yields by refluxing 3 with methyl iodide, propyl iodide, or benzyl chloride with or without a solvent.

Reaction scheme 1:

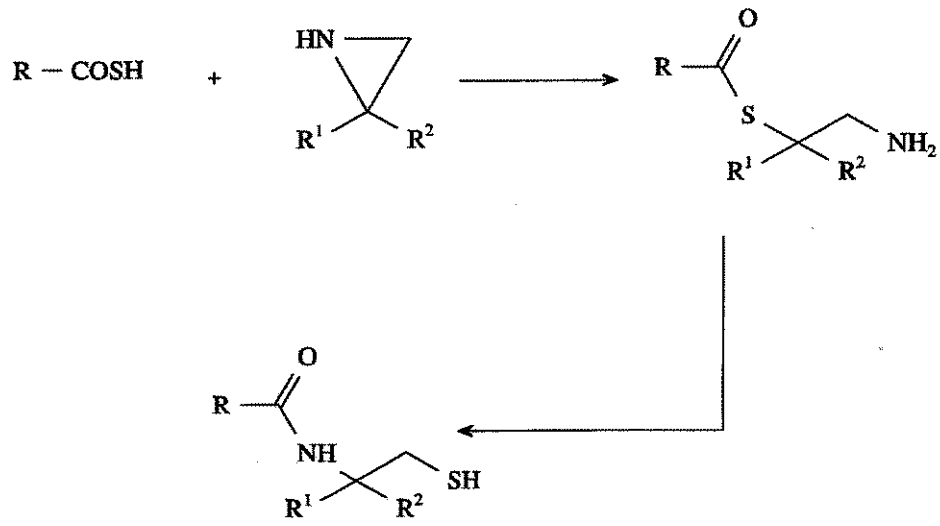

1	R	R^1	R^2
a	CH_3	H	H
b	CH_3	H	CH_3
c	C_6H_5	H	H
d	C_6H_5	H	CH_3
e	C_5H_4N	H	CH_3
f	C_5H_4N	H	CH_3

The crucial point of the synthesis of the mercapto ligand is the removal of the protective benzoyl group. Treatment of 3 with sodium methylate followed by acidification of the mixture converts 3 completely into 5 even at 0 °C in about half an hour, but a large amount of disulphide is formed as a side product. The reaction conditions must therefore be modified.

Reaction scheme 2:

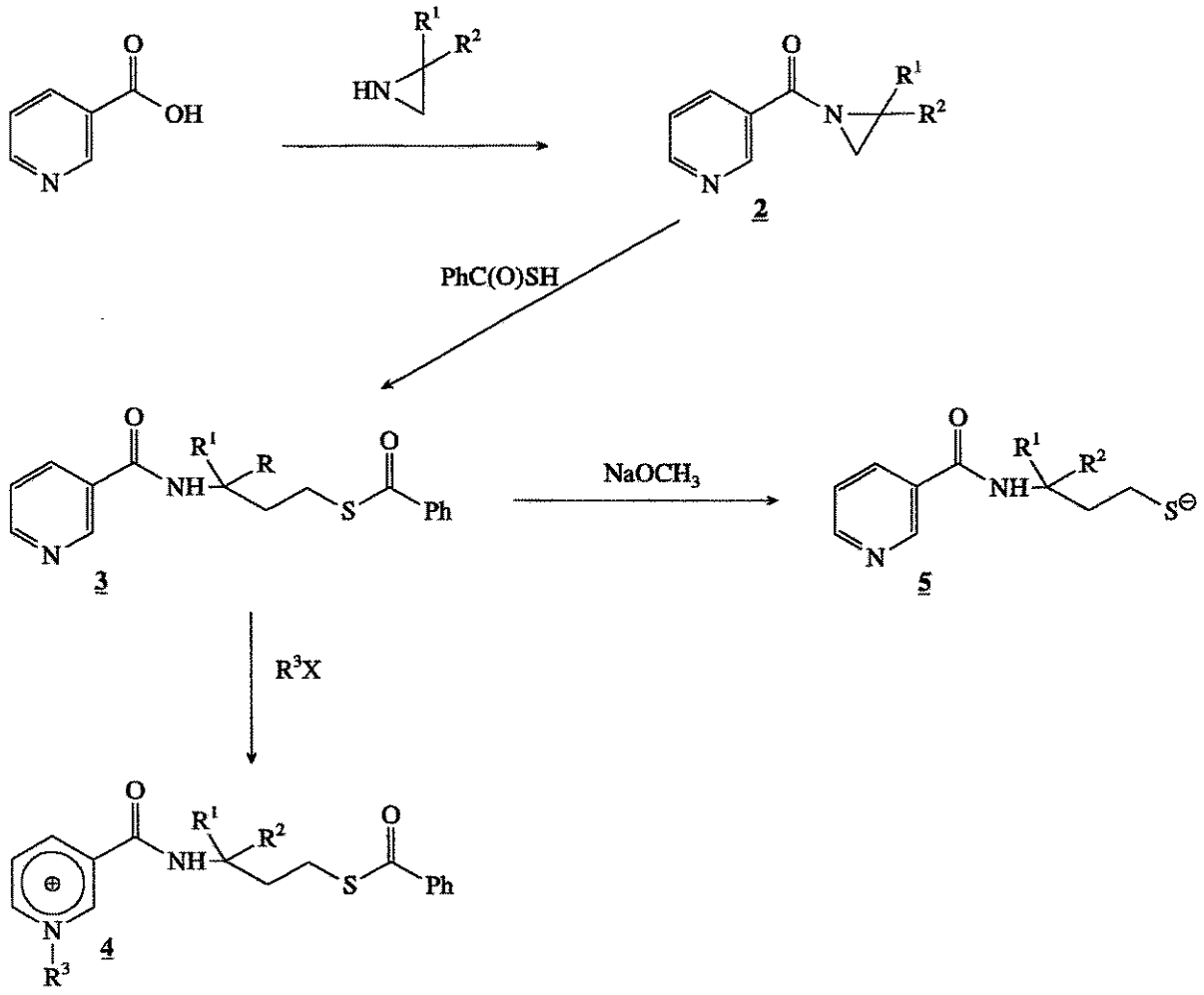

2, 3	R^1	R^2	4	R^1	R^2	R^3	X
a	H	H	a	H	H	CH_3	I
b	H	CH_3	b	H	H	$CH_2CH_2CH_3$	I
c	CH_3	CH_3	c	H	H	$CH_2C_6H_5$	Cl
			d	H	CH_3	CH_3	I
			e	H	CH_3	$CH_2CH_2CH_3$	I
			f	CH_3	CH_3	CH_3	I

References

[1] Bodor, N. and A. M. Abd el Alim, J. Pharm. Soc. **74** (1985) 241

[2] Spies, H. et al., Annual Report 1992, p. 94, Institute of Bioinorganic and Radiopharmaceutical Chemistry, FZR 93-12

[3] Bergmann, R. et al., Annual Report 1992, p. 122, Institute of Bioinorganic and Radiopharmaceutical Chemistry, FZR 93-12

[4] Kuhn, R. and G. Quadbeck, Chem. Ber. **84** (1951) 844

[5] Ross,W. C. J. et al., J. Med. Chem. **10** (1967) 257

19. RADIOCHEMICAL PURITY OF ^{99M}Tc-HM-PAO: CRITICAL PARAMETERS DURING KIT PREPARATION

S. Seifert, O. Muth[1], K. Jantsch[1], B. Johannsen

[1]Verein für Kernverfahrenstechnik und Analytik, Rossendorf

The instability of the reconstituted HM-PAO kit is characterized by the tendency of the primary lipophilic complex content to diminish with time, producing a secondary, less lipophilic, complex and pertechnetate. Factors which favour the decomposition of the lipophilic complex are its own instability, high doses of radiation, the presence of excess Sn^{2+} ions and a pH greater than 9 [1,2]. The radiochemical purity specification of not less than 80 % lipophilic complex requires that the kit be used within 30 min of reconstitution.

A number of approaches have been tried to extend the post-reconstitution shelf life from 30 min and to overcome the restrictions imposed on the eluate used [3,4,5]. Additions of weak chelating agents, oxidizing agents, free radical scavengers, ethanol, pH-adjusting agents and metal ions which could form complexes with HM-PAO were tested. The best results were achieved by the addition of cobalt chloride to the reconstituted kit, which can extend the shelf life to at least 5 h post reconstitution [6].

The time and temperature proved to be critical parameters during the kit preparation. We found that without adding any stabilizing agents a higher stability of the

reconstituted kit is obtained, if the Sn^{2+}/HM-PAO solution is allowed to stand at room temperature for at least 1 h before freeze-drying.

Following the regulations of a usual kit preparation, the ligand and the reducing agent are dissolved in saline or other solvents and mixed to give the stock solution. The solution is cooled and bubbled with nitrogen to prevent a rapid oxidation of stannous chloride. Aliquots of this solution are bottled as quickly as possible into the kit vials, immediately frozen in liquid nitrogen and freeze-dried. Hundreds of vials have to be filled at this step of kit production. That results in time differences of 30 or more minutes between bottling of the first and the last vial. As this could be the reason of the differences in radiochemical purity observed for individual vials of one batch, we made the following experiments:

As a first step the time before bottling was extended to 1 and 2 h. As a second step the cooling was omitted and the time was reduced again to one hour.

Using kits containing 0.5 mg HM-PAO (94 % d,l form), 5.0 µg $SnCl_2 \times 2H_2O$ and 4.5 mg NaCl in freeze-dried form results in the specified stabilities of the primary complex (Table 1). The yields of primary and secondary complex and pertechnetate were determined by HPLC (Fig. 1) according to [7]. Only traces of pertechnetate were detected after 60 min. 2 - 3 % of reduced hydrolysed technetium were found on an average by TLC. The results are reproducible and only small differences in radiochemical purity are observed from vial to vial.

The same results were obtained using 7.5 µg $SnCl_2 \times 2\ H_2O$ per vial as described for the original kit formulation.

Table 1: Stability of the primary complex as a function of time and temperature used during kit preparation

t[min]	T[°C]	Number of batches	Stability as % primary complex 10 - 120 min post reconstitution		
			10	60	120
10	0	6	90 ± 3	58 ± 8	
60	0	2	92 ± 3	78 ± 3	
60	20	6	94 ± 2	86 ± 6	77 ± 12
120	0	2	94 ± 2	85 ± 3	78 ± 9

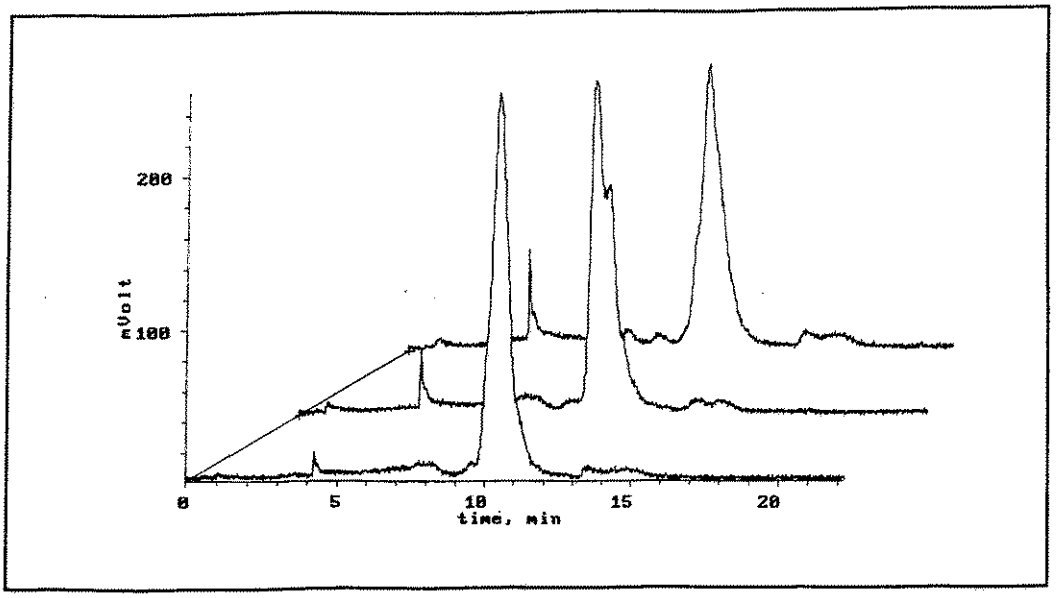

Fig. 1: HPLC analyses of ^{99m}Tc d,l-HM-PAO 10, 35 and 60 min post reconstitution with 1.5 GBq $^{99m}TcO_4^-$

The relatively high background of the chromatograms between 5 and 10 min at 1.0 GBq or more seems to be caused by the instability of the primary complex, which increases dramatically if the ligand excess is removed. That is the case during the HPLC analysis, because the free ligand is eluted from the column with another elution time than the primary complex. We separated the primary complex fraction and reinjected it after 15 and 35 min. The chromatograms show a nearly quantitative decomposition of the primary complex, mainly to pertechnetate (Fig. 2). That means, that small amounts of the primary complex decompose during the analysis.

At present not enough information is available to explain the higher stability of ^{99m}Tc-HM-PAO preparations. A possible explanation could be that time-dependent complex formation of Sn^{2+} and HM-PAO, which is accelerated at room temperature, is responsible for the higher stability of the primary complex. Corresponding investigations by HPLC, TLC and electrophoresis studies with non-radioactive and radioactive ^{113}Sn were carried out. The results obtained do not indicate any complex formation of Sn^{2+} with HM-PAO. .

A time-dependent hydrolysis of stannous ions to a colloidal solution of stannous hydroxide should also be discussed as an explanation of the improvement of the quality of the kit. Investigations of freeze-dried samples of various Sn^{2+} / HM-PAO /

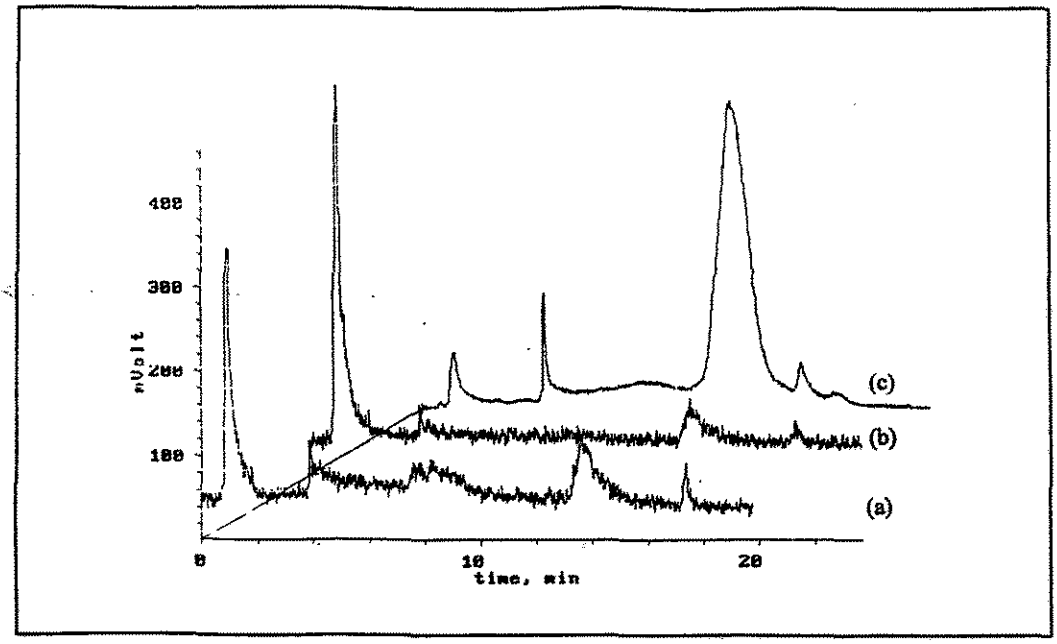

Fig 2: HPLC analyses of ^{99m}Tc-HM-PAO after 35 min (a) and reinjection of the separated primary complex fraction after 15 (b) and 35 min (c)

NaCl solutions by electron microscope studies showed only little change in microscopic appearance. No differences were observed between kit samples freeze-dried after 5 and 120 min.

Acknowledgements

The authors wish to thank Dr. (Mrs.) R. Müller and Mrs. E. Christalle (FWAS) for electron microscope studies.

References

[1] Ramamoorthy, N. et al., Nucl. Med. Biol. **20** (1993) 307

[2] Hung, J. C. et al., J. Nucl. Med. **29** (1988) 1568

[3] Reymen, M. et al., Eur. J. Nucl. Med. **18** (1991) 532

[4] Bayne, V. J. et al., Nucl. Med. Commun. **10** (1989) 29

[5] Lang, J. et al., Eur. J. Nucl. Med. **15** (1989) 424

[6] Weisner, P. S. et al., Eur. J. Nucl. Med. **20** (1993) 661

[7] Neirinckx, R. D. et al., J. Nucl. Med. **28** (1987) 191

20. PREPARATION OF 2-[^{18}F]FLUORO-2-DEOXY-D-GLUCOSE BY ALKALINE HYDROLYSIS OF 2-[^{18}F]FLUORO-1,3,4,6-TETRA-O-ACETYL-D-GLUCOSE

1. ELECTROPHILIC REACTION

F. Füchtner, J. Steinbach, R. Lücke, R. Scholz[1], K. Neubert

[1]Technische Universität Dresden, Klinik für Nuklearmedizin

Introduction

Quite a few methods to prepare ^{18}F labelled 2-[^{18}F]fluoro-2-deoxy-D-glucose ([^{18}F]FDG) have been reported in the literature [1]. The widespread use of the radiopharmaceutical [^{18}F]FDG in diagnostic procedures with Positron Emission Tomography (PET) means that efforts towards improving and simplifying the synthesis of [^{18}F]FDG are worthwhile.

In 1993 a remote controlled apparatus for routine preparation of [^{18}F]FDG on the basis of the electrophilic reaction according to Bida [2] was set up at Rossendorf [3]. Since then more than 70 preparations for animal and biochemical experiments and for optimization of the preparation procedure have been carried out. The preparation system proved to be simple and very reliable. During preparation and determination of the chemical and radiochemical purity [4] we found it possible to remove the acetyl groups of the 2-[^{18}F]fluoro-1,3,4,6-tetra-O-acetyl-D-glucose (TA-[^{18}F]FDG) by alkaline hydrolysis in a very short time and at room temperature.

This paper reports on the possibility of removing the protective groups by alkaline hydrolysis in contrast to the commonly used time-consuming acidic hydrolysis with thermal treatment.

Experimental

The investigations for optimizing the conditions for alkaline hydrolysis were carried out in the remote controlled laboratory system described in [3]. In contrast to the previous procedure we introduced the following modifications.

Fluorination

The absorption of the gaseous acetylhypofluorite ([^{18}F]AcOF) in a solution of 30 mg tri-O-acetyl-D-glucal (TAG, for synthesis, MERCK - Schuchardt) in 15 ml trichlorofluoromethane ($CFCl_3$, freon 11, for synthesis, MERCK - Schuchardt) at room

temperature led to TA-[^{18}F]FDG.

Removal of protective groups

Search for optimum conditions of alkaline hydrolysis

10 ml of distilled water were added to the remaining 5 ml of $CFCl_3$. By blowing in gaseous N_2 at a flow rate of about 100 ml/min, the remaining solvent was evaporated at room temperature. After the evaporation [^{18}F]F^- and TA-[^{18}F]FDG were in the aqueous phase. From the remaining aqueous solution a 1 ml aliquot was mixed with different amounts of a sodium hydroxide stock solution (prepared from a standard solution, MERCK) and distilled water, so that the final volume was always 2 ml. As a result we obtained solutions with sodium hydroxide concentrations of 0.01, 0.05, 0.1, 0.3, 0.5, 1, 2.5 and 4.5 M NaOH. From each of these solutions a sample was immediately analysed by thin-layer chromatography (TLC) [5] after adding the hydroxide solution and mixing it. Further samples were taken at time intervals of 0.5, 1, 2, 5, 10 and 20 min.

Standard preparation procedure

After the fluorination of the precursor, 2 ml of 0.3 M sodium hydroxide (prepared from a standard solution, MERCK) were added to the remaining solvent. By blowing in gaseous N_2 at a flow of about 100 ml/min the remaining 5 ml $CFCl_3$ were evaporated at room temperature. During evaporation the TA-[^{18}F]FDG was dissolved in the aqueous phase, the protective groups were removed and [^{18}F]FDG was formed.

Purification

The reaction mixture was purified by using a combination of liquid chromatographic columns. On the first column (d_i = 6 mm, L = 100 mm, OMNIFIT) filled with 2 ml cation exchanger (DOWEX 50 WX 8, 100 - 200 mesh, H^+-form, SERVA or for pharmaceutical use AG 50W-X, 200 - 400 mesh, H^+-form, BIO-RAD) the hydrolysis mixture was neutralized. To retain the partly hydrolysed intermediate products, a solid-phase extraction was employed on a styrene-divinylbenzene resin (LiChrolut® EN 1 g, MERCK) in an LC column (d_i = 6 mm, L = 100 mm, OMNIFIT) [6]. For this purpose charcoal (activated carbon, Darco G-90, ALDRICH, fraction > 50 µm) could also be used. The last column was a SEP-PAK cartridge ALUMINA A (Millipore) for retention of [^{18}F]F^-.

The [^{18}F]FDG was eluted from the columns with sterile water (aqua ad iniectabilia,

Serum-Werk Bernburg). For isotonic adjustment a calculated amount of NaCl (extra pure, MERCK) was added. The sterilization of the final product was achieved by sterile filtration (microporous membrane cellulose acetate, 0.22 µm, ALLTECH).

Results

Fluorination

After the reaction between TAG and the gaseous [^{18}F]AcOF had taken place about 5 ml of solvent remained in the reaction vessel. The step of fluorination took about 35 minutes, including 10 minutes for transporting the radioactivity from the cyclotron through a transporting tube over a distance of 500 m and the evaporation of the remaining solvent. The TA-[^{18}F]FDG yield was about 90 %.

Removal of protective groups

Search for optimum conditions of alkaline hydrolysis

The concentration of the sodium hydroxide was optimized so as to minimize both the alkaline concentration needed and the reaction time, on the one hand, and to maximize the yield of the reaction, on the other.

Fig. 1 gives an example of the kinetic investigations and shows an autoradiogram of the product of hydrolysis with 0.05 M NaOH after different reaction times. These conditions were suitable for following up the course of hydrolysis.

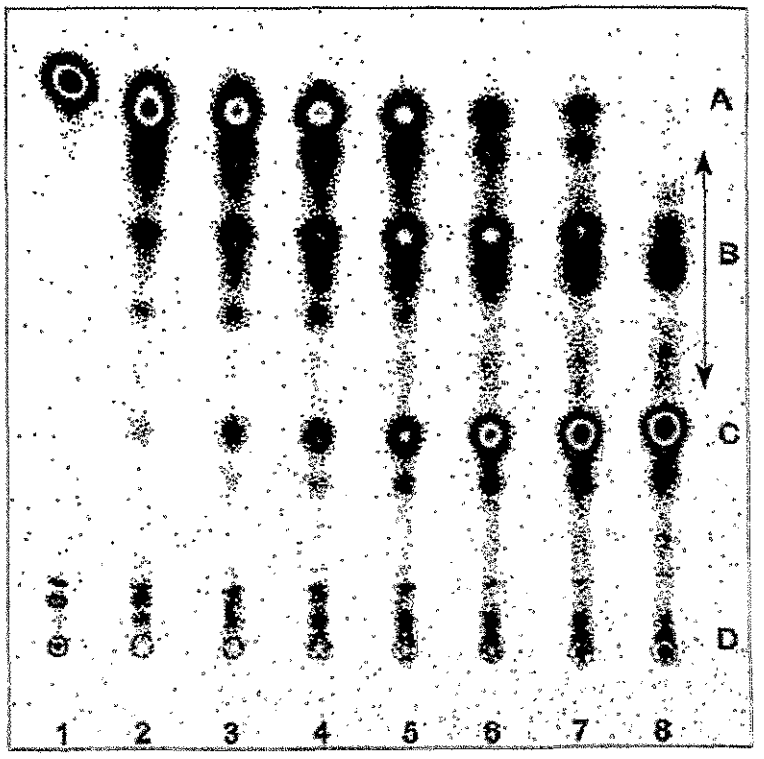

Fig. 1
Autoradiogram of a TLC plate used for kinetic study of alkaline hydrolysis (0.05 M NaOH)

A - TA-[^{18}F]FDG
B - partly hydrolysed TA-[^{18}F]FDG
C - [^{18}F]FDG + [^{18}F]FDM
D - [^{18}F]F$^-$
sampling time
1 - unhydrolysed TA-[^{18}F]FDG
2 - after mixing
3 - 0.5 min 4 - 1 min
5 - 2 min 6 - 5 min
7 - 10 min 8 - 20 min

Fig. 2 shows the forming rate and the yield of forming [^{18}F]FDG during conversion of TA-[^{18}F]FDG to [^{18}F]FDG depending on the concentration of sodium hydroxide. The figure shows that the forming rate for [^{18}F]FDG increases with increasing hydroxide concentration. However, the yield of forming [^{18}F]FDG reaches a maximum at a sodium hydroxide concentration of 0.3 M. In this case about 90 % of the TA-[^{18}F]FDG are converted into [^{18}F]FDG and the overall yield up to this step of synthesis is about 80 %.

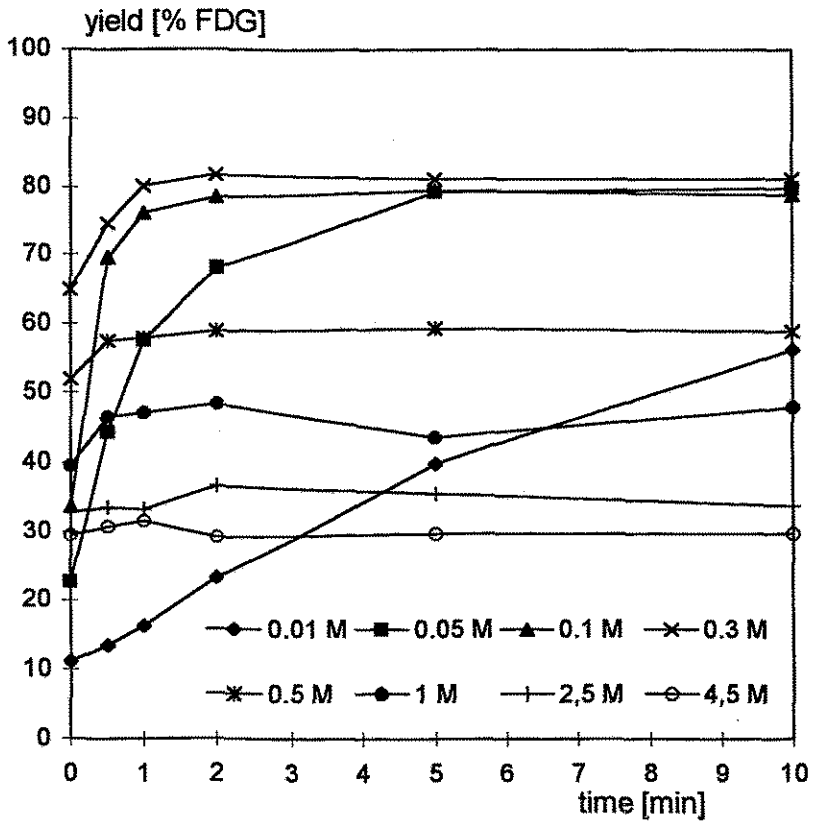

Fig.2 Dependence of forming [^{18}F]FDG on the sodium hydroxide concentration and reaction time during the alkaline hydrolysis starting with the reaction mixture after fluorination

Using a 0.3 M solution for hydrolysis, the maximum reaction yield is reached after about one minute. In addition, this concentration is favourable for the neutralization of the reaction mixture. A cation exchanger with a capacity of only 0.6 mmol is required in this case.

At higher hydroxide concentrations more [^{18}F]F$^-$ is formed and the yield for [^{18}F]FDG decreases.

Standard preparation procedure

The evaporation of the residual solvent takes about 7 minutes. The reaction product is a clear and colourless solution. Fig. 3 shows a series of thin-layer chromatograms

of the alkaline hydrolysis in comparison with acid hydrolysis.

The yield of forming [^{18}F]FDG and 2-[^{18}F]fluoro-2-deoxy-D-mannose ([^{18}F]FDM) under alkaline conditions is between 75 and 80 %. This is about 20 % higher than when using acid reaction conditions. However, without thermal treatment of the alkaline hydrolysis solution, a residue peak of a partly hydrolysed TA-[^{18}F]FDG or of a by-product is observed in the chromatogram (see peak in Fig. 3 marked *). This peak is found in all cases of alkaline hydrolysis and has a yield of about 5 % of the overall radioactivity.

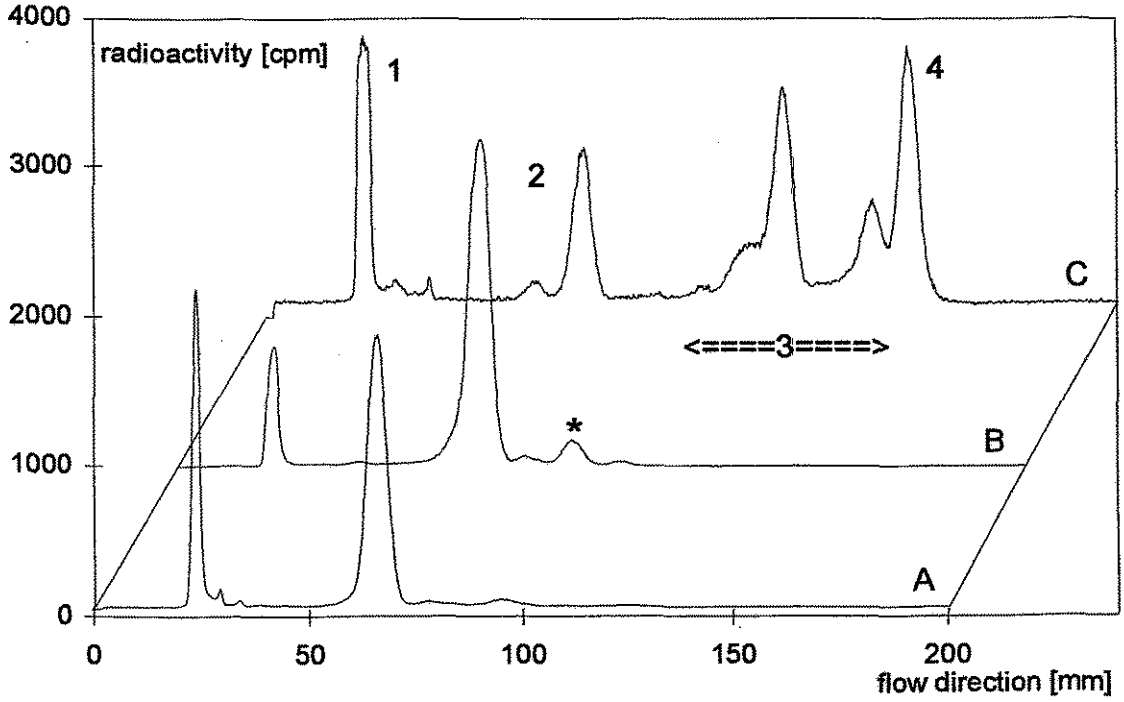

Fig. 3: TL chromatograms of different hydrolysates

A - acid hydrolysis, B - alkaline hydrolysis, C - alkaline hydrolysis (partly hydrolysed, 0.05 M NaOH, reaction time 2 min, compare Fig. 1)

1 - [^{18}F]F$^-$, 2 - [^{18}F]FDG + [^{18}F]FDM, 3 - partly hydrolysed TA-[^{18}F]FDG, 4 - TA-[^{18}F]FDG

Purification

The separation of compound " * " requires an additional purification step in contrast to the formerly described procedure [3]. A method for the separation of such a polar by-

product is the solid-phase extraction. Charcoal or polymeric resin is suitable for this purpose.

A separation of [^{18}F]FDG from the partly hydrolysed by-products by charcoal is only obtained under alkaline conditions. Using for example 0.1 M NaOH, [^{18}F]FDG and [^{18}F]F$^-$ are eluted from the charcoal column, whereas the by-product " * " is retained on the column. To reproduce charcoal columns with suitable chromatographic properties is difficult.

The polymer resin is simpler to handle and water can be employed as an eluent. A further advantage of resin is the possibility of regeneration of the whole chromatographic system for multiple use.

The radiochemical purity of the final product mixture of [^{18}F]FDG and [^{18}F]FDM is determined to >99 %. The concentration of the used solvent $CFCl_3$ in the final product is analysed by GC to < 10 µg/ml.

Synthesis in general

The total preparation time after EOB is about 40 minutes. Taking into consideration the splitting of the [^{18}F]F_2 radioactivity into [^{18}F]AcOF and [^{18}F]KF, the transporting losses and the synthesis and chromatographic separation, the total yield of [^{18}F]FDG is between 25 and 35 % EOS (uncorrected for decay). The yield starting from the fluorination step amounts to between 60 to 75 %.

Conclusion

The alkaline hydrolysis of TA-[^{18}F]FDG during the preparation of [^{18}F]FDG has the following advantages:

- Alkaline hydrolysis results in a reaction yield about 20 % higher than when using acid hydrolysis.
- All steps of synthesis can be performed at room temperature. The synthesis unit therefore becomes simpler, more reliable and easier to control.
- Because of the high speed of hydrolysis, the step of removing the protective groups does not take time in practice. Under acid conditions this step takes about 10 to 20 minutes. Therefore the yield of the preparation can be increased by 6 to 13 % by time saving.
- In the literature there is an indication of forming 2-deoxy-2-chloro-D-glucose (ClDG) as a chemical impurity during the preparation of [^{18}F]FDG, using acid hydrolysis with

HCl [7,8]. Using alkaline hydrolysis this by-product is not formed.

References

[1] Stöcklin, G. et al., "Radiopharmaceuticals for PET", Kluwer Academic Publisher, Dordrecht, 1993

[2] Bida, G.T. et al., J. Nucl. Med.. **25** (1984) 1227

[3] Füchtner, F. et al., Annual Report 1993, p. 14, Institute of Bioinorganic and Radiopharmaceutical Chemistry, FZR-32

[4] Füchtner, F. et al., Annual Report 1993, p. 17, Institute of Bioinorganic and Radiopharmaceutical Chemistry, FZR-32

[5] Füchtner, F. *et al., this report, p. 92*

[6] Hamacher, K., Forschungszentrum Jülich, Institut für Nuklearchemie, private communication

[7] Alexoff, D. L. et al., Appl. Radiat. Isot. **43** (1992) 1313

[8] Chaar, M. R. et al., Appl. Radiat. Isot. **45** (1994) 267

21. PREPARATION OF 2-[^{18}F]FLUORO-2-DEOXY-D-GLUCOSE BY ALKALINE HYDROLYSIS OF 2-[^{18}F]FLUORO-1,3,4,6-TETRA-O-ACETYL-D-GLUCOSE

2. NUCLEOPHILIC SUBSTITUTION

F.Füchtner, J. Steinbach, R.Lücke, R. Scholz[1], K. Neubert

[1]Technische Universität Dresden, Klinik für Nuklearmedizin

Introduction

The advanced procedures for routine preparation of 2-[^{18}F]fluoro-2-deoxy-D-glucose ([^{18}F]FDG) are based on nucleophilic substitution of the triflate leaving group in 1,3,4,6-tetra-O-acetyl-2-O-trifluoromethanesulphonyl-beta-D-mannopyranose (FDG-precursor) with [^{18}F]F$^-$ using a phase-transfer catalyst analogous to Hamacher et al. [1]. Many modifications of the [^{18}F]FDG synthesis have been described since its introduction to produce this important radiotracer more efficiently.

The aim of this paper is to report on the possibility of applying alkaline hydrolysis [2]

to prepare [^{18}F]FDG by nucleophilic substitution to shorten the preparation time.

Experimental

Fluorination

The non-carrier added [^{18}F]F$^-$ was produced via ^{18}O(p,n)^{18}F nuclear reaction using 200 µl ^{18}O (95 %) enriched water (Chemotrade ChemiehandelsgesellschaftmbH) in a silver target [3] using 13 MeV protons of the Rossendorf U-120 cyclotron.

The investigations for this synthesis were carried out in a simple experimental apparatus. The 200 µl [^{18}O]water/[^{18}F]F$^-$ were added to the reaction vessel (15 ml reaction vial with septum) containing a solution of 4.6 mg potassium carbonate (MERCK) and 7 mg Kryptofix^{TM} 2.2.2 (MERCK) in 1.5 ml acetonitrile/water (88 : 12). The solution was concentrated to dryness by heating to 90 °C in an oil bath and introducing an N_2 carrier gas flow of 100 ml/min. The process was repeated with 1 ml of anhydrous acetonitrile (MeCN, Fluka). A solution of 20 mg FDG-precursor (Fluka) in 1 ml anhydrous MeCN was added to the reaction vessel and the solution was refluxed for 5 minutes at a temperature of 90 °C yielding 2-[^{18}F]fluoro-1,3,4,6-tetra-O-acetyl-D-glucose (TA-[^{18}F]FDG) .

The reaction solution was evaporated to dryness by heating to 90 °C and using a carrier gas flow of N_2 at 100 ml/min.

Removal of protective groups

Search for optimum conditions of alkaline hydrolysis

The gas flow leaving the reaction vessel for analysing purposes was passed through a cooled vial to trap the condensate. 10 ml of distilled water were transferred to the reaction vial and the solution mixed by bubbling nitrogen gas through the liquid for one minute. A 1ml aliquot from this solution was mixed with different volumes of a sodium hydroxide stock solution (prepared from a standard solution, MERCK) and distilled water, so that the final volume was always 2 ml. As a result we obtained solutions with sodium hydroxide concentrations of 0.01, 0.05, 0.1, 0.2, 0.3, 0.5 and 1 M NaOH. From each of these solutions a sample was analysed by thin-layer chromatography (TLC) [4] immediately after adding the hydroxide and mixing it. Further samples were taken at time intervals of 0.5, 1, 2, 5, 10 and 20 min.

Standard preparation procedure

The fluorinated precursor was hydrolysed by adding 2 ml of 0.3 M NaOH to the reaction vessel. The hydrolysate was mixed by N_2 bubbles for one minute at room temperature.

Purification

For purification purposes the reaction mixture containing [^{18}F]FDG, partly hydrolysed TA-[^{18}F]FDG, [^{18}F]F$^-$, Kryptofix™ [2.2.2] and by-products was loaded on a column system. On the first column (d_i= 6 mm, L = 100 mm, OMNIFIT) filled with 2 ml cation exchanger (DOWEX 50 WX 8, 100 - 200 mesh, H^+-form, SERVA or for pharmaceutical use AG 50W-X8, 200 - 400 mesh, H^+-form, BIO-RAD) the hydrolysis mixture was neutralised and the Kryptofix™ 2.2.2 was separated. The concentration of Kryptofix™ 2.2.2 was determined by a spectrophotometric method using a lead(II) 1:1 complex (stock solution, $Pb(ClO_4)_2$, 1.5 mg/100 ml) and measuring the absorption of the complex at a wavelength of 250 nm [5].

To retain the partly hydrolysed intermediate products a solid-phase extraction on a cartridge of styrene-divinylbenzene resin (LiChrolut® EN 0.2 g, MERCK) is applied [6]. The last column is a SEP-PAK® cartridge ALUMINA A (Millipore) for retention of [^{18}F]F$^-$ The [^{18}F]FDG is eluted from the columns with sterile water (aqua ad iniectabilia, Serum-Werk Bernburg). For isotonic adjustment a calculated amount of NaCl (extra pure, MERCK) is added. The sterilization of the final product is achieved by sterile filtration (microporous membrane cellulose acetate, 0.22 µm, ALLTECH).

Results

Fluorination

The step of fluorination including all the drying processes, takes about 25 minutes. The yield of the substitution step and forming TA-[^{18}F]FDG is about 80 - 90 %, using freshly prepared precursor solution. During evaporation up to 20 % of the radioactive substances are lost, depending on the quality of the precursor. Using a freshly prepared charge of FDG-precursor solution, this amount can be reduced to 5 %. Analysing the condensate from the cooling trap, we found that about 98 % of all radioactive substances are [^{18}F]F$^-$ and the residual activity is TA-[^{18}F]FDG. For radiation protection it is useful to apply an absorption vessel filled with 1 M NaOH to trap the volatile radioactive substances.

Removal of protective groups

Search for optimum conditions of alkaline hydrolysis

Fig. 1 shows the time needed to reach maximum yield and the yield of forming [^{18}F]FDG during alkaline hydrolysis depending on the concentration of sodium hydroxide.

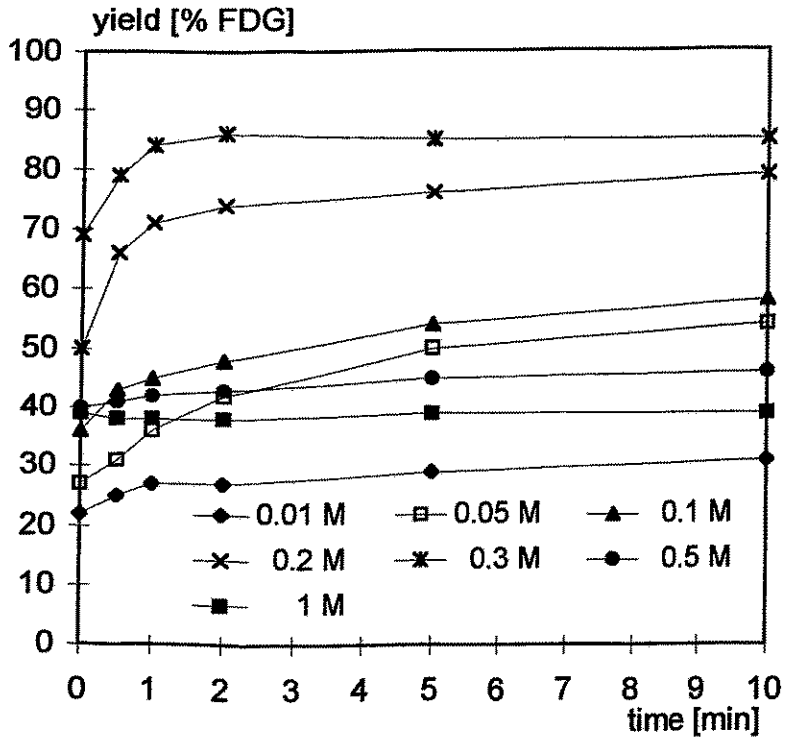

Fig.1
Dependence of forming [^{18}F]FDG on sodium hydroxide concentration and reaction time during alkaline hydrolysis, starting with the reaction mixture after fluorination

The figure demonstrates that the forming rate for [^{18}F]FDG increases with increasing hydroxide concentration. The maximum yield of forming [^{18}F]FDG is obtained at a sodium hydroxide concentration of 0.3 M. Under these conditions, all the starting TA-[^{18}F]FDG is converted into [^{18}F]FDG (about 100 % yield for hydrolysis, s. Fig. 2) and the yield of the synthesis up to this step is therefore determined only by the fluorination step. The hydrolysis using 0.3 M NaOH is suitable for realization of the routine synthesis. The time for reaching the maximum yield is only one minute and the capacity of cation exchanger needed for neutralizing the reaction mixture is only 0.6 mmol.

At higher hydroxide concentrations more [^{18}F]F$^-$ is formed and the yield of [^{18}F]FDG decreases.

The results of alkaline hydrolysis of nucleophilic and electrophilic [2] FDG-synthesis

are very similar. However, there are also some differences. The region of base concentration for the hydrolysis to reach the maximium [^{18}F]FDG yield is relatively small. In addition, we observe lower conversion rates of TA-[^{18}F]FDG for the nucleophilic reaction, using hydroxide concentrations lower than 0.3 M (see Fig. 1 and Fig. 2 [2], the slope of the graph is lower).

Standard preparation procedure

The product of hydrolysis is a clear and light brown solution. Fig. 2 demonstrates thin-layer chromatograms of reaction samples after fluorination and hydrolysis.

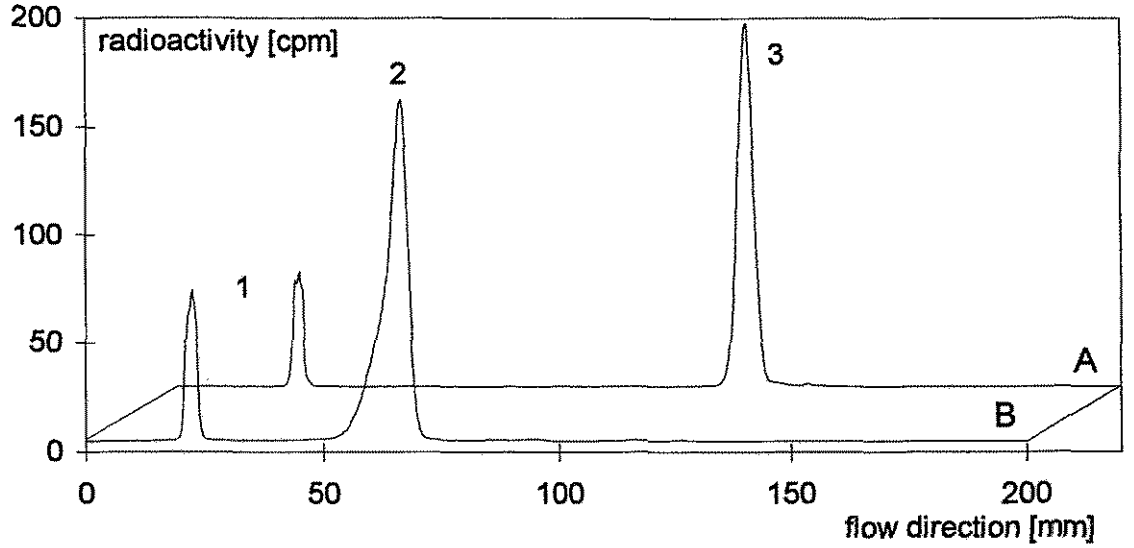

Fig. 2: TL chromatograms

A - product after fluorination, 1 - [^{18}F]F$^-$ = 14 %, 3 - TA-[^{18}F]FDG = 86 %,

B - alkaline hydrolysate of product A, 1 - [^{18}F]F$^-$ = 14 %, 2 - [^{18}F]FDG = 86 %,

The overall [^{18}F]FDG yield using 0.3 M NaOH for hydrolysis is between 80 and 90 %. In contrast to the electrophilic reaction the removal of protective groups in these non-carrier added solutions is nearly complete (> 99 %) and no by-products are formed.

Purification

From the final product after purification we determined the radiochemical purity by TLC and HPLC [7] to > 99 %. The main problems concerning chemical purity refer to the content of Kryptofix™ [2.2.2] and MeCN in the final product. Kryptofix™ [2.2.2] in the final formulation of [^{18}F]FDG has been proved to be toxic [8]. The efficiency of

separating Kryptofix™ [2.2.2] by cation exchange is sufficient. The concentration is determined by UV-spectroscopy to < 10 µg/ml. The concentration of the used solvent MeCN is analysed by GC to < 20 µg/ml.

Synthesis in general

The total preparation time is about 40 minutes. The total yield of the whole procedure (EOS) is about 30 to 40 %. The preparation was carried out 24 times with a starting radioactivity level of 500 - 1000 MBq per batch. As a result we obtain a final product suitable for radiopharmaceutical use. The preparation time can be reduced by using a preparation unit specially designed for the [^{18}F]FDG synthesis, e.g. using a more efficient heating and evaporation system.

Conclusion

Alkaline hydrolysis of TA-[^{18}F]FDG during the preparation of [^{18}F]FDG has the following advantages:

- The yield of removing the protective groups is about 100 %.
- Because of the high speed of hydrolysis, the step of removing the protective groups does not take time in practice. Under acid conditions this step takes about 10 to 20 minutes. Therefore the yield of the preparation can be increased by about 6 to 13 % by time saving.
- The reaction process makes it possible to perform the FDG preparation as a one pot synthesis in a very simple way.
- In the literature there is an indication of forming 2-deoxy-2-chloro-D-glucose (CIDG) as a chemical impurity during the preparation of [^{18}F]FDG, using acid hydrolysis with HCl [9,10]. Using alkaline hydrolysis this by-product is not formed.

Acknowledgments

The authors thank Kurt Hamacher at the Forschungszentrum Jülich, Institut für Nuklearchemie, for the helpful discussion.

References

[1] Hamacher, K. et al., J. Nucl. Med., **27** (1986) 235

[2] Füchtner, F. et al., this report, p. 81

[3] Steinbach, J. et al., Appl. Radiat. Isot. **41** (1990)753

[4] Füchtner, F. et al., this report, p. 92
[5] Drumhiller, J.A. et al., Anal. Chim. Acta, **162** (1984) 315
[6] Hamacher, K., Forschungszentrum Jülich, Institut für Nuklearchemie, private communication
[7] Füchtner, F. et al., Annual Report 1993, p. 17, Institute of Bioinorganic and Radiopharmaceutical Chemistry, FZR-32
[8] Chaly, T. et al., Nucl. Med. Bio. **16** (1989) 385
[9] Alexoff, D. L. et al., Appl. Radiat. Isot. **43** (1992) 1313
[10] Chaar, M. R. et al., Appl. Radiat. Isot. **45** (1994) 267

22. ASPECTS OF QUALITY CONTROL FOR PET-RADIOPHARMACEUTICALS

1. DETERMINATION OF RADIOCHENICAL PURITY OF 2-[^{18}F]FLUORO-2-DEOXY-D-GLUCOSE

F.Füchtner, J. Steinbach, R. Scholz[1], R.Lücke, K. Neubert
[1]Technische Universität Dresden, Klinik für Nuclearmedizin

Introduction

Radiopharmaceuticals of the highest achievable radiochemical purity are an important prerequisite for obtaining reliable quantitative data of PET-studies as well as for minimized radiation doses of patients [1]. Therefore, the correct determination of radiochemical purity is one of the most important criteria of the quality control of the final product of 2-[^{18}F]fluoro-2-deoxy-D-glucose ([^{18}F]FDG) preparation.

High performance liquid chromatography (HPLC) with an anion exchange separation column using a strong basic eluent was reported to be an up-to-date method for determining radiochemical purity. In combination with radioactivity detection, it seemed to be the best control method for the radiochemical purity of [^{18}F]FDG [2]. Last year we reported on the determination of the chemical and radiochemical purity of [^{18}F]FDG, applying this method [3].

In the search for optimum [^{18}F]FDG-preparation conditions [4,5] the quoted HPLC method was used as an analytical technique and we found that using alkaline eluent (0.1 M NaOH) during the HPLC separation, the fluorinated precursor 2-[^{18}F]fluoro-

1,3,4,6-tetra-O-acetyl-D-glucose (TA-[^{18}F]FDG) was converted into [^{18}F]FDG.
This paper focuses on the difference of analytical results obtained by common thin-layer chromatography (TLC) and HPLC. As a result we propose a reliable method for determining radiochemical purity of [^{18}F]FDG.

Experimental

To assess the reliability of both analytical methods we analysed various samples during the whole [^{18}F]FDG preparation procedure. The investigations were carried out in the remote controlled laboratory system described in [6]. The TA-[^{18}F]FDG was synthesized from gaseous acetylhypofluorite ([^{18}F]AcOF) and tri-O-acetyl-D-glucal (TAG) using the electrophilic addition reaction according to Bida [6]. After evaporation of the remaining solvent $CFCl_3$, 2 ml of 1 M HCl were added. The solution was heated to 135 °C in order to remove the protective acetyl groups from the TA-[^{18}F]FDG forming [^{18}F]FDG. In addition, the generated epimer 2-[^{18}F]fluoro-1,3,4,6-tetra-O-acetyl-D-mannosese was hydrolysed to 2-[^{18}F]fluoro-2-deoxy-D-mannose ([^{18}F]FDM). The hydrolysate was purified by using a combination of an anion exchange column (d_i = 6 mm, L = 100 mm, OMNIFIT, filled with 2 ml anion resin AG® 4-X4, 100 - 200 mesh, free base form, BIO-RAD) with a SEP-PAK cartridge ALUMINA A (Millipore).
Samples (100 µl) were taken from the reaction mixture after fluorination (A), during hydrolysis (B), at the end of hydrolysis (C) and from the final product after the purification step (D). The samples were analysed immediately by TLC and HPLC.
The conditions for the HPLC analysis are described in detail in [3]. TLC analysis was performed on plates with a stationary phase of silica gel (DC-Alufolien, Kieselgel 60, MERCK). All samples (about 0.5 µl) were spotted on a TLC plate using glass capillaries. The chromatographic development was carried out in a chamber filled with acetonitrile/water (95:5). For the visualization of the chromatograms the dried TLC plates were contacted with an imaging plate (IP-BAS-III, 20x25, FUJI) and spent an exposure time of 1 min per 2 KBq/cm^2. The information about the distribution of radioactivity on the TLC plate was read by a scanner (bio-imaging analyser, BAS2000, FUJI).

Results

Chromatograms of identical samples of the hydrolysis experiment and of the final product obtained by TLC and HPLC are shown in Fig. 1 and 2.

The TL chromatograms (Fig. 1) demonstrate clearly the different compounds during different stages of reaction progress. The running time for developing the TLC plates is about 20 minutes. The conversion of the TA-[^{18}F]FDG (A) into intermediate products (partly acetylated [^{18}F]FDG derivates, B) and into [^{18}F]FDG (C) during hydrolysis is visible. The radiochemical purity of the final product (D) for [^{18}F]FDG and [^{18}F]FDM is determined to > 99 %.However, a separation of [^{18}F]FDG and [^{18}F]FDM is not achieved, both compounds have similar R_f-values. The R_f-values of the main products analysed are given in Table 1.

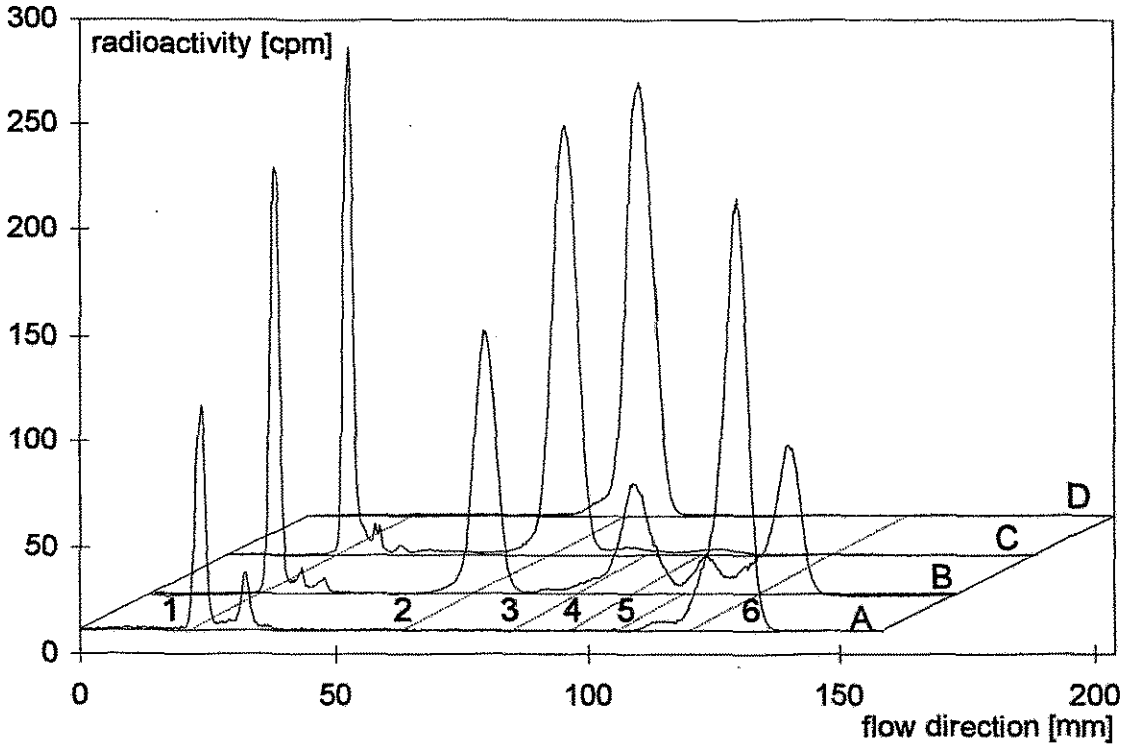

Fig. 1: TL chromatograms of reaxtion mixture

A - after fluorination, B - during hydrolysis, C - after hydrolysis,

D - final product after purification

1 - [^{18}F]F$^-$, 2 - [^{18}F]FDG+[^{18}F]FDM, 3 to 5 - partly hydrolysed TA-[^{18}F]FDG,

6 - TA-[^{18}F]FDG

Using HPLC the analytical results are very similar even of very different samples as shown in Fig. 2. The samples (A) and (B) are spontaneously and nearly completely converted into [^{18}F]FDG. In analogy with the results of alkaline hydrolysis of TA-[^{18}F]FDG [4], residual peaks are observed, however eluted before [^{18}F]F$^-$. By the

following thermal treatment during hydrolysis in the final hydrolysate (C) these peaks become smaller and eventually disappear except for two of them which we can still find a long time after thermal treatment. In the chromatogram of the final product obtained after purification (D), we observe a small radiochemical impurity (generated during hydrolysis) apart from the [^{18}F]FDG and [^{18}F]FDM. The radiochemical purity for [^{18}F]FDG and [^{18}F]FDM is measured to > 99 %.

Table: 1 R_f-values of the main constituent parts of the analysed samples

Compound	Peak N°	R_f-value
[^{18}F]F$^-$	1	0.00
[^{18}F]FDG	2	31
3rd product, (probably mono-acetyl-[^{18}F]FDG)	3	50
2nd product, (probably di-acetyl-[^{18}F]FDG)	4	56
1st product, (probably tri-acetyl-[^{18}F]FDG)	5	68
TA-[^{18}F]FDG	6	72

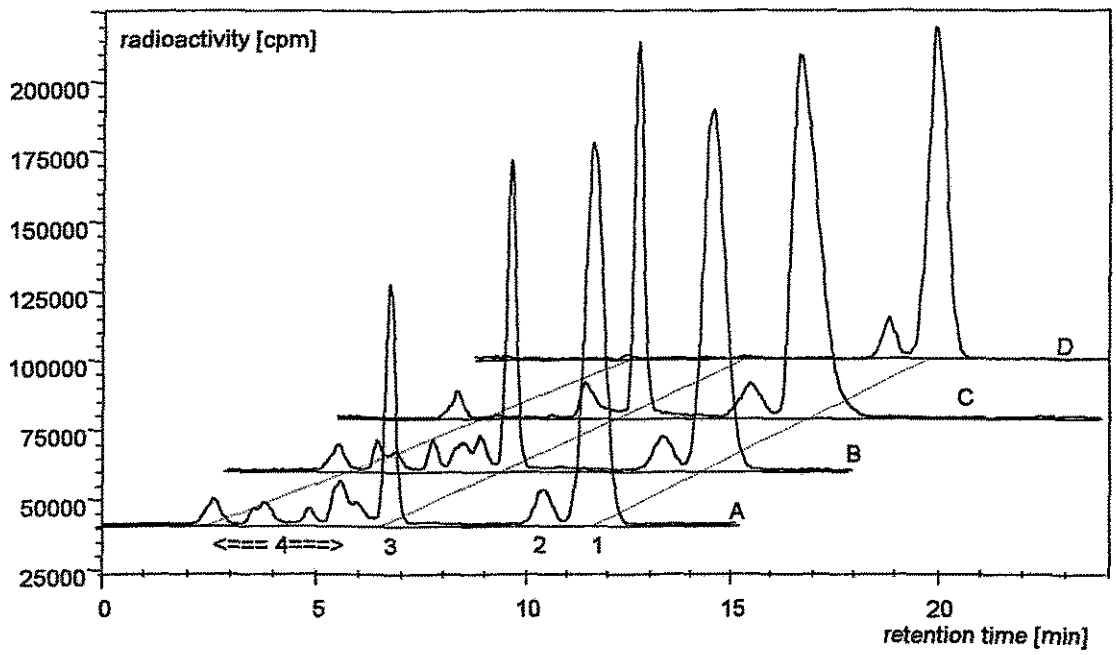

Fig. 2: HPLC chromatograms of reaction mixture

A - after fluorination, B - during hydrolysis, C - after hydrolysis,

D - final product after purification

1 - [^{18}F]FDG, 2 - [^{18}F]FDM, 3 - [^{18}F]F$^-$, 4 - partly hydrolysed TA-[^{18}F]FDG and by-products

Conclusion

- As a result of the self-conversion of TA-[^{18}F]FDG during the HPLC analysis using alkaline eluents, the obtained results do not describe the real course of the preparation of [^{18}F]FDG and the radiochemical purity determined is not identical with the real radiochemical purity in the sample. Only the peak pattern of hydrolysis products (4) gives evidence that the thermal treatment was performed successfully. The described HPLC method is therefore not suitable for determining the radiochemical purity of the final [^{18}F]FDG product.
- TLC is a reliable method for determination of the radiochemical purity during the preparation of [^{18}F]FDG. An advantage of the TLC method is the possibility to analyse several samples (double determination) simultaneously. However, the determination of the [^{18}F]FDG/[^{18}F]FDM ratio in the final product is not possible.
- For the determination of chemical purity and thus for the specific radioactivity of FDG (especially for the nucleophilic substitution reaction) HPLC using an anion exchange separation with the basic eluent in combination with a sensitive mass detector (electrochemical detection) is the best analytical technique. With this method the determination of the [^{18}F]FDG/[^{18}F]FDM ratio (especially for the electrophilic addition reaction) becomes possible, too.
- The HPLC is an analytical method easy to automate. Efforts should therefore be made to find an HPLC separation of [^{18}F]FDG, [^{18}F]FDM, [^{18}F]F$^-$, TA-[^{18}F]FDG and partly hydrolysed TA-[^{18}F]FDG, using radioactivity and electrochemical detection, which allows both the determination of radiochemical and chemical purity simultaneously.

References

[1] "Die Neufassung der Richtlinie Strahlenschutz in der Medizin", 3. Auflage, Verl. H. Hoffmann GmbH, Berlin, 1992, p. 32

[2] Meyer, G.-J. et al., "Quality assurance and quality control of short-lived radiopharmaceuticals for PET", in Stöcklin, G. et al., "Radiopharmaceuticals for PET", Kluwer Academic Publisher, Dordrecht, 1993, p. 91

[3] Füchtner, F. et al., Annual Report 1993, p. 17, Institute of Bioinorganic and

Radiopharmaceutical Chemistry, FZR-32
[4] Füchtner, F. et al., this report, p. 81
[5] Füchtner, F. et al., this report, p. 87
[6] Füchtner, F. et al., Annual Report 1993, p. 14, Institute of Bioinorganic and Radiopharmaceutical Chemistry, FZR-32
[7] Bida, G.T. et al., J. Nucl. Med. **25** (1984) 1227

23. SUBSTANCES LABELLED IN METABOLICALLY STABLE POSITIONS: 5. A PRECURSOR FOR THE SYNTHESIS OF 3-NITRO-[3-^{11}C]ANISOLE

P. Mäding, J. Steinbach, H. Kasper

Introduction

The synthesis of nitro-[1-^{11}C]benzene, the first n.c.a. ^{11}C-ring labelled benzenoid compound, was described in [1,2] using the principle of synchronous six-electron cyclization of hexatriene systems into aromatics. We now try to extend the basic principle to other substituted ^{11}C-ring labelled benzenoid compounds.

A prerequisite for ^{11}C-ring labelling of other benzenoid compounds according to this method is the existence of suitable nonradioactive precursors. For synthesizing 3-nitro-[3-^{11}C]anisole, the preparation of 5-dimethylamino-4-methoxy-penta-2,4-dienylidene-1-dimethylammonium salt (a pentamethinium salt) as a precursor is essential. The synthetic method for the generation of the unsubstituted pentamethinium salt, the 5-dimethylaminopenta-2,4-dienylidene-dimethylammonium perchlorate, according to [3,4] was therefore modified.

Experimental conditions and results

The starting material was 3-hydroxypyridine (Aldrich). At first the 3-hydroxy group had to be protected to avoid undesirable side reactions. The protection was carried out by means of the Williamson ether synthesis:

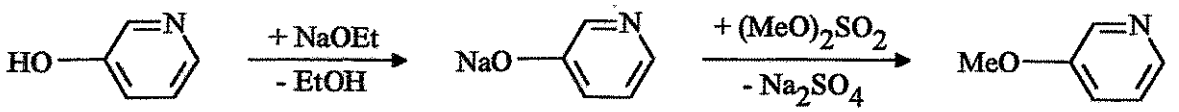

In this way 3-methoxypyridine was obtained in about a 20 % yield. When KOH was

used instead of NaOEt, there was a lower yield of 3-methoxypyridine (12 %). The methylation of 3-hydroxypyridine with methyl iodide in connection with NaOEt produced a yield of only about 10 % of 3-methoxypyridine.

3-Methoxypyridine is reacted with 1-chloro-2,4-dinitrobenzene to form N-(2,4-dinitro-phenyl)-3-methoxy-pyridinium chloride (yield: 31 %):

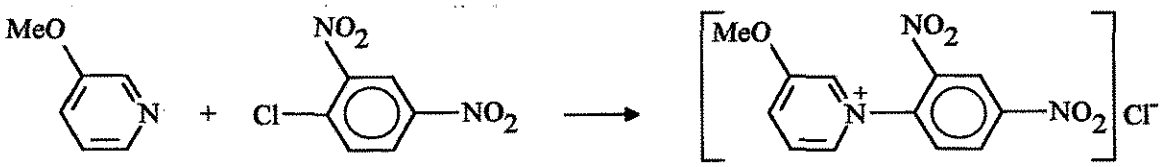

The instability of such a pyridinium salt against bases is used to open the pyridine ring by removing the pyridine nitrogen. Reaction of this pyridinium salt with dimethyl-amine produces the 5-dimethylamino-4-methoxy-penta-2,4-dien-1-al (yield: 53 %) and 2,4-dinitroaniline:

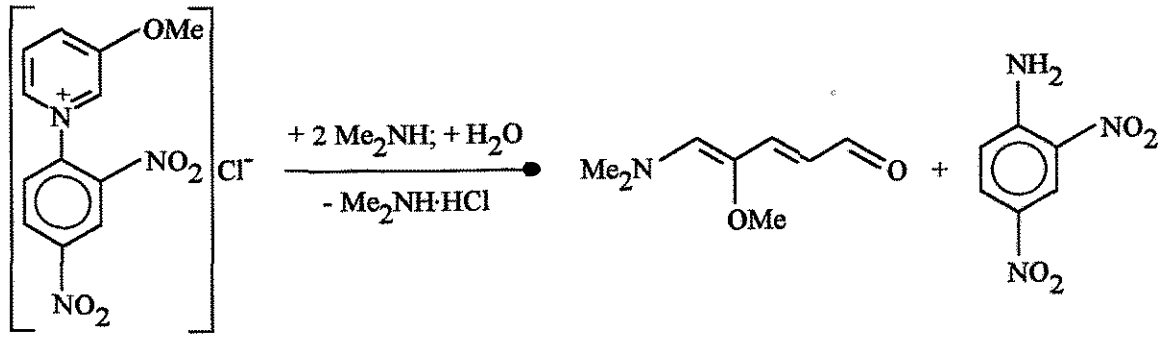

The 5-dimethylamino-4-methoxy-penta-2,4-dien-1-al reacts with dimethylamine per-chlorate or tetrafluoroborate to form the desired pentamethinium salt, the 5-dimethyl-amino-4-methoxy-penta-2,4-dienylidene-1-dimethylammonium perchlorate (yield: 18 %) and tetrafluoroborate (yield: 46 %):

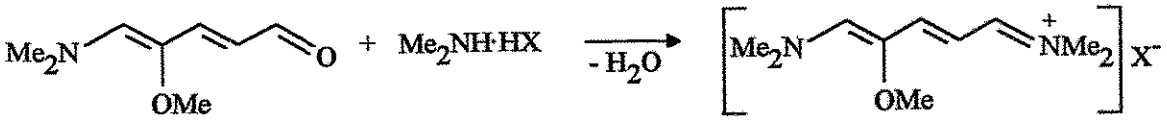

$X = ClO_4; BF_4$

The structures of 5-dimethylamino-4-methoxy-penta-2,4-dien-1-al and the 5-di-methyl-amino-4-methoxy-penta-2,4-dienylidene-1-dimethylammonium salts were confirmed by ^{13}C NMR data.

References

[1] Mäding, P. et al., Annual Report 1993, p. 4, Institute of Bioinorganic and Radiopharmaceutical Chemistry, FZR-32

[2] Steinbach, J. et al., J. Labelled Compd. Radiopharm. 36 (1995) 33

[3] Zincke, Th., Lieb. Ann. 333 (1904) 296

[4] Malhotra, S.S., et al., J. Chem. Soc. (1960) 3812

24. SUBSTANCES LABELLED IN METABOLICALLY STABLE POSITIONS:
6. THE SYNTHESIS OF 3-NITRO-[3-^{11}C]ANISOLE

P. Mäding, J. Steinbach, H. Kasper

Introduction

The applicability of the principle of synchronous six-electron cyclization of hexatriene systems into aromatics for ^{11}C-ring labelling of benzenoid compounds is described in [1, 2]. Based on this method, the synthesis of 3-nitro-[3-^{11}C]anisole being a further new ^{11}C-ring-labelled benzenoid compound was worked out using an appropriate precursor [3].

Principle of the synthesis

[^{11}C]Nitromethane (**1**) reacts in the presence of a base with the homemade precursor 5-dimethylamino-4-methoxy-penta-2,4-dienylidene-1-dimethylammonium perchlorate or tetrafluoroborate (**2**) [3] to form 1-dimethylamino-4-methoxy-6-nitro-[6-^{11}C]hexatriene (**3a**, **3b**) followed by cyclization/ aromatization into 3-nitro-[3-^{11}C]-anisole (**4**) at increased temperatures according to the following equation:

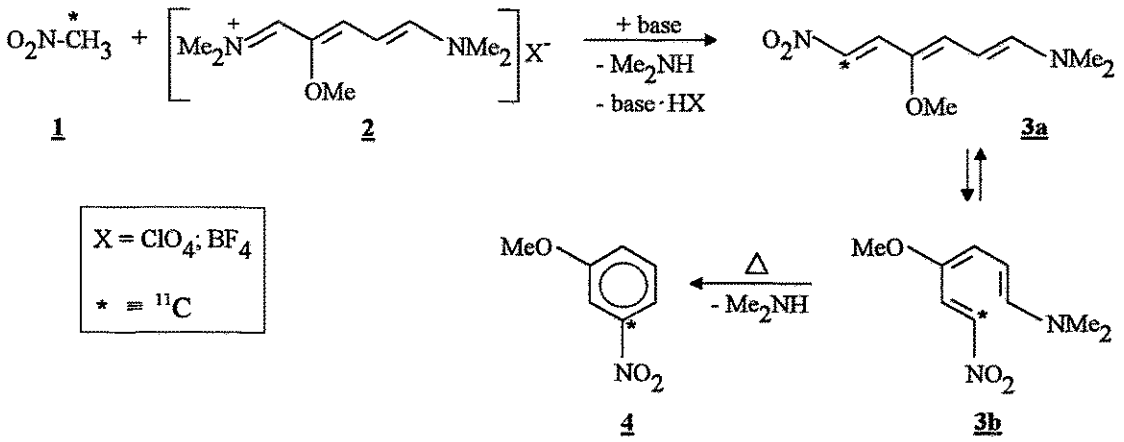

1 2 3a 3b 4

Experimental conditions

To determine the extent of conversion and the radiochemical purity, an HPLC system (Merck-Hitachi) was used, including a pump, a Rheodyne injector with a 20 µl loop, a LiChrospher 100 RP-18 endcapped column (5µm, 150 x 3.3 mm, Merck) and a UV-detector coupled in series with a radioactivity detector FLO-ONE\Beta A500 (Canberra Packard). In the course of experiments the mobile phase was optimized as regards the composition of the eluents and their linear gradient at a flow rate of 0.5 ml/min.

The results of the product distribution of the ^{11}C-labelled compounds after ring closure experiments are listed in Table 1. It was worked at various reaction times using 30 µmol precursor **2** (as tetrafluoroborate), [^{11}C]nitromethane and different kinds and amounts of bases at 170 °C in HMPT. The footnotes [c)d)e)] of Table 1 describe the various linear gradients of the eluents for HPLC investigations.

Optimization of the reaction conditions:

At the beginning the reaction conditions worked out for synthesizing nitro-[1-^{11}C]-benzene [1, 2] were transferred to this process: The gaseous [^{11}C]nitromethane produced according to [1, 2] was introduced in a cooled mixture of 8 mg (30 µmol) precursor **2** (as tetrafluoroborate) and 3.5 mg (30 µmol) solid t-BuOK in 250 µl HMPT followed by heating the well sealed vessel at 170 °C for 7 min. But these conditions are not suitable for synthesizing **4**. In this way only small amounts of **4** (13.2 %) as well as unconverted **1** (76.1 %) were found by HPLC investigations. Potassium tert.-

Table 1: Product distribution of the ^{11}C-labelled compounds after ring closure experiments under various conditions. General conditions: 30 µmol precursor **2** (as tetrafluoroborate), [^{11}C]CH_3NO_2 from [^{11}C]CH_3I, reaction temperature of 170 °C, HMPT as solvent

Experiment no.	Base	Amount of base [µmol]	Reaction time [min]	Product distribution (radioactivity [%] is decay-corrected)			
				[^{11}C]methyl-nitrite	[^{11}C]nitro-methane	unidentified ^{11}C-labelled product[a] **3a**	3-nitro-[3-^{11}C]-anisole **4**
1	t-BuOK	30	7	10.7	76.1	13.2[c]	
2	t-BuOK	30	20	31.4	43.4	21.9[c]	
3	t-BuOK	60	20	24.7	24.0	49.0[c]	
4[b]	t-BuOK	60	20	35.4	13.2	41.3[c]	
5	t-BuOK	120	20	68.1	-	25.4[c]	
6	NaH	30	7	24.9	57.5	17.6[c]	
7	NaH	130	7	83.0	-	-	
8	BuLi	30	20	8.3	0.7	89.0[c]	
9	BuLi	30	10	5.3	0.3	27.2[d]	65.1
10	BuLi	40	10	9.7	-	18.9[d]	70.3
11	BuLi	40	10	12.6	-	23.2[e]	61.5[e]
12	BuLi	50	10	14.2	-	24.5[d]	56.6
13	BuLi	60	10	40.0	-	-	50.9

[a] Probably 1-dimethylamino-4-methoxy-6-nitro-[6-^{11}C]hexatriene (**3a**)

[b] Use of 30 µmol precursor **2** as perchlorate

[c] This peak is the sum of **3a** and **4**, because the following linear gradient of the eluents was not able to separate these two compounds: 0 min - 70 % water/ 30 % MeCN; 10 min - 0 % water/ 100% MeCN; 20 min - 0 % water/ 100 % MeCN

[d] Shoulder of **3a** at the peak of **4**, because the following linear gradient of the eluents is not able to separate completely the peaks of **3a** and **4**: 0 min - 70 % buffer/ 30 % MeCN; 10 min - 0 % buffer/ 100% MeCN; 20 min - 0 % buffer/ 100 % MeCN; buffer = phosphate buffer pH 7 (c[NaH_2PO_4] = 2.6 mM; c[Na_2HPO_4] = 5.1 mM)

[e] First efficient and complete separation of the peaks of **3a** and **4** by using the suitable linear gradient of the eluents: 0 min - 70 % buffer/ 30 % MeCN; 20 min - 0 % buffer/ 100 % MeCN; buffer = phosphate buffer pH 7 (c[NaH_2PO_4] = 0.26 mM; c[Na_2HPO_4] = 0.51 mM)

butylate, the base used proved to be too weak. Similar amounts of **4** (17.6 %) were obtained using 1.3 mg NaH, 60 % dispersion in mineral oil (30 µmol) instead of t-BuOK. But in this way an undesired isomerization reaction took place: **1** was probably converted into [^{11}C]methylnitrite (24.9 %). With 130 µmol NaH this conversion was the main reaction (83.0 % [^{11}C]methylnitrite). The amount of **4** was increased to 21.9 % by extension of the reaction time to 20 min using 30 µmol t-BuOK. A further increase of **4** (49.0 %) could be obtained by use of 7 mg (60 µmol) t-BuOK and 20 min reaction time. With 14 mg (120 µmol) t-BuOK and 20 min reaction time a decrease of **4** (25.4 %) was found as well as an increase of [^{11}C]methylnitrite (68.1 %). The best yields of **4** were obtained using precursor **2** and BuLi in a molar ratio of 1:1 or 3:4 and a reaction time of 10 min (65±5 %). A greater excess of base relating to the precursor should be avoided because of the increasing isomerization of [^{11}C]CH_3NO_2 into [^{11}C]CH_3ONO.

Results and discussion

The reaction conditions worked out for synthesizing nitro-[1-^{11}C]benzene [1, 2] are not suitable for synthesizing **4**. Potassium tert.butylate, the base used proved to be too weak. Lithium butyl (1.6 M solution in hexane) is a suitable base for the desired ring closure reaction, although a complete cyclization/ aromatization is not possible. Steric reasons could be responsible for this phenomenon.

The optimized conditions for the synthesis of **4** are:

Solvent:	250 µl HMPT
Precursor:	8 mg (30 µmol) 5-dimethylamino-4-methoxy-penta-2,4-dienylidene-1-dimethylammonium tetrafluoroborate (**2**)
Base:	20 - 25 µl 1.6 M BuLi in hexane (30 - 40 µmol)
Reaction temperature:	170 °C
Reaction time:	10 min

In this way 3-nitro-[3-^{11}C]anisole was prepared with a radiochemical purity of 65±5 %.

The reproducible radiochemical yields of **4** (decay-corrected) are in the range of 60±5 %, within a synthesis time from [^{11}C]CH_3NO_2 of 10 min. An HPLC radiogram of *unpurified* **4** *is shown* in Fig. 1. The efficient and complete separation of the peaks of probably **3a** and **4** could be obtained at a flow rate of 0.5 ml/min by using the following linear gradient of the eluents:

0 min - 70 % buffer/ 30 % MeCN; 20 min - 0 % buffer/ 100 % MeCN; buffer = phosphate buffer pH 7 (c[NaH_2PO_4] = 0.26 mM; c[Na_2HPO_4] = 0.51 mM)

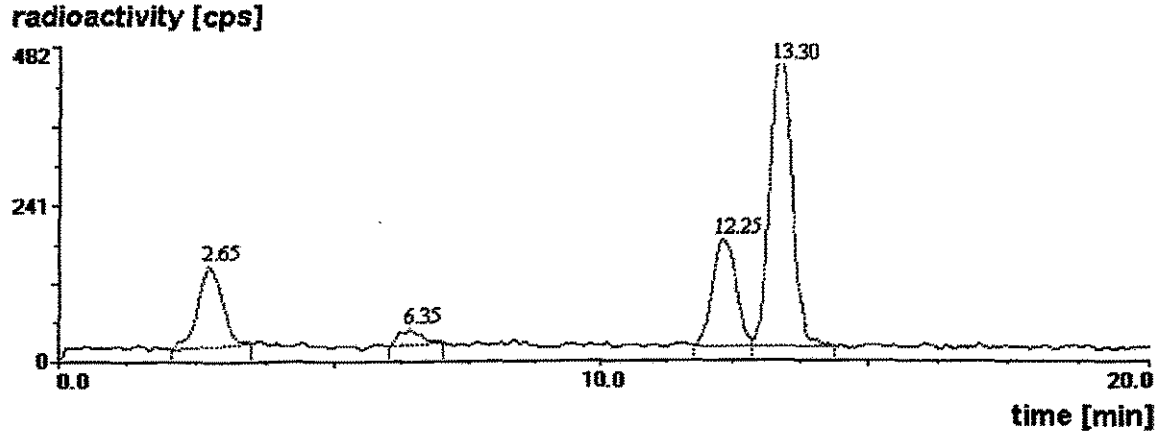

Fig. 1: HPLC radiogram obtained from the reaction mixture of the 3-nitro-[3-^{11}C]-anisole synthesis

2.65 min: [^{11}C]CH_3ONO; 12.6 %

6.35 min: 3-amino-[3-^{11}C]anisole; 2.6 %

12.25 min: unidentified product, probably 1-dimethylamino-4-methoxy-6-nitro-[6-^{11}C]-hexatriene (**3a**); 23.2 %

13.30 min: 3-nitro-[3-^{11}C]anisole (**4**); 61.5 %

(yield [%], decay-corrected)

References

[1] Mäding, P. et al., Annual Report 1993, p. 4, Institute of Bioinorganic and Radiopharmaceutical Chemistry, FZR-32

[2] Steinbach, J. et al., J. Labelled Compd. Radiopharm. **36** (1995) 33

[3] Mäding, P. *et al., this report, p. 98*

25. SUBSTANCES LABELLED IN METABOLICALLY STABLE POSITIONS:

7. THE SYNTHESIS OF 3-AMINO-[3-^{11}C]ANISOLE - A ^{11}C-RING-LABELLED SYNTHONE

P. Mäding, J. Steinbach, H. Kasper

Introduction

The synthesis of 3-nitro-[3-^{11}C]anisole is described in [1]. In continuation of this work the 3-nitro-[3-^{11}C]anisole was converted into 3-amino-[3-^{11}C]anisole, another ^{11}C-ring-labelled benzenoid synthone.

Experimental conditions and results

The required 3-nitro-[3-^{11}C]anisole (**4**) was prepared in a special cyclization/ aromatization reaction by conversion of [^{11}C]CH_3NO_2 (**1**) with 5-dimethylamino-4-methoxy-penta-2,4-dienylidene-1-dimethylammonium tetrafluoroborate (**2**) in the presence of BuLi in HMPT according to the following equation:

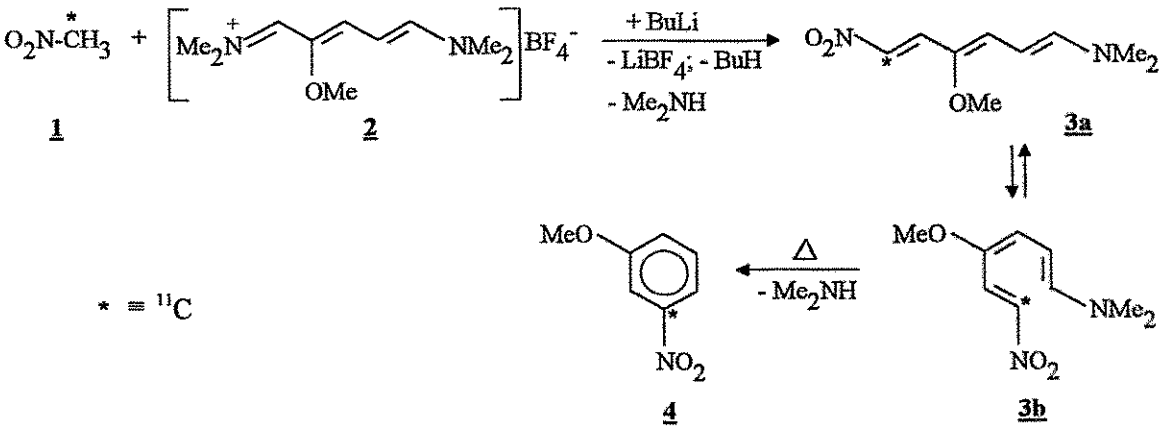

1 **2** **3a** **4** **3b**

Starting from the above reaction mixture, the following reduction was carried out by addition of an aqueous solution of sodium sulphide and subsequent heating:

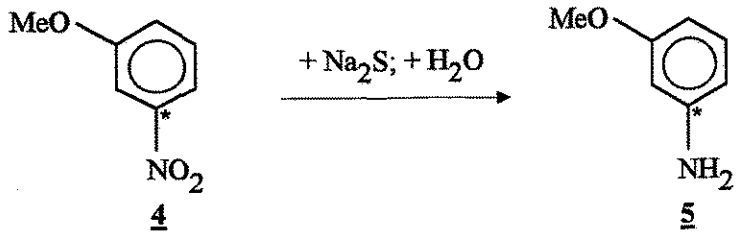

4 5

* ≡ ^{11}C

To determine the extent of conversion and the radiochemical purity of **5**, an HPLC system (Merck-Hitachi) was used, including a pump, a Rheodyne injector with a 20 µl loop, a LiChrospher 100 RP-18 endcapped column (5µm, 150 x 3.3 mm, Merck) and a UV-detector coupled in series with a radioactivity detector FLO-ONE\Beta A500 (Canberra Packard). In the course of experiments the mobile phase was optimized as regards composition of the eluents and their linear gradient at a flow rate of 0.5 ml/min. The footnotes [c)d)] of Table 1 describe the various linear gradients of the eluents for HPLC investigations.

Procedure:

3-Amino-[3-^{11}C]anisole (**5**) is generated by reduction of the reaction mixture of **4** in a one-pot process. 3-Nitro-[3-^{11}C]anisole (**4**), synthesized from **1**, 8 mg (30 µmol) of **2** and various amounts of BuLi - hexane solution (30, 40 and 60 µmol) in 250 µl HMPT at 170 °C and 10 min (see [1]), was reduced by adding a solution of 8 mg of $Na_2S{\cdot}5H_2O$ in 100 µl H_2O (50 µmol) and heating at 170 °C. The results of the product distribution of the ^{11}C-labelled compounds are listed in Table 1.

5 could be prepared from **4** with a radiochemical purity of 49 ± 4 %, if **4** was synthesized by use of 30...40 µmol BuLi. The reproducible radiochemical yields of **5** (decay-corrected) are in the range of 45±5 %, within a synthesis time from [^{11}C]CH_3NO_2 of 16 min. An HPLC radiogram of unpurified **5** is shown in Fig. 1. The peak at 12.30 min is probably **3a**, which was not isomerized into **3b**, and a complete cyclization/ aromatization was not possible. Steric reasons could be responsible for this phenomenon. The reducing power of sodium sulphide is not strong enough for the reduction of the aliphatic nitro group of **3a**.

Table 1: Product distribution of the ^{11}C-labelled products after reduction of several batches of 3-nitro-[3-^{11}C]anisole with sodium sulphide

Experiment no.	[%] of radioactivity of **4**[a)] in the starting reaction mixture	Reaction time [min]	Product distribution (radioactivity [%] is decay-corrected)			
			[^{11}C]methyl-nitrite	3-amino-[3-^{11}C]anisole (**5**)	unidentified ^{11}C-labelled product[b)]	3-nitro-[3-^{11}C]anisole (**4**)
1[c)]	65.1[a1)]	10	11.6	48.5	37.7	-
2[c)]	70.3[a2)]	5	23.0	53.0	23.5	-
3[d)]	61.5[a2)]	5	19.5	45.2	24.7	8.5
4[c)]	50.9[a3)]	10	58.1	32.2	-	-

[a)] See Table 1 in [1]; used amounts of BuLi for synthesis of **4**: [a1)] 30 µmol, [a2)] 40 µmol, [a3)] 60 µmol

[b)] Probably 1-dimethylamino-4-methoxy-6-nitro-[6-^{11}C]hexatriene (**3a**)

[c)] Linear gradient of the eluents for HPLC: 0 min - 70 % buffer/ 30 % MeCN; 10 min - 0 % buffer/ 100% MeCN; 20 min - 0 % buffer/ 100 % MeCN; buffer = phosphate buffer pH 7 (c[NaH_2PO_4] = 2.6 mM; c[Na_2HPO_4] = 5.1 mM)

[d)] Linear gradient of the eluents for HPLC: 0 min - 70 % buffer/ 30 % MeCN; 20 min - 0 % buffer/ 100 % MeCN; buffer = phosphate buffer pH 7 (c[NaH_2PO_4] = 0.26 mM; c[Na_2HPO_4] = 0.51 mM)

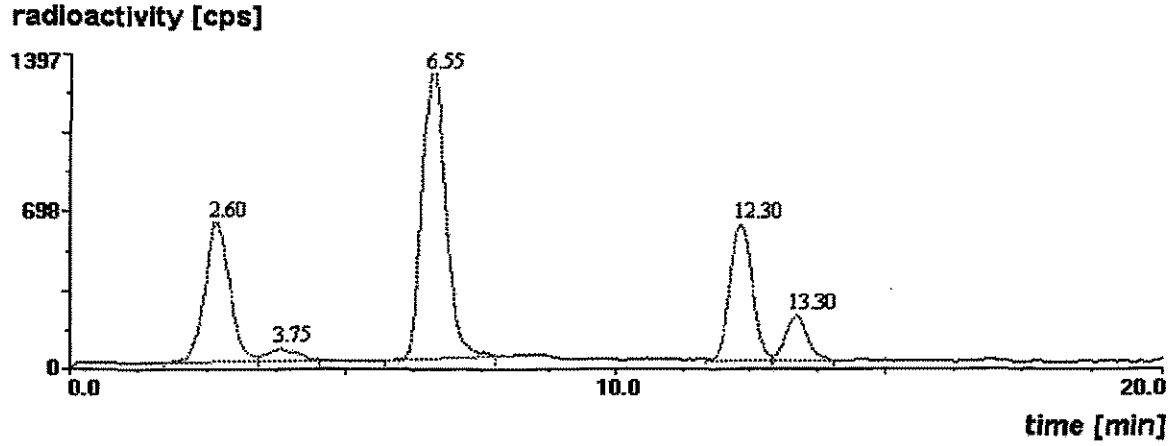

Fig. 1: HPLC radiogram obtained from the reaction mixture of the 3-amino-[3-^{11}C]-anisole synthesis

2.60 min: [^{11}C]CH_3ONO; 19.5 %

3.75 min: unidentified product; 2.0 %

6.55 min: 3-amino-[3-^{11}C]anisole (**5**); 45.2 %

12.30 min: unidentified product, probably 1-dimethylamino-4-methoxy-6-nitro-[6-^{11}C]-hexatriene (**3a**); 24.7 %

13.30 min: 3-nitro-[3-^{11}C]anisole (**4**); 8.5 %

(yield [%], decay-corrected)

References

[1] Mäding, P. et al., this report, p. 100

26. SUBSTANCES LABELLED IN METABOLICALLY STABLE POSITIONS:

8. PRECURSOR SYNTHESIS FOR ^{11}C-RING-LABELLED PYRIDINE DERIVATIVES

K. Chebani, P. Mäding, W. D. Habicher, D. Scheller, J. Steinbach

Introduction

This is a progress report on our attempts to synthesize precursors for ^{11}C-ring labelled pyridine derivatives [1]. The 3-bromo-malein-dialdehyde-4,4-dimethylacetal (I) was thought to be a precursor for reaction with [^{11}C]nitromethane according to equation (1).

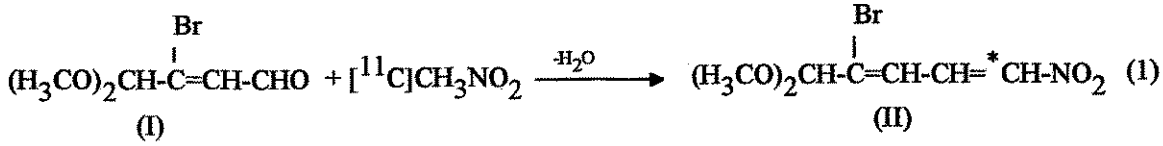

$(H_3CO)_2CH\text{-}C(Br)=CH\text{-}CHO + [^{11}C]CH_3NO_2 \xrightarrow{-H_2O} (H_3CO)_2CH\text{-}C(Br)=CH\text{-}CH=^{*}CH\text{-}NO_2$ (1)

(I) (II)

*: ^{11}C

The further steps were planned as follows (2):

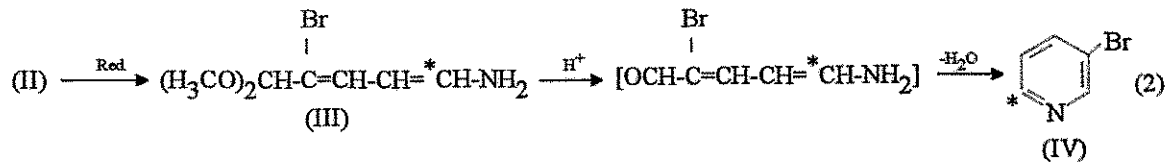

(II) $\xrightarrow{Red}$ $(H_3CO)_2CH\text{-}C(Br)=CH\text{-}CH=^{*}CH\text{-}NH_2$ (III) $\xrightarrow{H^+}$ $[OCH\text{-}C(Br)=CH\text{-}CH=^{*}CH\text{-}NH_2]$ $\xrightarrow{-H_2O}$ (IV) (2)

The synthesizing of (I) had to be performed via equation (3).

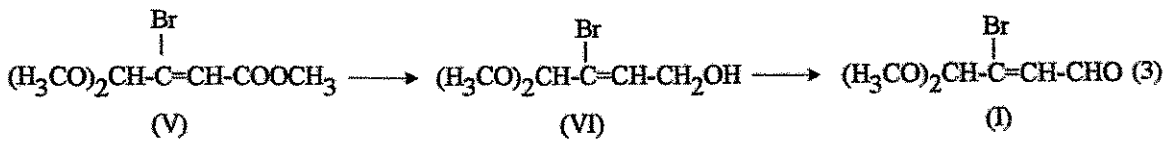

$(H_3CO)_2CH\text{-}C(Br)=CH\text{-}COOCH_3$ (V) $\longrightarrow$ $(H_3CO)_2CH\text{-}C(Br)=CH\text{-}CH_2OH$ (VI) $\longrightarrow$ $(H_3CO)_2CH\text{-}C(Br)=CH\text{-}CHO$ (I) (3)

In our last annual report [1] we described the synthesis of (V). Its conversion to (VI) and the problem involved are the content of this paper.

Experimental and results

Reaction of $(CH_3O)_2CH$-CBr=CH-$COOCH_3$ (V) with $NaBH_4$+LiCl in diglycol

The reaction of the ester group in (V) with $NaBH_4$ and LiCl in diglycol at 25 °C according to [2,3] was not successful. The conditions directed the E/Z-isomeric ratio of (V) from 90:10 to 50:50.

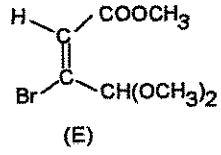

(E)

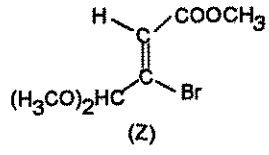

(Z)

Attempts at 110 °C lead to a transesterification reaction yielding (VII) with about 70 % with only one isomeric form (E) (equation 4).

$$(V) \xrightarrow[\text{diglycol/110°C}]{NaBH_4+LiCl} \underset{(VII)}{(H_3CO)_2CH\text{-}CBr{=}CH\text{-}COOCH_2\text{-}CH_2\text{-}O\text{-}CH_2\text{-}CH_2\text{-}OH} \quad (4)$$

The structures of (E-V) , (Z-V) and (VII) were proved by ^1H NMR spectra.

Reaction of $(CH_3O)_2CH$-CBr=CH-$COOCH_3$ (V) with a surplus of $NaBH_4$ in methanol

The (E) and (Z) isomers of (V) were treated for 3 h with 25 % surplus of $NaBH_4$ in methanol under reflux according to [4]. The ^{13}C and ^1H NMR spectroscopic investigations of the reaction products showed that no reduction took place. Instead of this a Br to CH_3O exchange was observed. This can be explained by the vinyl-homologue structure of the molecule, which enables the substitution of the Br atom at the olefinic carbon.

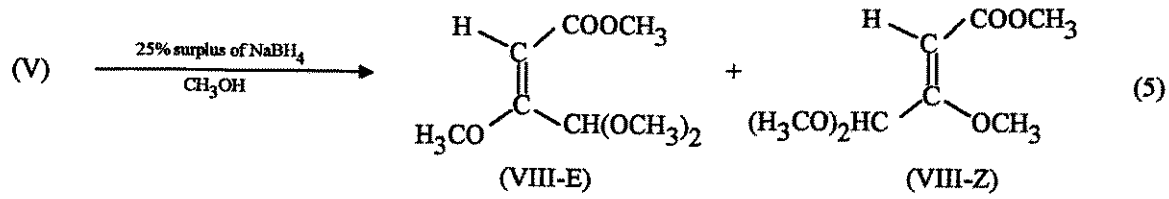

(5)

The E/Z isomeric ratio of (VIII) was about 60/40.

Reduction of $(CH_3O)_2CH$-CBr=CH-$COOCH_3$ (V) with $LiAlH_4$

Compound (V) was reacted with $LiAlH_4$ with the molar ratio 1 : 0.5 at -20 °C in ether according to [2]. The reaction mixture was distilled between 65 - 77 °C at 400 Pa. An HPLC- investi-gation of the distilled product showed a mixture of compounds.

The main product was the 3-bromo-4-methoxy-3-butenol-1 (IX) with an overall yield of about 7 %. The desired compound (VI) was found to be only a by-product with an overall yield of at most 2 %.

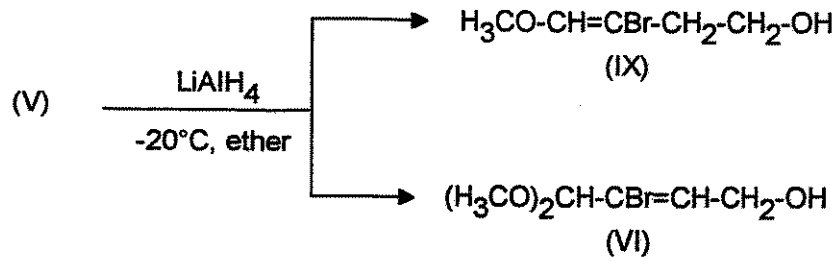

(6)

The structures of (IX) and (VI) were proved by ^{13}C and ^{1}H NMR spectra (Fig. 1and 2).

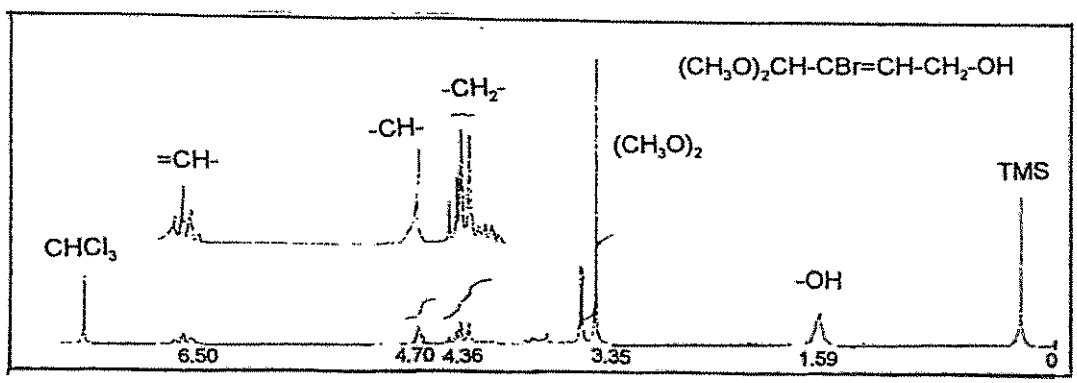

Fig. 1: ^{1}H NMR spectrum of (IX)

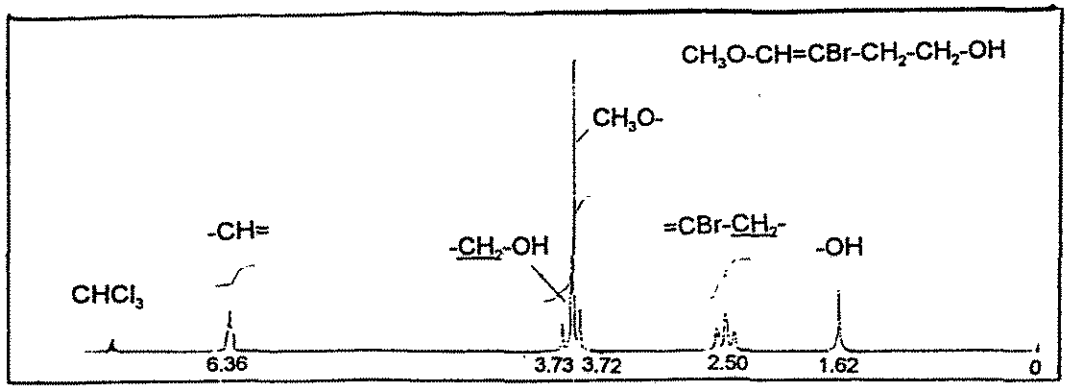

Fig. 2: ^{1}H NMR spectrum of (VI)

Other reactions to yield (VI) from (V) by means of $LiAlH_4 + AlCl_3$ in ether, $(C_4H_9)_2AlH$ in tetrahydrofurane and $NaBH_4 + LiCl$ in diethylenglycol-diethylether were not successful.

The poor yield of (VI) in the overall synthetic route caused us to change the strategies for [^{11}C]pyridine generation [5,6].

References

[1] Chebani, K. et al., Annual Report 1993, p. 10, Institute of Bioinorganic and Radiopharmaceutical Chemistry, FZR-32

[2] Organikum, Organisch-chemisches Grundpraktikum, 16., bearbeitete Auflage, VEB Deutscher Verlag der Wissenschaften, Berlin 1986, p. 493

[3] Houben-Weyl, Methoden der Organischen Chemie, Stuttgart, New York : Verlag Georg Thieme, 1981, Band IV/1d, Teil (II), p. 212

[4] Angew. Chem., Neuere Methoden der präparativen organischen Chemie IV, 73. Jahrg. Nr. 3, 1961, p. 81

[5] Kopinke, F.-D. et al., Journal of Analytical and Applied Pyrolysis, **13** (1988) 259

[6] Chebani, K. et al., this report, p. 113

27. SUBSTANCES LABELLED IN METABOLICALLY STABLE POSITIONS: 9. SYNTHESIS OF PYRIDINE BY THERMAL REARRANGEMENT OF AMINES CONTAINING THE C_5N STRUCTURE

K. Chebani, J. Zessin, J. Steinbach

Introduction

In continuation of our efforts to introduce ^{11}C into the pyridine ring we shifted from a synthetic route [1,2] to thermal rearrangement reactions.

For a derivative of pyridine, Chebani et al. describe a synthetic route which contains the formation of an unsaturated C_5N structure followed by an intramolecular cyclization reaction. Because of poor yields and unforeseeable reactions we cut short the synthetic program. We decided to construct an ^{11}C-labelled C_5N structure, which could be converted to pyridine by high temperatures. Such conversions are well known in reforming processes [3] and should be possible as an alternative and fast synthetic route.

Bell et al. [4] describe the high temperature dehydrocyclization of various aliphatic amines in the presence of iodine. They found that these reactions produce pyridine with yields between 9.5 and 41.5 %. The presence of calcium oxide increases the yield of pyridine. Pyridine can also be formed by thermal conversion of N-methylpyrrole in the absence [5] and in the precense of iodine, using a reactor filled with calcium oxide [6]. The ^{11}C labelled compounds with the required C_5N structure were synthesized by addition of $[^{11}C]CH_3I$ to C_4 amines in general. n-Butylamine (1), pyrrole sodium (2), 4-aminobutanol (3) and 3-pyrrolidinole (4) were selected. (3) and (4) were thought to be compounds which should lead to unsaturated amines by dehydration, thinkable precursors of aromatic N-heterocycles.

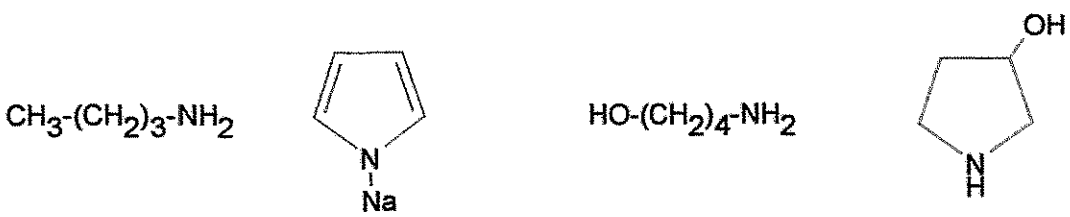

(1) (2) (3) (4)

In the first experiments, the thermal conversion of the unlabelled N-methyl derivatives of (1) to (4) were investigated more closely in order to select suitable precursors and

conditions for the generation of [^{11}C]pyridine.

Experimental

Formation of the N-methyl amines:

(1), (3) and (4) were reacted with methyl iodide in molar amounts, using absolute ethanol as a solvent to yield the appropriate N-methyl derivatives. For the further experiments the ammonium salts generated were used directly. Only N-methyl butylamine was isolated by adding sodium hydroxide solution and extraction with diethylether. N-methylpyrrole (6) was prepared from methyliodide and pyrrole sodium, which was synthesized from pyrrole and sodium hydride. N-methyl-3-pyrrolidinol (8) was commercially available and was used without further purification.

Thermal conversions:

The thermal conversions of the methylated compounds (5) - (8) were carried out in two various, vertically arranged quartz glass tubular reactors (220 mm x 15 mm and 400 mm x 12 mm). Nitrogen acted as an inert carrier gas. The volumetric flow rate was in the order of 30 ml per minute. The substances were directly injected at the beginning of the hot zone of the oven. The temperature range of the different experiments varied from 400 to 600 °C. The residence time was in the order of 5 to 15 seconds.
The following configurations were investigated:

1. The compounds (5) to (8) passed through the empty reactor.
2. A stoichiometric amount of iodine was added to the N-methylated substances. This mixture passed through the empty oven.
3. According to 2 iodine was added, but the reactor was filled with calcium oxide.
4. The C_5N-compounds passed through the reactor filled with a dehydrogenation catalyst (Pd/activated carbon/magnesium oxide).

The products of the thermal conversion were collected in 2 ml of absolute ethanol and ana-lysed by HPLC (HPLC system from Merck-Hitachi, injector with 20 µl loop, RP-18 column (150 x 3.3 mm) filled with LiChrospher (5 µm) from Merck, DAD detector). The mobile phase started with 100 % phosphate buffer according to Sörensen (2.6 mM NaH_2PO_4 + 5.1 mM Na_2HPO_4; pH 7) and changed with the following linear gradient to acetonitrile: 0 min: 100 % buffer/0 % MeCN; 10 min: 0 % buffer/100 % MeCN; 20 min: 0 % buffer/100 % MeCN. The interesting compounds were identified by comparing the

retention times. In some cases the products were analysed by GC-MS by use of a GC system HP5890 with the MSD HP5972 (column: Chrompack HP-5, 30 m, 0.25 mm; helium with 65 ml/min; temperature: 45 °C (2 min) to 150 °C at 8 K/min).

Results

General rules

The thermal conversion of the N-methyl derivatives of the compounds (1) - (4) yields a mixture of various substances. The composition of this product was nearly constant between 400 and 600 °C .

The use of ethanol as a solvent does not lead to pyridine. Only substituted N-heterocycles were obtained under these conditions. The use of benzene as a solvent does not produce significant modifications of the product composition in comparison with the thermal conversion of the pure substances (5) to (8).

N-Methylbutylamine (5)

Between 400 and 600 °C, the thermal conversion of (5) by application of the empty reactor produce only small amounts of pyridine as well as substituted pyridines. The quantity of pyridine did not increase significantly if iodine was added to (5) and the reactor was filled with calcium oxide. But in this case, pyrrole was obtained as an additional product.

By application of the palladium-based dehydrogenation catalyst, the same products were formed. The amount of pyrrole increased clearly, but the quantity of pyridine was unchanged. Apart from pyrrole and pyridine, the analysis of the fluid products by GC-MS showed various methyl and dimethylpyridines, butylpyridine, methyl and dimethylpyrroles, nitriles and indole. Under this conditions the share of pyridine lies between 7 and 17 % (determined by GC-MS).

N-Methylpyrrole (6)

In the empty reactor, N-methylpyrrole rearranges thermically in contrast to [5] into two main products, which could be identified with GC-MS as 2- and 3-methylpyrrole. Pyrrole and pyridine were only obtained as by-products in very small quantities.

By application of the reactor filled with the dehydrogenation catalyst, the thermal conversion of (6) yields - in contrast to the other investigated N-methyl compounds - a smaller number of secondary compounds. The analysis of the product mixture shows pyridine,

pyrrole as well as various methyl and dimethyl pyrroles. The percentage of pyridine increases by the use of this catalyst and lies between 8 and 18 % (determined by GC-MS).

4-(N-methylamino)-butanol (7)

Between 400 and 600 °C, thermal rearrangement of (7) in the empty reactor yields pyridine, pyrrole, N-methylpyrrole and various methyl pyridines.

The application of iodine in combination with the calcium-oxide-filled reactor produces smaller amounts of pyrrole and N-methylpyrrole. In comparison to the N-methyl derivatives (5) and (6), the yield of pyridine does not obviously increase.

N-Methyl-3-pyrrolidinol (8)

The thermal conversion of (8) by use of the empty reactor or with the addition of iodine leads to comparable results as the pyrolysis of (7).

Conclusions

In all cases the thermal rearrangement of the N-methyl compounds (5) - (8) produces mixtures of various substances, which contain pyridine as the basic structure. Additional pyrrole is generated. That means that only aromatic systems are stable under the reaction conditions. The occurrence of alkylated compounds demonstrates, that besides cyclization or isomerization reactions also the cleavage of the C-N bonds takes place. The attachment of the alkyl fragments causes the high quantities of alkylpyridines and alkylpyrroles.

Thermal rearrangment of (5) - (8) without dehydrogenation catalysts yields the broadest spectrum of products. The application of palladium or iodine in combination with a calcium oxide filled reactor leads to a decreasing number of by-products. By use of the dehydro-genation catalysts, the percentage of pyridine was nearly unchanged. The presence of a hydroxy group in the molecule does not produce the desired results.

The highest yields of pyridine (up to 18 %) were obtained by thermal conversion of N-methylbutylamine (5) and N-methylpyrrole (6), if the dehydrogenation catalysts were used. The thermal rearrangment of (6) leads to a small number of by-products. Thus, after optimization of the reaction conditions, the thermal rearrangement of these two compounds should be a possible way of synthesizing ^{11}C-ring labelled pyridine.

This work will be continued by thermal rearrangement of the ^{11}C-labelled substances (5) and (6).

References

[1] Chebani, K. et al., Annual Report 1993, p. 10, Institute of Bioinorganic and Radiopharmaceutical Chemistry, FZR-32

[2] Chebani, K. et al., this report, p. 109

[3] Kopinke, F.-D. et al., J. Anal. Appl. Pyrolysis **13** (1988) 259

[4] Bell, W. H. et al., J. Chem. Soc. (C) **1969** 352

[5] Patterson, J. M. and P. Drenchko, J. Org. Chem. **27** (1962) 1650

[6] Bell, W. H. and P. M. Quan , Brit. Pat. 1,184,244 (1970)

28. PET - CAMERA POSITOME IIIp, PROGRESS IN HARD UND SOFTWARE

H. Linemann[1], C. Thompson[2], E. Will

[1]Technische Universität Dresden, Klinik für Nuklearmedizin

[2]Montreal Neurological Institute, Canada

The efforts to complete the hard and software of the PET-camera POSITOME IIIp were related to the quantitative analyses of FDG studies, the increase of the measurable count rate, the realisation of the measured attenuation correction and the improvement of the quality control conditions.

Programs for the calculation of glucose metabolic rates in brain

We have written FORTRAN programs (GLUCOSN; TCN) to calculate the glucose metabolic rate from the measured activity concentration of ROI's and have compared the results with values taken from the literature. A program (TCNP) for computing the metabolic rate by the graphic method giving parametric pictures on pixel base is in progress.

The program GLUCOSN, based on the program GLUCOS developed in Montreal, uses the autoradiographic method. For this method a single PET scan, usually started 40 minutes after injection, and the time function of the plasma activity concentration have to be measured [3].

In the program TCN the graphic method, the so called PATLAK plot, is applied. It uses a set of PET images, measured in the first hour after injection, and the corresponding plasma samples.

Both methods are widely used for the calculation of glucose metabolic rates in brain. A three-compartment model for FDG uptake is the base for these methods.
If the rate constants are known the metabolic glucose rate MRGl can be calculated as:

$$MRGl = C_g / LC * k_1k_3 / (k_2+k_3)$$

C_g = plasma glucose concentration
LC = lumped constant (converts from FDG to glucose)

The determination of the rate constants is possible on the base of the three-compartment model. It requires to measure the complete time functions of the plasma activity concentration and also of the tissue activity concentration. This extensive dynamic method is usually replaced by the autoradiographic method or the graphic one. Both methods allow to determine the quotient $k_1k_3 / (k_2+k_3)$ which is proportional to the metabolic glucose rate.
The autographic method uses the normal values of the rate constants and the measured PET and plasma concentration results to determine the actual value of this quotient. The PATLAK plot gives this quotient as the slope of a linear regression using the results of the PET scan and plasma concentration measurement.
We have tested our programs with data from a dynamic patient study performed in Montreal. Slope values calculated by the program TCN for three small ROI's in grey matter and two large ROI's over a half of the slice are shown in the following table :

ROI - diameter (in cm)	ROI - position	$k_1k_3 / (k_2+k_3)$ (in min^{-1})
0.8	grey matter, front side	0.029
0.8	grey matter, right side	0.027
0.8	grey matter, back side	0.030
8.0	frontal half of the slice	0.016
8.0	back half of the slice	0.018

The large ROI's contain a mixture of grey and white matter. All calculated slope values for grey matter agree with the values of about 0.028...0.033 min^{-1} given in the literature

[3]. The slope values for the large ROI's are between the values for grey matter and white matter (0.014 min^{-1}) as expected.
To test the program GLUCOSN with the same ROI's we used only the last frames of the dynamic study. The $k_1k_3 / (k_2+k_3)$ - values are 15% smaller than the one determined with the PATLAK plot.

Stabilization of data acquisition for high count rates

The PET-studies with the POSITOME IIIp in Montreal were performed up to an activity concentration of 40 kBq/cm^3 [2]. In our measurements the camera became instable, if we used activities of more than 20 KBq/cm^3. The reason for these instabilities was a bad synchronization of the three parallel switched FIFO's (74S225), used as a fast buffer for the coincidences. We changed the form of the reset signal and the acquisition software to reset the interface after each 30 seconds. Tests with an activity concentration of up to 60 KBq/cm^3 indicate no failure.

Transmission sources

The POSITOME IIIp PET camera can measure the transmission and emission coincidences simultaneously. The transmission sources were prepared by DUPONT using electroplated ^{68}Ge on a 0.5 mm thick nickel foil 5 mm in diameter and a second one as a cover [1] .
We have manufactured lead collimators as described in [1] to install the ^{68}Ge sources into the PET camera. This new mechanical arrangement of the sources and collimators requires also a new EPROM-mask to decide which coincidences are emission or transmission one. This mask was calculated on the base of the data measured with the transmission sources in defined positions.

Cross phantom

The daily check of the PET camera and the weekly comparison with the well counter have to be done with a phantom of homogeneous and constant activity concentration. This cross phantom we have filled with the ^{68}Ge chloride in a hydrochloric acid solution. The phantom was made from a PVC cylinder of 15 cm diameter. We used PVC to avoid corrosion of the cover. The phantom is enclosed in a second cylinder of metal sheet to guarantee a correct location in the camera port and to prevent contamination.

References

[1] Thompson, C. et al., IEEE Trans. Nucl. Science **35** (1989) 1011

[2] Thompson, C. et al., IEEE Trans. Med. Imaging **MI-5** (1986) 183

[3] Wienhard, K. et al., "PET-Grundlagen und Anwendungen der PET", Berlin 1989

[4] Hutchins, G. et al., J. Cereb. Blood Flow and Metabol. **4** (1984) 35

29. QUANTITATIVE AUTORADIOGRAPHIC STUDIES OF THE DISTRIBUTION OF [^{3}H]KETANSERIN IN HORIZONTAL RAT BRAIN SECTIONS AFTER INFLUENCE OF SEVERAL DISPLACING COMPOUNDS INCLUDING Re COMPLEXES

M. Kretzschmar, P. Brust

Introduction

For the development of radioligands with affinity to serotonin receptors it is necessary to use reference methods with known serotonergic compounds. [^{3}H]ketanserin shows high-affinity binding to 5-HT_2 receptors in brain tissues of several species [1-4]. The characteristic parameters of receptor binding, K_D and B_{max}, and the distribution of the 5-HT_2 binding sites were therefore studied in several rat brain regions using [^{3}H]ketanserin.

The density of 5-HT_2 receptor binding sites was measured by quantitative in vitro autoradiography on horizontal rat brain sections using the FUJI BAS 2000 bio-imaging analyzer (FUJI Photo Film Co., Tokyo), which resulted in one tenth of the exposition time compared with the conventional film autoradiography.

Two rhenium complexes were studied to search for possible serotonergic receptor-affine properties. These compounds inhibited [^{3}H]ketanserin binding in homogenates of rat frontal cortex with IC_{50} values of 1.25 µM and 0.93 µM [6]. The Re complexes were used as model compounds for planned [^{99m}Tc]complexes. The receptor-binding properties of compounds were gained indirectly by comparison of their inhibition of [^{3}H]ketanserin binding with mianserin, as a displacer which has high affinity to 5-HT_2 receptors.

Materials and methods

6 male Wistar rats weighing 229 - 300 g were used. The rats were sacrificed by CO_2 inhalation and their brains rapidly removed, frozen quickly in an isopentane/dry ice solution at -70 °C.

To prepare sections, the brains were mounted on cryostat chucks and 20 µm horizontal sections were cut at -20 °C, thaw-mounted onto gelatin-coated microscope slides, dried at room temperature and kept at -20 °C until used. Every 10th

section was stained with cresyl violet to facilitate identification of brain regions by using the atlas of Paxinos and Watson [5].

Serotonin-binding sites in brain tissue were labelled as described by Hrdina, P. D. et al. [1]. In brief, the frozen sections were warmed to room temperature and pre-incubated for 15 min in 50 ml Coplin jars containing 50 mM tris - HCl buffer (pH 7.6) to remove endogenous ligands. The sections were then incubated in a solution of 50 mM tris - HCl buffer (pH 7.6), 1 nM [^{3}H]ketanserin (sp.act. 2.99 TBq/mmol) and 2 µM tetrabenazine to mask the vesicular amine uptake sites, and incubated for 40 min at room temperature.

The nonspecific binding was determined by incubating adjacent sections of the same brain areas in the presence of 2 µM tetrabenazine and 10 µM mianserin.

To examine the inhibition of [^{3}H]ketanserin binding by the two Re complexes compounds 16 and 17 [7], adjacent sections of the same brain areas were incubated under the same conditions. The test substance was used at a concentration of 1 µM, which is close to the IC_{50} value measured in binding studies with homogenates [6].

The sections were washed for 2 x 10 min in ice cold buffer, rinsed in distilled water, and dried with cold air.

For autoradiography, the sections together with tritium labelled polymer layer standards (Amersham, Braunschweig) calibrated for intact brain grey matter were apposed to tritium-sensitive imaging plates and kept at 4 °C for one week. The exposed imaging plates were inserted into an image reading unit and then scanned with a fine laser beam in the FUJI BAS 2000 device. The image data were recorded as digital values and evaluated with the TINA 2.07c program (Raytest, Straubenhardt).

In addition, the equilibrium dissociation constants (K_D) and receptor densities (B_{max}) were estimated. For this purpose, saturation experiments were performed in several rat brain regions. Alternating adjacent sections were incubated with increasing concentrations of the radioligand [^{3}H]ketanserin (0.3 - 5 nM).The incubation and the determinations of the specific and nonspecific binding were carried out as described above. The data were analysed by Eadie-Hofstee plots and with the figure P computer program.

Furthermore, the radioactivity in some of the slide-mounted tissue sections adjacent to those used for autoradiography was measured after incubation, using the LS counter 6000 (Beckman Instruments, Fullerton).

Results and discussion

From the LSC measurement of the sections a relatively high nonspecific binding (defined with mianserin as a displacer) of about 64 % was calculated. However, this measurement includes the whole brain, i.e. also areas with low receptor densities Using compounds 16 and 17 as displacer, about 78 and 72 %, respectively, of the total binding remained on the sections. That means that these compounds inhibited

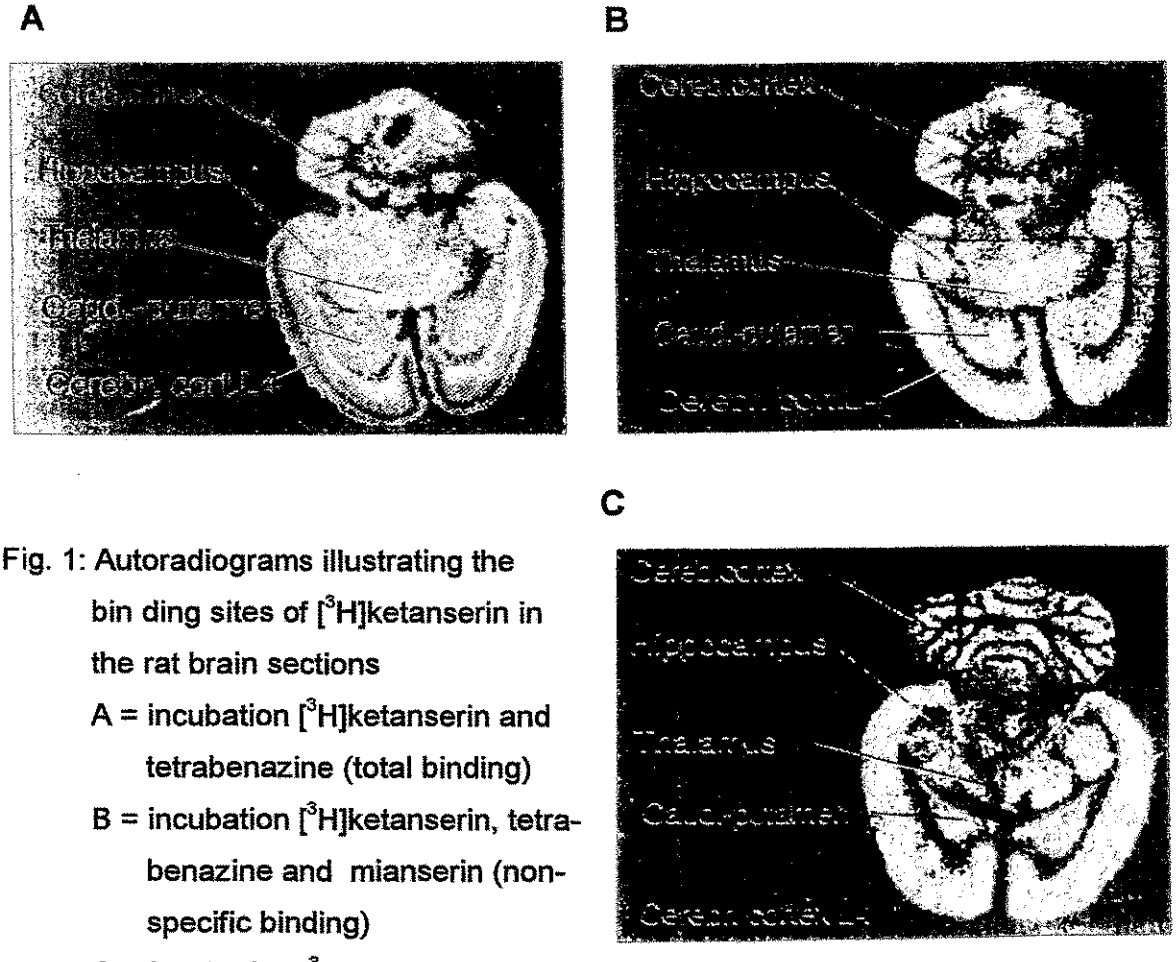

Fig. 1: Autoradiograms illustrating the bin ding sites of [^{3}H]ketanserin in the rat brain sections
A = incubation [^{3}H]ketanserin and tetrabenazine (total binding)
B = incubation [^{3}H]ketanserin, tetra-benazine and mianserin (non-specific binding)
C = incubation [^{3}H]ketanserin and compound 17
The radioactive concentration decreases from red to yellow and green
(Cereb. cortex = cerebellar cortex, Cerebr.cort. L4 = cerebral cortex lamina 4)

the specific binding of [^{3}H]ketanserin by more than 50 %, which corresponds to the data obtained from binding studies with homogenates [6]. These results are also confirmed by the autoradiograms. Fig. 1 shows the distribution of total [^{3}H]ketanserin binding (A), nonspecific binding (B) and the autoradiogram obtained after inhibition with compound 17 (C). Fig. 1A shows a highly selective distribution of [^{3}H]ketanserin in various brain areas, with the highest labelling in the frontal and parietal cortex, in which different binding of the label in certain laminae is evident. A medium level of 5-HT_2 receptor density is visible in the caudate-putamen and thalamus, as also demonstrated in Fig. 2. The image of the nonspecific [^{3}H]ketanserin binding (Fig. 1B) displayed a homogeneous low level of labelling.

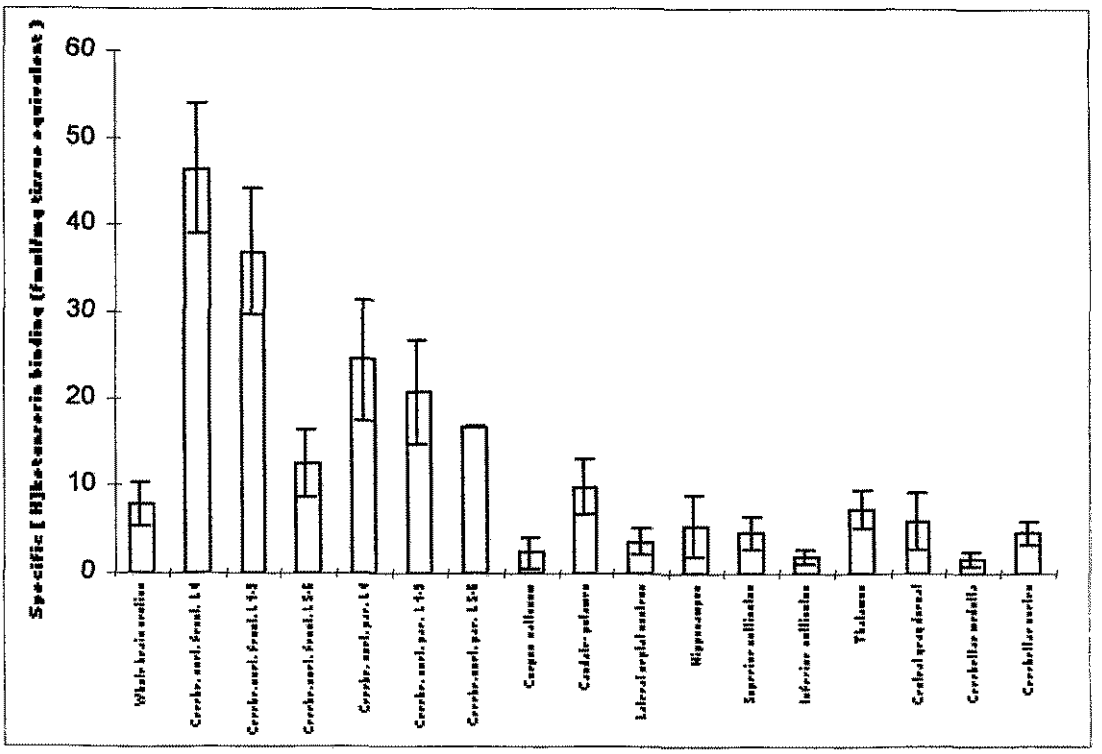

Fig. 2: Specific binding of [^{3}H]ketanserin in different areas of the rat brain, n = 6
Cerebr.cort. front. L4 = cerebral cortex frontal lamina 4;
Cerebr.cort.par. L 1-3 = cerebral cortex parietal lamina 1-3

Preliminary results from the saturation experiments are shown in Table 1.

Table 1: Parameters of [^{3}H]ketanserin binding in different brain areas

Area	K_D (nM)	B_{max} (fmol/mg tissue equivalent)
Whole brain section	2.32 ± 0.73	23.07 ± 3.32
Cortex right	1.56 ± 0.75	43.35 ± 8.22
Cortex left	1.64 ± 0.8	49.67 ± 9.1

The affinity of the ligand estimated for the whole section is lower than for the cortical region, which may be explained by a different contribution of 5-HT_2 receptor subtypes to the total binding.

Fig. 3 shows the percentage of total binding which remained after inhibition with mianserin and the Re complexes, respectively, in several areas of the brain (see also Fig. 1B and 1C).

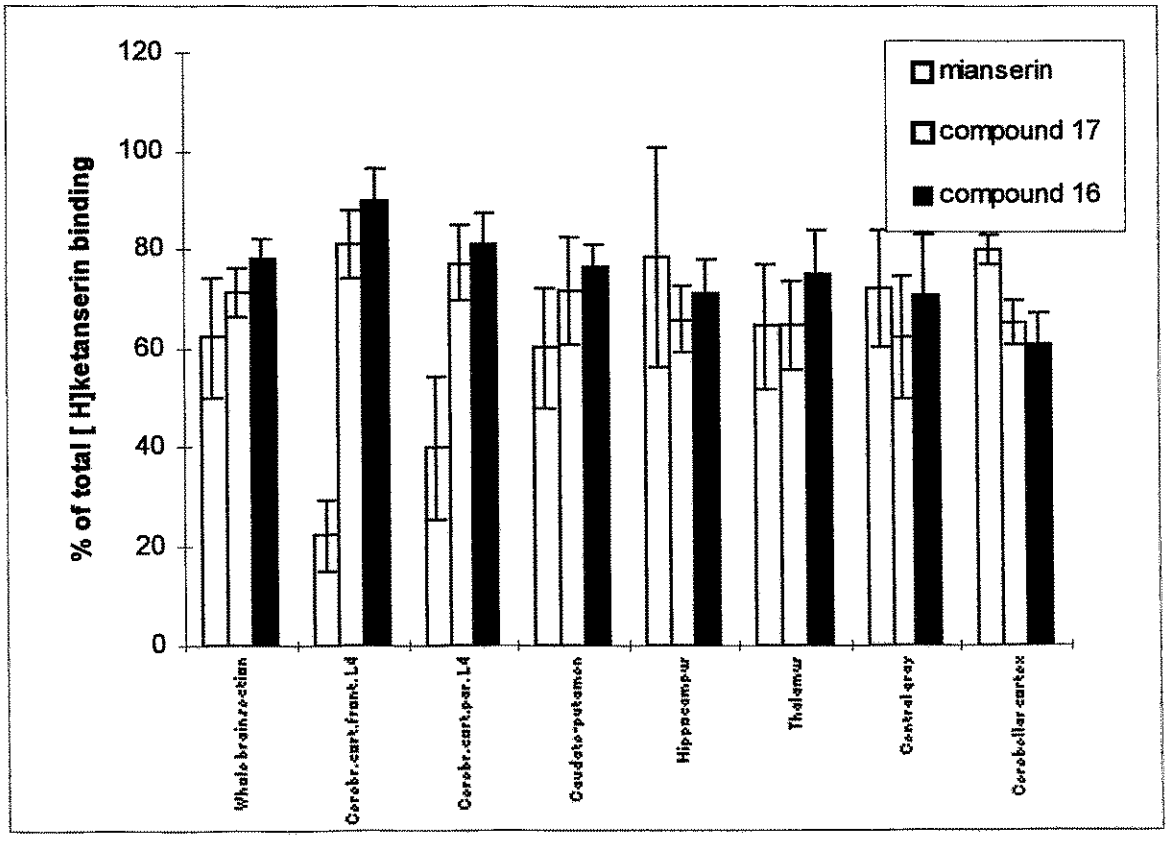

Fig. 3: Inhibition of [^{3}H]ketanserin binding (percentage of total binding) by various compounds, n = 6

The amount of nonspecific binding, measured with mianserin, varied between 20 and 40 % of the total binding in cortical areas and 60 and 80 % in the other structures of the brain. The values for the remaining [^{3}H]ketanserin binding sites after inhibition with the Re compounds displayed in Fig. 3 show a relatively small decrease of the total binding to about 80 - 90 % in the cortical areas. However, a higher inhibition of [^{3}H]ketanserin binding was found in the hippocampal region and cortical area of the cerebellum. Compounds 16 and 17 inhibit [^{3}H]ketanserin binding even more than mianserin. This is confirmed more clearly in Fig. 4, which shows the part of the specific [^{3}H]ketanserin binding (measured with mianserin) which is not inhibited after use of the Re complexes.

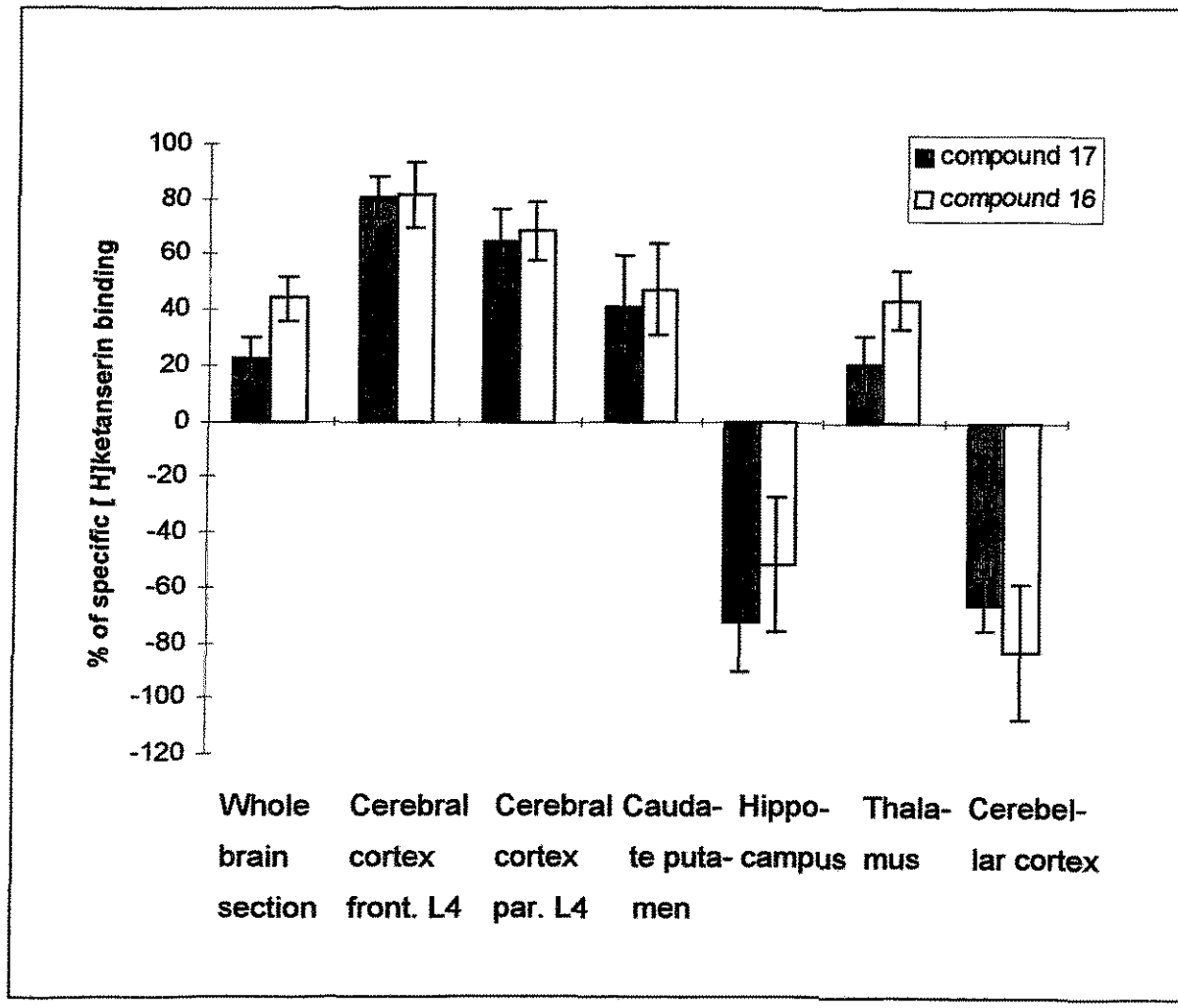

Fig. 4: Percentage of the specific [^{3}H]ketanserin binding which remained after addition of the Re compounds to the incubation medium, n = 6

The specific [^{3}H]ketanserin binding which remained after the use of compounds 16 and 17 as displacers was about 40 % and 20 %, respectively, in the whole brain section. The non-displaceable specific [^{3}H]ketanserin binding was about 60 - 80 % in the cortical areas and 20 - 50 % in the caudate putamen and thalamus. The greater inhibition in the hippocampus and cerebellar cortex indicates that [^{3}H]ketanserin probably binds to a heterogeneous population of receptors. This ligand can probably label both 5-HT_{2C} and 5-HT_{2A} receptors. In addition, it binds with low affinity to α_1 - adrenoceptors or histamine H_1 receptors [8]. Further studies are planned with displacer compounds for the identification of these different binding sites.

The Re complexes used in this study suggest that it might be possible to obtain ^{99m}Tc-labelled serotonergic ligands. The fact that the two Re compounds inhibit [^{3}H]ketanserin binding in the hippocampus and cerebellum more than mianserin indicates that they have an affinity to a second binding site which is labelled by [^{3}H]ketanserin. They have a higher affinity than mianserin to this binding site.

References

[1] Hrdina, P.D. et al., Synapse **14** (1993) 324

[2] Leysen, J. E. et al., Mol. Pharmacol. **21** (1982) 301

[3] Schotte, A. et al., Brain Res. **276** (1983) 231

[4] Pazos, A. et al., Brain Res. **346** (1985) 231

[5] Paxinos, G. et al., The rat brain in stereotaxic coordinates, Academic Press, New York 1986

[6] Brust, P. et al., unpublished data

[7] Pietzsch, H.-J. et al., unpublished data

[8] Waeber, C. et al., Mol. Brain Res. **24** (1994) 199

30. BIOLOGICAL CHARACTERIZATION OF ^{99m}Tc-DMS ESTER COMPLEXES IN RATS

R. Syhre, S. Seifert, H. Spies, B. Johannsen

Studies of the biological behaviour of ^{99m}Tc-DMS esters in rats were carried out to test the influence on distribution and excretion of ester functions and the number of ester groups within the molecule. Furthermore it seems to be interesting to study the effect on biodistribution of the arrangement of ester groups in the molecule.

Experimental

Table 1 gives a summary of the ^{99m}Tc-DMS compounds used for the investigations.

Table 1: ^{99m}Tc-DMS compounds used for investigations

COMPLEX	FORMULA
1 **R = Ethyl-** **1-1** **R = Methyl-** **1-2** **R = Diisobutyl-**	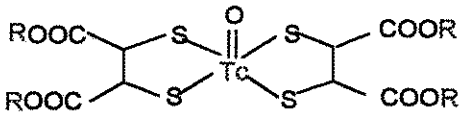
2	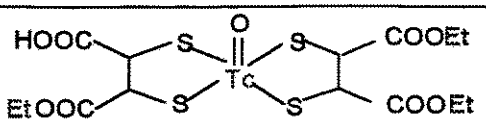
3	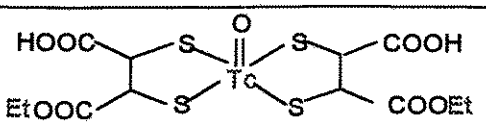
4	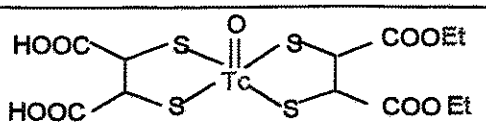
5	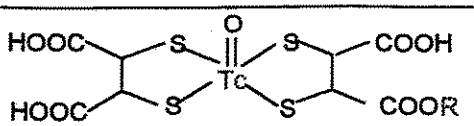
6	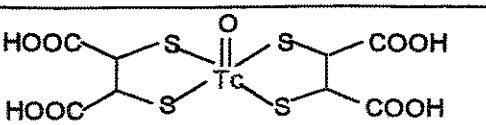

Preparation, characterization and enzymatic hydrolysis of the ester complexes are described in [1] and [2]. The reference substance for these studies was ^{99m}Tc(V)-DMSA (complex 6), a radiopharmaceutical used for tumour diagnosis.

For *in vivo* studies 0.5 ml complex solution (5 - 10 MBq ^{99m}Tc) are injected into the tail vein of male Wistar rats (5 - 6 weeks old). After the incubation time the rats were sacrificed by heart puncture under light ether anaesthetic and the selected organs were isolated for weighing and counting.

Table 2: Distribution of ^{99m}Tc-DMS compounds in rats (means ± SD; n ≥ 6)

Complex	Time p.i. [min.]	Blood % D/g	Heart % D/g	Lung % D/g	Kidney % D/g	Liver % D/g	Femure % D
1	10	0,7 ± 0,2	0,5 ± 0,3	0,5±0,3	2,2 ± 0,5	4,2 ± 0,9	≤0,1
	60	0,6 ± 0,1	0,3 ± 0,2	0,3 ± 0,1	1,3 ±0,3	1,5 ± 0,3	≤0,1
	120	0,4 ± 0,1	0,2 ± 0,1	0,3 ± 0,3	1,3 ± 0,2	1,4 ± 0,2	≤0,1
2	10	1,7 ± 0,3	0,7 ± 0,3	1,2 ± 0,2	2,0 ± 0,4	4,3 ± 1,0	0,3
	60	1,4 ± 0,3	0,5 ± 0,2	0,6 ± 0,1	1,7 ± 0,3	2,0 ± 0,5	0,2
	120	0,7 ± 0,2	0,3 ± 0,1	0,5 ± 0,2	0,9 ± 0,1	1,4 ± 0,4	≤0,1
3	10	1,9 ± 0,3	0,8 ± 0,2	1,7 ± 0,4	1,9 ± 0,4	1,5 ± 0,4	0,4
	60	1,3 ± 0,3	0,5 ± 0,1	1,1 ± 0,1	1,5 ± 0,2	1,2 ± 0,3	0,2
	120	1,2 ± 0,3	0,4 ± 0,2	0,8 ± 0,1	1,3 ± 0,2	1,2 ± 0,2	0,2
4	10	2,4 ± 0,3	0,8 ± 0,2	1,7 ± 0,4	2,9 ± 0,2	4,4 ± 0,9	0,4
	60	1,8 ± 0,3	0,6 ± 0,1	1,2 ± 0,2	3,4 ± 0,5	5,6 ± 0,4	0,3
	120	1,3 ± 0,3	0,5 ± 0,1	0,7 ± 0,2	4,5 ± 0,5	6,5 ± 0,4	0,2
5	10	2,2 ± 0,3	0,9 ± 0,2	1,8 ± 0,3	1,8 ± 0,3	2,0 ± 0,4	0,5
	60	1,1 ± 0,1	0,6 ± 0,2	1,1 ± 0,2	1,2 ± 0,1	1,9 ± 0,5	0,4
	120	0,9 ± 0,1	0,4 ± 0,1	0,9 ± 0,1	1,1 ± 0,1	1,3 ± 0,2	0,3
6	10	1,1 ± 0,2	0,5 ± 0,3	0,5 ± 0,2	2,1 ± 0,3	0,3 ± 0,1	1,2 ± 0,1
	60	0,4 ± 0,1	0,3 ± 0,2	0,3 ± 0,1	2,0 ± 0,2	0,3 ± 0,1	1,5 ± 0,1
	120	0,2 ± 0,1	0,1 ± 0,1	0,2 ± 0,1	1,9 ± 0,3	0,2 ± 0,05	1,6 ± 0,2
1-1	10	1,3 ± 0,2	0,6 ± 0,1	1,1 ± 0,2	3,9 ± 0,2	4,8 ± 0,9	0,2
	60	1,0 ± 0,4	0,3 ± 0,1	0,6 ± 0,1	3,3 ± 0,4	2,6 ± 0,5	0,1
	120	0,7 ± 0,1	0,3 ± 0,2	0,4 ± 0,1	2,9 ± 0,5	1,0 ± 0,4	0,1
1-2	10	1,5 ± 0,3	0,5 ± 0,3	1,2 ± 0,3	0,5 ± 0,2	11,6 ± 2,5	0,2
	60	1,2 ± 0,3	0 4 ± 0,3	0,9 ± 0,2	0,5 ± 0,2	8,2 ± 1,9	0,2
	120	0,4 ± 0,1	0,2 ± 0,2	0,4 ± 0,3	0,2 ± 0,1	6,2 ± 1,3	0,1

Results and discussion

No target organ was found for the ester complexes. The radioactivity in the brain, in the spleen and the pancreas was not higher than the background activity in the remaining parts of the animal. Table 2 shows the distribution data 10, 60 and 120 minutes after injection for some interesting organs. With the exception of complex 4 the blood elimination and the distribution data are within the normal range. The renal and the hepatobiliary parts of distribution and excretion are demonstrated in Figs. 1 and 2, depending on the number of carboxyl groups and the nature of the alcohol function of the complexes.

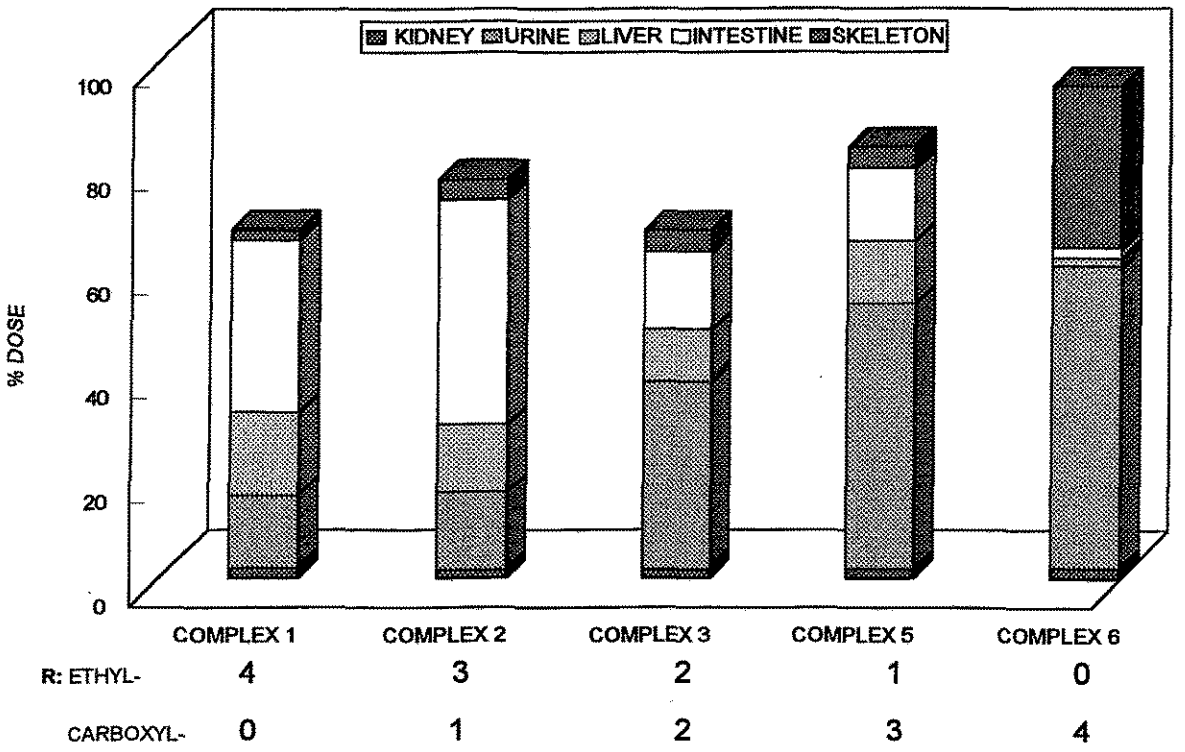

Fig. 1: ^{99m}Tc-DMS complexes - renal and hepatobiliary parts of excretion and accumulation and skeleton uptake in rats (60 min. p.i.; means; $n \geq 6$)

Fig. 1 shows that the renal part increases with the number of carboxyl groups in the molecules, which is consistent with a decrease of lipophilicity [2]. The results also demonstrate that the affinity of ^{99m}Tc(V)-DMSA to the bone disappears in the presence of only one ester group (complex 5). Fig. 2 documents that the hepatobiliary part of distribution and excretion increases with increasing lipophilicity

from methyl (complex **1-1** ; log P ~ -1) to diisobutyl (complex **1-2** ; log P ~ +1) derivatives.

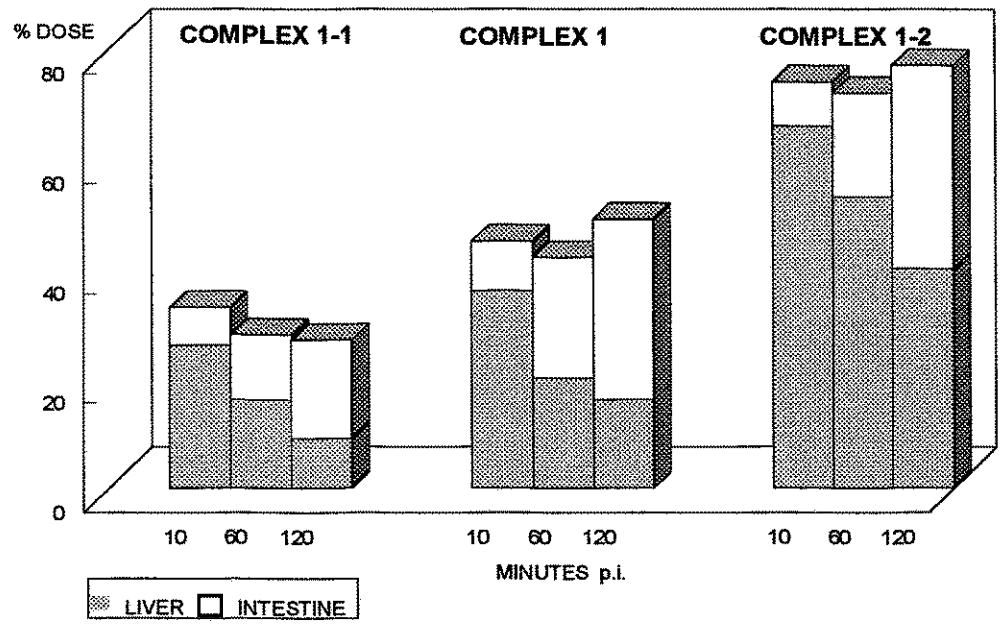

Fig. 2: ^{99m}Tc-DMS tetraester compounds - hepatobiliary parts of excretion and accumulation in rats (means; n ≥ 6)

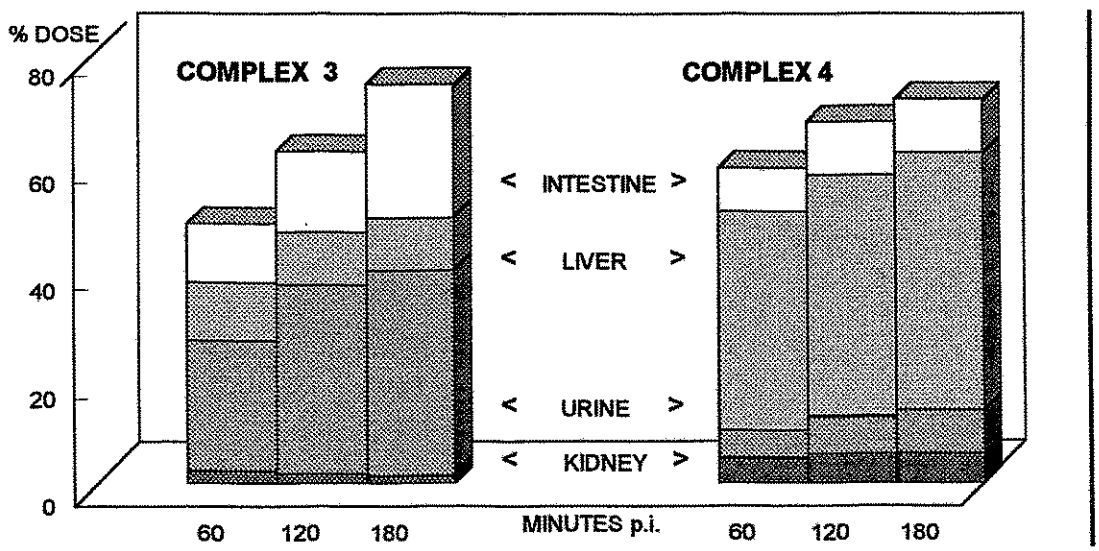

Fig. 3: ^{99m}Tc-DMS diester complexes - comparison of symmetric and asymmetric form in rats (means; n ≥ 6)

The *in vivo* behaviour differs significantly between symmetric (complex 3) and an asymmetric (complex 4) diester complex (Fig. 3). After injection of complex 4 a very high accumulation in the liver was observed. The activity is not much excreted via the biliary tract.

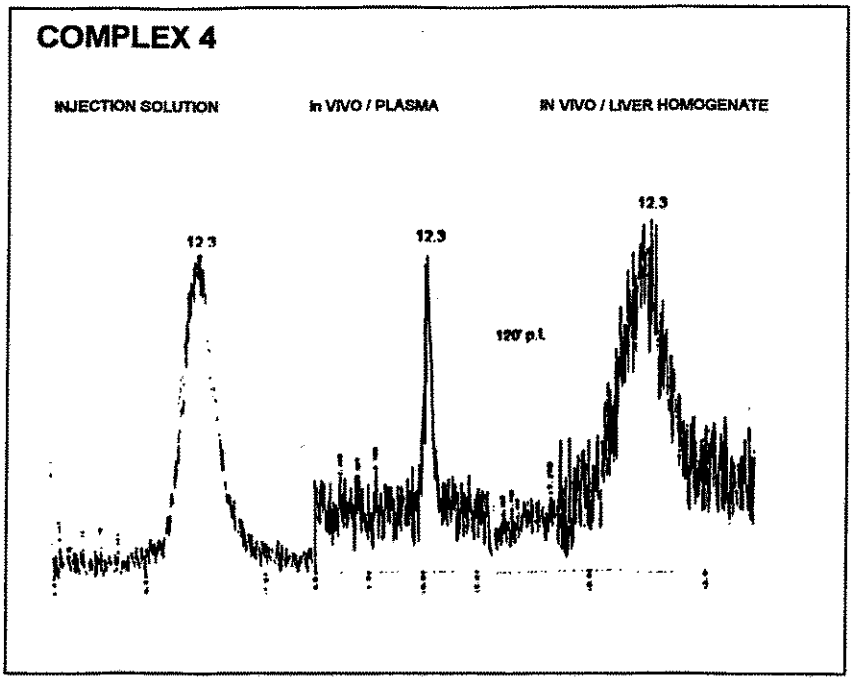

Fig. 4: *In vivo* stability of asymmetric ^{99m}Tc-DMS diester (complex 4) in the blood and liver of rats

The chromatography of the liver extract shows that the complex is not metabolized *in vivo* in the liver (Fig. 4). The high accumulation of complex 4 in the liver cannot be explained.

References

[1] Syhre, R. et al., Annual Report 1992, p. 61, Institute of Bioinorganic and Radiopharmaceutical Chemistry, FZR 93-12

[2] Seifert, S. et al., this report, p. 38

31. IN VITRO EVALUATION OF ^{99m}Tc-ESTER COMPLEXES BY ENZYMATIC METHODS IN COMPARISON WITH *IN VIVO* METABOLISM AND BIODISTRIBUTION IN RATS

R. Syhre, S. Seifert, H. Spies, B. Johannsen

The biological screening of potential radiopharmaceuticals in rats is more complicated when the tracers are subject to *in vivo* metabolism as well as to a significant species- dependent variation of this metabolism. This is to be expected for ester groups bearing ^{99m}Tc -complexes if the ester bonds are metabolizable.

Unfortunately, compounds with metabolizable ester groups show wide interspecies variations in biological behaviour [1,2,3,4]. The reason for these variations is, that the metabolic enzymes, especially the esterases, vary considerably from tissue to tissue and from one species to another. The esterases of blood and liver, for instance, have a low specificity to substrates and a high specificity to stereoisomeric compounds. The activity of these enzymes is variable in different animals and in man. Because of the different behaviour of the species, especially between humans and rats, the extrapolation from animal to man of the biodistribution data is limited [5,6,7].

In screening new ^{99m}Tc-ester complexes it appears reasonable to clarify whether the complexes actually may be metabolized under the conditions of interest.

Systematic investigations of the enzymatic hydrolysis from ^{99m}Tc-DMS esters are carried out:

- to find a simple and reliable *in vitro* test system. This system is supposed to show differences in metabolism and biodistribution in species prior to animal experiments.
- to compare the *in vitro* and *in vivo* data in order to extrapolate from rat to man

Experimental

The ^{99m}Tc-DMS-ester complexes used for the investigations are already described in an other article of this report [10]. ^{99m}Tc-ECD was used as reference compound. The

conditions of the *in vitro* hydrolysis are summarized in Table 1. Analytical data of metabolites have been described in this report [9].

For *in vivo* studies 0.5 ml complex solution (5 - 10 MBq ^{99m}Tc) are injected in the tail vein of male Wistar rats. After the incubation time rats were sacrificed by heart puncture under a light ether anaesthetic. Blood plasma and urine were analysed by HPLC.

Table 1: Conditions of enzymatic hydrolysis of ^{99m}Tc-ester complexes

VOLUME	→	1 ml
RADIOACTIVITY	→	> 5 - 10 MBq 99mTc-COMPLEX (n.c.a.)
ENZYME MEDIA	→	• PLASMA / 1:1 / PHOSPHATE BUFFER , pH 7.4 • HOMOGENATE / 1:20 / PHOSPHATE BUFFER, pH 7.4 • PIG LIVER ESTERASE, PLE (EC.3.1.1.1) ; / 100 U / ml
INCUBATION	→	≥ 10 ≤ 120 MINUTES; 37°C; SHAKE
ANALYSIS	→	COMPLEX, METABOLITES : HPLC SEPARATION *PRP-1*

Results and discussion

Hydrolysis of the DMS-ester complexes is markedly species dependent. The *complexes* **1**, **2**, **1-1** *and* **1-2** *are partially hydrolysed in rat plasma, in rat liver* homogenates and in pig liver esterase (PLE), as exemplified in Fig. 1 and Fig. 2. In rats, *in vitro* and *in vivo* data are consistent. The HPLC analysis of urine 120 minutes p. i. shows only the metabolites. No metabolism can be observed for complexes **3**, **4** *and* **5** *under the same conditions. In vitro non hydrolysable esters (complexes* **3**, **4**, **5**) are also stable *in vivo* (Fig. 3). All complexes (**1** - **5** ; 1-1 and **1-2**) are stable in human plasma [8,9].

As seen in Figs. 1 and 2, only 20 - 40 % of the parent compounds are found hydrolysed in the blood of rats 10 minutes after injection.

From the results obtained with complex **1** and complex **2**, as seen in Figs. 1 and 2, the following conclusions can be drawn:

- The complexes investigated represent a type of ester- bearing compounds which is metabolized in rat plasma both *in vitro* and *in vivo*, but not in human plasma. In this case, metabolites are not of interest for the evaluation of the potential radiopharmaceutical. Therefore only the data of initial biodistribution during the first minutes after injection as obtained in rats should be used for an extrapolation from rat to man.
- The identification of a possible target organ depends on the speed of the hydrolysis and on the portion of parent complex still present in the blood pool of test animals.

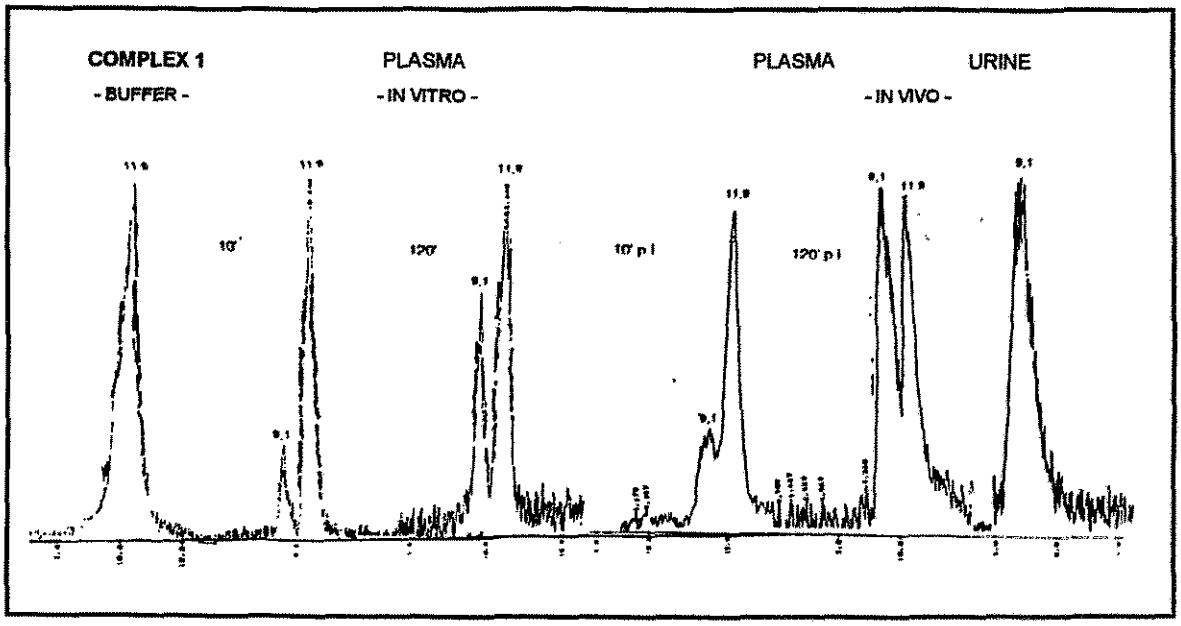

Fig. 1: Comparison of *in vitro* and *in vivo* metabolism of complex 1 in rats (HPLC patterns)

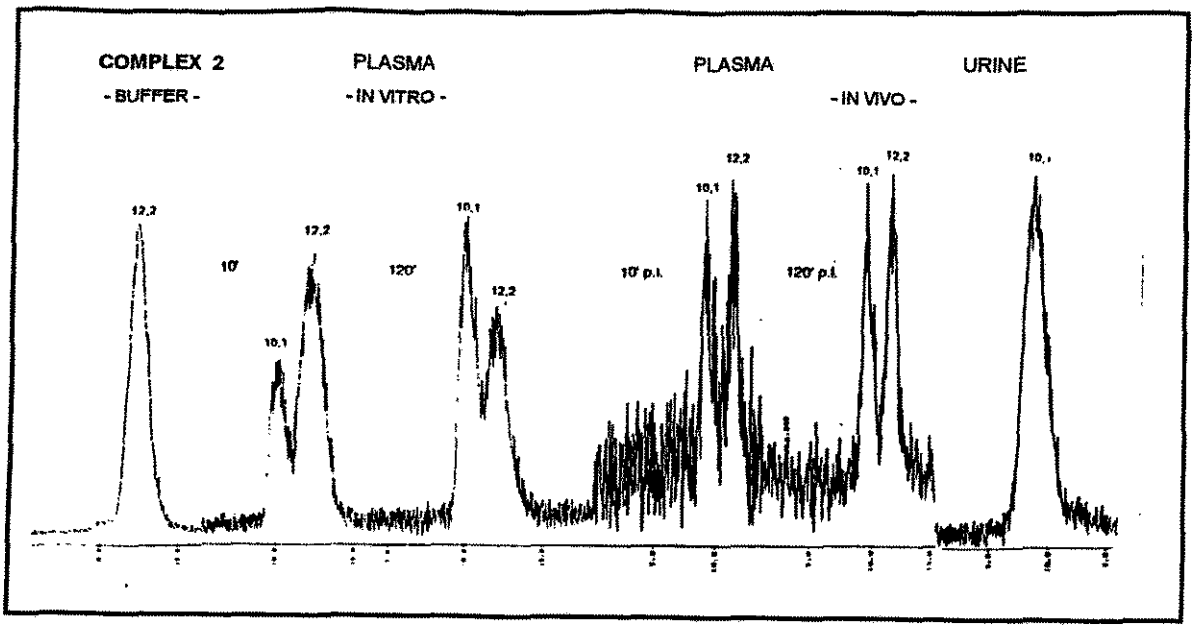

Fig. 2: Comparison of *in vitro* and *in vivo* metabolism of complex 2 in rats (HPLC patterns)

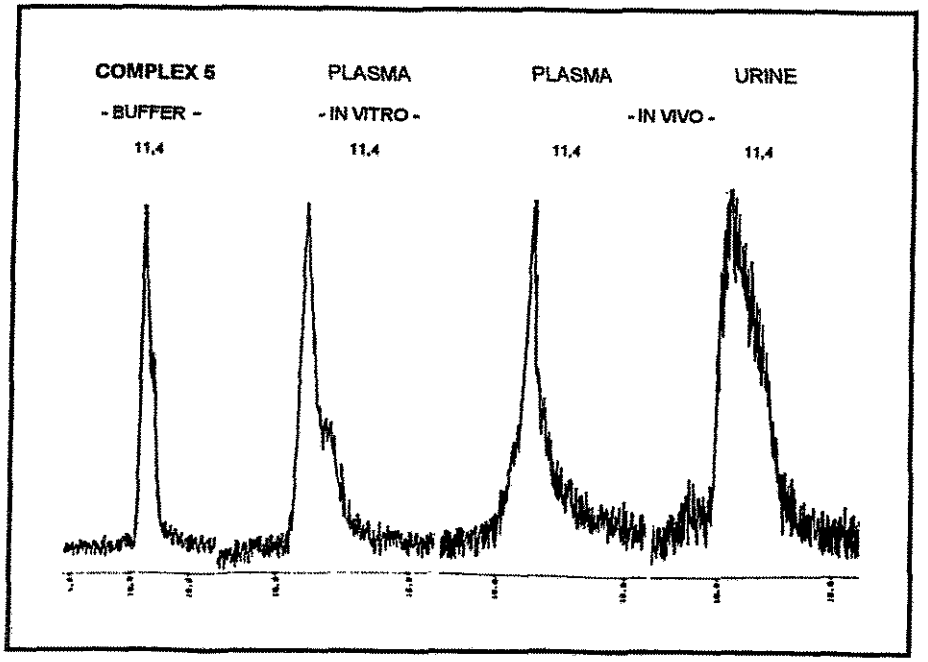

Fig. 3: Comparison of *in vitro* and *in vivo* stability of complex 3 in rats (HPLC patterns)

In the following, these conclusions have been applied to a known ester- bearing radiopharmaceutical in order to validate the conclusions. We tested the brain perfusion imaging agent ^{99m}Tc-ECD (Fig. 4), for which species dependent enzymatic hydrolysis to its mono and diacid form is known [1,2].

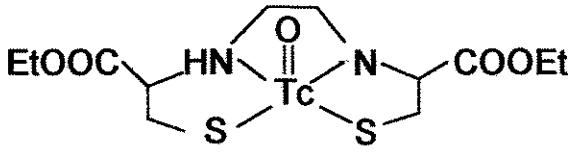

Fig. 4: ^{99m}Tc-ECD (^{99m}Tc-N,N'-1,2-ethylene-diylbis-L-cysteine diethyl ester)

Our results of *in vitro* and *in vivo* hydrolysis are demonstrated in Fig. 5, which agree well with the literature. In human plasma, only a small percentage of the parent compound (^{99m}Tc-ECD) is partially hydrolysed to the monoacid compound (^{99m}Tc-ECM). In rat plasma however, the monoacid metabolite and a small amount of diacid complex is quickly formed *in vitro* and *in vivo*. The rapid brain uptake in rats shows the ability of ^{99m}Tc-ECD to pass the blood-brain barrier of the rat. The slow wash out of the brain activity 10 - 60 minutes after injection documents the affinity to the brain (Fig. 6).

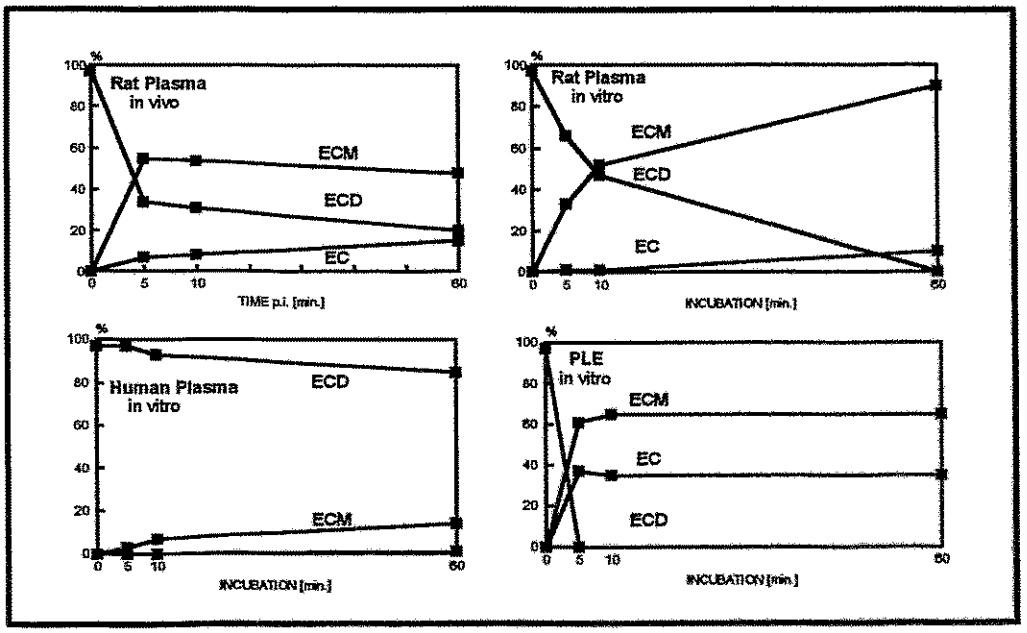

Fig. 5: Comparison of *in vitro* and *in vivo* metabolism of ^{99m}Tc-ECD in rats

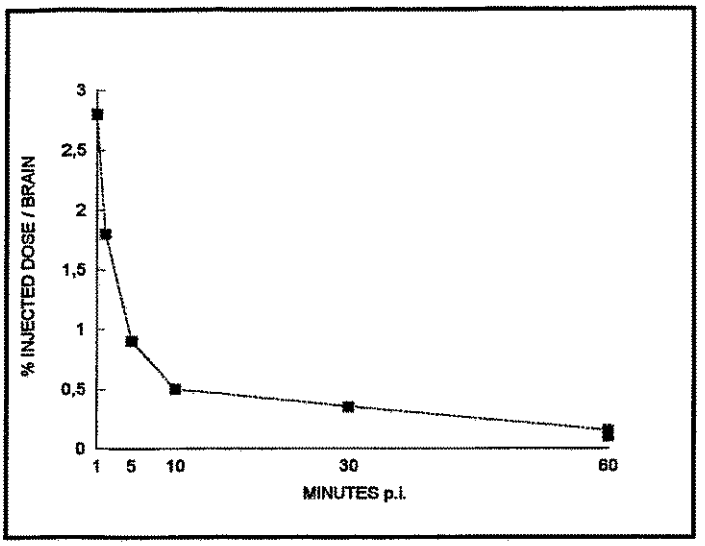

Fig. 6: Brain uptake and brain wash out after injection of ^{99m}Tc-ECD in rats (mean; n = 3)

Actually, according to our results, ^{99m}Tc-ECD behaves similarly to the complexes 1 and 2 described above and thus belongs to the type of compounds for which we have drawn our conclusions. ^{99m}Tc-ECD is quickly metabolized in rat plasma both *in vitro* and *in vivo* but in human plasma only a small percentage is hydrolysed to the monoacid compound, as illustrated in Fig 5. According to our hypothesis, the early biodistribution patterns in rats, the rapid brain uptake and the slow wash out (Fig. 6) are pedictive for man.

References

[1] Walovitch, R. C. et al., J. Cereb. Blood Flow Metab. **14** (1994) 4

[2] Verbruggen, A. et al., in: Technetium and Rhenium in Chemistry and Nuclear Medicine 3 (M. Nicolini, G. Bandoli, U. Mazzi Eds.) Cortina International, Verona 1990, p. 445

[3] Pasqualini, R. et al., Eur. J. Nucl. Med. **20** (1993) (abstr.)

[4] Vanbilloen, H. et al., Eur. J. Nucl. Med. **20** (1993) (abstr.)

[5] La Du, B. et al., in: Concepts in Biochemical Pharmacology, Part.2 (B. B. Brodie, J. R. Gillette Eds.) Springer, Berlin, Heidelberg, New York 1971

[6] Bergmeyer, H. U., Methods of Enzymatic Analysis IV,

Verlag Chemie, Weinheim 1967

[7] Paul, J., Biochem. J. **78** (1961) 418

[8] Syhre, R. et al., Annual Report 1992, p. 61, Institute of Bioinorganic and Radiopharmaceutical Chemistry, FZR 93-12

[9] Seifert, S. et al., this report, p. 38

[10] Syhre, R. et al., this report, p. 129

32. UPTAKE OF ^{99m}Tc(V)-DMS COMPLEXES IN TUMOUR CELLS *IN VITRO*

G. Kampf[1], U. Wenzel[1], W.-G. Franke[1], S. Seifert, P. Brust, B. Johannsen

[1] Klinik und Poliklinik für Nuklearmedizin, Universitätsklinikum "Carl Gustav Carus", Technische Universität Dresden

^{99m}Tc(V)-dimercaptosuccinic acid (DMSA) has proved to be a useful imaging agent mainly for medullary thyroid carcinoma [1-4] but also for bone and soft tissue tumours and their metastases [5,6]. Replacement of the technetium by the ß-emitter rhenium-186 [7] is of high therapeutic interest for palliation of metastatic pain, provided the nuclide can be enriched in the malignant tissue in an amount sufficient to yield an effective dose.

Since the compounds of the pentavalent technetium with DMSA are accumulated by some tumours in imaging-relevant amounts, it seems reasonable to synthesize and study derivatives of the compound with the aim to find a modified tracer which accumulates still higher in these or other tumours.

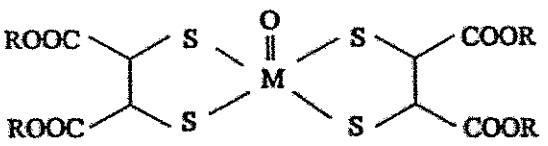

M = Tc, Re

R = H, Me, Et, Isobut

In this sense the methyl, ethyl, and isobutyl esters of the ^{99m}Tc(V)-DMSA, where all carboxylic groups are esterified, were to be studied for their uptake in tumour cells *in vitro*. With the introduction of the ester groups a change from the hydrophilic DMSA molecule to more lipophilic compounds occurs with the lipophilicity increasing with the chain length of the alkyl group. This may have consequences for attachment at the cellular membrane and for cellular uptake. Therefore their uptake by human adenocarcinoma cells of the kidney has been studied; the first results are presented in this contribution.

Materials and methods

The ^{99m}Tc(V)-DMS esters were synthesized according to the method described [8].
The cell strain used was the line KTCTL-2, a human adenocarcinoma of the kidney from the DKFZ Heidelberg. The methods for growing the cells and preparing them for radioactivity measurement have been reported in [9].
Incubation of the cell monolayers with the radiotracers was performed in cell culture medium RPMI 1640 for 1 h at 37 °C. In order to study the influence of plasma proteins on the uptake of the complexes, medium without and with 10 % of fetal calf serum (FCS) was used.The concentration of the radiotracers was varied between 37 and 600 KBq/ml (1 - 16 µCi/ml).

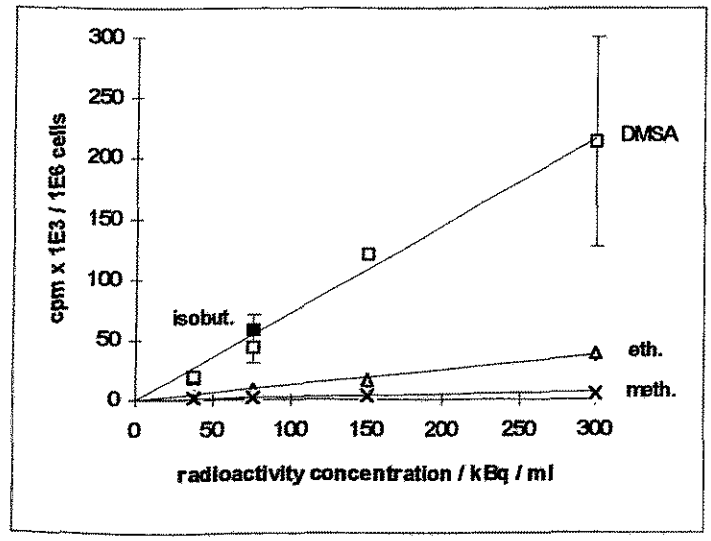

Fig.1. Uptake of ^{99m}Tc(V)-DMS complexes by KTCTL-2 cells in dependence on the radiotracer concentration, n = 4.

Results and discussion

Fig.1 shows that cellular association of all four complexes studied in medium without serum grows linearly with tracer concentration. ^{99m}Tc(V)-DMSA shows the highest uptake into the cells, with the isobutyl ester adequate radioactivity in the cell pellet was measured with the two lowest concentrations. With the methyl and ethyl esters, however, uptake is strongly diminished.

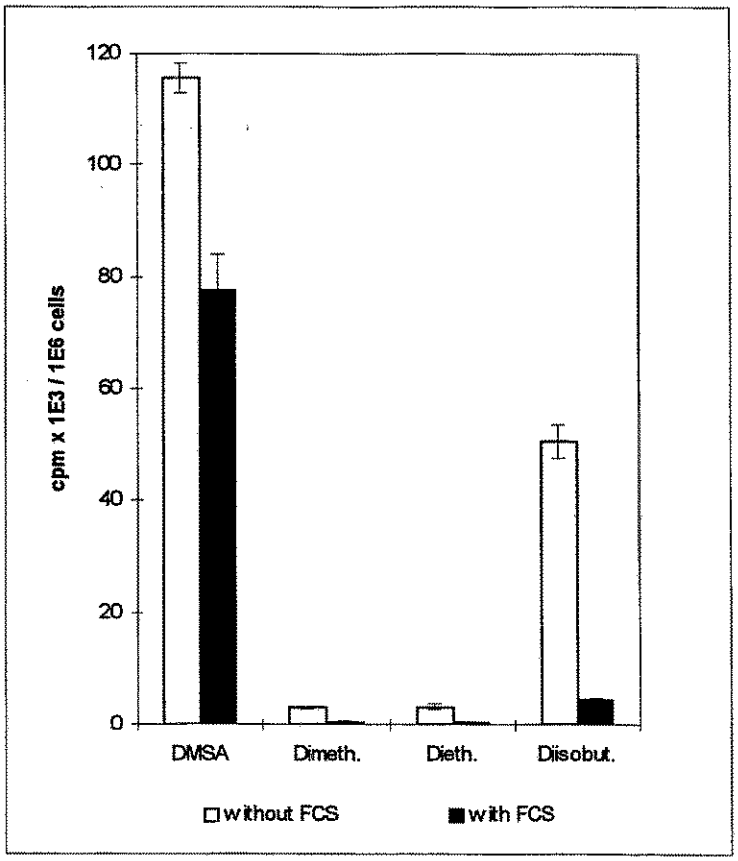

Fig.2. Uptake of ^{99m}Tc(V)-DMS complexes by KTCTL-2 cells in the absence and presence of serum proteins, n = 6
FCS = fetal calf serum.

The higher cell association of the isobutyl ester is not readily interpretable, possibly it does not represent a real cellular uptake but only an outer attachment at the cell membrane as a sequel of the high lipophilicity.

It has to be noted that with all compounds studied at concentrations above 300 KBq/ml, representing of course a correspondingly high concentration of the free ligand, the cells began to detach themselves from the plastic dish, i. e. their normal adherence is disturbed. With the isobutyl ester, this signal was already observed at 150 kBq/ml, therefore in Fig.1 only the first two concentrations were utilized. Hence the following experiments were performed with radiotracer concentrations of 100 kBq/ml.

In Fig. 2 the influence of serum proteins on the uptake of the complexes is represented. It is evident that the addition of FCS leads to a strong diminution of the cellular uptake resp. the association of the compounds. The effect is especially pro-

nounced with ester substitution, and increases with the chain length of the alkyl group: in these experiments uptake in the presence of serum decreases to 66 % with the DMSA complex, to 16 % with the methyl and ethyl esters, and to only 8 % with the isobutyl ester. It may be a consequence of the growing lipophilicity of the compounds that their affinity to the serum proteins increases, and the protein-bound portion is no longer available for cellular uptake. The same phenomenon is observed with the ^{169}Yb citrate complex [10].

Additional information is provided by a comparison of the ratios of radioactivities released by the trypsin-EDTA treatment of the cells to the radioactivities in the cell pellets. After incubation with the radiotracer and 12-fold rinsing of the monolayers with buffer solution, the cells are dissociated from the surface of the petri dish by trypsin-EDTA solution. This treatment also dissociates the protein particles or complex molecules attached outside at the cell membrane.

Table 1. Ratio of radioactivities released by trypsin to the radioactivities of the cell pellets, using the ^{99m}Tc(V)-DMSA complex and three ^{99m}Tc(V)-DMS complexes

Compound Condition	R = H	R = CH_3	R = C_2H_5	R = C_4H_9
without FCS	0.26	1.14	1.76	0.86
with FCS	0.23	1.42	1.62	0.48

As is shown in Table 1, with the methyl and ethyl esters more radioactivity is found in the trypsin-EDTA solution than in the cell pellet itself, and this ratio seems to be independent of the serum content of the medium. This means that the complexes attach to the cells but they are not incorporated - in contrast to the DMSA complex. For interpretation of the results with the isobutyl ester further studies will be necessary.

These investigations show that the ^{99m}Tc(V)-DMSA complex exhibits the highest cellular uptake *in vitro* of the four complexes studied and is least affected by the presence of serum proteins.

Analogous studies with the normal fibroblast cell line could not yet be performed.

References

[1] Ohta, H. et al., J. Nucl. Med. **25** (1984) 323

[2] Yokoyama, A. et al., Int. J. Nucl. Med. Biol. **12** (1985) 273

[3] Clarke, S. E. M. et al., J. Nucl. Med. **29** (1988) 33

[4] Horiuchi, K. et al., Eur. J. Nucl. Med. **18** (1991) 796

[5] Wey, S. P. et al., in: New Trends in Radiopharmaceutical Synthesis, Quality Assurance, and Regulatory Control (ed. A.M.Emran), New York, Plenum Press, 1991, p.193

[6] Chauhan, U. P. S. et al., Nucl. Med. Biol. **19** (1992) 825

[7] Bisunadan, M. M. et al., Int. J. Appl. Radiat. Isot. **42** (1991) 167

[8] Kampf, G. et al., Annual Report 1993, p. 146, Institute of Bioinorganic and Radiopharmaceutical Chemistry, FZR-32

[9] Seifert, S. et al., this report, p. 38

[10] Kampf, G. et al., this report, p. 144

33. EVIDENCE OF ACTIVE UPTAKE OF ^{169}Yb COMPLEXES INTO TUMOUR CELLS *IN VITRO*, STABILITY OF THEIR CELLULAR FIXATION, AND THE ROLE OF THEIR PROTEIN BINDING

G. Kampf[1], G. Knop[1], U. Wenzel[1], W.-G. Franke[1], P. Brust, B. Johannsen

[1]Klinik und Poliklinik für Nuklearmedizin, Universitätsklinikum "Carl Gustav Carus", Technische Universität Dresden

In our endeavour to improve the uptake of metal complexes in tumour tissue we performed *in vitro* cell uptake studies with various ^{169}Yb complexes. These studies showed a clear dependence of the uptake on the complex stability [1] and of ^{169}Yb citrate (CIT) uptake on the metabolic activity of normal and tumour cells as measured by [^{18}F]FDG trapping, but this was not exhibited with ^{169}Yb-NTA (nitrilotriacetate) nor with ^{169}Yb-DTPA (diethylenetriaminepentaacetic acid) [2].

The recent investigations were aimed at elucidating the following points:

1. The question of active uptake of the complexes by the cell.
2. The stability of the metal-cell association.

3. The influence of protein-binding of the Yb complexes on their cellular uptake.

Materials and methods

The methods for growing, incubating, and preparing cells for radioactivity measuring were described in [2]. The cell lines used were also the KTCTL-2 cells from a human adenocarcinoma of the kidney (Heidelberg) and the V79/4 hamster lung fibroblasts.

The studies of the role of metabolic activity for the cellular uptake of both complexes were extended to other approaches: to the influences of the growth stage of the culture and the incubation temperature. The stability of the fixation of the incorporated ^{169}Yb was checked by postincubation with the strong complexing agent DTPA.

The determination of protein-binding was performed by separating the protein-bound portion of the radiometal or its ligand complex from the non-bound part by ultrafiltration. For the protein-binding assay 100 - 200 µl of the M^{3+} complex solution are added to 1 ml of the protein solution, and the mixture is incubated for 30 min at 37 °C. 1 ml of this mixture is then put into a Centricon tube (Amicon) with an ultrafilter (pore diameter for 10,000 or 30,000 daltons), which is centrifuged for 30 min at 5,000 g. Big particles as proteins are concentrated on the filter. The full volume of the concentrate can be easily recovered by reverse centrifugation of the filter membrane. The volumes of concentrate and filtrate and their radioactivity as well as that of the membrane are measured (calibrator). Since there are still small residual amounts of non-bound complex in the volume of the concentrate, the radioactivity value of the concentrate has to be corrected according to the volumes of the filtrate and concentrate. The protein-associated radioactivity is determined in percent of the whole radioactivity concentration added to the tube, considering the corrected radioactivity content of the concentrate.

Results and discussion

Evidence of active uptake

Influence of the growth stage of the culture:

When cells are propagating in a culture, they consume the nutrients and produce metabolites so that the growth conditions are impaired up to standstill of mitotic activity. In these cases metabolic activity decreases to a minimum of breathing.

With cultures of different cell densities on the petri dish reflecting different growth stages the uptake of ^{169}Yb-CIT and ^{169}Yb-NTA was checked. The different cell densities were reached by inoculating different cell numbers in the dishes and assaying them at the same time, 48 h later. With 7 - 8 x 10^6 cells the petri dish (60 mm diameter) is completely full, the cells can scarcely divide further.

The uptake of the ^{169}Yb-NTA complex per cell is independent of the cell density on the petri dish in the range studied, whether incubated for 2 or 4 h. The uptake of the ^{169}Yb-CIT complex, however, shows a dependence on cell density after 4 h incubation. Overpopulation leads to a diminished uptake (not shown).

These observations confirm the results observed with [^{18}F]FDG [2]: the metabolic activity of the cell culture exhibits a clear influence on the uptake of ^{169}Yb-CIT, but not of ^{169}Yb-NTA. That is to say that the uptake of ^{169}Yb-CIT proceeds via an active cellular transport process, but there is no indication as to the way of Yb uptake from the aminopolycarboxylic acid complex.

Does this mean that there is no cellular activity at all necessary for ^{169}Yb-NTA uptake? We tried to answer this question using the well-known test of temperature dependence.

Influence of temperature:

In these experiments cells were incubated in RPMI 1640 medium without and with 10 % of fetal calf serum (FCS, Sigma), and radioactivity concentration after incubation was checked not only in the cell pellet, but also in the trypsin-EDTA solution used for cell dissociation after incubation and 10 - 12 rinsings of the monolayer with buffer. We suppose that this is a measure for labile association of complex molecules to the cells.

As can be seen from Fig. 1, with both complex species the cellular uptake is drastically diminished by low temperatures, the great jump occurring between 37 and

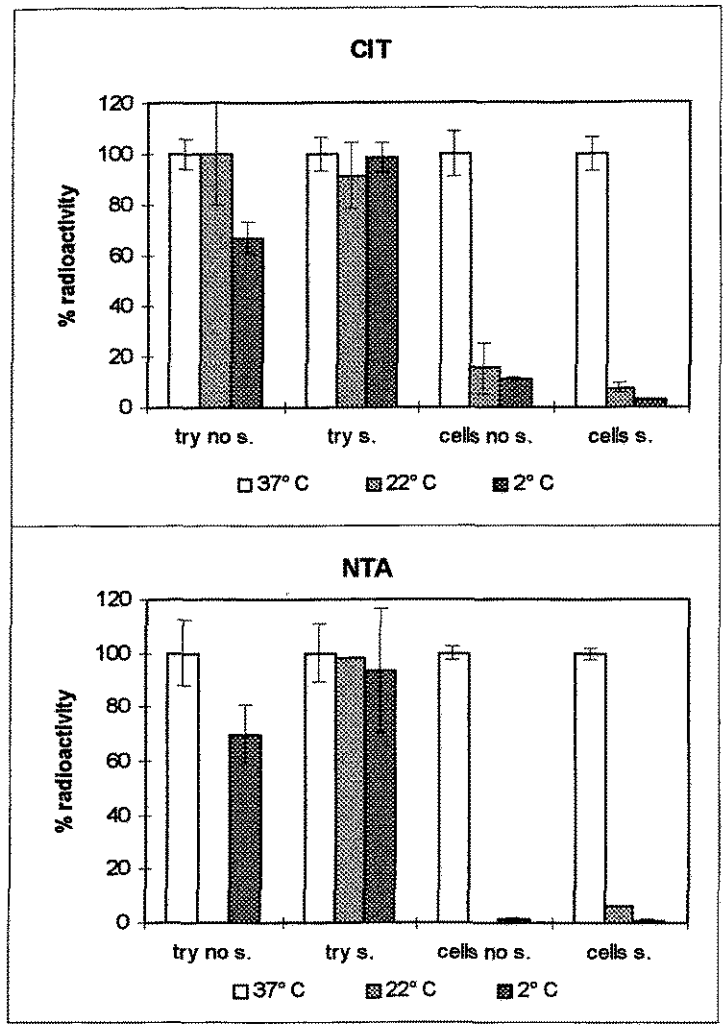

Fig.1: Temperature dependence of ^{169}Yb uptake using the CIT and NTA complexes incubation time: CIT - 2 h, NTA - 4 h; radioactivity at 37 °C was taken as 100 % in each group; try = trypsin, cells = cell pellet, s resp. no s = 10 % FCS resp. no serum; n = 6

22 °C (analogous results were obtained with the fibroblast line V 79/4). However, the mere adsorption of the complex molecules to the cell monolayer is not impaired by the low temperature with the exception of a moderate drop in the assay without serum at 2 °C. These results show that also in the cold the complex molecules adhere to the cell surface as they do at 37 °C, but they are not incorporated.

Stability of ^{169}Yb incorporation

We performed experiments of postincubation with Na-DTPA (0.25 mg/ml) dissolved in RPMI 1640 medium without or with 10 % FCS. As controls cell monolayers were incubated with the radiotracer and not postincubated (K_1), and postincubated with RPMI 1640 (K_2). The results of the assays with and without FCS showed no difference. Neither the RPMI 1640 medium a-lone nor the DTPA-containing me-dium released any considerable a-mount of radioactivity from the cells (Fig. 2). Results with the fibroblasts were analogous.

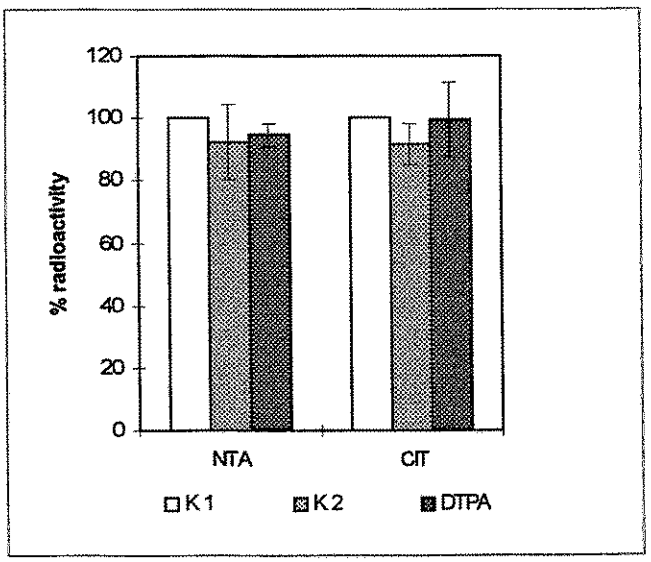

Fig. 2: Effect of 60 min postincubation without (K 2) and with DTPA on ^{169}Yb release after 2 h (CIT) and 4 h (NTA) incubation with the ^{169}Yb complexes. n = 8, K 1 is taken as 100 %

Influence of protein-binding

Binding of metals to plasma proteins plays an important role for their uptake into tumours. Unlike gallium, the lanthanides thulium and ytterbium are reported to bind scarcely to transferrin, but with moderate stability to albumin [3,4,5].

The following experiments were performed in order to elucidate the protein-binding of Yb complexes in the incubation medium and its influence on their cellular uptake in dependence on the ligands CIT and NTA.

For protein-binding studies as well as for incubation of the cells with the radiotracers different portions of fetal calf serum (FCS), human serum albumin (HSA), or human transferrin (TF) (all products from Sigma) were added to the incubation medium:
40 mg/ml HSA resp. 3 mg/ml TF corresponding to 100 % of their natural plasma concentration were dissolved in fresh RPMI 1640 and diluted with the same medium.
The complexes ^{169}Yb-CIT and ^{169}Yb-NTA behave quite differently when contacting the plasma proteins in the incubation medium (Fig. 3). ^{169}Yb-CIT binds to nearly 100 % already to small amounts (3 %) of FCS, much less to HSA and, surprisingly, up to about 80 % to rising portions of TF. This protein-association of the ^{169}Yb-CIT complex has consequences for the cellular uptake of the radiotracer: the highest uptake occurs in medium where protein is absent; with increasing serum or protein concentrations in the medium cellular uptake drops down to 3 % (FCS) resp. 15 % (TF) of the level in protein-free medium.
These results can only be interpreted in that protein association withdraws a great portion of the radiotracer from the pool available for cellular uptake.
By contrast, ^{169}Yb-NTA shows no protein association at all in the incubation medium, and the addition of increasing amounts of serum even stimulates uptake. HSA also shows an uptake-stimulating effect, but only at higher concentrations, and TF with maximum 3 mg/ml protein shows no effect. This stimulating effect is interpreted as a simple matrix support of cellular adherence by the proteins.
Comparing the absolute uptake amounts of both ^{169}Yb complexes in pure serum (Fig. 4), it becomes evident that there is no difference.
Though the pool of bioavailable ^{169}Yb-NTA should be much greater than that of ^{169}Yb-CIT, which is trapped by protein-binding, the uptake of the Yb complexes with the aminopolycarboxylic acids NTA, EDTA, and DTPA occurs only to a small extent [1].
In these studies no differences in the principal uptake behaviour were observed between the fibroblasts and the tumour cells, the uptake pathways seem to be the same in both cell types and possibly represent a general cellular feature.
On the basis of earlier animal experiments and theoretical calculations it was assumed that the tumour accumulates metallic radionuclides preferably in protein-bound form [6]. The results presented here with cultured fibroblast and tumour cells, indicate, however, other relations: ^{169}Yb-CIT showing high protein affinity is not taken

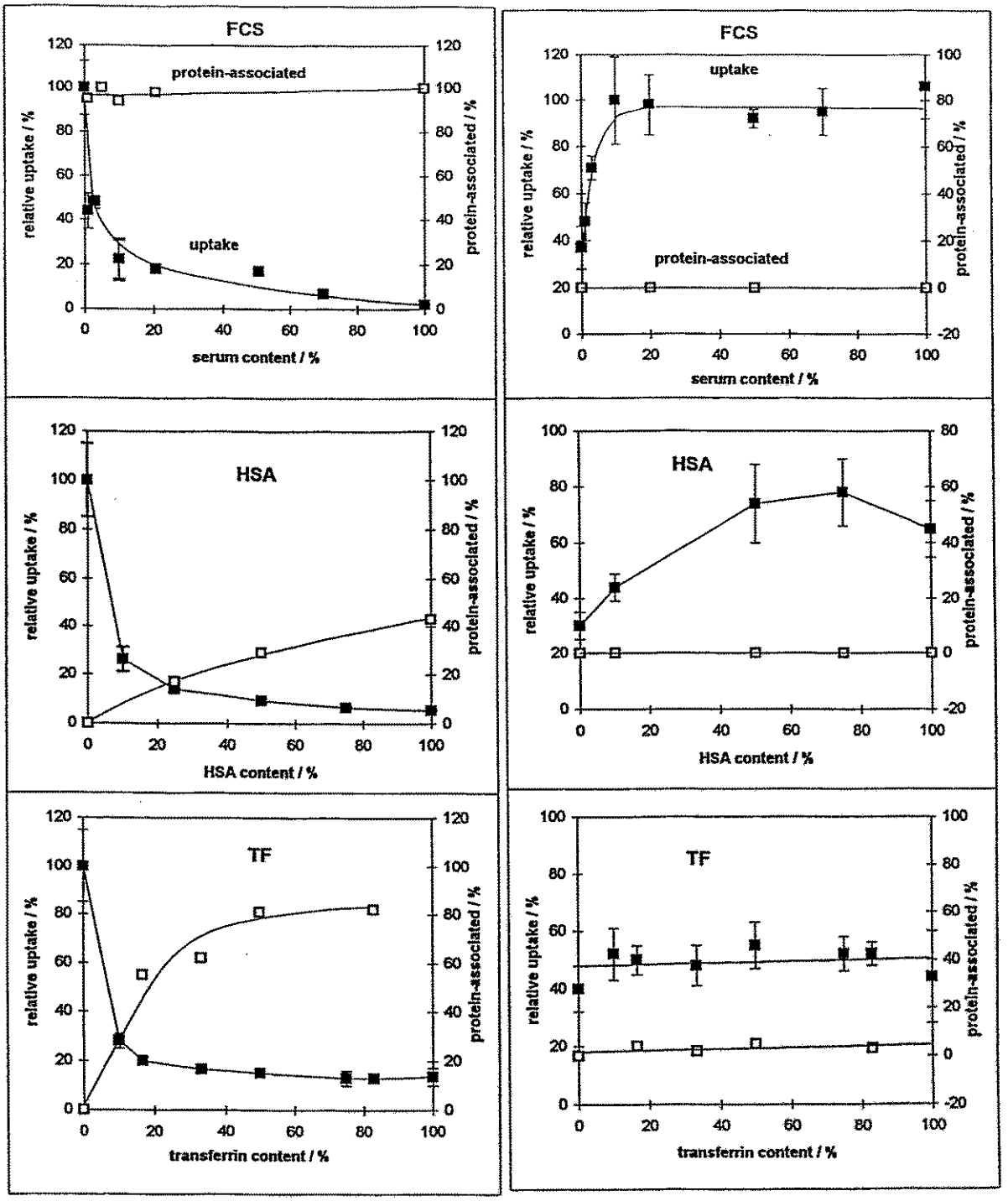

Fig.3. Relative uptake by KTCTL-2 cells (■) and protein-binding (□) of ^{169}Yb using the CIT and NTA complexes. Incubation with different portions of fetal calf serum (FCS), human serum albumin (HSA), and human apotransferrin (TF). Incubation times: CIT - 2 hrs, NTA - 4 hrs, n = 4 - 8.
x-axis: concentration in pure serum is taken as 100% level, correspondingly 40 mg/ml HSA or 3 mg/ml TF. y-axis:conditions for the highest uptake (100% level) are with ^{169}Yb-CIT : medium without FCS or other proteins, with ^{169}Yb-NTA : medium with 10% FCS.

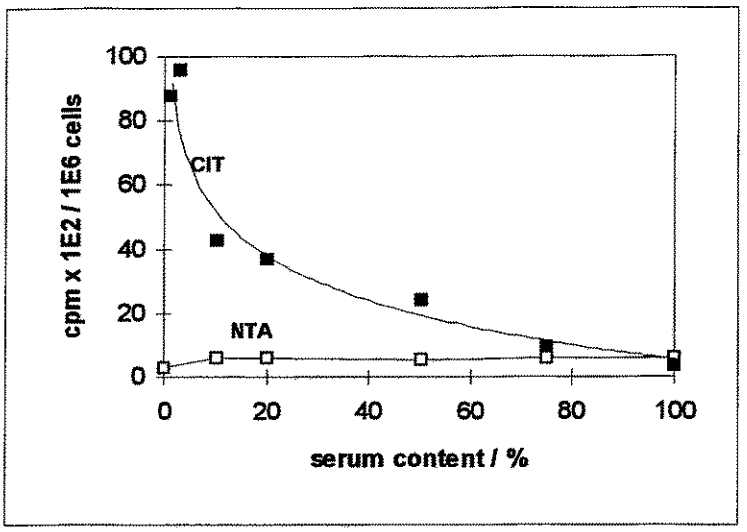

Fig. 4: Comparison of absolute uptake of ^{169}Yb-CIT and ^{169}Yb-NTA by KTCTL-2 cells in the presence of different concentrations of FCS; data corresponding to Fig. 3

up in protein-bound form, and only the non-bound residue enters the cell. ^{169}Yb-NTA does not associate with any of the offered proteins and consequently is also taken up in non-bound form. Control experiments with [^{123}I]labelled HSA showed almost no uptake of the protein by the cells (not shown).

Summarizing the results, the following statements can be made:

- Uptake of ^{169}Yb-CIT into the cells is strongly dependent on their metabolic activity; it is an active cellular transport process.
- Uptake of ^{169}Yb-NTA into the cells shows no direct relation to their metabolism, but is, nevertheless, temperature-dependent.
- Uptake of both ^{169}Yb complexes leads to a stable association to cellular compounds. ^{169}Yb is not releasable by a stronger complexing agent.
- ^{169}Yb-CIT binds strongly to the proteins in the medium, ^{169}Yb-NTA does not. Both ^{169}Yb complexes are not taken up in protein-bound form.

References

[1] Kampf, G. et al., Annual Report 1993, p. 150, Institute of Bioinorganic and Radiopharmaceutical Chemistry, FZR-32

[2] Kampf, G. et al., Annual Report 1993, p. 146, Institute of Bioinorganic and Radiopharmaceutical Chemistry, FZR-32

[3] Franke, W.-G. et al., In: Radioaktive Isotope in Klinik und Forschung, Gasteiner Internationales Symposium 1984, Vol.2 (Ed. R.Höfer, H.Bergmann), Egermann, Wien, p. 545

[4] Schomäcker, K. et al., in: Nuclear Medicine in Clinical Oncology (Ed. C. Winkler), Springer Berlin Heidelberg, 1986, p. 397

[5] Schomäcker, K. et al., Int. J. Appl. Radiat. Isot. **39** (1988) 261

[6] Schomäcker, K. et al., Annual Report 1986, p. 76, ZfK-622

These studies were enabled by grant Fr 883/1-1 by the Deutsche Forschungsgemeinschaft.

34. USE OF BRAIN MICRODIALYSIS FOR STUDYING CHANGES OF AMINO ACID CONCENTRATIONS IN THE BRAIN INTERSTITIAL SPACE

R. Bergmann, P. Brust

Introduction

Microdialysis is a new bioanalytical sampling technique with remarkable potential. It opens up the possibility of sampling substances from the extracellular space of essentially any tissue in the body - including the blood [1]. It provides a sample which is already clean and ready to be analysed.

Brain microdialysis as an *in vivo* perfusion method was originally used by Ungerstedt and his group at the beginning of the 1980s to measure the release of rat striatal dopamine [2,3].

The analysis of microdialysis perfusates using HPLC provides a method with the high sensitivity and selectivity necessary to detect low levels of endogenous substances (e.g. neurotransmitter, amino acids) in the brain extracellular space with a few minutes time resolution. The technique of microdialysis may also be used to recover exogenous substances and their metabolites such as drugs. Furthermore, it

is possible to study the direct effects of drugs upon neurotransmission and metabolism.

Here we report on attemps to establish microdialysis as a tool to study the transport and metabolism of radiopharmaceuticals for PET and SPECT, among them amino acids such as [^{11}C]methionine or [^{18}F]DOPA. First we used microdialysis to monitor changes in the extracellular concentration of endogenous amino acids. It is known that stimulation with KCl elicits increases of excitatory amino acids. Therefore we used this model in our investigation.

Materials and methods

Microdialysis

Animal experiments were carried out in compliance with the relevant national laws relating to the conduct of animal experimentation (registration number 75/9185.81-4). Male Wistar rats (weighing 300 - 400 g) were tracheotomized and anesthetized with a mixture of 40 % oxygen and 60 % N_2O containing 0.8 % halothane. The body temperature was kept at 37 °C. The rats were mounted in a stereotaxic instrument (Stoelting Inc.). The skull was exposed, and a burr hole was made. After a small tear was made in the dura, the dialysis probe (CMA/10; Carnegie Medicin, Sweden) was implanted in the dorsal hippocampus at the coordinates anteroposterior with respect to the bregma of +3.0 mm, lateral with respect to the midline suture of +2.5 mm, and dorsoventral with respect to the dura of 3.0 mm. The position of the probes implanted in the brain was verified after termination of the experiment. The probes were continuously perfused at 2.0 µl min^{-1} with Krebs-Ringer bicarbonate solution (155 mM NaCl, 5.5 mM KCl, and 2.3 mM $CaCl_2$). Perfusate samples were collected every 10 min. Upon collection of 3 samples for determination of the basal amino acid concentration (starting 30 min after insertion of the probe, see results) 50 mM of KCl (equal reduction in NaCl) was periodically (10 min on, 40 min off) added to the perfusate.

HPLC

Aliquots of each dialysis sample (10 µl) were injected into the HPLC system (Hewlett Packard). Amino acids were detected fluorimetrically after precolumn derivatization with ortho-phthalaldehyde (OPA) and fluorenylmethoxychloroformate (FMOC) [4].

Mobile Phase A

1.0 ml EDTA solution (4.0 g EDTA disodium salt (dihydrate) in 100 ml water) and 180 µl sequencer-grade triethylamine (TEA) were added to 1000 ml of HPLC-grade water. The pH was adjusted to 7.2 with 1-2 % acetic acid. After pH adjustment 3.0 ml of unstabilized, UV-grade tetrahydrofuran (THF) was added and the pH rechecked.

Mobile Phase B

2.72 g sodium acetate trihydrate was dissolved in 200 ml of HPLC-grade water. The pH was adjusted to 7.2 with 1-2 % acetic acid. 400 ml methanol and 400 ml acetonitrile were added and mixed well.

Amino acid standards

Individual amino acids and a mixed standard were purchased from Sigma.

Derivatization

Derivatization was done using an automatic sampler (Hewlett Packard). Ampoules of OPA and FMOC (Hewlett Packard) were used. They were transferred to microvials in 50 - 100 µl aliquots and capped. Borate buffer (0.4 N, pH 10.4) was pipetted into 2.0 ml sampler vials for pH control during derivatization. HPLC-grade water was placed into a 2.0 ml sampler vial for use as a needle wash.

Results and discussion

Fig. 1 shows an example of a standard chromatogram obtained under the conditions defined in "Materials and methods".

The concentrations of nearly all amino acids detected by HPLC were artificially high immediately after insertion of the dialysis fiber into the brain (see Fig. 3). This is a well known phenomenon, since acute intracerebral implantation of probes leads immediately to a number of reversable disturbances in the vicinity, including spreading depression, damage to the blood-brain barrier and disrupted glucose metabolism [3,5].

A stable level was reached about 30 min after insertion. Perfusate samples collected over the first 30 min after surgery have therefore to be discarded. The concentrations of the different amino acids detected in the dialysates were between 0.1 µmol/l (aspartate) and 9.8 µmol/l (glutamine) (Table 1). They are in the range which may be expected from data published by others [6,7].

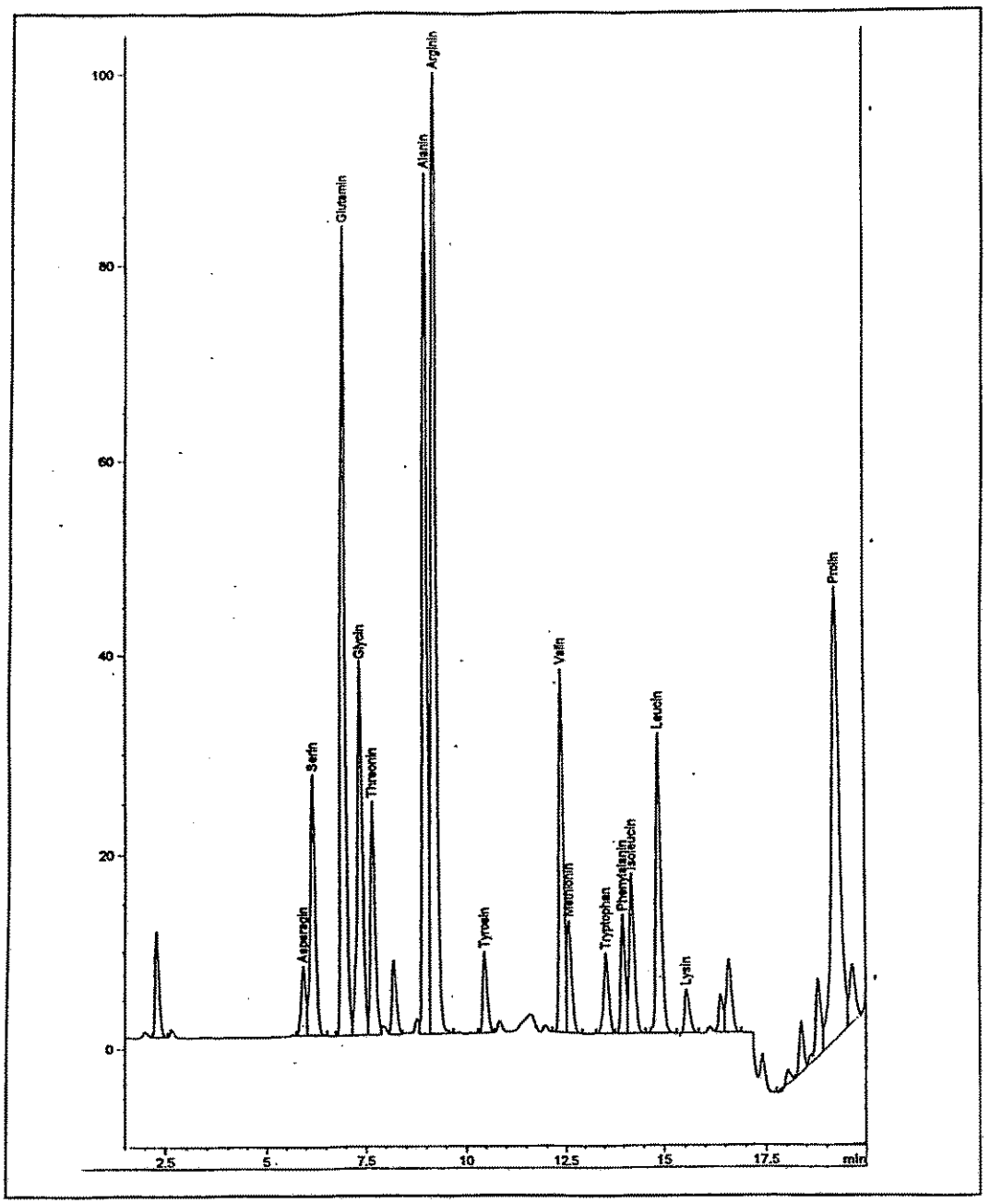

Fig. 1: Chromatogram obtained with a sample of a standard mixture of amino acids (0.5 mmol/l).

This standard chromatogram was used to define the peaks in chromatograms of dialysate samples (Fig. 2).

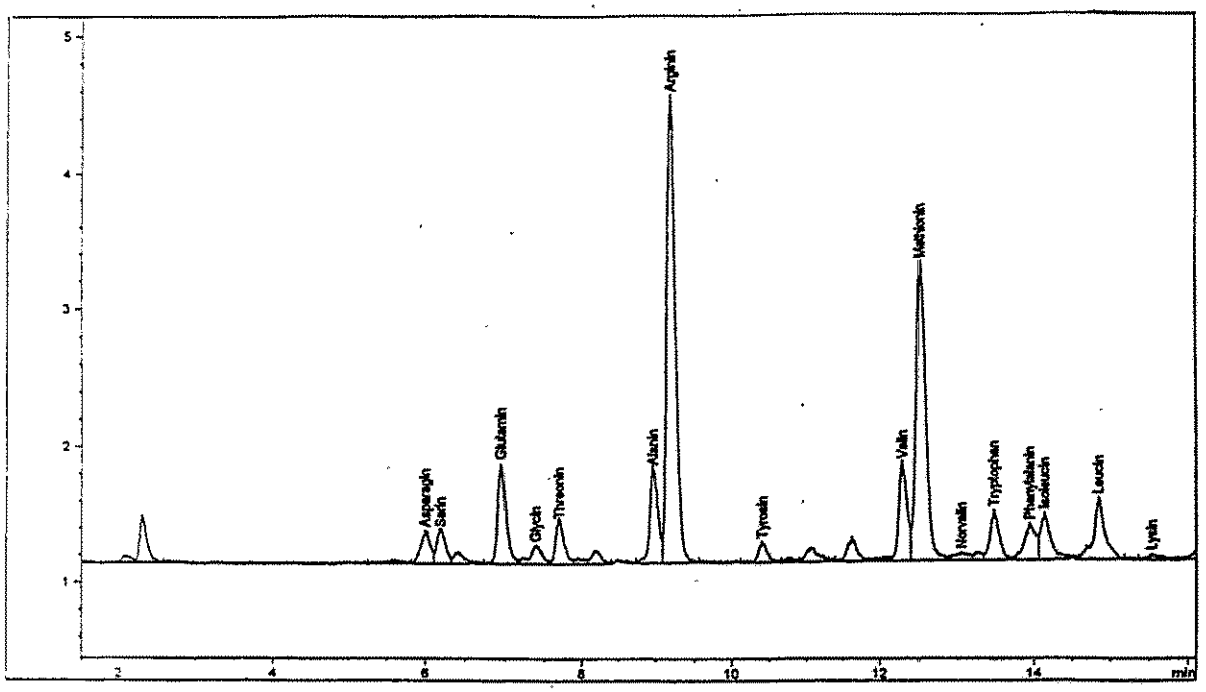

Fig. 2: Chromatogram of a dialysate sample obtained from a probe inserted into the dorsal hippocampus of rats

Stimulation with KCl induces a massive depolarization of nerve cells and is known to evoke a marked and short-lived increase in neurotransmitter output [3]. In our study it elicited an immediate increase in the concentrations of the amino acid neurotransmitters glutamate and aspartate (Fig. 3) by about the factors 10 and 5.

However, also the concentrations of most other amino acids were more or less increased during the period of stimulation while methionine remained quite stable under these circumstances (Table 1).

In conclusion, we have set up a standard microdialysis procedure which should allow to study the transport and metabolism of radiopharmaceuticals for PET and SPECT. To obtain quantitative data in absolute terms it will be necessary to estimate the in vivo recovery of these substances and to establish an HPLC procedure with radioactive detection. Because of the expected low recovery of most of the radiopharmaceuticals, a high sensitivity of detection will be a crucial point.

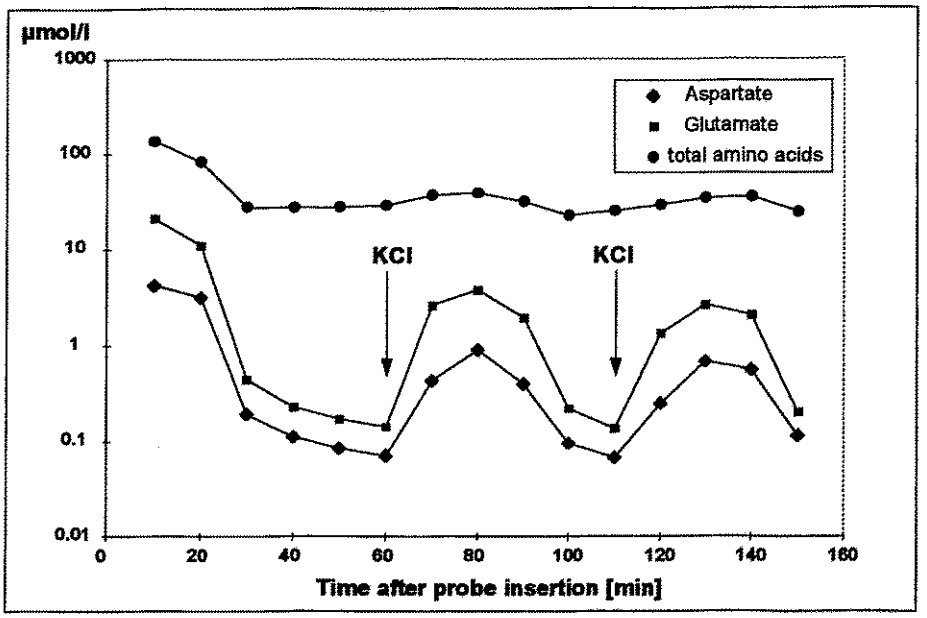

Fig. 3: Changes of amino acid concentrations in microdialysates from the rat dorsal hippocampus during the study. Arrows indicate stimulation with 50 mM KCl (10 min) in the perfusate.

Table 1: Concentrations of amino acids in microdialysates (µmol/l) from the dorsal hippocampus of rats before and after stimulation with KCl in the perfusate

	Before stimulation		After stimulation	
	Mean	SD	Mean	SD
Aspartate	0.129	0.057	0.670	0.334
Glutamate	0.283	0.145	3.205	0.842
Asparagine	2.094	0.073	3.010	0.834
Glutamine	9.776	2.507	13.610	2.317
Glycine	0.646	0.096	0.818	0.368
Threonine	0.824	0.031	1.150	0.260
Alanine	1.140	0.160	1.879	0.243
Arginine	5.774	2.071	6.315	0.318
Methionine	6.460	0.269	6.210	0.390
Tryptophan	0.259	0.045	0.556	0.535
Phenylalanine	0.265	0.004	0.303	0.045
Leucine	0.378	0.012	0.609	0.317

References

[1] Collin, A.-K. and U. Ungerstedt, Microdialysis, Carnegie Medicine 1988, p. 1-64

[2] Ungerstedt, U. et al., Advances in Dopamine Research (Kohsaka et al., eds.) Pergamon Press, New York, 1982, p. 219

[3] Sharp, T. and T. Zetterström, Monitoring Neuronal Activity (Stamford J.A., Ed.) Oxford University Press, Oxford, 1992, p. 147

[4] Fleming, J. et al., Bioscience 10/92 (43) 5091-5615E, Hewlett-Packard Company, (1992) 1

[5] Benveniste, H., J. Neurochem. **52** (1989) 1667

[6] Korf, J. et al., J. Neurochem. **50** (1988) 1087

[7] Lehmann, A., J. Neurochem. **53** (1989) 525

35. CEREBRAL CAPILLARY ENDOTHELIAL CELLS OF ADULT PIG AS AN *IN VITRO* MODEL FOR THE BLOOD-BRAIN BARRIER

B. Ahlemeyer, S. Matys, P. Brust

Introduction

The blood-brain barrier regulates the transfer of water, electrolytes and nutrients between the blood and the extracellular fluid of the brain. Cerebral endothelial cells are the main constituents to form this selective permeability barrier because of their characteristic properties, e.g. formation of tight junctions, lack of fenestrations and low vesicular transport. Numerous in vitro studies revealed that brain endothelial cells possess biochemical and functional features of the BBB, such as different receptors, transporters, enzyme activities and ion channels [1]. In order to examine the characteristics and mechanism of the transport of radiotracers across the BBB, it was the aim of our work to establish an *in vitro* model of the blood-brain barrier.

Materials and methods

Materials

Dispase, fetal calf serum, collagen type III, percoll, dextran, glycylglycine, N(-3-(2-furyl) acryloyl-)-phenylalanylglycylglycine, captopril, levamisol, mouse anti α-smooth

muscle actin, ALP reaction mixture Sigma kit N°85 and protein assay kit were purchased from Sigma Chemicals, Deisenhofen, Germany. Collagenase/dispase, *L-glutamic acid α-(4-methoxy-β-naphthylamide)*, *p-nitrophenylphosphate*, Ig G fractions of mouse anti-human factor VIII, mouse anti-vimentin, mouse anti-neurofilament, mouse anti-galactocerebroside, mouse anti-fibronectin and rat anti-mouse Ig G fluorescein were from Boehringer, Mannheim, Germany. Medium 199 and antibiotics were obtained from Gibco BRL, Eggenstein, Germany. MiniMacs separator, MiniMacs separaration columns and rabbit anti-rat Ig G microbeads were obtained from Miltenyi Biotec GmbH, Bergisch Gladbach, Germany. Ig G fractions from rat anti-alkaline phosphatase were from BioTrend, Köln, Germany. All other chemicals were derived from Merck, Darmstadt, Germany.

Cell cultures

Primary cultures of porcine brain microvessel endothelial cells were obtained according to [2]. Briefly, pig brains, cleaned of meninges and white matter, were minced and incubated for 3 h at 37 °C in medium 199 containing 0.8 % dispase. After centrifugation with 15 % dextran at 6800 x g for 10 min, isolated capillaries were digested with 1 % collagenase for 3 h. Endothelial cells were separated from erythrocytes and cell debris by a percoll-gradient. Cells were seeded on collagen type III coated petri dishes (Becton Dickinson, Heidelberg, Germany) with a density of 10-20 000 cells/cm² and on 12-well Costar filters, 0.45 µm pore size (Bodenheim, Germany), or Nunc filters, 0.45 µm pore size (Wiesbaden, Germany), with a 3-times higher seeding density. The cells were cultivated for 7 days in medium 199 with 10 % fetal calf serum, 100 U/ml penicillin, 100 µg/ml streptomycin and 2.5 µg/ml amphotericin at 37 °C with 5 % CO_2 and 95 % air. The medium was changed every second day.

Astrocytes were derived from white matter of porcine brain according to [2]. The minced tissue was incubated for 30 min in 1 % dispase. The homogenate was then centrifuged at 200 x g for 10 min and the pellet was pressed through nylon meshes of 250 µm, 125 µm and 50 µm pore size, successively. Cell suspension was seeded in uncoated petri dishes and cells were cultivated until confluence at 37 °C in MEM with 10 % fetal calf serum, 100 U/ml penicillin, 100 µg/ml streptomycin and 2.5 µg/ml amphotericin at 37 °C with 5 % CO_2 and 95 % air. The medium was changed every second day.

Chondrocyte-derived matrix was produced by a chondrocytic cell line after confluence in uncoated petri dishes. The cell layer was washed extensively with bidistilled sterile water until the cells were disrupted osmotically. Complete removal of the cells was controlled microscopically. Chondrocyte-derived matrix was always prepared immediately before use.

Immunostaining

Cells were washed three times with PBS^{++} and fixed with 99 % ethanol for 20 min at room temperature. In order to reduce unspecific binding the monolayer was preincubated with 1 % BSA in PBS^{++} for 30 min before addition of mouse anti-human factor VIII-related antigen (dilution 1:10). After 30 min the cells were washed several times and fluorescein conjugated sheep anti-mouse-IgG (1:20) was added for 1 h. Thereafter, the cells were washed and observed in an inverted Olympus IMT 2 microscope equipped for epifluorescence and photography.

Enzyme assays

Histochemistry

ALP activity was determined histochemically, using the reaction mixture Sigma kit N°85 according to manufacturers´ instructions with naphthol AS-Bi phosphate as substrate and Fast blue RR as diazonium salt for 15 min. γ-GT activity was determined histochemically, using a reaction mixture containing L-glutamic acid α-(4-methoxy-β-naphthylamide) as substrate and glycylglycine as acceptor (60 min). A red azo dye was produced by reaction with Fast blue BB.

Biochemistry

For the biochemical ALP and γ-GT assay, the cells were washed 3-times with saline, then scraped from the petri dish and homogenized by short sonification. Cell suspension was used for both enzyme activity and protein determination.

ALP activity was determined by incubating the cell suspension with substrate solution containing 4 mM p-nitrophenylphosphate, pH 10.37. Formation of p-nitrophenol was measured kinetically at 420 nm and was compared to the saline/ substrate solution. Specificity of the test was demonstrated with levamisol (5 mM) which inhibited ALP activity completely. One unit of enzyme activity was defined by formation of 1 µmol p-nitrophenol per min at 25 °C, using an extinction coefficient of 17300 l M^{-1} cm^{-1}.

γ-GT activity was determined by incubating the cell suspension with substrate solution containing 2.7 mM L-γ-glutamyl-3-carboxy-4-nitroanilide and 20 mM glycylglycine in Tris-buffer pH 9. Formation of carboxy-4-nitroanilide was measured kinetically at 410 nm and was compared to the saline/substrate solution. One unit of enzyme activity was defined by formation of 1 nmol carboxynitroanilide per min at 25 °C, using an extinction coefficient of 9500 l M^{-1} cm^{-1}.

Angiotensin-converting enzyme (ACE) activity was determined by incubating the cell suspension with substrate solution containing 0.8 mM N(-3-(2-furyl)acryloyl-)-phenylalanylglycylglycine in Tris-buffer pH 7.5. Formation of N(-3-(2-furyl)acryloyl)-phenylalanine was measured kinetically at 340 nm and was compared to the saline/substrate solution. Specificity of the test was demonstrated with captopril (1 mM), which inhibited ACE activity completely. One unit of enzyme activity was defined by formation of 1 nmol N(-3-(2-furyl)acryloyl)-phenylalanine per min at 25 °C, using an extinction coefficient of 2750 l M^{-1} cm^{-1}.

Protein determination

Cell protein was determined by a modified Lowry test.

Results and discussion

Characterization of endothelial cells and astrocytes

1) Immunohistochemical studies were performed to ensure the identity and purification of endothelial and astrocyte cell cultures (Table 1).

Contamination was lower than 5 % after 6 days in endothelial cell cultures. After 4 - 5 days some cells appear on the top of the monolayer. These cells are mainly endothelial cells (with a higher content of smooth muscle actin and vimentin) and pericytes (because of the absence of factor VIII immunoreactivity). Astrocytes were of 99 % purity.

2) For transport studies low permeability of cerebral capillary endothelial cells is necessary. Determination of the electrical resistance, an indication of continuous tight junctions and therefore of low permeability, was performed in endothelial cells grown on Costar filters using the EVOM system from WPI, Wiesbaden, Germany.

Table 1: Immunofluorescence of endothelial cells of porcine microvessels after incubation with various antigen Ig-G-fractions and a second incubation with anti-IgG antibodies coupled with FITC (lit.= data of the literature, GFAP= glial fibrillary acidic protein)

Antigen	Endothelial cells	Lit.	Astrocytes	Lit.
Factor VIII	+	+++	-	-
Neurofilament	-	-	-	-
GFAP	-	-	++	++
Galactocerebroside	-	-	-	-
Fibronectin	-	-	+	(+)
Vimentin	+	+	+	+
Smooth muscle actin	- (+)	-	-	-

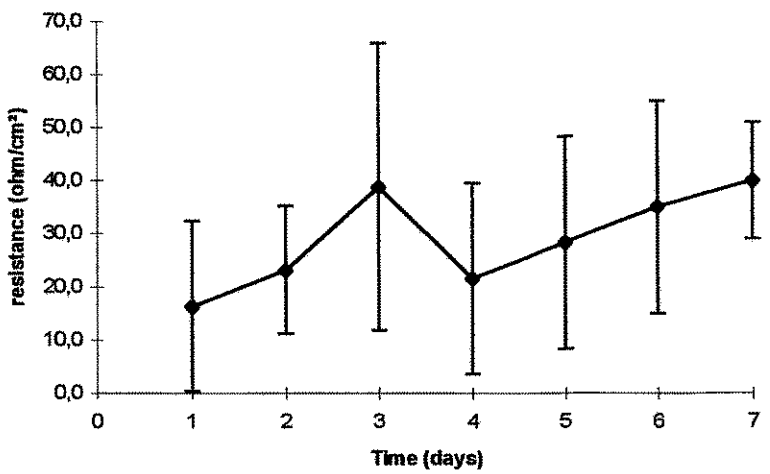

Fig. 1: Electrical resistance of cerebral capillary endothelial cells grown on Costar filters (subtracted by the resistance of the cell-free filters) as a function of time. Mean values of 6 - 8 filters +/- standard deviation are shown

For comparison, [3] measured 800 Ohm/cm² for cloned endothelial cells of mouse microvessels, [4] measured 160 Ohm/cm² for bovine brain endothelial cells, [5] found 30 - 35 and [6] 14 - 20 Ohm/cm² for murine and bovine brain endothelial cells, respectively.

3) Endothelial cells and astrocytes were also characterized by enzyme activities.

Table 2: Enzyme activities of endothelial cells and astrocytes in culture. All values are in the same range found in the literature. Values are given as mean +/- standard deviation of 4 petri dishes (n.d. = not detectable, DIV = days *in vitro*).

Activity [U/mg protein]:	ALP	γ-GT	ACE
Endothelial cells (0 DIV)	1.10 +/- 0.38	26 +/- 12	n.d.
Endothelial cells (4 DIV)	0.28 +/- 0.01	2.1 +/- 0.7	55.7 +/- 11
Astrocytes	n.d.	n.d.	n.d.

4) Electron microscopy. The growth of cells on Costar filters may induce polarization of the cells. Fig. 2 shows an electron micrograph of endothelial cells (6 DIV) grown on a filter.

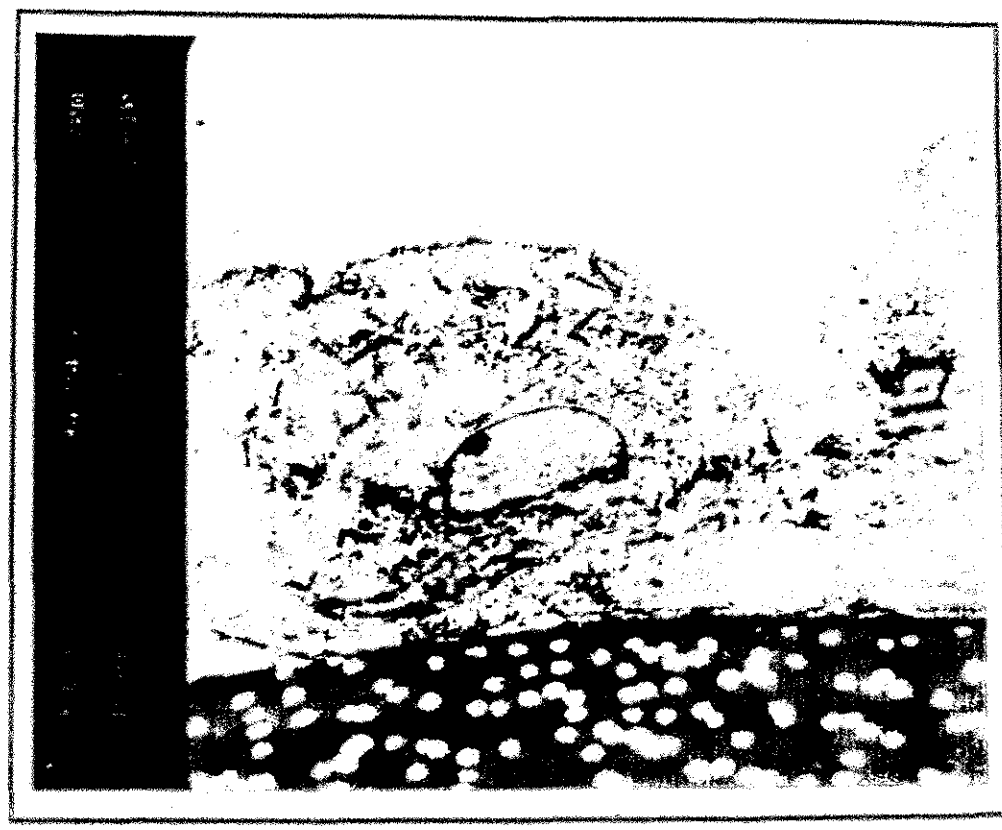

Fig. 2: Electron micrograph of endothelial cells after 6 days in culture grown on Costar filters (magnification 1 : 6000).

Close apposition of the cells is visible. Electron micrographs reveal that the cells sometimes grow as multilayers, that they are not confluent over the whole area of the filter and that they contain villi on the luminal side - an indication for polarization.

Cerebral endothelial cells as an in vitro model for the blood-brain barrier

Two enzymes are considered as marker enzymes of endothelial cells of the BBB: γ-glutamyltranspeptidase (γ-GT) [7-8] and alkaline phosphatase (ALP) [9-11]. Both enzymes are highly concentrated in brain endothelia in contrast to peripheral endothelia, astrocytes and neurons. In primary cultures of endothelial cells of porcine brain microvessels the activities of both enzymes decrease as a function of time [12-13] leading to the debate whether a differentiated function of the BBB is preserved in culture.

It was the aim of our studies to increase the activities of ALP and γ-GT by variations in culture conditions:

a) culturing endothelial cells on petri dishes and on Costar filters
b) culturing endothelial cells with or without serum and drugs and on various extracellular matrices
c) culturing endothelial cells as "sandwich" cultures

a) Endothelial cells on petri dishes and on Costar filters. Fig. 3 shows the activities of ALP and γ-GT as a function of time in collagen-coated petri dishes and Costar filters.

Histochemical analysis revealed a decrease in ALP and γ-GT activities during cell cultivation, mainly due to a decrease in cell clusters with extremely high enzyme activities. We found higher enzyme activities on Costar filters than on petri dishes (data not shown). Biochemical analysis shows a decrease in ALP and γ-GT activities/mg protein as a function of time (Fig. 3), but in Costar filters ALP and γ-GT activities/mg protein were significantly lower than in collagen-coated petri dishes. However, calculating both enzyme activities in relation to the area of growth surface (cm^2), they *were higher in Costar filters than in collagen-coated petri dishes* (data not shown). We suggest that permeable supports induce a polarized distribution of both enzymes at the luminal side of the plasma membrane. This would explain why ALP

and γ-GT activities related to protein are lower in Costar filters than on collagen-coated petri dishes.

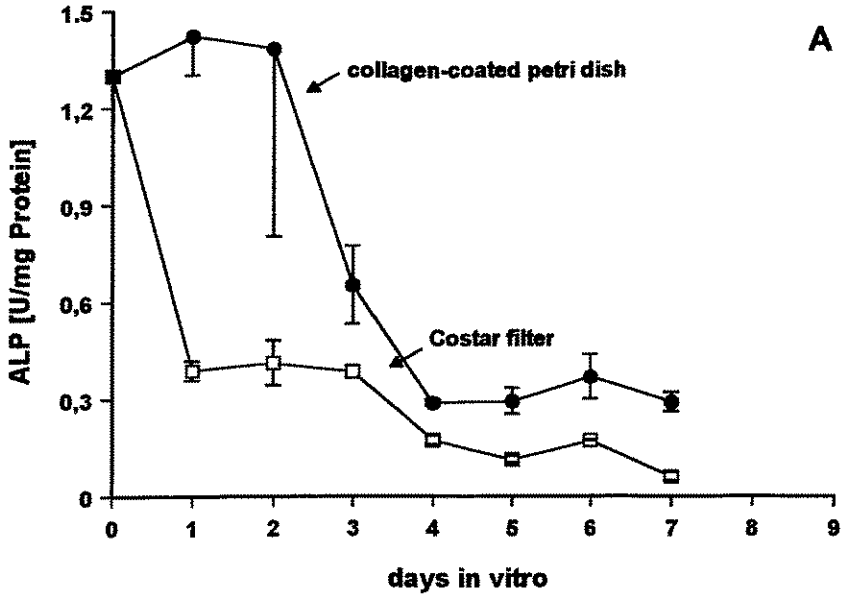

Fig. 3A: ALP-activities as a function of time in endothelial cells grown on collagen coated petri dishes and filters. Values are given as means +/- standard deviation of 4 petri dishes and 6 Costar filters

b) Enzyme activities of endothelial cells grown under the influence of various medium additives and on various extracellular matrices.

We did not find any change in ALP and γ-GT activities after 7 days in culture by adding to the culture medium 0.4 mg molsidomine (release NO), 20 mg/l phenylbutazone (increase γ-GT activity in the liver) or 20 mM ATP (increase the $[Ca^{2+}]_i$) one day after seeding. Phenylbutazone and molsidomine increase the contamination with astrocytes, probably due to toxic effects on endothelial cells.

Addition of several growth factors (endothelial growth factor, basic fibroblast growth factor) to medium 199 did not enhance the low resting ALP or reinduce lacking γ-GT activities as revealed by histochemistry after 6 days in culture. Interestingly, culturing cells in serum-free medium with and without antibiotics for 7 days resulted in an increase in γ-GT activity from 2 U/mg protein to 7.5 and 14.5 U/mg protein,

respectively. However, a lack of serum reduced the cell density and changed cell morphology (retained differentiation). Cell protein/dish decreased from 30 µg/petri dish (with serum, with antibiotics) to 3 µg/petri dish (without serum, with antibiotics) and 6.5 µg/petri dish (without serum, without antibiotics). Because the cell density was strongly reduced, these cultures cannot be used for BBB transport studies.

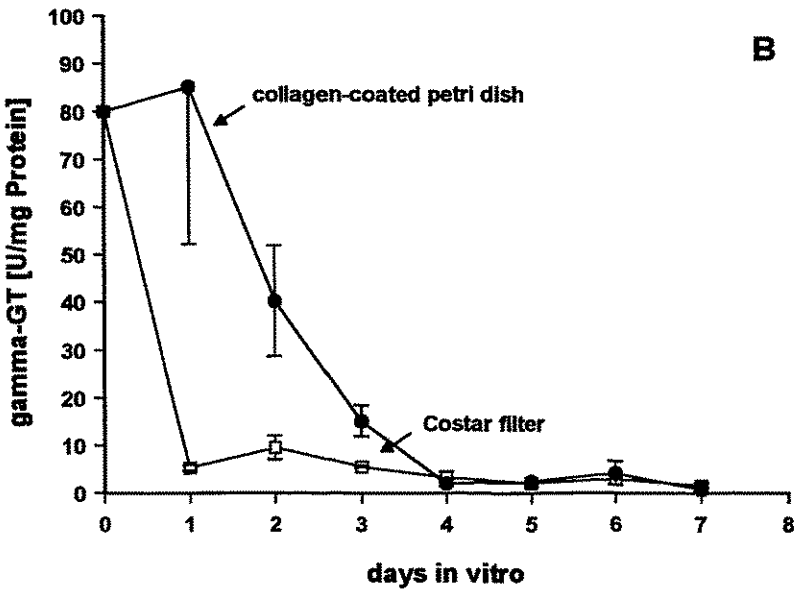

Fig. 3B: γ-GT-activities as a function of time in endothelial cells grown on collagen coated petri dishes and filters. Values are given as means +/- standard deviation of 4 petri dishes and 6 Costar filters.

By coating petri dishes with gelatin, we observed - after 6 days - the same low resting level of ALP and no γ-GT activity of the cells as in collagen-coated petri dishes. With a matrix derived from a chondrocytic cell line as growth surface, adherence of the endothelial cells was reduced. After 6 days, no induction of ALP and γ-GT was observed by histochemistry (data not shown).

c) Endothelial cells as "sandwich" cultures

In sandwich cultures, a cellular monolayer is covered with a coverslip or, as in our case, with extracellular matrices. Sandwich cultures could be used to reinforce cellular differentiation. We covered 4 day-old endothelial cell cultures grown on

collagen coated petri dishes with collagen (10 µg/cm²), gelatin (10 µg/cm²) and fibronectin (5 µg/cm²).

As shown in Table 3 covering endothelial cell monolayers with gelatin on day 4 increases ALP activity by about 60 % on day 7. However, we observed cell-free areas in the monolayer, probably due to the stress of covering the cells with matrices on day 4. Nonconfluent cell layers could not be used for transport studies. Further studies (e.g with Costar filters) will be carried out to reach *confluent* sandwich cultures with increased ALP activities.

Table 3: ALP activities in endothelial cells after 7 days under sandwich conditions. Values are given as mean +/- standard deviation of 4 petri dishes.

Matrix	ALP [U/mg protein]	µg protein/petri dish
Collagen	0.413 +/- 0.025	63.2 +/- 1.4
Fibronectin	0.353 +/- 0.014	53.8 +/- 0.6
Gelatin	0.451 +/- 0.029	65.3 +/- 4.4
Control	0.264 +/- 0.01	104 +/- 7

Conclusions

In order to establish an *in vitro* model for the blood-brain barrier, our studies have shown that it is useful to culture endothelial cells on permeable supports (e.g. Costar filters). This resulted in a polarized distribution of ALP and γ-GT as revealed by a comparison of histochemical and biochemical analyses. On the other hand, filters offer the possibility to study not only the uptake of drugs or tracers into the cell, but also mechanism and direction of the transcellular transport. However, before using permeable supports for BBB transport studies, the quality of the monolayer have be carefully checked.

References

[1] Joó, F., J. Neurochem. **58** (1992) 1

[2] Mischek, U. et al., Cell. Tiss. Res. **256** (1989) 221

[3] Krause, D.N. et al., Fed. Proc. **41** (1982) 1760

[4] Raub, T.J. et al., Exp. Cell. Res. **199** (1992) 330

[5] Hart, M. N. et al., J. Neuropathol. Exp. Neurol. **46** (1987) 141
[6] Jaehde, U. et al., Eur. J. Pharm. Sci. **1** (1993) 49
[7] Ghandour, M.S. et al., Neurosci. Lett. **20** (1980) 125
[8] Orlowski, M. et al., Science **184** (1974) 66
[9] Brightman, M. W. Implications of the blood-brain barrier and its manipulation. Vol. 1 Sciences Aspects. E.A. Neuwelt, ed. Plenum, New York, 1989, p. 53
[10] Vorbrodt, A. W. et al., Devel. Neurosci. **8** (1990) 1
[11] Vorbrodt, A. W., Prog. Histochem. Cytochem. **18** (1988) 1
[12] Meyer, J. et al., Brain Res. **514** (1990) 305
[13] Fukushima, H. et al., In Vitro Cell. Dev. Biol. **26** (1990) 612

We gratefully thank the colleagues of the Technical University of Dresden (group of Dr. Fischer) for transmission electron microscopy. This study was supported by the Saxon Ministry of Science and Art (Grant 7541.82-FZR/309).

36. HETEROGENEITY OF ALP AND γ-GT ACTIVITIES IN CEREBRAL ENDOTHELIAL CELLS

B. Ahlemeyer, S. Matys, P. Brust

Introduction

It was the aim of our work to establish an *in vitro* model for the blood-brain barrier to characterize the transport of radiotracers [1]. Cerebral capillary endothelial cell cultures with high activities of the marker enzymes ALP and γ-GT, as found *in vivo*, are desired.

Materials and methods

Materials, cell cultures, enzyme assays as previously described [1]

Magnetic cell sorting

Freshly isolated endothelial cells were incubated for 10 min with anti-ALP antibodies and for 15 min with anti-Ig G magnetic antibodies (microbeads). Thereafter, cells containing the first and second antibody were separated by magnetic columns. Cells

without microbeads ("ALP negative cells") passed the column and were collected separately, whereas cells with microbeads ("ALP positive cells") were retained on the column. After removal of the magnet, cells with microbeads were washed from the column and collected. Thereafter, we cultured separate monolayers of "ALP positive" and "ALP negative" cells with a seeding density of 5×10^4 cells per petri dish. Control cells were seeded with a density of 1.5×10^5 cells per dish.

Results and discussion

Heterogeneity of ALP and γ-GT activity

During preparation of pig brain endothelial cells we measured the ALP and γ-GT activities in endothelial cells after the second digestion and purification with a percoll gradient. We observed variations in the ALP and γ-GT activities between the preparations and in the same preparation after various times of storage in liquid nitrogen (Table 1).

Table 1: ALP and γ-GT activity of endothelial cells after preparation and storage in liquid nitrogen. The coefficient of variance for the ALP and γ-GT assay is 2 % and 5 %, respectively.

Preparation	ALP [U/mg protein]	γ-GT [U/mg protein]
I	0.80	11.6
II	0.83	18.5
III	1.80	46.8
IV	1.26	20.9
Storage in liquid nitrogen		
0	0.83	18.5
3 weeks	1.83	39.1
5 weeks	0.85	43.2
6 weeks	1.19	18.9

Histochemical analysis revealed heterogeneity of ALP and γ-GT activity in purified endothelial cells before seeding. Fig. 1 shows heterogeneity of the ALP activity in

endothelial cells at the end of the second digestion - the capillary structure is still visible. Similar heterogeneity was found for γ-GT (data not shown).

During the first 3 days of cell culture, we found high ALP and γ-GT acitivities of the cells on collagen-coated petri dishes exclusively in cell aggregates or clusters as already mentioned by [2]. Cell clusters disappear after 3 - 4 days, resulting in an overall decrease of ALP and γ-GT activity. We observed no γ-GT, but resting ALP activity after 6 days with great intercellular differences as shown in Fig. 2. Heterogeneity is also found for ALP *and* γ-GT by cultivating the cells on permeable supports (data not shown).

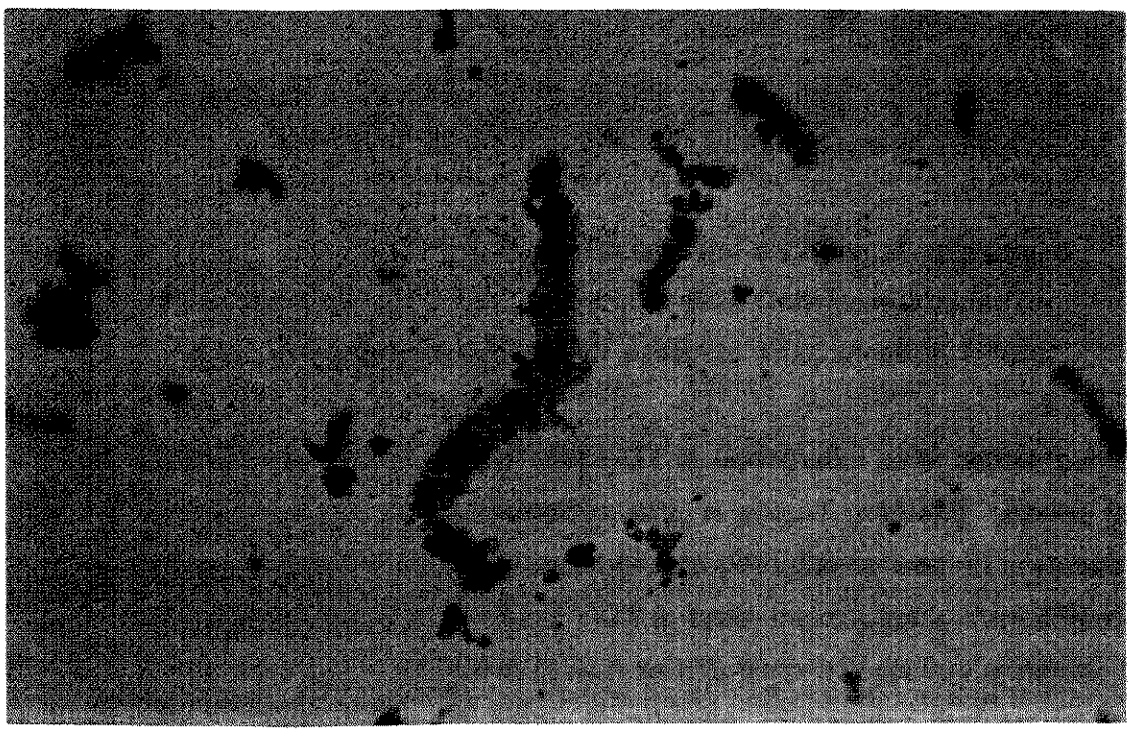

Fig. 1: Histochemical localization of ALP in endothelial cells of porcine microvessels before seeding. Cells were stained for ALP after 15 min of incubation with substrate (magnification 1:100)

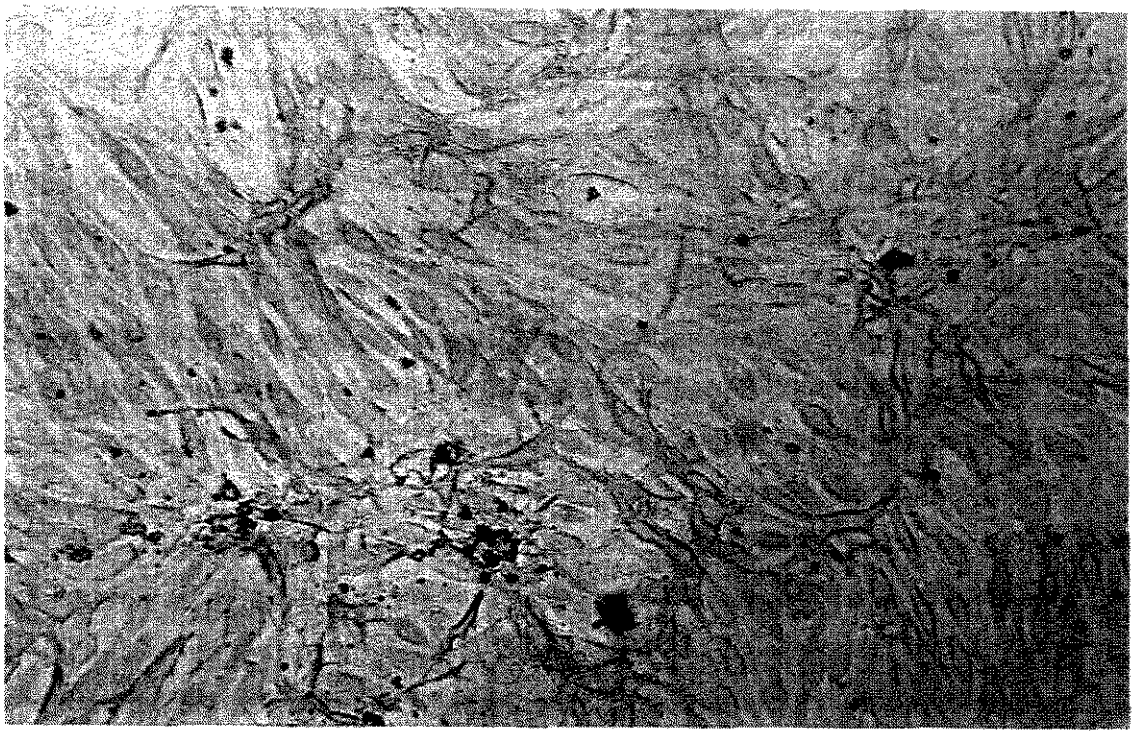

Fig. 2: Histochemical localization of ALP in cerebral endothelial cells after 6 days cultured in a collagen-coated petri dish. Cells were stained for ALP after 15 min of incubation with substrate (magnification 1:100).

We suggest that heterogeneity of ALP and γ-GT in endothelial cells before culture (after the second digestion and purification with a percoll gradient) caused the heterogeneity during cell culture on collagen-coated petri dishes and on permeable filters. Heterogeneity in the distribution of γ-GT in brain microvessels from different regions of the brain [3] and a decrease in ALP activity from precapillary arterioles to venules [4] have already been described. In addition, [5] showed that endothelial cells from larger vessels with more pericytes had higher levels of γ-GT than cells from smaller vessels and they found a heterogeneity of γ-GT in pericytes. Here we demonstrate (Fig. 2) that even porcine brain endothelial cells from the same section of microvessel (and therefore from the same brain region) show a heterogeneous distribution of ALP (the same was found for γ-GT, data not shown). Enzyme heterogeneities presumably depend on various parameters.

Our results suggest that endothelial cells of porcine brain microvessels consist of different cell populations with high and low activities of the marker enzymes ALP and

γ-GT. There was no correlation between ALP and γ-GT activity. Obviously, the existence of two or more endothelial cell populations with different activities of marker enzymes would complicate the establishment of an in vitro model for the blood-brain barrier. Therefore, we separate endothelial cells with a high ALP activity from those with low activity by magnetic cell sorting.

Separation of cell populations with different ALP activities

Endothelial cells were separated by magnetic cell sorting into two fractions: one with a high expression of ALP ("ALP positive cells") and another with a low expression of ALP ("ALP negative cells"). During the very short time of incubation (10 min) with anti-ALP antibodies, we suppose that only cells with a high concentration of ALP in the plasma membrane bind the first antibody. The second magnetic antibody binds only to cells containing the first antibody. Magnetic columns allowed the separation of cells with different expression of ALP.

We measured the ALP activity of each fraction of separation and found only a very low activity in the "ALP positive cells". The antibody complex (first and second antibodies) on the "ALP positive cells" probably binds to the catalytic side of the enzyme. However, the antibody complex is biodegradable (according to information from Miltenyi Biotech) and will disturb the biochemical assay only in the first 2 days after separation. Each fraction was cultivated for at least 7 days. ALP activity was determined by histochemistry:

"ALP positive cells"

Until day 4, the "ALP positive fraction" shows homogenous ALP activity. The cells were flat and larger than control cells. We observed only a few clusters and cell density was low. The cultures did not reach confluence at all. After 4 days, the heterogeneity of the ALP activity reappeared - in contrast to the aim of our separation. However, greater areas of the monolayer showed the same ALP activity. The intensity of histochemical staining was the same as in the "ALP negative fraction" and control cells.

"ALP negative fraction"

Until day 3, the "ALP negative cells" showed homogenous ALP activity. The cells were elongated and we observed fewer clusters than in control cultures. The cell density was lower than in control cultures and higher than in the "ALP positive cell

cultures". Confluence was reached after 6 days in culture. Heterogeneity reappeared on day 4 and was found to be diffuse, e.g. neighbouring cells show different ALP activity.

Control cultures

Until day 3, many cell clusters with a high ALP activity were found. The cells were elongated and confluence was reached on day 5. Heterogeneity reappeared on day 4 and was found to be diffuse, e.g. neighbouring cells show different ALP activity.

Biochemical analysis of the ALP activity as a function of culture time will be performed to clarify the success of our separation and the utility of enriched cultures as an *in vitro* model of the blood-brain barrier.

Conclusions

Although we separated cells with a high ALP activity from those with a low ALP activity, heterogeneity reappeared, suggesting that heterogeneity may be a prerequisite for the differentiated function of endothelial cells. The existence of cell prerequisite for the differentiated function of endothelial cells. The existence of cell populations with different ALP activity may complicate the establishment of an *in vitro* model of the blood-brain barrier. Transport characteristics of each cell population may be different.

References

[1] Ahlemeyer, B. et al., this report, p. 157

[2] Meyer, J. et al., J. Neurochem. **57** (1991) 1971

[3] Wolff, J. E. et al., J. Neurochem. **58** (1992) 909

[4] Bell, M. A. et al., Microvasc. Res. **27** (1984) 189

[5] Risau, W. et al., J. Neurochem. **58** (1992) 667

37. ANALYSES OF AN IMAGE OF A HUMAN BRAIN OBTAINED BY POSITRON EMISSION TOMOGRAPHY IN TERMS OF FRACTAL AND MULTIFRACTAL GEOMETRY

M. Obert, P. Brust, R. Bergmann

In recent years many different investigations have shown how successfully the irregularity of biological shapes can be described in terms of fractal theory [1]. The branching structures of neurons [2], arterial vessel systems [3], or the heart rate variability [4] have all been studied. In most examinations it is very difficult (especially for living organisms) to obtain unambiguous digitized data sets of the structures of interest. In our analysis positron emission tomography (PET) is applied as a method which allows the noninvasive in vivo mapping of dynamic structures of biochemical or physiological processes, e.g. in the human brain [5]. The resulting space-time distributions are characteristic with respect to the physics and chemistry of a special marker molecule and to the biological function of that tracer. An example: [^{18}F]2-fluoro-2-deoxy-D-glucose (FDG) mimics glucose and allows the estimation of the spatial and temporal distribution of the glucose metabolism. Depending on the actual activation of certain regions of a volunteer's brain, an FDG-PET image of the brain looks different at rest or during visual stimulation [6]: Investigations of functional neuroanatomy are possible.

We introduce the concept of fractal and multifractal geometry to describe the irregular spatial distribution of FDG in a section of a human brain [7, 8]. A contour diagram of the spatial radioactivity distribution of the analyzed section is shown below. The higher the radioactivity, the denser are the contour lines. The given units are lattice sites or pixels of the PET scan.

In order to investigate the fractal properties of the image, we construct binary subsets from the image data for different ranges of radioactivity. Such subsets contain only spatial information, which allows the determination of selfsimilar properties. A detailed description of how to conduct the fractal and multifractal analysis is given in Refs. 7, 8. For a subset generated from low to high radioactivity we find a fractal dimension D of 1.9. For a subset representing basically high radioactivity we find a D of 1.2. This indicates a multifractal behaviour of the set.

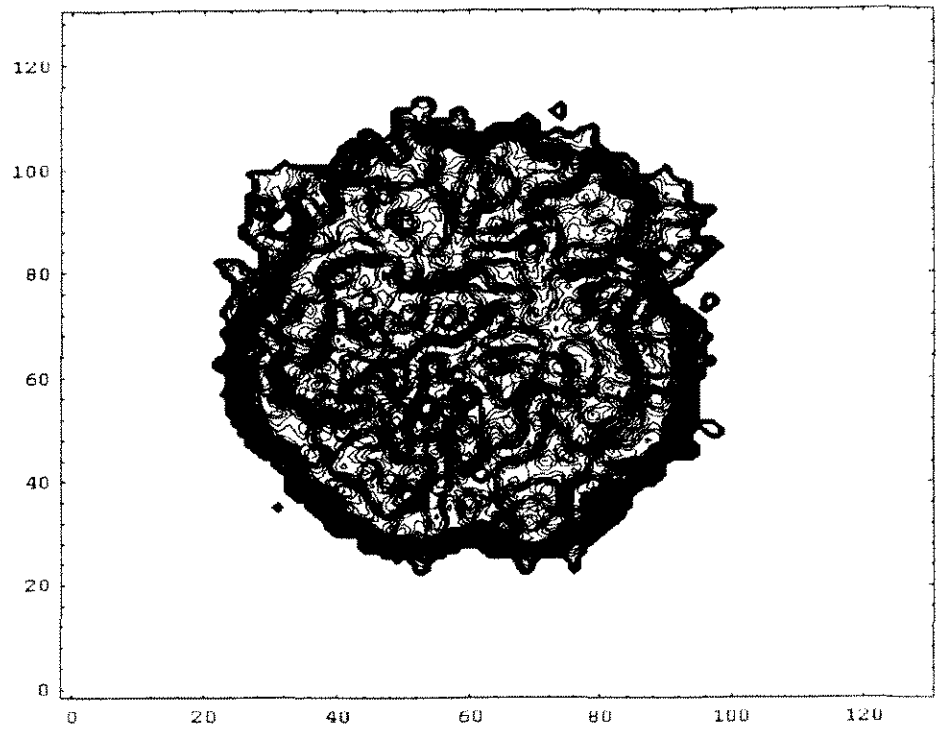

Further, the data is analyzed as a "landscape" where 2 dimensions are given by the spatial coordinates of the cross section of the brain and the third dimension, the height of the "landscape", is defined by the radioactivity at the spatial position on the slice. The analysis of this selfaffine set with the mass radius relation [1] gives a D of 2.3.

We have shown in preliminary studies [7, 8] that D can serve as a mathematically well-defined measure to describe the global irregularity of a PET image. The power of the software methods (e.g. the clinical relevance as a tool of computer aided and automated diagnosis) will be examined as soon as image data of patients are available, which are produced at the PET center Rossendorf.

Acknowledgments:

The authors wish to thank W. Enghardt for the permission to analyze the PET data. We further thank H. Linemann and E. Will for the transmission of the image data.

References

[1] Avnir, D. The Fractal Approach to Heterogeneous Chemistry: Surfaces, Colloids, Polymers, Wiley, Chichester, 1989

[2] Smith Jr., T. G. et al., Brain Research **634** (1994) 181

[3] Sernetz, M. et al., Physica A **191** (1992) 13

[4] Meesmann, M. et al., Biol. Cybern. **68** (1993) 299

[5] Phelps, M. Positron Emission Tomography and Autoradiography: Principles and Applications for the Brain and Heart, Raven, N.Y., 1986

[6] Fox, P.T. et al., Science **241** (1988) 462

[7] Obert, M. et al., Fractal 95 - 3rd International Working Conference, Marseille, 1995

[8] Obert, M. et al., International Workshop on Nonlinear Dynamics, Fractality, and Selforganization of Complex Systems, Würzburg, 1994

III.

PUBLICATIONS, LECTURES AND POSTERS

PUBLICATIONS

Bergmann R., P. Brust, H. Coenen, G. Stöcklin
Compartmental analysis of blood brain transfer and protein incorporation of L-[^{75}Se]seleno methionine in rat brain
J. Neurochem. **63** (1994) (Suppl. 1) S78C

Brandsch M, P. Brust, K. Neubert, A. Ermisch
ß-Casomorphins - chemical signals of intestinal transport systems
in: ß-Casomorphins and Related Peptides: Recent Developments (Brantl V. and Teschemacher H., eds.) VCH, Weinheim, 1994, pp. 207-219.

Brust P, A. Bech, R. Kretzschmar, R. Bergmann
Developmental changes of enzymes involved in peptide degradation in isolated rat brain microvessels
Peptides **15** (1994) 1085

Brust P., R. Bergmann
Characterization of serotonin uptake sites on the blood brain barrier
J. Neurochem. **63** (1994) (Suppl. 1) S13C

Kampf G., G. Knop, S. Matys, G. Kunz, U. Wenzel, R. Bergmann, W.-G. Franke
Beziehungen zwischen der ^{169}Yb-Aufnahme in Normal- und Tumorzellen und deren metabolischer Aktivität in Abhängigkeit von der Ligandspezies
Nuklearmedizin **33** (1994) A 82

Kampf G., G. Knop, U. Wenzel, G. Wunderlich, R. Bergmann, W.-G. Franke
Studies of radiometal uptake by cultured normal and tumour cells
Eur. J. Nucl. Med. **21** (1994) 874

Mihail J. D., M. Obert, S. J. Taylor, J. N. Bruhn
The fractal dimension of young colonies of *macrophomina phaseolina* produced from microsclerotia
Mycologia **86** (1994) 350

Johannsen B.
Entwicklungen in der Technetiumchemie für die Nuklearmedizin
Nucl.-Med. **33** (1994) A 90 (Abstract)

Seifert S., G. Wagner, A. Eckardt
Highly concentrated [^{99m}Tc]pertechnetate solutions from (n,γ)^{99}Mo/^{99m}Tc generators for nuclear medical use
Appl. Radiat. Isot. **45** (1994) 577

Spies H., M. Glaser, H.-J. Pietzsch, F. E. Hahn, O. Kintzel, T. Lügger
Trigonal-bipyramidale Technetium- und Rhenium-Komplexe mit vierzähnigen tripodalen NS_3-Liganden
Angew. Chem. **106** (1994) 1416

Steinbach J., P. Mäding, F. Füchtner
N. c. a. ^{11}C-labelling of benzenoid compounds in ring positions: Synthesis of nitro-[1-^{11}C]benzene and [1-^{11}C]aniline
J. Labelled Compd. Radiopharm. **36** (1995) 33

LECTURES

Ahlemeyer B.
Die Schilddrüse
im Rahmen der Physiologie- und Pharmakologievorlesung des Fachbereichs Pharmazie der Philipps-Universität Marburg, 5. Mai 1994

Ahlemeyer B.
Histamin und Antihistaminika
im Rahmen der Physiologie- und Pharmakologievorlesung des Fachbereichs Pharmazie der Philipps-Universität Marburg, 17. November 1994

Ahlemeyer B.
Glatte Muskulatur
im Rahmen der Physiologie- und Pharmakologievorlesung des Fachbereichs Pharmazie der Philipps-Universität Marburg, 18. November 1994

Ahlemeyer B.
Physiologie der Niere, Gefäßsystem und Blutdruck, Pharmakologie Blutdruck, Pharmakotherapie des Herzens
im Rahmen der Physiologie- und Pharmakologievorlesung des Fachbereichs Pharmazie der Philipps-Universität Marburg, 22. April - 9. Mai 1994 und 11. - 28. November 1994

Brust P.
Aspekte der Positronen-Emissions-Tomografie aus neurobiologischer Sicht
Institut für Pharmakologie und Toxikologie der TU Dresden, 14. Juni 1994

Brust P., R. Bergmann
Characterization of serotonin uptake sites on the blood brain barrier
10th Meeting of the European Society for Neurochemistry, Jerusalem, Israel, August 14 - 19, 1994

Brust P., H.-J. Pietzsch, M. Scheunemann, H. Spies, B. Johannsen
Biochemische Charakterisierung von potentiell rezeptoraffinen Re-Koordinationsverbindungen
AG Radiochemie/Radiopharmazie, Brüggen, 20. - 22. Oktober1994

Brust P.
Peptide und Blut-Hirn-Schranke: Ergebnisse verschiedener *in vivo* Methoden einschließlich der Positronen-Emissions-Tomographie
Institut für Pathologische Physiologie Jena und BMFT-Verbundvorhaben "Klinisch orientierte Neurowissenschaften", Jena, 8. Dezember 1994

Brust P.
Peptide als auslösende Signale von Transportveränderungen an der Blut-Hirn-Schranke
Habilitationsvortrag, 11. Dezember 1994

Johannsen B.
Technetiumkomplexe von Peptiden
Institut für Diagnostikforschung Berlin, 14. Januar 1994

Johannsen B.
Möglichkeiten und Grenzen von Technetium in der Medizin
Seminar über theoretische Grundlagen der Radiologie, Radiologisches Zentrum, Klinikum Essen, 4. Februar 1994

Johannsen B.
The technetium/MAG_3 sytem: Reactions and sources of by-products
Mallinckrodt Medical Petten, Holland, February 16, 1994

Johannsen B.
Studies of technetium(V)/S-donor ligand systems
Mallinckrodt Medical St. Louis, USA, April 12, 1994

Johannsen B.
Entwicklungen in der Technetiumchemie für die Nuklearmedizin
Deutsche Ges. f. Nuklearmedizin, 32. Intern. Jahrestagung, Kiel, 27. - 30. April 1994

Johannsen B.
Radiotracer in der Medizin
Festkolloquium Inst. f. Lebensmittelchemie der TU Dresden, Dresden,
18. Oktober 1994

Johannsen, B, H. Spies
Functionalisation of technetium and rhenium complexes to make them active *in vivo*
3rd Intern. Symp. on Applied Bioinorganic Chemistry, Fremantle-Perth, Australien,
Dezember 11 - 15, 1994

Noll B., St. Noll, B. Johannsen
Sources of radiochemical impurities in the ^{99m}Tc/S-unprotected MAG_3 system
VIII. Böttstein-Kolloquium, Villigen, Switzerland, October 6 - 7, 1994

Noll B., St. Noll, H. Spies, B. Johannsen, L. Dinckelborg, W. Semmler
Technetiumkomplexe mit N-Alkyl-Mercaptoacetyltriglycinen als potentielle Tracer zur Diagnostik von Arteriosklerose
2. Arbeitstagung AG Radiochemie/Radiopharmazie, Brüggen, 21. Oktober 1994

Obert M.
Anwendung der fraktalen Geometrie in der Medizin
Konferenz der Klinik und Poliklinik für Nuklearmedizin der Technischen Universität Dresden, 19. November 1994

Preusche St.
Probleme der Installation und Besonderheiten des Rossendorfer PET-Zyklotrons
Arbeitsaufenthalt, Deutsches Krebsforschungszentrum Heidelberg, 13. Juni 1994

Preusche St.
An overview of the Rossendorf PET Center
Montreal Neurological Institute, Neuroimaging Laboratory, McConnell Brain Imaging Centre, Montreal, Canada, November 17, 1994

Seifert S., G. Wagner, A. Eckardt
Highly concentrated [^{99m}Tc]pertechnetate solutions from (n,γ)^{99}Mo/^{99m}Tc generators for nuclear medical use
Final Research Coordination Meeting of the CRP on "Alternative technologies for ^{99m}Tc generators based on low temperature sublimation and gel elution"
IAEA Headquarters Vienna, Austria, May 3 - 6, 1994

Seifert S., R. Syhre, H. Spies, B. Johannsen
Reaktionen isomerer Technetium- und Rhenium-Komplexe mit 2,3-Dimercapto-bernsteinsäure und deren Ester
GDCh-Fachgruppe Nuklearchemie, Berlin, 6. September 1994

Seifert S., O. Muth, K. Jantsch, B. Johannsen
Radiochemical purity of ^{99m}Tc-HMPAO: Critical parameters during kit preparation
VIII. Böttstein-Kolloquium, Villigen, Switzerland, October 6 - 7, 1994

Spies H., B. Johannsen
Functionalization of technetium complexes to make them *in vivo* reactive
5th Nordic Symposium on "Trace elements in human health and disease"
Loen, Norway, June 19 - 22, 1994

Spies H., T. Fietz, H.-J. Pietzsch, R. Syhre, B. Johannsen
Das 3+1-Konzept in der Synthesestrategie neuer funktionalisierter Technetium- und Rheniumtracer, GDCh-Fachgruppe Nuklearchemie, Berlin, 6. September 1994

Spies H.
Wege zu neuen Technetium- und Rheniumtracern
2. Arbeitstagung AG Radiochemie/Radiopharmazie, Brüggen, 21.Oktober 1994

Steinbach J., F. Füchtner, K. Neubert
Arbeiten zur PET-Radiochemie im FZ Rossendorf und alternative Ansätze zu eingeführten Synthesen mit [^{11}C]CO_2, Max-Planck-Gesellschaft, Arbeitsgruppe "CO_2-Chemie", Universität Jena, 16. Juni 1994

Steinbach J.
PET- mehr als ein neues bildgebendes Verfahren in der Medizin
Fortbildungsveranstaltung mittleres medizin. Personal, Fortbildungswerk Bischofswerda, Bischofswerda, 15. November 1994

Syhre R., S. Seifert, H. Spies, B. Johannsen
Beziehungen zwischen in vitro Hydrolyseeigenschaften und in vivo Verhalten von ^{99m}Tc-DMSA-Ethylestern mit unterschiedlichem Veresterungsgrad.
AG Radiochemie/Radiopharmazie, Brüggen, 20. - 22. Oktober 1994

POSTERS

Ahlemeyer B, S. Matys, R. Bergmann, P. Brust
Alkaline phosphatase and g-glutamyltransferase in cultured endothelial cells of adult pig show changes in the activities by variations in culture conditions
VIIIth International Symposium on the Biology of Vascular Cells,
Heidelberg, August 30 - September 4, 1994

Bergmann R., P. Brust, H. Coenen, G. Stöcklin
Compartmental analysis of blood-brain transfer and protein incorporation of L-[^{75}Se]seleno methionine in rat brain
10th Meeting of the European Society for Neurochemistry, Jerusalem, Israel,
August 14 - 19, 1994

Kampf G., G. Knop, S. Matys, G. Kunz, U. Wenzel, R. Bergmann, W.-G. Franke
Beziehungen zwischen der ^{169}Yb-Aufnahme in Normal- und Tumorzellen und deren metabolischer Aktivität in Abhängigkeit von der Ligandspezies

Deutsche Gesellschaft für Nuklearmedizin, Jahrestagung, Kiel, 27. - 30. April 1994

Kampf G., G. Knop, S. Matys, G. Kunz, U. Wenzel, R. Bergmann, W.-G. Franke
Studies of radiometal uptake by cultured normal and tumour cells
European Association of Nuclear Medicine Congress, Düsseldorf,
August 20 - 24, 1994

Mäding P., F. Füchtner, J. Steinbach
N. c. a. ^{11}C-ring labelling of aromatic compounds: Synthesis of nitro-[1-^{11}C]benzene and [1-^{11}C]aniline
5th International Symposium on the Synthesis and Applications of Isotopes and Isotopically Labelled Compounds, Strasbourg, France, June 20 - 24, 1994

Noll B., P. Leibnitz, St. Noll, B. Johannsen, G. Reck, H. Spies, H.-J. Pietzsch
Synthesis and X-ray structures of $AsPh_4$ [$ReO(MAG_2)$] and $AsPh_4$ [$TcO(MAG_2)$]
30th Intern. Conf. Coord. Chem., Kyoto, Japan, July 24 - 29, 1994

Noll B., St. Noll, H. Spies, B. Johannsen, L. Dinkelborg, W. Semmler
Technetium complexes of N-alkylated mercaptoacetyl glycines as potential unspecific tracers in arteriosclerotic diagnostics
4th Intern. Symp.on Technetium in Chemistry and Nuclear Medicine, Bressanone, Italy, September 12 - 14, 1994

Obert M., P. Brust, H. Linemann, R. Bergmann, F. Jestczemski
The distribution of a radiotracer in a human brain is a multifractal - A novel approach for the analysis of positron emission tomography images
Intern. Workshop on Nonlinear Dynamics, Fractality, and Selforganization of Complex Systems, Würzburg, October 1 - 3, 1994

Pietzsch H.-J., H. Spies, K. Klostermann, P. Leibnitz, G. Reck
Rhenium complexes with bi- and tetradentate thioether ligands
30th Intern. Conf. Coord. Chem., Kyoto, Japan, July 24 - 29, 1994

Pietzsch H.-J., M. Glaser, H. Spies, F. E Hahn, O. Kintzel, T. Lügger
Trigonal-bipyramidal rhenium and technetium complexes containing tris(2-thiolato-ethyl)amine
30th Intern. Conf. Coord. Chem., Kyoto, Japan, July 24 - 29, 1994

Pietzsch H.-J., H. Spies, P. Leibnitz, G. Reck, K. Klostermann
Technetium and rhenium complexes with multidentate thioether ligands
4th Intern. Symp.on Technetium in Chemistry and Nuclear Medicine, Bressanone, Italy, September 12 - 14, 1994

Seifert S., R. Syhre, H. Spies, B. Johannsen
Enzymatic cleavage of technetium and rhenium complexes with DMSA ester ligands
4th Intern. Symp.on Technetium in Chemistry and Nuclear Medicine, Bressanone, Italy, September 12 - 14, 1994

Spies H., T. Fietz, H.-J. Pietzsch, P. Leibnitz, G. Reck
Neutral oxorhenium(V) complexes with tridentate/monodentate coordination
30th Intern. Conf. Coord. Chem., Kyoto, Japan, July 24 - 29, 1994

Spies H., T. Fietz, M. Glaser, H.-J. Pietzsch, B. Johannsen
The n+1 concept in the synthesis strategy of novel technetium and rhenium tracers
4th Intern. Symp.on Technetium in Chemistry and Nuclear Medicine, Bressanone, Italy, September 12 - 14, 1994

IV.

POSTDOCTORAL QUALIFICATION

Peter Brust Ph.D.

Habilitation

Thesis: "Peptide als auslösende Signale von Transportveränderungen an der Blut-Hirn-Schranke"

November 1994

V.

SCIENTIFIC COOPERATION

In multidisciplinary research such as carried out by this Institute, collaboration, the sharing of advanced equipment, and above all, exchanges of ideas and information obviously play an important role. Effective collaboration has been established with colleagues at universities, in research centres and hospitals.

Cooperative relations and joint projects

The *Technische Universität Dresden* (Dr. Scheller, Dr. Klostermann, Inst. of Analytical Chemistry) plays an essential part in SPECT tracer research by performing analytical characterization of new tracers and providing support with the synthesis of organic compounds (Dr. Habicher, Inst. of Organic Chemistry), as well as in biochemical research (Dr. Fischer, Dr. Kaspar, Institut für Pathologie).

Common objects of radiopharmacological and medical research link the Institute with the *Universitätsklinikum "Carl Gustav Carus"*, above all with its Department of Nuclear Medicine (Prof. Franke). A joint team of staff members from both the Institute and the Clinic of Nuclear Medicine are currently working at the Rossendorf PET centre.

Very effective cooperation also exists with the *Bundesanstalt für Materialforschung* Berlin (Dr. Reck, Mr. Leibnitz) who have carried out X-ray crystal structure analyses of new technetium and rhenium complexes.

Our long-standing cooperation in technetium chemistry with the *University of Padua* (Prof. Mazzi) and the *"Demokritos" National Research Centre for Physical Sciences* in Athens (Dr. Chiotellis) has been continued.

Joint work on technetium complexes with tripodal ligands has been carried out with the *Freie Universität Berlin* (Prof. Hahn, Inst. of Inorganic and Analytical Chemistry).

Cooperation on a special topic concerning bioinorganic chemistry is in progress with the *Arzneimittelwerk Dresden* (Dr. Unverferth).

Identification of common objects in PET radiopharmacy has led to collaborative research with the *Humboldt-Universität Berlin* (Dr. Michael of the "Charité" Hospitals, Clinic of Nuclear Medicine) and the *Universität Leipzig* (Dr. Günther, Radiology, Nuclear Medicine).

In the field of PET tracers, cooperation exists with the *Montreal Neurological Institute* (Prof. Gjedde, Prof. Thompson), the *Turku Medical PET Centre* (Prof. Wegelius, Dr. Solin), the CO_2-Group of the *Max-Planck-Gesellschaft* an der Universität Jena (Prof. Dinjus) and the *Hans-Knöll-Institut* Jena (Dr. Kasch).
The fruitful contacts to the *Paul Scheerer Institut,* Villigen, Switzerland, are very appreciated.

Cooperation on the biochemical aspects of radiotracer research exists with the *Universität Münster* (Prof. H.-J. Galla, Institute of Biochemistry), the *University of Minnesota* in Duluth (Prof. L.R. Drewes, Department of Biochemistry and Molecular Biology) and the *Friedrich-Schiller-Universität* Jena (Dr. R. Bauer, Institute of Patho-physiology).

In helpful discussions both abroad and at Rossendorf numerous colleagues have contributed to defining areas of cooperation and shaping projects.

Special thanks go to Dr. K. Deutsch, Mallinckrodt Medical Inc., St. Louis, USA, Dr. U. Scheffel, The Johns Hopkins Institutions, Baltimore, USA, Prof. Yoshihara, Tohoku University Sendai, Japan, and Prof. C.J. Thompson, Montreal Neurological Institute, Canada.

VI.

INTERNATIONAL ACTIVITIES

TEACHING ACTIVITIES FOR THE INTERNATIONAL ATOMIC ENERGY AGENCY (IAEA)

B. Johannsen
One week course within the Regional Training Course on the Production and Control of Tc-99m Generators and Tc-99m Radiopharmaceuticals, Tehran, Iran,
May 14 - 30, 1994

B. Johannsen
One week course within the Regional Training Course on Hospital Radiopharmacy, Rabat, Morocco, November 14 - 25, 1994

EUROPEAN RESEARCH PROGRAMME

H. Spies
Set up and chairing a working group on "New chelating systems for Tc and Re for medical application" within the EU research programme COST-B3

VII.

SEMINARS

Prof. H.-J. Galla, Institut für Biochemie, Westfäl. Wilhelms-Universität Münster
Kapillarendothelien in Kultur: Ein *in vitro*-Modell der Blut-Hirn-Schranke
27. Januar 1994

Dr. W. Burchert, Medizin. Hochschule Hannover
PET in der klinischen Praxis
11. Februar 1994

Dr. U. Scheffel, The Johns Hopkins Institutions, Baltimore, USA
New ligands for dopamine and serotonin transporters
March 11, 1994

Prof. J. Krieglstein, Institut für Pharmakologie und Toxikologie der Philipps-Universität Marburg
Experimentelle Nachweise von neuroprotektiver Arzneistoffwirkung
25. März 1994

Prof. W. Forth, Walter-Straub-Institut für Pharmakologie und Toxikologie, Universität München
Interaktionen von Metallen bei der Aufnahme in den Organismus
15. April 1994

Prof. E. Hoyer, Universität Leipzig
Neues über Schwefelliganden
22. April 1994

Prof. M. Eisenhut, Radiologische Universitäts-Klinik Heidelberg, Abt. Nuklearmedizin
^{123}I markierte, paraphenylenverbrückte Fettsäuren: Verlängerung der Herzmuskelretention durch metabolischen Einfang
6. Mai 1994

Dr. M. Gerlach, Universität Würzburg
Interaktionen von Neurotransmittersystemen in den Basalganglien und ihre Relevanz für die Pathophysiologie neurodegenerativer und psychiatrischer Erkrankungen
13. Juni 1994

Dr.Dr. H.J.Gross, University of Texas, MD Anderson Cancer Center Houston, USA
Rare Event Analysis: Eine Herausforderung für die Flow Cytometrie-Grundlage zum Nachweis von Minimal Residual Disease
August 22, 1994

Prof.Dr. F.F. Knapp, Jr., Oak Ridge Nat. Laboratory, USA
New developments at Oak Ridge ($^{188}W/^{188}Re$ generator; mACh receptor ligand)
August 30, 1994

O. Knoesen, Atomic Energy Corporation, Pretoria, Süd-Afrika
Current research and development program on radiopharmaceuticals at the AEC
September 9, 1994

Prof. C.J. Thompson, Montreal Neurological Inst., Canada
Quantitative Auswertealgorithmen am POSITOME IIIp am Beispiel von FDG-Studien (Demonstration am Tomografen)
12. September 1994

Prof. Yoshihara, Tohoku University Sendai, Japan
Trajectory of technetium chemistry of the group of Tohoku University
September 16, 1994

Dr. Kasch, Hans-Knöll-Institut Jena
Immunregulierende und anticancerogene Wirkung von DHEA (Dehydro-epiandrosteron) und seiner Derivate
23. September 1994

Prof. Dinjus, Arb.-Gruppe CO_2-Chemie der Max-Planck-Ges. an der Universität Jena
Zur Chemie des CO_2
28. Oktober 1994

Prof. Joó, Szeged, Ungarn
Regulation by second messenger molecules of the permeability of the blood-brain barrier: basic research and clinical applications
November 24, 1994

VIII.

ACKNOWLEDGEMENTS FOR FINANCIAL AND MATERIAL SUPPORT

The Institute is part of the Research Center Rossendorf Inc., which is financed by the Federal Republic of Germany and the Free State of Saxony on a fifty-fifty basis. In addition, the Free State of Saxony provided support for a project (7541.82-FZR/309) covering the establishment of cell cultures as a tool to replace animal experiments.

The research projects concerning technetium tracer design and PET radiochemistry were supported by the *Deutsche Forschungsgemeinschaft* and the *Fonds der Chemischen Industrie.*

Support by *Mallinckrodt Medical Inc.,* Petten, is highly appreciated.

The work on technetium chemistry was supported in part by a contract with the *Institut für Diagnostikforschung,* Berlin.

A number of projects were facilitated by financial and material support provided within a scientific job-creating programme (ABM).